The crucial roles played by HNF1β during kidney development

Filippo Maria Massa

THESE DE DOCTORAT DE

L'UNIVERSITE PARIS DESCARTES

Ecole doctorale « Génétique, Cellules, Immunologie, Infectiologie, Développement », ED 157

Spécialité : Développement

Présentée pour obtenir le titre de

DOCTEUR de l'Université Paris Descartes

"The crucial roles played by HNF1β during kidney development"

Par

M. Filippo Maria Massa

Soutenance le 14 novembre 2012

Composition du jury:

M. Marco Pontoglio	Directeur de thèse
Mme Evelyne Fischer	Codirectrice de thèse
M. Michel Cohen-Tannoudji	Rapporteur
Mme Brigitte Lelongt	Rapportrice
M. Bertrand Knebelmann	Examinateur
M. Gerard Waltz	Examinateur
M. Rémi Salomon	Examinateur
M. Weitzman Jonathan	Examinateur

Equipe "Expression Génique, Développement et Maladies" (EGDM)
INSERM U1016/ CNRS UMR 8104 / Université Paris-Descartes
Institut Cochin, Dpt. Génétique et Développement
24, Rue du Faubourg Saint Jacques, 75014 Paris, France

« Considerate la vostra semenza:
fatti non foste a viver come bruti
ma per seguir virtute e canoscenza»

Ulisse

(*Divina Commedia,* Inferno canto XXVI, 118-120, Dante Alighieri)

Aknowledgments - Remerciements – Ringraziamenti

Four years of thesis are a long journey; fortunately I have be surrounded and supported by a lot of people that I will try to thank in this page, too short to be exhaustive for all the gratitude I have to them.

In first place, I would like to thank the members of the jury that have kindly accepted to evaluate my work: Pr. Knebelmann, Pr Waltz, Pr Knebelman, Pr Salomon. A special thank goes to Mme Lelongt and M Cohen-Tannoudji to have reviewed my thesis and to give very useful suggestions in order to ameliorate it.

A long journey needs good leading. For the precious and irreplaceable help and support I would like to thank Marco and Evelyne that overviewed all my work (and corrected the not-so-few mistakes I did on the way). They avoid me to get lost in failing experiments and frustrating periods, as well as to encourage my enthusiasm. I'm still in love with the research!

Once the journey has started, I found a very important help from the entire group of colleagues: the "*Pontoglio's team*" crew always supported me and offered me the pratical/technical/moral support to achieve my work. I would like to thank the actual members of the lab (Serge, Michel, Magali, Jon, Cecile and Claire) and the people I have the pleasure to meet in the lab and that are now in the different corner of the world (the spanish Miguel and Kiko, Celine and Tristan).

A big thank to all the friends that I meet during my thesis: too many to number them without forgiving someone… Thanks for the support you gave me, for the antibodies protocols and suggestion you gave me, without forgetting the long nights spent partying around!

In conclusion, useless to check the list of the names, I could not double the size of my thesis!! But I will remember all of you wherever I will go ☺

Of course, a very special thank goes to my parents Ezio and Grazia that supported me (even with excellent food supplies) all along my thesis and to my brothers Corrado and Emanuele! Thanks also to Giulia and Veronica to support and stand my bros, and without forgetting the newcomer Edoardo.

Finally, THE very special thanks to Eva that stand me all along the way and gave me the strength to keep going on, even if sometimes the things seem not to work and I was tempted to give up. Thank youuuu!!

Table of Contents

Introduction I

Introduction II

Introduction III

Introduction IV

Introduction V

Results Part I

Results Part II

Discussion

Perspectives

Bibliography

Introduction I

I. **Kidney morphology and functions**

The kidney is a complex organ, located at the rear of the abdominal cavity in the retroperitoneum (figure 1A). The kidneys play crucial roles in the maintenance of the homeostasis including the regulation of blood pressure (salts and water balance), the modulation of acid-base balance and the elimination of wastes derived from the metabolism. The tight controlled balance between glomerular filtration, tubular excretion and reabsorption is at the basis of kidney functions and importance. Around 40 highly specialized cell types are organized in peculiar compartments of the kidney to exert all these functions. The kidney has also endocrine functions: it produces erythropoietin, responsible for inducing red blood cells maturation, active Vitamin D that participates to the homeostasis of calcium and phosphorus, important for bone morphogenesis and maintenance, and renin, an active actor in the blood pressure regulation.

The functional unit of the kidney is the nephron. It is composed by a blood filtration unit, called glomerulus, and a tubular part in charge of processing the primary urine filtered by the glomerulus. The epithelial tubular portion of the nephron is divided in successive segments, composed by highly specialized cells: starting from the Bowman's capsule of the glomerulus, the nephron is composed by the Proximal Tubule (subdivided in S1, S2 and S3 segments), the Henle's Loop, the Distal Convoluted Tubule and the Collecting Duct system (figure 1C-D). Morphologically, the kidney is formed by the cortex, characterized by the presence of S1 and S2 convoluted segments of proximal tubules, the globular structures of the glomeruli and the convoluted distal tubules that are connected to collecting tubules via a short connecting segment. The inner part of the kidney, the medulla, contains the straight S3 segment of proximal tubule, the Henle's loop branches and the collecting duct system. The collecting system will progressively form pyramids (that is a single structure in mouse and rat), renal calyces, pelvis and finally the ureter that will flow the urine into the bladder (figure 1B).

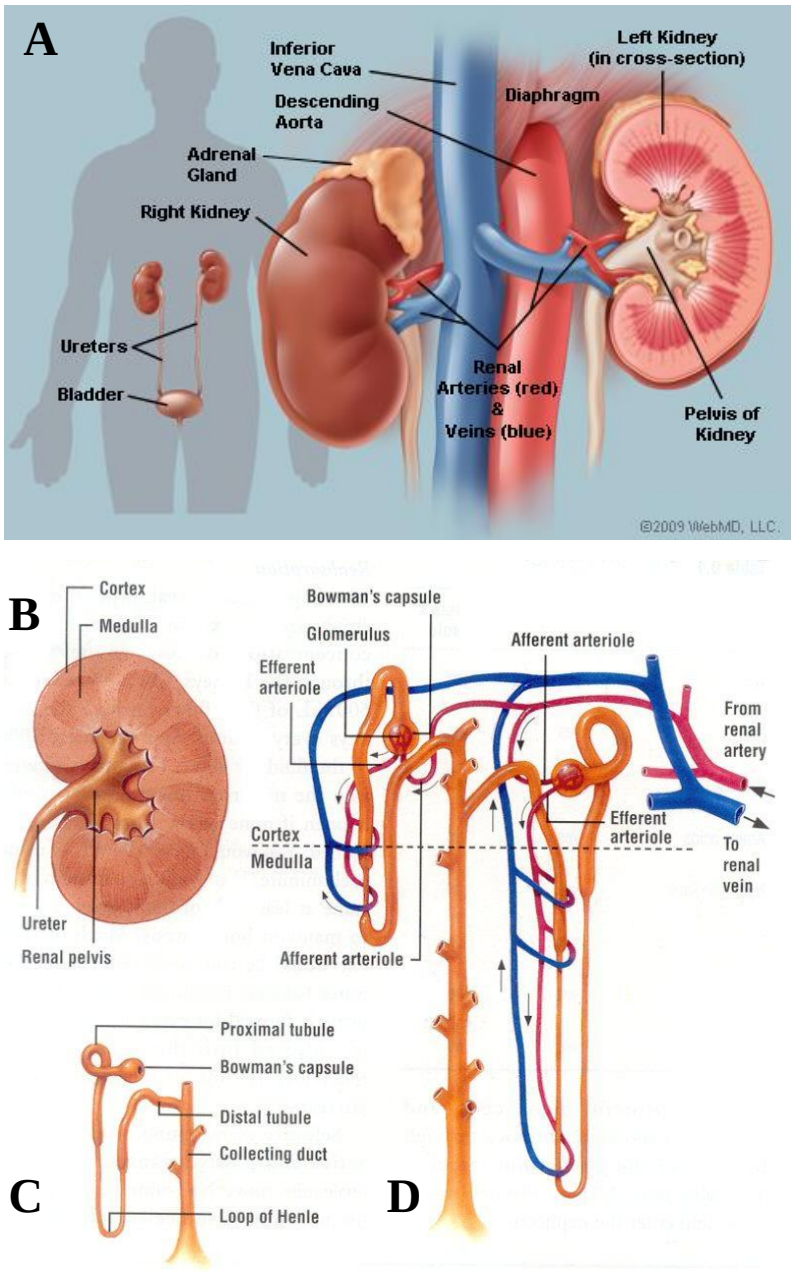

Figure 1. Anatomical structure of the kidney. (A) Macroscopical representation of kidneys and their connections with the vascular system: the renal artery coming from the aorta in red and the renal vein going to the vena cava in blue (adapted from http://www.webmd.com). (B) The kidney is composed by a cortex that contains glomeruli, proximal and distal convoluted tubular portions of the nephron, and a medulla that contains the straight part of the proximal tubule, Henle's loop and part of the collecting system. (C) Representation of the different segments of the nephron and (D) their interaction with the peritubular capillaries network (adapted from: http://classconnection.s3.amazonaws.com).

The **glomerulus** is formed by a complex net of anastomosed capillaries that arises from a single afferent artery and that finally converges into a single efferent artery: the glomerular capillaries are fenestrated and surrounded by a specific cell type, the podocytes. The structural support to the vascular flocculus is provided by the mesangial cells. The blood is filtered through a filtration barrier that allows only small molecules (low molecular weight proteins or ions) to pass. This barrier is composed by a fenestrated endothelial layer, a basal membrane and a podocyte zip-shaped slit diaphragm. Cells and high molecular weight proteins (for example, albumin) are normally retained in the circulation and their presence in the urine is a symptom of alteration of this filtration barrier. The vascular tuft is surrounded by the Bowman's capsule that collects the primary urine derived from filtration in the urinary space. The Bowman space is in direct connection with the proximal tubule at the urinary pole (figure 2).

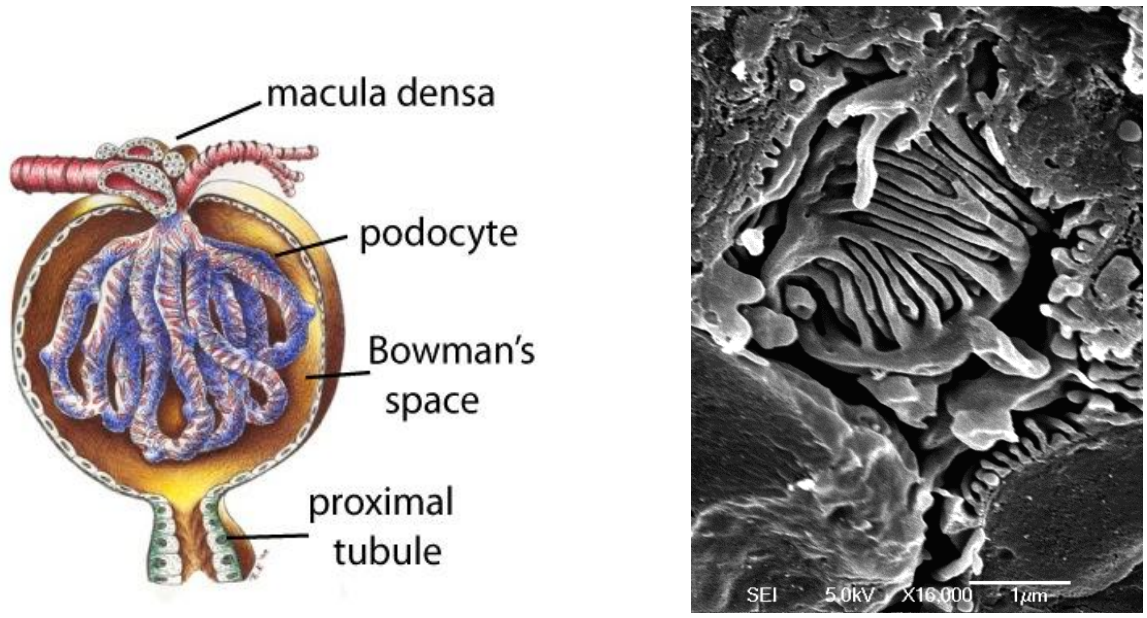

Figure 2. Structure of the glomerulus. The glomerulus (on the left panel) is composed by a net of capillaries, arising from the afferent artery and flowing into the efferent artery. These capillaries are wrapped by the podocytes. After the filtration process, the primary urine flows in the urinary space of Bowman's capsule and is drained away by the proximal tubule (image adapted from http://www.sharinginhealth.ca). In the right panel, a scanning electron microscopy picture of the podocytes and their foot processes. These foot processes are linked by a zip-shaped slight diaphragm, which is part of the filtration barrier (this image has been gently provided by Michel Leibovici).

The **Proximal Tubule** (**PT**) is responsible for the massive reabsorption of most of the primitive urine components. Around 60% of the water and salt and up to 95% of phosphate, glucose and amino acids filtered by the glomerulus are reabsorbed in this segment (figure 3). To perform this massive reabsorption, the surface of tubular cells is increased by the presence of brush borders on the apical membrane and by interdigitations of the basal membrane. In the proximal tubule, the passive reabsorption of ions occurs via several Na^+-coupled cotransporters that are located on the luminal surface. The driving force of this reabsorption is generated by an electrochemical gradient of Na^+ that is performed and maintained by the Na^+-K^+-ATPase, an active transporter located baso-laterally and intimately associated with large prominent mitochondria (Brenner, 1996). The transport of water through the epithelial layer is a passive mechanism, while the reabsorption of small molecular weight proteins physiologically filtered by the glomerulus requires a lysosomal system, known as apical vacuolar endocytotic apparatus. A more detailed observation shows a sub-compartmentalization of the PT in three different segments called S1, S2 (convoluted segments) and S3 (straight segment). These segments are characterized by the expression of a different set of genes that confer to each subdomain specific functions. As an example, among the small molecules that pass the glomerular filter, the glucose is an important metabolite that is reabsorbed entirely in the proximal tubule via the glucose transporters Slc5a1 and Slc5a2. These glucose transporters present different affinity and stochiometries for the glucose and they are specifically expressed in sub-segments according to the concentration of the glucose along the tubule. The low affinity Na^+/glucose transporter Slc5a2 is present mostly in the first convoluted segment S1 where the concentration of glucose is high in the primary urine, whereas the Na^+/glucose high affinity transporter Slc5a1 is located in the straight segment S3 where only few molecules of glucose have still to be reabsorbed (Kamiyama et al., 2012; Kanai et al., 1994).

Henle's Loop segment is composed by the thin descending limb (TDL), which is in direct continuation with the S3 segment, and the thick ascending limb (TAL). The Henle's loop has a characteristic U conformation that enters in the medulla of the kidney and that goes up again in the cortex where it is in contact with its own glomerulus. The major role of Henle's loop is to generate the cortico-medullary gradient that plays a crucial role in the ability of the kidney to concentrate or dilute urine (figure 3). The TDL is extremely permeable to water and less permeable to ions. In this portion of Henle's loop, the reabsorption is limited to water, whereas the solutes are retained in the urine (Kokko, 1970). This process increases

the concentration of the urine that reaches its maximum around the tip of the loop in the medulla. In the TAL the situation is reversed: the tubule becomes impermeable to water and permeable to ions principally via active transports. The ions are reabsorbed mainly via the Na-K-2Cl cotransporter (Slc12a1), localized at the apical pole of tubular cells. The intracellular ion gradient is maintained by a Na^+/K ATPase that actively pumps Na+ ions in the peritubular compartment, that will ultimately be reabsorbed by the vasa recta (Greger, 1985), (Imai and Kokko, 1976).

A specific set of cells, composing the **Macula Densa**, is localized at the end of the Henle's loop segment. This peculiar tubular portion, with the two glomerular arteries and the extraglomerular mesangium, forms the juxta-glomerular apparatus (Barajas, 1970) (Barajas, 1979). This specific domain, through its peculiar anatomical conformation has been demonstrated to be important for the regulation of blood pressure, via the renin angiotensin system. It is also acting as chemo-mechanical sensor of the urine and it participates to the tubulo-glomerular feedback via mechanisms that are not yet completely elucidated (Brenner, 1996).

The **Distal Convoluted Tubule** (DCT) is the last portion of the nephron before the connection to the collecting system. The DCT plays a crucial role in refining the urine composition and concentration, via the action of circulating hormones on the distal tubule cells (Greger and Velazquez, 1987) (figure 3). In particular, the DCT participates to the homeostasis of Na^+, mediated by aldosterone, and to the reabsorption of Ca^+(Borke et al., 1987).

The DCT is then connected via a short connecting duct to the **Collecting Duct** (CD) system. This set of tubules collects the urine produced by the nephrons and brings it via a series of structures (the pyramids, the calices, the pelvis and the ureter) into the bladder. The CD has a different embryological origin than the other tubules from the nephron as we will discuss it later. It is separated in cortical and medullary collecting ducts, according to the kidney compartments it crosses. It is composed mainly by "principal cells" (around 60%), rich in transporters and channels located at the apical membrane, that are mainly sensible to the action of hormones (figure 3). For example, the aldosterone increases the activity and, later, the number of Na+/K+ transporters to increase the sodium reabsorption and the potassium secretion, whereas the vasopressin modulates the localization of aquaporin channels on the cell surface. Together, aldosterone and vasopressin are key players in the final regulation of

urine volume and concentration in this last portion of the nephron (Naray-Fejes-Toth and Fejes-Toth, 1990) (Verrey et al., 1987). The other 20% of cells composing the CD are "intercalated cells" type α and β: they participate to the acid-base homeostasis by regulating the absorption/excretion of acid and bicarbonates (Malnic et al., 1994), (Brenner, 1996).

In conclusion, the kidney fulfills several important functions in order to maintain the body homeostasis through the filtration, reabsorption or secretion of water and small molecules present in the blood. These functions are accomplished thanks to the cellular and anatomical complexity of the kidney: the adult kidney is composed by around 40 different cell types. Its functional unit, the nephron, is composed by highly differentiated segments that have different characteristic and perform specific functions (figure 3). Such high level of complexity is achieved by a tightly controlled and regulated developmental process during embryogenesis: several signaling pathways and crosstalk take place since the early steps of nephrogenesis and lead an aggregate of multipotent cells to become a complete and functional organ. In the next chapter I will introduce the state of the art in the knowledge of these processes during the embryonic development and their implication in renal morphogenesis.

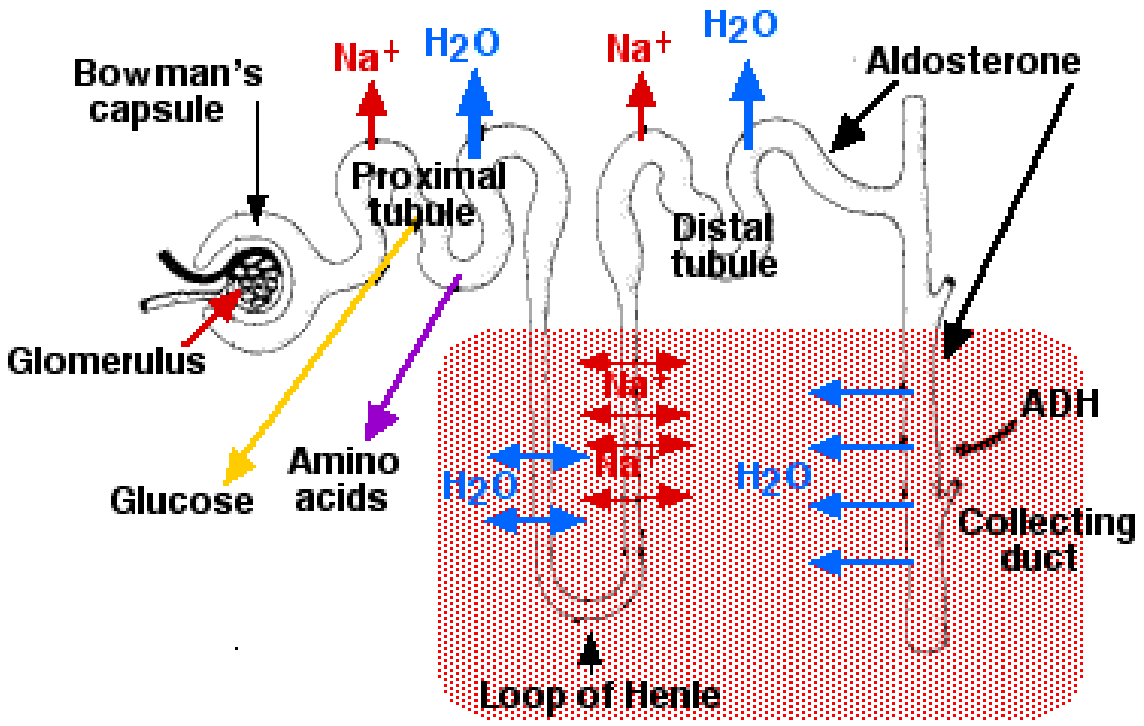

Figure 3. Schematic representation of tubular absorption and secretion functions. After glomerular filtration, the primary urine is processed all along the tubule in order to reach its final concentration and composition. The proximal convoluted part is responsible of massive reabsorption of water, solutes and glucose, whereas the successive segments refine the urine composition.

Image adapted from http://users.rcn.com/jkimball.ma.ultranet/BiologyPages/W/Welcome.html

Introduction II

II. Principal signaling pathways during renal morphogenesis

In higher organisms, the interactions and communications between different cells and with environment are crucial. Autocrine or paracrine signals deliver information to cells via short range signaling whereas hormones and soluble molecules can act via long range signalization. These external signals can modify cell behavior through multiple aspects, from structural cell modification to gene expression modulation. The ability of cells to perceive and correctly respond to their environment is at the basis of normal tissue homeostasis, tissue repair, as well as development. During embryonic development, several signaling pathways are involved in organ morphogenesis: despite the huge difference in shape and function between different organs and different species, most of the signaling pathways are evolutionary conserved and are able to fulfill different roles according to the environment in which they act.

In order to have a general overview of the pathways I will discuss during my thesis, I will briefly illustrate the principal signaling pathways that are implicated in kidney morphogenesis. In particular, I will focus on:

- Notch pathway
- Wnt canonical (β-catenin dependent) and Wnt non-canonical (β-catenin independent) signaling
- Bone Morphogenic Proteins (BMPs) signaling pathways
- Fibroblast Growth Factors (FGFs) signaling

The Notch Pathway

The Notch signaling pathway is a highly conserved cell signaling system present in most of multicellular organisms. The canonical Notch pathway is considered as a short range signaling, involving cell-to-cell contact. Indeed, both ligand and receptor are membrane proteins. In order to initiate the pathway, the signal-sending cell has to express the ligand at the cell membrane, whereas the adjacent signal-receiving cell must expose the receptor on its surface. In mammals, the Notch receptors family is composed by four members (Notch1 to 4) and they can interact with five ligands, two Jagged proteins (Jag1 and Jag2, homologous of Serrate in *Drosophila*) and three Delta-like ligands (Dll1, Dll3 and Dll4). Notch signaling can elicit opposite responses depending on the cell nature, such as proliferation or apoptosis program, can drive the acquisition of a specific cell fate or the maintenance of self-renewing status. The peculiar characteristic of the canonical Notch pathway depends on the mechanism of signal transduction. Once a ligand is bound to the receptor, a complex set of events leads to the release of the extracellular portion of the receptor after cleavage. The intracellular domain of the receptor is then able to translocate into the nucleus, where it plays the role of a transcriptional co-activator.

After their synthesis in the endoplasmic reticulum, Notch receptors undergo a first cleavage (S1) by a furin-like convertase in the trans-Golgi. This cleavage converts the original molecule in a heterodimeric molecule joined by non-covalent interactions (Logeat et al., 1998). The mature Notch receptor is composed by an extra cellular domain, a transmembrane part and an intracellular domain.

The extracellular portion is composed by a conserved array of 36 Epidermal Growth Factor (EGF) like repeats that are involved in the binding of the ligand (Wharton et al., 1985). In addition, three juxtamembrane repeats of cysteine rich regions, known as Lin-12, modulate the interaction with the juxtamembrane portion of the intracellular domain. These repeats compose the negative regulatory region (NRR). In the absence of ligand, the receptor is folded in a structure that makes the S2 cleavage site inaccessible and the receptor inactive (Gordon et al., 2007). The large modular Notch intracellular domain (NICD) is composed, starting from the juxtamembrane domain, by a region called RAM (RBPjκ associated molecule) that is followed be a repeated structural motif, flanked by nuclear localization signals. This repeated structural domain is composed by seven Ankirin, in charge of modulating the interaction with CBF1/Su(H). The N-terminal part of NCID domain is

composed by a transactivation domain (TAD, only in Notch1 and 2) and a proline-glutamine-serine-threonine rich domain (PEST) that is involved in the degradation/recycling of Notch (Oberg et al., 2001) (figure 4).

All the Notch ligands are, as well, membrane proteins, composed by a short N-terminal intracellular domain and a large extracellular domain. The major difference between Jag and Dll ligands is represented by the length of EGF-like domains, composed by 16 repeats for Jag and 6-8 repeats for the three Dll homologous. In addition to the number of EGF-like-tandem repeats, Jag differs from Dll by the presence of a cysteine rich domain close to the transmembrane region. The most important part for the signaling role of the ligand is located in the C-terminal portion of the extracellular part of the protein and it is common to both Jag and Dll. This domain is known as DSL (*Delta-Serrate-Lag2*) and is responsible for interaction with Notch receptor at the level of EGF-like repeat 11 and 12 (reviewed in (D'Souza et al., 2010)) (figure 4).

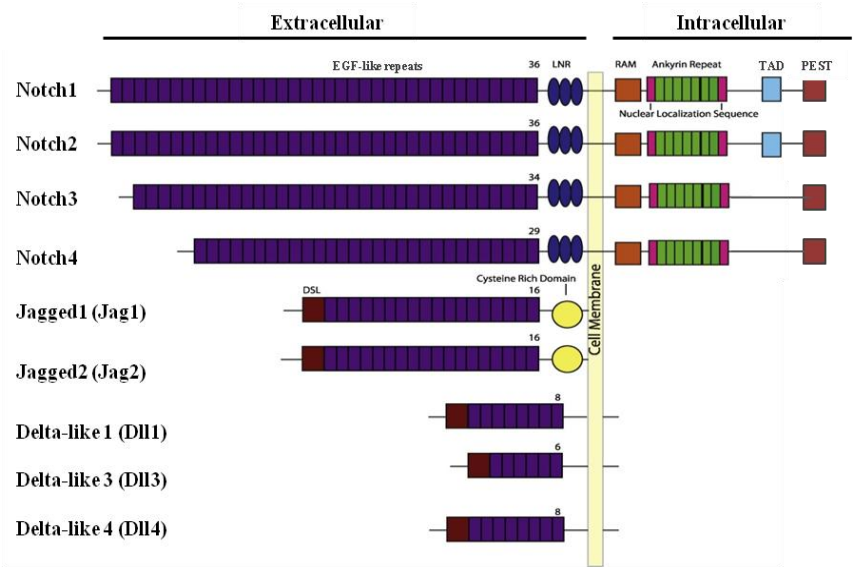

Figure 4. Schematic representation of the four Notch receptors (Notch1 to 4) and the five ligands present in mammals (Jag1 and 2, Dll1-2 and 4). The receptors differ mainly by the number of EGF-like repeats and the presence of a TAD domain in the intracellular portion of Notch1 and 2. All the ligands are characterized by a DSL sequence at the C-terminal part, whereas the cysteine rich domain is specific for the two Jagged ligands (adapted from (Wang, 2011)).

The activation of the pathway via ligand-receptor binding is known as **canonical Notch signaling pathway** (figure 5, left panel). In order to be active, the Notch receptor needs to undergo a first cleavage of the extracellular portion. Constitutively, the cleavage site is not accessible due to the 3D protein conformation that maintains the receptor in an inactive configuration. The binding of the ligand is able to modify this conformation, resulting in the exposition of a metalloproteinase site (S2) to the caspase activity and the shedding of the ectodomain. The enzyme in charge of this cleavage is a membrane bound complex, composed by ADAM (a desintegrin and metallopeptidase) and TACE (tumor necrosis factor α converting enzyme) (Brou et al., 2000).

The cleaved extracellular domain of the receptor is transferred inside the cell expressing the ligand by trans-cytosis. This complex is then disassembled inside the endosome and the ligand is again able to be expressed on the cell surface. The remnant cleaved part of the receptor, still inserted in the membrane, is a transient intermediate called Notch extracellular truncation (NEXT). NEXT becomes now accessible to another caspase, the γ-secretase, a multicomponent member of the intramembrane cleaving proteases (I-CLiPs). The γ-secretase is able to progressively cut NEXT at S3 and S4 sites, probably after endocytosis of the complex NEXT/γ-secretase. This process leads to the release of the transcriptionally active Notch intracellular domain (NICD). Its translocation in the nucleus leads to its interaction with different DNA-binding CSL proteins through the RAM domain. These proteins, also known as CBF1, Su(H), Lag1 contain RBPjκ binding interfaces. Subsequently, the Ankirin domain of NICD interacts with CSL to recruit another co-activator, Mastermind (Mam) (reviewed in (Kovall, 2008)). In order to elicit a transcriptional response, this complex has to bind RBPjk. In fact, in absence of NICD, RBPjk is bound to a co-repressor complex and silences gene expression. The intervention of NICD displaces the co-repressors complex from RBPjk, that switches from repressor to activator via the recruitment of the described transcriptional co-activators. The best known target genes of Notch canonical pathway are the members of hairy/enhancer of split (HES/HEY) family: they are helix-loop-helix transcription factors that mainly act as repressor during the embryonic development and the modulation of cell fate (Iso et al., 2003)

Recent experimental evidences disclosed the importance of a second Notch signaling pathway, known as **non-canonical Notch pathway** (figure 5, right panel). Preliminary experiments suggest that activation of Notch could be either independent from ligand-receptor interaction or uncoupled from the canonical intracellular action of the NICD. In this context, the extracellular domain of Notch could be bound by non canonical ligands or soluble proteins. This binding could modulate Notch pathway in several ways, including competitive inhibition, dissociation of the receptor or enhanced endocytosis (review in (Wang, 2011)). As an alternative, non canonical signaling can also act via the intracellular domain of Notch, which can behave separately from the canonical CSL-dependent way. Some genes have been shown to be affected, in different models and cell types, by non-canonical Notch signaling, but the precise mechanisms are still elusive. The most studied and well conserved non-canonical Notch pathway is the regulation of Wnt/β-catenin signaling: NICD domain can bind and titrate the active β-catenin, the major component of the Wnt/β-catenin pathway, as we will discuss it later (reviewed in (Andersen et al., 2012)).

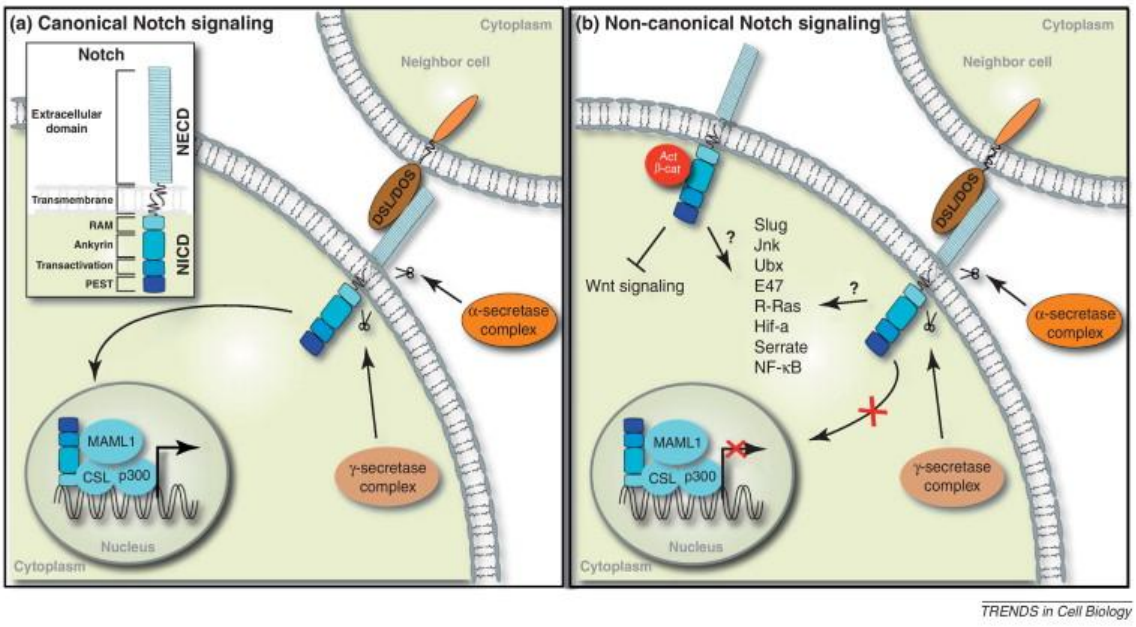

Figure 5. Canonical and non-canonical activation of Notch intracellular signaling. (A) The canonical Notch pathway involves the translocation of the NICD (once released by the secreatase) in the nucleus, necessary to the expression of target genes. (B) In the non-canonical pathway, NICD does not migrate in the nucleus, and more and more evidences suggest an interaction with other partners to elicit the modulation of several intracellular cascades (from (Andersen et al., 2012))

The Wnt signaling pathways

The *Wingless-related MMTV integration site (Wnt)* genes were first identified in the *Drosophila*. They were called *Wingless* (*Wg*) due to the absence of wings in the mutant flies. (Nusslein-Volhard et al., 1980). In mammals, the Wnt family is composed by 19 different soluble ligands that act, in association with lipoproteins, as middle-long range morphogens in a classical concentration-dependent manner (Panakova et al., 2005). Many of the 19 members are conserved in several multicellular organisms: the fact that monocellular organisms lack Wnt proteins suggests its importance for the development of more complex organims (reviewed in (Petersen and Reddien, 2009)). Wnt members are 40kDa proteins that contain many conserved cysteines, but their biochemical characterization still remains challenging. During the transit in the endoplasmatic reticulum, Wnt undergoes a lipid modification by the Porcupine (Porc) enzyme before being shuttled in Golgi vesicles and released outside the cell. The interaction of these ligands with the signaling receiving cell can give rise to two different cellular responses, according to the intracellular mechanisms involved: similar to Notch pathway, we can distinguish between a canonical and non-canonical Wnt signaling pathway.

The **canonical Wnt signaling pathway**, also known as **Wnt/β-catenin signaling**, involves a complex network of proteins that is activated once the ligand/receptor interaction occurs on the surface of the cell (figure 6). This signaling cascade ends up with the transcription of specific target genes in the nucleus. The canonical Wnt/β-catenin signaling is involved in several aspects of embryo and adult biology: its main role is the maintenance of self-renewal properties of stem cells and altered Wnt/β-catenin signaling is correlated with cancer and developmental abnormalities. The β-catenin is an important component of the cytoskeleton interacting complexes at the adherent junctions: these proteins have multiple copies of the so-called armadillo repeat domain, which is specialized for protein-protein interaction and allows the β-catenin to interact with cadherins and alpha-catenin. When β-catenin is not involved in membrane complexes, it can interact with other proteins and, in particular, it plays a role in Wnt intracellular signaling pathway. In absence of Wnt signalling, the cytoplasmic β-catenin is constantly degraded by the action of a complex composed by the scaffold protein Axin, the modular protein Dishevelled (Dsh, composed by three domains DIX, PDZ and DEP), the tumor suppressor *adenomatous polyposis coli* gene product (APC), and two different kinases, the casein kinase 1 (CK1) and the glycogen synthase kinase 3 (GSK3). The two kinases act sequentially by phosphorylating the amino

terminal region of β-catenin. This modification results in β-catenin recognition by β-Trcp, an E3 ubiquitin ligase subunit, and subsequent β-catenin ubiquitination and targeting to proteasome for degradation (Ha et al., 2004). The continuous elimination of β-catenin prevents its cytoplasmic accumulation and its migration in the nucleus: the β-catenin target genes are maintained repressed by the DNA-bound T cell factor/lymphoid enhancer factor (TCF/LEF) family members. In fact, in absence of β-catenin, these factors act as transcription repressors via the binding of a co-repressor Groucho that can both modify chromatin conformation and recruiting other co-repressors (Jennings and Ish-Horowicz, 2008).

The signaling becomes active when Wnt proteins interact with a surface heterodimeric receptor complex, composed by the transmembrane receptor Frizzled (Fz) and the single-pass transmembrane receptor LRP5/6 protein. The N-terminal cysteine-rich domain of Fz (CRD) contains a hydrophobic groove that gives a docking platform for the lipid component of Wnt (Janda et al., 2012). Once bound by Wnt, Fz undergoes a conformational modification that leads to its heterodimerization with LRP5/6 and the recruitment of Dsh. The activation of Dsh induces the successive phosphorylation of the LRP5/6 receptor by CK1 and GSK3 that allows the binding of the Axin complex and its sequestration at the membrane (Tamai et al., 2004). The new conformation leads to the inhibition of β-catenin ubiquitination. Two different models have been proposed. The current model suggests that Axin segregation at the membrane disassembles partially the complex leading to the absence of β-catenin phosphorylation and its subsequent β-Trcp-mediated ubiquitination (figure 6A). Recent studies have proposed a new model, suggesting that the relocalisation of the whole Axin complex leads, instead of disassociating the kinases, to the recruitment and phosphorylation of β-catenin that rapidly saturates the complex. In this context, the new produced non-phosphorylated β-catenin accumulates in the cytoplasm and finally translocates in the nucleus (Li et al., 2012) (figure 6B). In the nucleus, β-catenin interacts with TCF/LEF transcription factors. The β-catenin is able to displace Groucho and recruit several elements (as CBP, Cdc47, Bcl9 and Pygous), switching the TCF/LEF transcription factors from a repressor status to an activator of gene expression (figure 7).

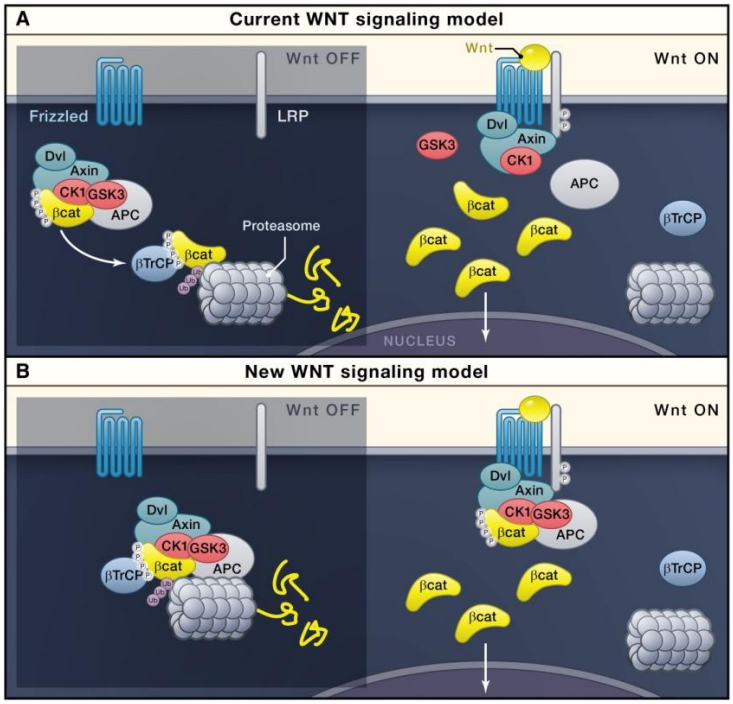

Figure 6. Schematic representation of Canonical Wnt/β-catenin signaling. (A) According to the current hypothesis, in absence of Wnt signaling, the β-catenin is rapidly phosphorylated and degraded by the proteasome via βTrCP transport (left panel). In the presence of Wnt, the phosphorylation complex is sequestered and dismantled by the receptor, leading to the β-catenin accumulation in the cytoplasm and finally to its migration into the nucleus (right panel). **(B)** An alternative hypothesis suggests that in absence of signaling, β-catenin is directly transported by the phosphorylating complex to the proteasome (left panel). In the presence of Wnt, the complex is sequestrated at the membrane by the activated receptor, rapidly saturated by phosphorylated β-catenin and not more able to interact with βTrCP and the proteasome: newly synthesized β-catenin is able to accumulate in the cytoplasm and migrate then in the nucleus (right panel) (Clevers and Nusse, 2012).

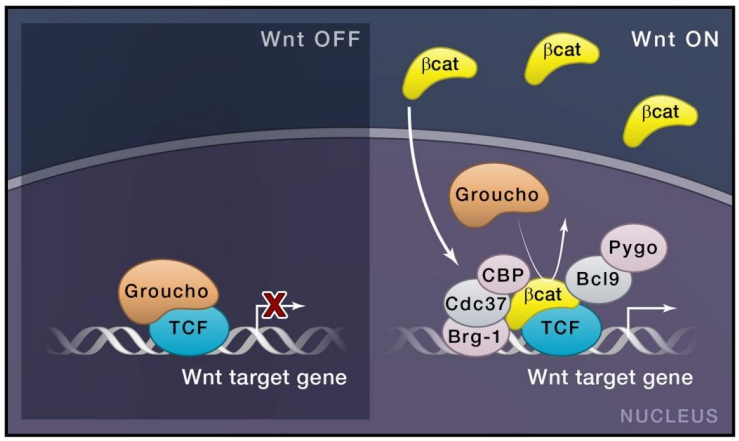

Figure 7. β-catenin mediated transcription. In absence of β-catenin, the transcription factors TCF/LEF are bound to the target genes, but in a repressive status, via the binding to the inhibitor Groucho (left panel). When the β-catenin enters the nucleus, Groucho is displaced and the newly recruited co-activators can assemble with TCF/LEF transcription factors and elicit gene transcription (right panel) (Clevers and Nusse, 2012).

The second pathway involving Wnt is the **non-canonical Wnt signaling**: this pathway acts in a β-catenin independent way and involves a central role for Dishevelled (Dsh). Until today, two main non-canonical pathways involving Wnt signaling have been indentified: the planar cell polarity pathway (PCP) and the non-canonical Wnt/Ca^+ pathway. The planar cell polarity is an intrinsic property that confers to the cell a specific orientation in the plan. As an example, it has been shown that planar cell polarity is crucial during cell division to maintain a correct orientation of the mitosis axis during tubular elongation (Fischer et al., 2006) .

The ***non-canonical Wnt PCP pathway*** emerged from the study of the *Drosophila* in which Wnt mutations affected the orientation of several structures such as hair, sensory bristles and ommatidia in the eye (Mlodzik, 2002) (figure 8). In this pathway, Wnt signaling is mediated by Fz alone, without interaction with LRP receptor. Once activated, Fz is then able to recruit and activate Dsh. Dsh is composed by three different domains, DIX, PDZ and DEP. These domains are involved in the interaction with specific partners that can activate different signals, such as Rho or Rac signaling cascades, involved in different cell responses (Wallingford and Habas, 2005). To activate the GTPase Rho pathway, Dsh interacts, via its PDZ and DEP domains, with Daam1 (Dishevelled associated activator morphogenesis-1), a Formin homologous protein able to bind Dsh and RhoA. This interaction activates, via Rho, the downstream Rho-associated kinase (ROCK) and JNK1, which are responsible for cytoskeletal rearrangement and actin modification. The parallel activation of Rac GTPase is Daam1 independent and is mediated by the DEP domain of Dsh and leads to JNK activation, even if the downstream effectors are not clear. Rho and Rac are known to have opposite functions: it is then considered that both pathways are responsible for cytoskeletal rearrangments during morphological convergent extension movements (Veeman et al., 2003).

The second non-canonical pathway is ***Wnt/Ca^+ pathway***: it has been noticed that the interaction Wnt/Fz can stimulate intracellular Ca^+ release from the endothelial reticulum in G-protein dependent way without affecting β-catenin stabilization (Harada et al., 2007). Ca^+ waves have been demonstrated to be crucial for early embryo patterning in *Xenopus* and *Zebrafish* (Wallingford et al., 2001), (Gilland et al., 1999) (figure 8). Intracellular release of calcium activates Ca^+ sensitive proteins such as protein kinase C (PKC) and calcium/calmodulin-dependent kinase II (CamKII): the downstream pathways result in the regulation of important morphological events during embryonic development. These processes include the regulation of cell fate in the blastula stage and the modulation of morphogenetic convergent extension movements during gastrulation via phosphorylation of

Dsh and Lef. This phosphorilation leads to their inactivation and has as a consequence the downregulation of the convergent extension movements (reviewed in (De, 2011)).

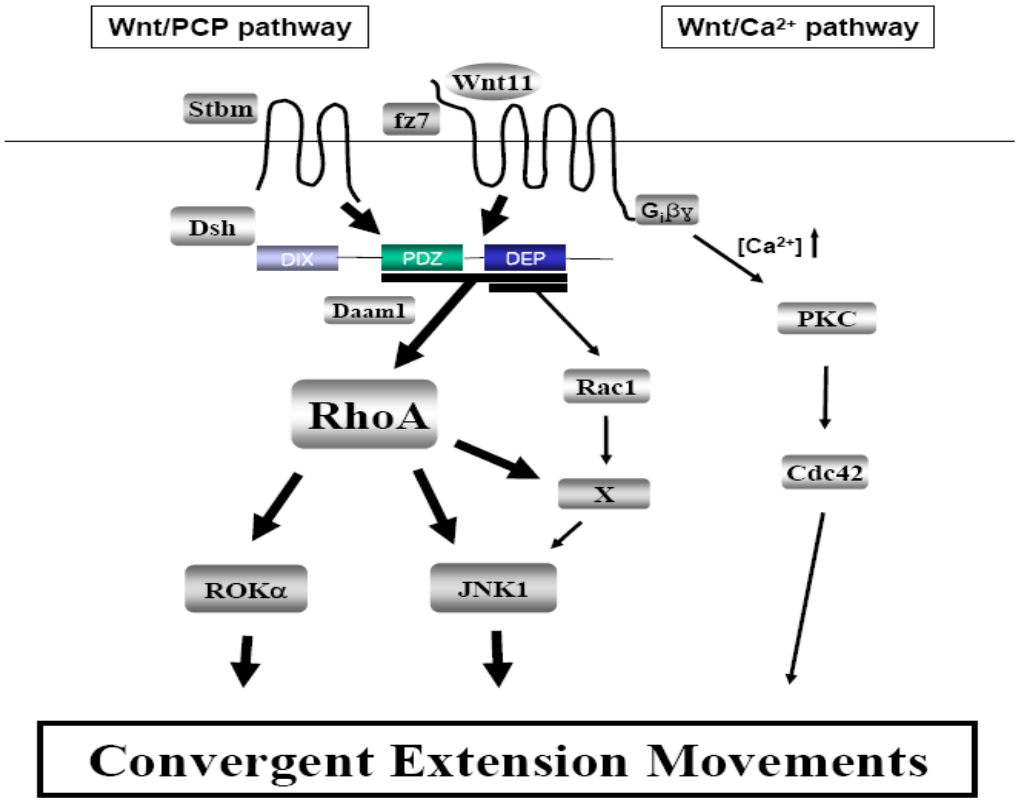

Figure 8. Schematic representation of Non-canonical Wnt signaling. The two non-canonical Wnt pathways are mediated by the interaction of Wnt with Fz alone, without any interaction with LRP receptors. In the *Wnt-PCP* pathway, Fz recruits the protein Dsh which in turn interacts with Daam1 in order to elicit the signalization cascade of RhoA and the activation of ROKα and JNK1. Fz activation can also act in a Daam1independent way and activate Rac1: this cascade leads to the activation of JNK1and its downstream effectors.. The second non canonical pathway is known as Wnt-Ca^+ pathway: the interaction of Wnt with Fz is able to elicit intracellular release of Ca^+ that activates PKC cascade. These pathways (PCP signaling and Wnt-Ca^+) are known to modulate the convergent extension movements during embryogenesis.

Picture adapted from http://www.postech.ac.kr/life/DB/%B0%C7%C8%AD-1.htm

Bone Morphogenic Proteins (BMPs) signaling pathways

BMPs (Bone morphogenic proteins) are a subgroup of growth factors belonging to the TGF-β superfamily, except for BMP1 that is a metalloprotease. BMPs were originally discovered by their ability to induce the formation of bone and cartilage (Urist, 1965). Nowadays, a more precise knowledge of BMPs functions pointed out their important morphogenetic functions during embryonic development. The BMP signalling is mediated by the interaction of BMP proteins with BMP receptors type I and type II. These two groups of receptors are composed by serine/threonine kinase receptors. The BMPR class II is composed by three types of proteins that share similar structures: BMP type II receptor (BMPR-II), Activin type II receptor (ActR-II) and Activin type IIb receptor (ActR-IIb). All the members of these receptor subgroups can interact with all the different BMPs. The BMPR class I is composed by seven members of Activin receptor-like kinase (Alk1 to Alk7). These receprtors show different affinity for the TGFβ-BMPs ligands: in particular, BMPs bind to the receptors Alk1 Alk2, Alk3 and Alk6 with different specificity, whereas the other receptors of the group are involved specifically in the TGFβ signaling pathway (reviewed in (Miyazono et al., 2010)) (figure 9).

The binding of BMPs to the BMPR type II allows its heterodimerisation with the type I receptor. This heterodimerisation promotes the phosphorylation of Gly-Ser (GS) domain of the intracellular part of the type I receptor, via the constitutively active serine/threonine kinase present on type II receptor. This type I receptor phosphorylation leads to the activation of its own kinase. Therefore, intracellular specificity of the signal is dictated by the type I intracellular domain: the activated type I receptor kinase propagate the signal by phosphorylating proteins of the Smad family transcription factors. In mammals, eight different Smad proteins are identified: Smad1, Smad5 and Smad8 are receptor-regulated Smads (R-Smad) involved in the transmission of BMPR signaling whereas Smad2 and Smad3 are involved in TGFβ specific pathways. Smad4 is a Co-Smad, common to both pathways, whereas Smad6 and Smad7 fulfill inhibitory functions (I-Smad). Structurally, all the Smad family members share a highly conserved Mad homology domain in N-terminal region (MH2), whereas a second Mad homology domain (MH1) is conserved only in R-Smad and Co-Smad. MH2 domain is responsible for interaction with type I BMPR, dimerization with other Smads and activation of transcription, whereas MH1 is responsible for DNA binding (reviewed in (Miyazono et al., 2005)). In the absence of phosphorylation, MH1 and MH2 are

folded together by a linker of variable amino acids length: the inactive conformation of R-Smad cannot dimerize with other Smads and it is anchored to the membrane via transmembrane proteins as SARA (Qin et al., 2002).

R-Smads have a characteristic Ser-Ser-Val/Met-Ser (SSXS) sequence at their C-terminal part, through which they can transiently and directly interact with activated type I receptors: the activated kinase in the intracellular N-terminal of BMPR-I phosphorylates the SSXS sequence, disrupting the MH1-MH2 bridge. This disruption allows R-Smads to form hetero-oligo dimers that are translocated into the nucleus via interaction via Co-Smad (Qin et al., 2001). In the nucleus, Smad complex can bind gene promoter regions and interact with other DNA binding proteins, Co-activator/repressor, in order to modulate downstream target gene expression (reviewed in (Miyazono et al., 2010)).

The I-Smads negatively control the Smad intracellular signaling: Smad6 preferentially inhibits the BMP signaling, whereas Smad7 is involved in both TGFβ-BMP signaling pathways inhibition via different mechanisms (figure 10). The first mechanism of regulation involves the capacity of I-Smad to interact directly with R-Smads, inhibiting their heterodimerization with Co-Smad and the subsequent translocation in the nucleus. On the other hand, I-Smad can directly degrade BMPR by interacting with the Smurf proteins. Smurf1 and Smurf2 proteins are members of HECT type E3 ligase, known to directly regulate the R-Smad cellular pool (Zhang et al., 2001). In the nucleus, Smurf proteins can also bind to I-Smad, and translocate outside the nucleus. The complex Smurf/I-Smad directly targets the active BMPR type I and promote its ubiquitination and proteasome-dependent degradation (Horiki et al., 2004). In addition to Smurf driven degradation, the I-Smad can negatively regulate the BMPR signaling via protein phosphatase-1 (PP1): I-Smad, in fact, interacts with a regulatory subunit of PP1, recruiting the catalytic domain (PP1c) to dephosphorylate and silence the active BMPR type I (Shi et al., 2004). The I-Smads are modulated by Arkadia-mediated dowregulation. The expression of this RING type ligase is downregulated by TGFβ, suggesting a negative feedback control of TGFβ on Smad signaling. Contrary to Smurf complex, Arkadia does not interact with the BMPR type I when engaged by Smad7, but it elicit the ubiquitin-depend degradation of Smad7 that can not anymore play is role in the control of TGFβ-BMP signaling (Koinuma et al., 2003).

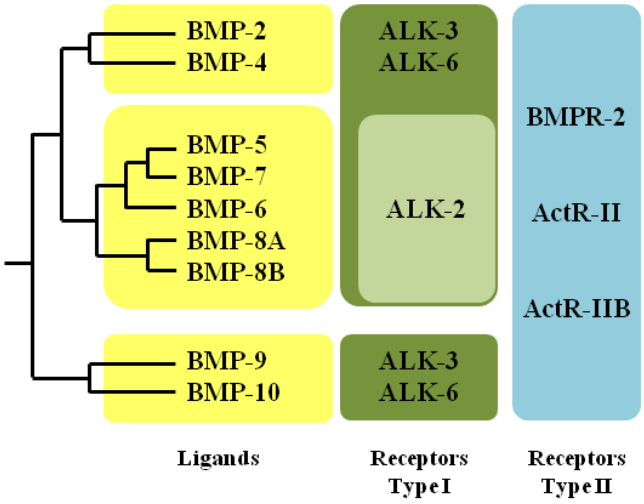

Figure 9. Schematic representation of BMPs family. The bone morphogenic proteins can be subdivided in three major groups according to their homology degree: BMP2 and 4 belongs to the first group, BMP5 to BMP-8B to the second group, and BMP-9 and 10 form the third group. All the BMPs members are able to bind to type II receptors (BMPRII, ActR-II and ActR-IIB). In the type I group, ALK2 can be bound only by the second group of BMP members, i.e. BMP5 to BMP8B. (Modified from (Miyazono et al., 2010))

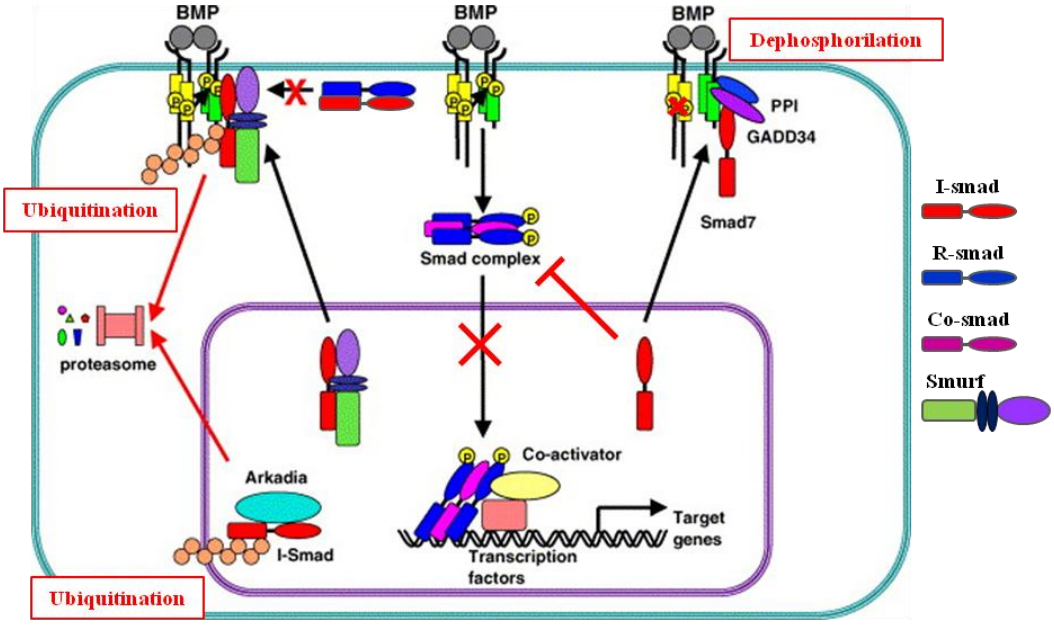

Figure 10. Schematic representation of Smad signaling modulation by I-Smad. The inhibitory Smads can regulate the intracellular signaling in several ways: they can either dephosphorylate directly the receptor or degrade it via Smurf ubiquitination. The I-Smad can also interfere in the interaction R-Smad/Co-Smad and block the nuclear translocation of this complex. In addition, I-Smad directly interferes with R-Smad phosphorylation at the membrane. In the nucleus, the I-Smad are modulated by Arkadia (Modified from (Miyazono et al., 2010)).

Fibroblast Growth Factor (FGF) signaling pathway

Fibroblast Growth Factors (FGFs) and their specific cell surface receptors (FGFR) make up a large and complex family of signaling molecules that have been shown to play an important role in several crucial processes ranging from embryonic development to tissue homeostasis: the importance of this pathway is underlined by its role in a wide range of organisms, from the nematode to the human. In vertebrates, FGFs family counts 22 members, whose molecular weight varies from 17 to 34 kDa. These members share a high affinity for heparin or heparan sulfate proteoglycan and are composed by a central domain of 28 highly conserved amino acids: among them, six amino acids residues are identical in all the FGF members and are in charge of the interaction with FGFRs (Plotnikov et al., 2000). These proteins are almost all readily secreted molecules even if some of them (FGF9, FGF16 and FGF20) lack the amino-terminal sequence peptide, common to the other members. On the contrary FGF1 and FGF2 are not secreted, but released from damaged cells in exocytotic mechanism independent from endoplasmic/Golgi reticulum pathways (Mignatti et al., 1992). The signaling of the FGFs family members passes through their interaction with four high related members of tyrosine/kinase (RTKs) receptors.

The fibroblast growth factor receptors (FGFR1 to FGFR4) are composed by a single transmembrane domain that links the extracellular globular portion, in charge of ligand binding, with the intracellular domain that contains the tyrosine kinase activity domain. The extracellular domain is composed by three immunoglobulin-like domains (D1-3), a seven to eight acidic residues domain in the linker connecting D1 and D2, designated as "acid box", and finally a conserved positively charged region in D2 that serves as a binding site for heparin (reviewed in (Schlessinger et al., 2000)).

It is hypothesized that the acid box can participate to the inhibition of the FGFR auto induction. The multiple acidic sites carried by the acid box can mimic the negative potential surface of heparin-like compounds. Binding of the acid box to the heparin-binding sites on the D2 region of the FGF receptor leads to a 3D compacted conformation of D1 on D2, without initiating a biological response (figure 11). A peculiar characteristic of the FGFR family is that alternative splicing of FGFR transcripts generates a variety of FGFR isoforms: the different FGFR isoforms include receptors with extracellular domain composed of either two or three immunoglobulin-like domains or soluble secreted FGFR forms. In addition, alternative splicing in the D3 domain can profoundly modify the ligand-binding specificity

(reviewed in (Mohammadi et al., 2005)). Ligand-induced receptor dimerization is a prerequisite for PTK activation. Receptor dimerization brings the cytoplasmic domains of the receptors in close vicinity one to the other. This provides the opportunity for receptor *trans*-autophosphorylation, subsequent tyrosine kinase activation and initiation of downstream signaling pathways. The heparan sulfate (HS) proteoglycans have a very important role in the ligand-receptor interaction: in the inactive form of the receptor, the heparin is bound to a specific part of the D2 domain, preventing the juxtaposition of intracellular tyrosine kinase domain of adjacent receptors. The asymmetric binding of FGFs with D2-D3 receptor domains leads to their dimerization and the modification of heparin interaction: the heparin is reoriented by the binding of the ligand and stabilized by the receptor new conformation (Uematsu et al., 2000).

Once the receptor is activated, multiple tyrosines on its intracellular domain are phosphorylated by the intrinsic tyrosine kinase. These phosphorylated tyrosines allow the docking of regulatory proteins implicated in different intracellular signaling cascades (reviewed in (Eswarakumar et al., 2005)) (figure 12). One of the most studied and characterized pathway activated by FGF involves the docking of the protein FRS2α that serves as core for the assembling of Shp2-Grb2-GAB1 activating complex. On one hand, via the recruitment of the transmembrane guanine nucleotide exchange factor SOS, this complex is able to activate Ras and the downstream effectors of MAP kinase: these latter proteins regulate the activity of downstream kinases (as ERKs, P38 and JNKs families) or modulate the action of transcription factors. On the other hand, the FRS2α complex is also able to promote the anti-apoptotic pathways via AKT activation: the P-I-3 kinase signaling cascade activation leads to PDK dependent activation of AKT that is able to block or silence apoptotic effectors like Caspase9, FKHR and BAD (reviewed in (Schlessinger et al., 2000)). Another pathway mediated by the FGFR activation is the modulation of the cytoskeletal organization via PLCγ: the phospho tyrosine kinase part of the FGFRc can dock and activate PLCγ, that will hydrolize Pt-Ins-(4-5)P2 to form diacylglycerol (DAG) and Inositol triphosphate. Ins-(1-4-5)P3 release will stimulate intracellular calcium release and calcium-calmodulin dependent protein kinase activation. Finally, in some cell types, specific proteins (i.e. Src or Shc) are directly recruited to the active phosphorylation sites where they are, in turn, activated by addition of phosphate groups.

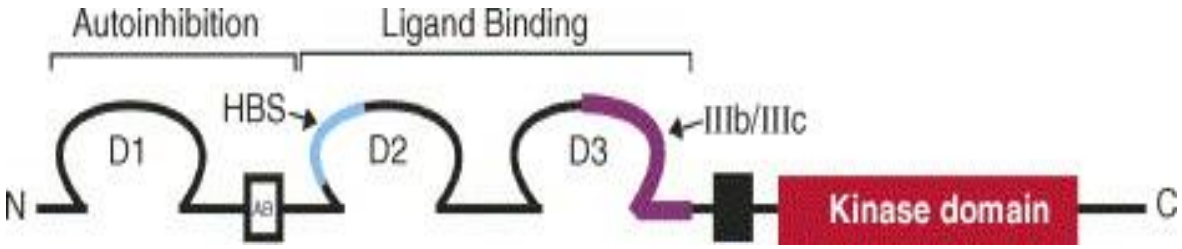

Figure 11. Structure of FGF receptors. FGFR are transmembrane receptors that are composed by an intracellular kinase domain and three conserved globular extracellular domains (D1-D3): the D1 and D2 domains are involved in the ligand binding, whereas the D1 and the acid box AB between D1 and D2 are responsible for the auto-inhibitory function. In the absence of the ligand, the D1 domain is folded on the HBS site, maintaining the receptor in a closed conformation. The binding of the ligand opens this conformation, which is stabilized by heparan sulfate interaction, via the Heparan binding site (HBS) in the domain D2. Different isoforms of the receptors have been described: as an example, different isoforms of the D3 domain of FGFR2 give rise to FGFR2-IIIb and FGFR2-IIIC (Mohammadi et al., 2005).

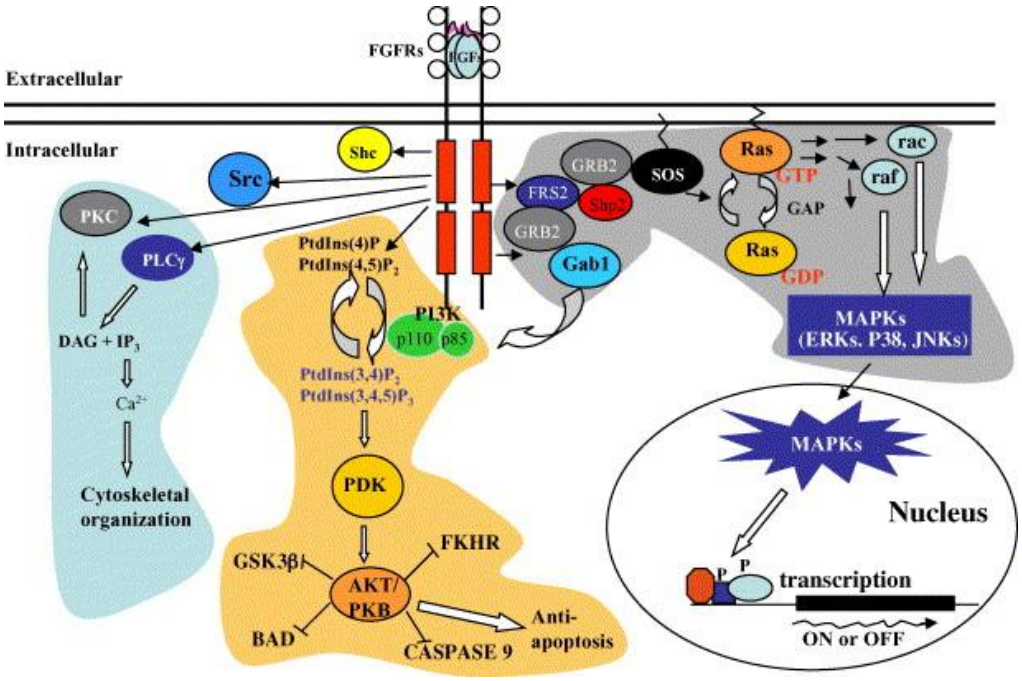

Figure 12. Schematic representation of FGF intracellular signal transduction. Activated FGFRs (red rectangles) can activate PLCγ cascade pathway (blue highlight) modulating the cytoskeletal organization, the P-I-3 Kinase-AKT/PKB pathway (yellow highlight) to elicit the cell surviving program and the FRS2-Ras-MAP kinase pathway (grey highlight). The activated MAP kinases (ERKs, p38, or JNKs) translocate into the nucleus where they phosphorylate specific transcription factors, regulating target genes expression (Dailey et al., 2005).

Introduction III

III. Kidney development

In human, renal morphogenesis is a tightly controlled process that starts with the specification of a condensed cluster of cells in the intermediate mesoderm, the metanephric mesenchyme. This structure will lead to the formation of a definitive kidney, composed by more than 40 different cell types. These cell types acquire during organogenesis a complex spatial organization and activate the expression of a peculiar subset of genes which is crucial for kidney functions. Kidney development is a morphogenetic process controlled mostly at the transcriptional level. A complex network of transcription factors regulate the expression of effectors of several signaling pathways that interact or act successively in a complex spatio-temporal process.

In mammals, kidney development is based on the formation of three successive structures: the pro-, meso- and metanephros (figure 13). The first two are transient structures, whereas the third one will give rise to the definitive kidney (figure 13). All these structures derive from a common nephrogenic territory in the intermediate mesoderm. They develop successively following a rostro-caudal pattern, the pronephros being the most rostral. During evolution, all these successive embryonic renal structures have been adopted to play a functional role. The pronephros is the functional kidney in the amphibious tadpole and in the fish larvae. The study of pronephros development in these animals has been very useful to identify some crucial genes involved in kidney development in mammals. In fact, the molecular mechanisms at the basis of the formation of this rudimentary kidney are conserved through evolution in different species (Drummond and Davidson, 2010). The mesonephros is the functional kidney for adult fishes and frogs, whereas in mammals this structure is able to perform some blood filtration, but it is functional only during a short period of time and rapidly degenerates. Only few vestigial tubular structures derived from the mesonephros are involved in the development of the male reproductive system. The metanephros is a much more complex organ, based on branching morphogenesis and it develops only in amniotes (mammals birds and reptiles), (reviewed in (Joseph et al., 2009)).

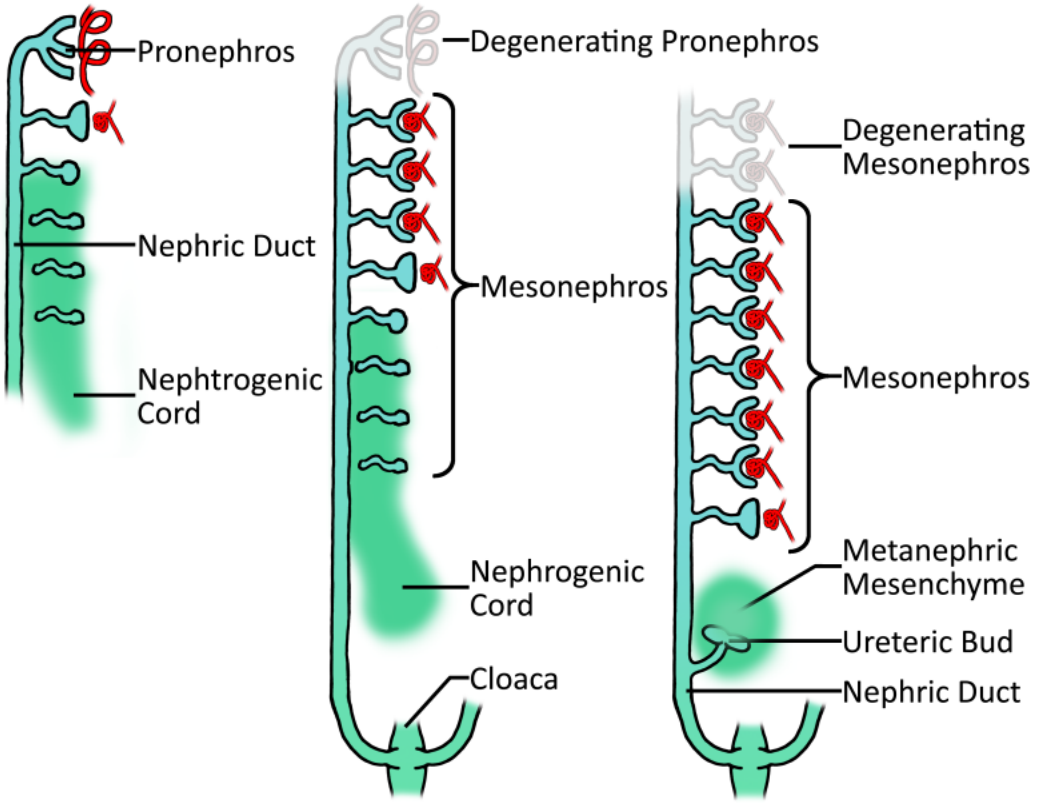

Figure 13. Schematic representation of kidney development during embryogenesis in mammals. Temporal succession of three structures during kidney morphogenesis: the pronephros, on the left, and the mesonephros, in the center, are transient organs that disappear when the definitive metanephros on the right starts to develop (adapted from (Sawle A, 2009)).

III.1 Pronephros and mesonephros

Morphology

During gastrulation, multipotent cells migrate from the primitive streak to form the endodermal and mesodermal layers (figure 14). The mesoderm is composed by paraxial mesoderm, intermediate mesoderm at the origin of the nephric field and lateral plate mesoderm. Intermediate mesoderm is further specified by dorsal-ventral gradient expression of morphogen proteins, such as the Bone Morphogenic Proteins (BMPs), and by signals from the paraxial mesoderm (De Robertis and Kuroda, 2004). In the mouse, at the 8^{th} day of embryonic development (around 3 weeks of human embryo development), a small cluster of cells, located around the 5^{th} and 6^{th} somites, generates the nephrogenic cord. Part of these cells undergo an epithelialisation process and form the primary nephric duct (ND), also known as Wolffian Duct (WD), that begins to elongate caudally. At the same time, some clusters of cells in the intermediate mesoderm facing the nephric duct start to condense to form tubules. The few pronephric tubules connect to the nephric duct to form the pronephros. In mouse embryos, in a matter of days, this first renal structure undergoes rapidly a massive apoptosis and degenerates around 12 days of gestation, reviewed in (Dressler, 2006).

After the formation of the pronephros, the more caudal part of the nephric duct continues to elongate in parallel with the migration of the nephric cord that will give rise to the mesonephric mesenchyme. This event takes place at 9 days of gestation in the mouse and 3.5 weeks in the human.

The mesonephros, located more caudally in respect to the pronephros (between somites 10-17) (Smith and Mackay, 1991) is composed by two different populations of tubules derived from the condensation of the mesonephric mesenchyme: they can be divided in cranial and caudal tubules (Sainio et al., 1997a). The cranial tubules are in number of 4-6 and they are formed by rudimentary glomeruli and short tubular structures. These tubules are directly connected to the Wolffian Duct (WD) by a short connecting portion derived from the nephric duct (Mugford et al., 2008a), (Brenner-Anantharam et al., 2007). In contrast, the caudal tubules (in number of 10-12) derive only from the nephrogenic mesenchyme and do not contact the WD. They are formed by condensation of cells that undergo mesenchymal-to-epithelial transition, forming the typical nephron precursors. The aggregates initially condense in “renal vesicles” and they rearrange until they assume the typical shape of “sigma-shaped bodies (S-shaped body)” (Smith and Mackay, 1991). However, the mesonephros is not able to

develop further and begins to degenerate by E14.5. The tubules disappear starting from the caudal to the cranial ones in 24 hours (Sainio et al., 1997a). In the male, some cranial tubules are maintained in the adult and they are part of the epididymis (Joseph et al., 2009).

Molecular mechanisms

A few genes have been identified to play a role in pronephros formation in vertebrates. Among them, in mouse, *Osr1* (Odd skipped related 1) and *Lhx1*, two transcription factors are expressed in the lateral mesoderm just after gastrulation. This territory is broader than the intermediate mesoderm, and progressively, the expression pattern of *Lhx1*, and to a lesser extent, of *Osr1* become restricted to the intermediate mesoderm around E8.5.

At this stage, the two paired-box homeotic transcription factors *Pax2* and *Pax8* start to be expressed in few cells of the intermediate mesoderm. These two factors represent the first markers of the nephric field (Bouchard et al., 2002). They are expressed both in the nephrogenic cord and in the nephric duct, an epithelial structure that form in the intermediate mesoderm. In mouse, the inactivation of *Pax8* doesn't affect the kidney development (Mansouri et al., 1998), whereas the absence of *Pax2* leads to a degeneration of the nephric duct that is not able to reach the urogenital sinus (Torres et al., 1995). Interestingly, in double *Pax2*/*Pax8* mutants, the nephric duct fails to form and the intermediate mesoderm undergoes a massive apoptosis (Bouchard et al., 2002). *Gata3* is a transcription factor whose expression has been shown to be controlled by *Pax2* and *Pax8*. Its expression pattern is restricted to the nephric duct. Inactivation of *Gata3* leads to morphogenic abnormalities in the mesonephros formation and to the absence of metanephros development due to a defective elongation of the nephric duct (Grote et al., 2006),(Pedersen et al., 2005). In the same way, inactivation of *Lhx1* leads to kidney agenesis, linked to a defective elongation and survival of the nephric duct. {Shawlot, 1995 #3131}(table1). In addition, *Lhx1* inactivation in early stage of gastrulation leads to severe defect in intermediate mesoderm differentiation (Tsang et al., 2000). Inactivation of *Osr1*, which is expressed only in the nephrogenic cord and is excluded from the nephric duct, leads to defective mesonephric tubule formation and absence of metanephric differentiation (James et al., 2006).

During pronephros formation, the epithelial derivatives emanating from the nephrogenic cord and the nephric duct form independently. On the contrary, the development of mesonephric tubules is due to the induction of the mesonephric blastema by inductive signals send by the nephric duct. *Wnt9b* encodes a member of the Wnt family signaling

molecules secreted by the nephric duct. Interestingly, the mutants lacking *Wnt9b* show also defective mesonephric tubules and metanephric nephrons formation (Carroll et al., 2005), suggesting a common mechanism of formation of epithelial derivatives from the mesonephric and metanephric mesenchymes. Several other genes involved in the mesonephros development play also a role in metanephric development, including the transcription factors *Pax2*, *Wt1*, *Osr1* and *Six1* and they will be discussed in detail later. Inactivation of these transcription factors leads to variable defects, ranging from total mesonephros agenesis (*Pax2* inactivation) or defective mesonephric tubules formation (*Wt1*, *Osr1* and *Six1* mutants) (Torres et al., 1995),(Sainio et al., 1997a),(James et al., 2006),(Mugford et al., 2008b).

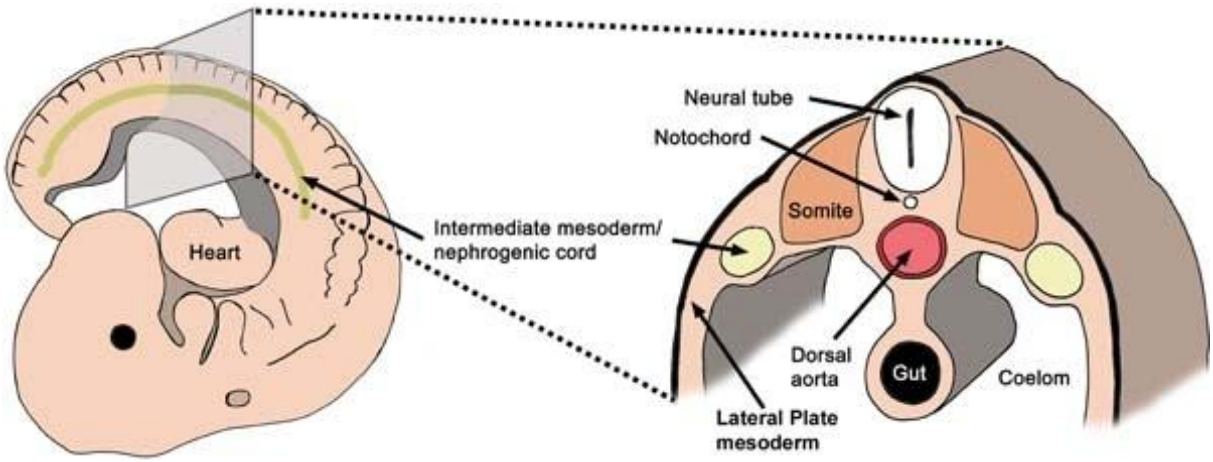

Figure 14. Schematic representation of intermediate mesoderm position. Lateral and transversal section of the mouse embryo showing the position of the nephrogenic cord (intermediate mesoderm) in respect of body axis (on the left) and of the other embryonic layers (on the right) (Davidson, 2008).

Table 1. Summary of the principle actors implicated in the nephric duct development in the mouse

Function	Gene involved	Malformation	Ref.
Nephric duct formation and elongation	**Pax2**	- Abortive ND elongation and degeneration	(Torres et al., 1995)
	Pax2/Pax8	- Absence of ND formation - Defect in epithelialization of ND	(Bouchard et al., 2002)
	Gata3	- Defective elongation of ND - Formation of ectopic NDs	(Grote et al., 2006)
	Lhx1	- Impaired ND extension - Absence of IM differentiation	(Pedersen et al., 2005) {Shawlot, 1995 #3131} (Tsang et al., 2000)

III.2 Metanephros Development

In mammals, the metanephros is the last and definitive kidney: it is a much more complex organ compared to the previous pro- and mesonephros. Evolutionary, the metanephros appeared when animals had to adapt to terrestrial life. The complex organization of the metanephros provides the capacity of efficient water reabsorption. In addition, metanephros structural modifications have been selected depending on the external environment. For example, small rodents that live in desertic areas have developed very long Henle's loops. This anatomical particularity confers to these rodents the capacity to concentrate very efficiently their urine.

The metanephros is formed mainly by the interaction between two different compartments: the ureteric bud, derived from the epithelial nephric duct, and the metanephric mesenchyme, a structure that differentiates from the intermediate mesoderm (Shah et al., 2009).

Metanephric mesenchyme identity.

The metanephric mesenchyme is a sub territory of the intermediate mesoderm that is characterized by the expression of a specific set of genes, whose expression can be partially activated even in the absence of the nephric duct elongation (Grote et al., 2006). The correct differentiation of this territory is crucial for the invasion of the ureteric bud, the first step of metanephros morphogenesis. This event occurs around E10.5 in the mouse and at five weeks of gestation in the human. Several genes has been demonstrated to have a crucial role in the metanephric mesenchyme specification and survival including *Alk3, COUP-TFII*, *Osr1*, *Eya1*, *Sall1*, *Wt1*, *Six1-4*, and the *Hox11* paralogous family (*Hoxa11*, *Hoxc11* and *Hoxd11*) (table 2). All these genes are important for the expression of *Gdnf*, a crucial molecule for the outgrowth of the ureteric bud (figure 15). I will discuss briefly the role of these different genes in the following paragraphs.

A very important role of the BMP signaling in the metanephric mesenchyme has been recently demonstrated by the selective inactivation in this territory of the receptor *Activin like Kinase 3* (*Alk3*). This receptor starts to be expressed at E9.5 in the nephric field in the intermediate mesoderm (Mishina et al., 1995), (Hartwig et al., 2008). The Rarb2-Cre inactivation of *Alk3* in the nephrogenic field leads to hypoplasia, characterized by a reduced number of normally developed nephrons. This defect is due to the reduction of the nephrogenic and mesenchymal precursor cells in the metanephric mesenchyme that lacks *Alk3*. This defect is correlated to the decreased expression of *Osr1,* one of the earliest marker of nephrogenic commitment in the intermediate mesenchyme (Di Giovanni et al., 2011).

Odd-skipped related1 (*Osr1)* encodes a zinc-finger transcription factor that is already expressed in some mesodermal cells just after their migration from the primitive streak (Wang et al., 2005a). Later on, it is restricted to the commited metanephric mesenchyme and is not expressed in the nephric duct (So and Danielian, 1999). Embryos lacking *Osr1* suffer from an absence of metanephric mesenchyme differentiation leading to renal agenesis. The metanephric mesenchymal cells lacking *Osr1* do not express *Eya1* and *Pax2* and show a drastic downregulation of *Wilm's tumor suppressor1 (Wt1)* expression (James et al., 2006), (Wang et al., 2005b). Since *Wt1* expression is necessary for metanephric mesenchyme cell survival, its downregulation in absence of *Osr1* causes a massive increase of apoptosis in the metanephric blastema (Donovan et al., 1999), (Davies et al., 2004).

Recent studies have defined the role of the orphan nuclear receptor Chicken Ovalbumin Upstream transcription factor II (*COUP-TFII*) in metanephric mesenchyme specification. During kidney development, it is expressed specifically in the nephrogenic field since E9.5 and later on in the metanephric mesenchyme and in the developing nephrons. The inactivation of COUP-TFII does not affect the mesonephros development, but it leads to the absence of all markers of metanephric mesenchyme specification (*Eya1, Pax2, Six2 and Gdnf*). COUP-TFII has been shown to directly regulate the expression of *Eya1* and *Six2* in an *Osr1*-independent way, suggesting an interaction between these two factors in the first steps of metanephric mesenchyme specification. Similarly, COUP-TFII is also able to control the expression of *Wt1* in order to maintain the metanephric mesenchyme survival (Yu et al., 2012a).

Eya-absent1 (Eya1) encodes a co-activator that can induce the transcription of target genes via its interaction with transcription factors (Jemc and Rebay, 2007). During kidney morphogenesis, *Eya1* expression is restricted to the metanephric mesenchyme around E11.5. Its expression is regulated by *COUP-TFII* and *Osr1* (Yu et al., 2012a), (Sajithlal et al., 2005). The inactivation of *Eya1* leads to the absence of *Pax2*, *Six2* and *Gdnf* expression accompanied by a significant apoptosis of the metanephric blastema (Xu et al., 1999). *Eya1* has been sown to regulate the expression of *Gdnf* via the interaction with *Hox11* members and *Pax2* (Gong et al., 2007). In addition, EYA1 is known to interact with the SIX family members in gene regulation (Ohto et al., 1999) and Chip experiments have shown that EYA1 and SIX1 are present on regulatory sequences of *Gdnf*. These results suggest an interaction between EYA1/SIX1 in the direct control of *Gdnf* expression. Thus, EYA1 acts, through different pathways, as a key co-activator of the metanephric mesenchyme differentiation and a regulator of *Gdnf* expression.

Hox genes have been recognized since a long time as important regulators during embryonic development. In the kidney, three paralogous members of *Hox11* (*Hoxa11*, *Hoxb11* and *Hoxc11*) play a role in the activation of the expression of crucial genes in the metanephric mesenchyme. Single inactivation experiments of *Hoxa11* and *Hoxb11* did not display any overt phenotype. On the contrary, the double inactivation of these two genes shows a renal phenotype of variable penetrance. In the double mutant animals, the ureteric bud emerges normally but, later on, it shows a defective and reduced number of branching events with a reduced expression of several genes implicated in this process (Patterson et al., 2001). As expected, the triple inactivation of the *Hox11* paralogous genes showed a more drastic kidney phenotype. The triple mutants have no kidneys due to the defective expression of *Six2* and *Gdnf* genes. Molecular analysis of the different transcriptional cascades during metanephric early development elucidated the role of the *Hox11* genes in *Six2* and *Gdnf* expression via their interaction with EYA1 and PAX2 (Wellik et al., 2002).

The *Sine-oculis* (*Six*) family is composed by homeobox transcription factors and some of these factors are directly involved in the metanephric differentiation. In particular, *Six1* and *Six4* are expressed in metanephric mesenchyme territory since E9.5. *Six1* deficient embryos suffer from renal agenesis due to a defective ureteric bud elongation into the metanephric mesenchyme. This defective mesenchyme still express *Wt1*, *Eya1* and *Gdnf* but is characterized by the downregulation of key genes such as *Pax2, Sall1* and *Six2* (Xu et al., 2003), (Kobayashi et al., 2007). More recently it has been shown that *Six1* controls also the expression of *Gremlin1*, involved in the outgrowth of the ureteric bud, as we will see in detail later (Nie et al., 2011). Inactivation of *Six4* does not show any obvious renal malformation, but *Six1*/*Six4* double inactivation is responsible for a more severe metanephric mesenchymal defect compare to the *Six1* inactivation alone. Double mutant embryos totally lack the expression of *Pax2*, *Six2*, *Gdnf* and *Pax8* in the metanephric domain that, however, still expresses *Wt1* and *Osr1* (Kobayashi et al., 2007).

Wilm's tumor suppressor-1 (*Wt1*) is a transcription factor expressed in the intermediate mesoderm since day E9.5 and it is restricted to the uninduced metanephric mesenchyme around E10.5. Later on, it is expressed in the condensed metanephric mesenchyme around the ureteric bud tip and it remains expressed in the podocyte precursors (Armstrong et al., 1993). Germline inactivation of *Wt1* is lethal during embryogenesis, mainly due to heart malformation (Kreidberg et al., 1993). In addition, mutant embryos suffer from kidney agenesis, due to the absence of ureteric bud emergence. In these embryos, despite normal levels of *Pax2*, *Gdnf* and *Six2,* the uninduced metanephric undergoes massive apoptosis. This observation suggests a role of Wt1 as an autonomous signal for metanephric mesenchyme survival (Kreidberg et al., 1993). siRNA inactivation of *Wt1* in metanephroi organ culture and animals carrying a BAC transgene that partially rescue the *Wt1* functions showed a drastic block of in the ureteric bud branching process and the absence of mesenchymal to epithelial transition (Davies et al., 2004), (Moore et al., 1999).

Table 2. Summary of the principal actors implicated in metanephric mesenchyme specification in the mouse

Function	Gene involved	Malformation	Ref.
Matanephric mesenchyme Specification-differentiation	**Alk3**	- Renal hypoplasia, reduction of nephrogenic cells pool	(Di Giovanni et al., 2011)
	Osr1	- Absence of MM specification - Renal agenesis	(James et al., 2006) (Wang et al., 2005b)
	COUP-TFII	- Defective MM specification	(Yu et al., 2012a)
	Eya	- Defective MM specification - Apoptotic MM	(Xu et al., 1999) (Gong et al., 2007)
	Six1	- Defective expression of MM differentiation markers	(Xu et al., 2003) (Kobayashi et al., 2007)
	Six1/4	- Lack of MM markers that are only downregulated in Six1 mutants	(Kobayashi et al., 2007)
	Wt1	- Degeneration by apoptosis of specified MM	(Kreidberg et al., 1993)

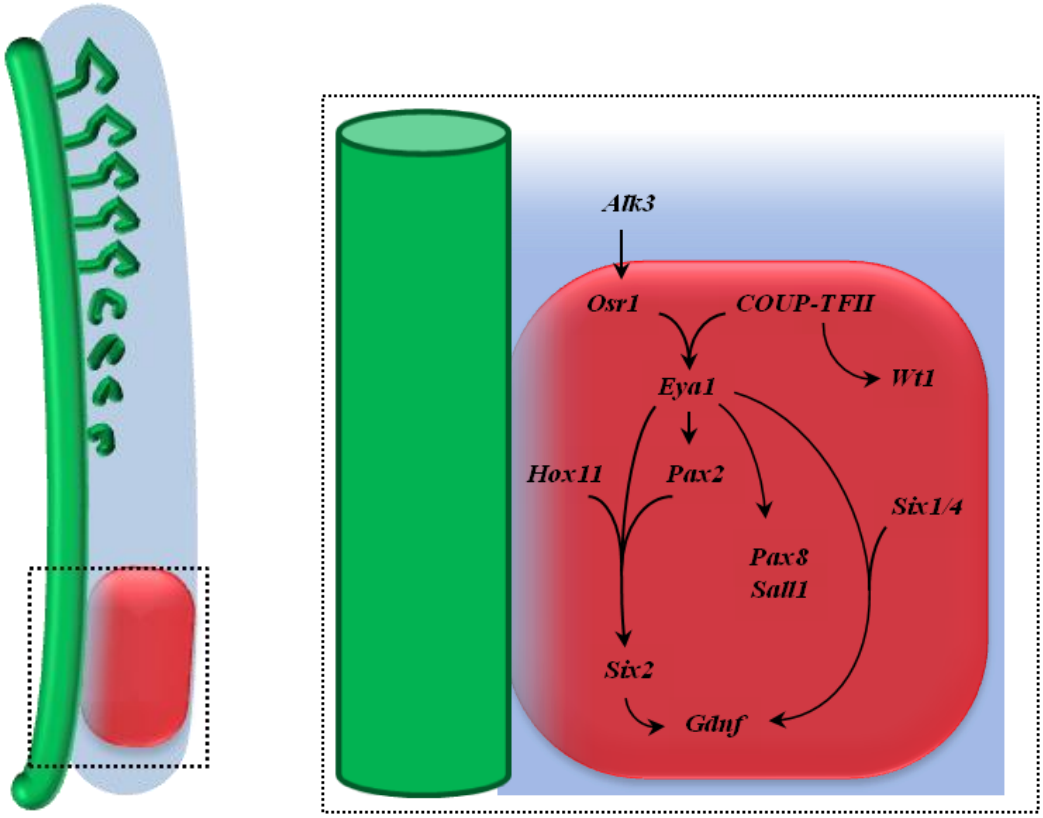

Figure 15. A model of epistatic interactions between transcription factors during early metanephric mesenchyme differentiation. The localization of the metanephric mesenchyme (red) in the nephrogenic field (light blue) in respect to the Wolffian duct is showed on the left panel. The right panel shows the potential interaction of early transcription factors in the metanephric mesenchyme differentiation

The emergence of the ureteric bud.

Once the metanephric mesenchyme identity has been determined, the second key event of metanephros formation occurs around E10.5 in mouse. The portion of the Wolffian duct facing the metanephric territory starts a process that leads to the outgrowth of the ureteric bud and its invasion into the metanephric mesenchyme.

The emergence of the ureteric bud is a tightly regulated process (figure 16). First, the metanephric mesenchyme facing the emergence needs to be properly positioned to provide diffusible molecules necessary for this process. Secondly, a combination of several pathways restricts the emergence of the UB to a unique event at the correct place (table 3). The most important inducer of the ureteric bud emergence and the successive branching process is the *Glial-cell-line Derived Neurotrophic Factor* (GDNF). GDNF is a soluble factor specifically expressed in the metanephric mesenchyme from E8.5. This growth factor binds and activates on the surface of the nephric duct cells, a tyrosine kinase membrane receptor called c-RET, coupled with the co-receptor Gfrα1 (Shakya et al., 2005). Alterations in the GDNF/RET signaling pathway may lead to the absence of ureteric bud emergence (reviewed in (Costantini and Shakya, 2006)). The activation of GDNF/RET signaling modifies the expression of several genes in the ureteric bud. The first consequence is the onset of a positive feedback loop: the GDNF/RET signaling increases the expression of *Wnt11* in the nephric duct. WNT11 in turn will diffuse in the mesenchyme to maintain a high expression of *Gdnf* (Pepicelli et al., 1997). This positive feedback loop is maintained all along the branching process of the ureteric bud, allowing a significant source of GDNF to be delivered to the ureteric bud tip cells. Another pathway downstream of RET involves the PI3-kinase dependent regulation of *Etv4* and *Etv5*. These two genes are part of the Ets transcription factors family. The inactivation of Etv4/5 in animal models showed either renal agenesis or dysplasia, secondary to a defective ureteric bud branching (Lu et al., 2009). The deficient ureteric bud tip is affected by the downregulation of a particular set of genes. These genes, *CxCr4*, *Myb* and *Mmp14* are involved in migration, proliferation and cell shape modifications. They are responsible for the pseudo stratified organization of the Wolffian duct cells facing the metanephric mesenchyme that precedes the outgrowth of the ureteric bud (Lu et al., 2009). More in detail, in human *CxCr4* is known to be involved in epithelial cell migration (Chi et al., 2009), (Murdoch, 2000); *Myb* is a transcription factor involved in proliferation in several

organs during morphogenesis (Ramsay and Gonda, 2008) and it is expressed in the ureteric bud tips where an active proliferation takes place (Michael and Davies, 2004); *Mmp14,* a member of the metalloproteinase family, is known to play a role in the branching events of the ureteric bud in vitro (Kanwar et al., 1999). One can hypothetize that this protein could play a role in the remodeling of the basal membrane to promote the ureteric bud outgrowth or in the release of bound growth factors in an autocrine/paracrine signaling way.

FgF10, a member of the diffusible Fibroblast Growth Factors family, is expressed in the metanephric mesenchyme since E10.5. It signals to the nephric duct (and later on to the branching ureteric bud) mainly via the receptor FGFR2 (Ohuchi et al., 2000). Inactivation of *Fgf10* does not lead to the drastic phenotype showed by *Gdnf* or *Ret* inactivation. *Fgf10* mutants suffer only from a defective branching pattern of the ureteric bud, comparable to what is observed in animals lacking *Fgfr2* (Zhao et al., 2004). The complementary role of *Fgf10* in the emergence of the ureteric bud has been elucidated studying mouse models carrying homozygous double mutation in *Gdnf-Spry1* or *Ret-Spry1*. In this context, the loss of one allele of *Fgf10* is sufficient to inactivate the ureteric bud outgrowth (Michos et al., 2010). The inductive action of *Fgf10* in absence of GDNF/RET signaling is obtained via its binding to the receptor Fgfr2. This binding activates a downstream pathway common to the one of GNDF/RET signaling. In metanephroi organ cultures, *Etv4* and *Etv5* expression have been shown to be directly activated by exogenous *Fgf10* in a RET independent way (Michos et al., 2010).

Sall1 is a zinc-finger transcription factor, able to act either a repressor or an activator. It is expressed in the metanephric mesenchyme from E10.5 before the ureteric bud outgrowth. The inactivation of *Sall1* leads to renal agenesis due to an abortive emergence of the ureteric bud. *Sall1* deficient metanephric mesenchyme continues to express some markers such as Pax2, Wt1 and Eya1. However, this mesenchyme undergoes a massive apoptosis and *Gdnf* expression is drastically downregulated (Nishinakamura et al., 2001). It has been shown that *Sall1* is essential to modulate β-catenin signaling in the ureteric bud. *Sall1* deficient mutants show an abnormal expression of *Wnt9b* and the β-catenin effector *Axin2* in the tip of the ureteric bud, whereas in the wild type they are restricted exclusively to the stalk, where the branching event is repressed via the stabilization of β-catenin (Kiefer et al., 2010). *Sall1* is absent in *Six1* mutants: in vitro experiments have shown that *Six1* and *Eya1* co-transfection is

able to synergistically activate the promoter of *Sall1*, suggesting that it is directly controlled by the *Eya-Six1* transcriptional complex (Chai et al., 2006).

In parallel with the induction of the ureteric bud outgrowth, its restriction to a unique place involves different mechanisms (table 3). One of these is the spatial restriction of the *Gdnf* expressing territory (metanephric mesenchyme) to a caudal position of the intermediate mesoderm. The signals that control this position involve either a crosstalk between the metanephric mesenchyme and the Wolffian duct (such as *Foxc1/2, Robo2/Slit2, Bmp2*) or genes that are expressed specifically by the nephric duct, such as *Sprouty1* and *Gata3.*

The two members of the forkhead/winged helix family, *Foxc1* and *Foxc2*, are expressed in the intermediate mesoderm since E10.5. Both *Foxc1*$^{+/-}$*/Foxc2*$^{+/-}$ animals and *Foxc1*-null animals show a rostral expansion of *Gdnf -Eya1* territory, that causes ectopic emergence of the ureteric bud and the formation of duplex kidneys (Kume et al., 2000). *Foxc1* may play a role in the cell fate regulation of mesodermal cells along the dorso-ventral axis. The size and the extent of the intermediate mesoderm depend on the balance between dorsalization and ventralization signals. In the *Foxc1* null animals, defective dorsalization signaling leads to a ventral expansion of *Gdnf* territory in the intermediate mesoderm (Kume et al., 2000).

ROBO2, a receptor implicated in axonal guidance, is expressed in the metanephric mesenchyme. Its ligand SLIT2 is, a large secreted molecule expressed in the nephric duct,. Mutations in *Robo* or *Slit2* lead also to an aberrant expansion of the metanephric domain. This rostral expansion is at the origin of the emergence of surnumerary ureteric buds (Grieshammer et al., 2004), as it was described for *Foxc1-Foxc2* mutants.

Heterozygous inactivation of *Bmp4*, a member of the Bone Morphogenic Protein (Bmps) family, leads to an anteriorization of the metanephric blastema (Miyazaki et al., 2000). In addition, *Bmp4* expression in the nephrogenic mesoderm surrounding the nephric duct inhibits ectopic buddings by counteracting the GDNF/WNT11 positive feedback loop. Later on, the inhibitory role of *Bmp4* is conserved during the ureteric bud branching. *Bmp4* expression in the mesenchyme surrounding the ureteric bud stalk prevents it to branch (Miyazaki et al., 2000). The inhibitory function of *Bmp4* is counteracted by its antagonist

Gremlin1 (*Grem1*). This antagonist is a soluble ligand that binds preferentially to BMP4 and BMP2 (Hsu et al., 1998). It is expressed in the mesenchyme surrounding the ureteric bud outgrowth site and around the newly formed tips during the branching process. Its expression is important for the maintenance of *Wnt11* expression in the tips and *Gdnf* in the mesenchyme (Michos et al., 2007). The absence of *Grem1* leads to renal agenesis due to a defective ureteric bud outgrowth (Michos et al., 2004). The importance of controlling *Bmp4* function is reinforced by the recent observation that *Cerberus1* (*Cer1*), another member of secreted BMPs inhibitors, can refine the spatial organization of the ureteric bud tree (Chi et al., 2011).

Gata3 is a transcription factor of the Zinc-finger family, expressed during kidney development in the nephric duct. Its specific inactivation in this compartment leads to ectopic emergence of multiple ureteric buds, giving rise to a variety of urogenital malformations. The mechanisms of extrabudding in this model is quite complex and involves c-Ret/Gdnf and Fgf signalings, and leads to a premature differentiation of nephric duct cells (Grote et al., 2008).

Sprouty (Spry1) is an inhibitor of the c-Ret kinase activity and acts downstream of the GDNF/RET signaling. *Spry1* is expressed mainly in the nephric duct and more faintly in the surrounding mesenchyme (Mason et al., 2006). Inactivation of *Spry1* leads to ectopic emergence of several buds in the Wolffian duct and in the stalk of the ureteric bud. This abnormality is due to the absence of the inhibition of the GDNF/RET signaling along the stalk of the ureteric bud. In fact, mutants lacking *Spry1* show an abnormal persistence of *Wnt11* expression in the trunk (Basson et al., 2005), (Basson et al., 2006). A precise balance between the expression of *Gdnf* and *Spry1* is critical for the correct emergence of the ureteric bud: heterozygous inactivation of *Spry1* (*Spry* $^{+/-}$) is sufficient to rescue the *Gdnf* haplo-insufficiency. Embryos totally lacking either *Spry1-Gdnf* or *Spry1-Ret* do not show anomalies in the emergence of the ureteric bud (Michos et al., 2010). In this context, *Fgf10* replaces the GDNF-RET signaling by activating part of the RET downstream cascade.

Table 3. Summary of the major actors implicated in the ureteric bud (UB) outgrowth

Function	Gene involved	Role and Malformations	Ref.
Induction of ureteric bud emergence	**GDNF**	Renal agenesis due to absence of UB emergence	(Sanchez et al., 1996) (Moore et al., 1996)
	RET	Renal agenesis due to absence of UB emergence	(Schuchardt et al., 1994)
	Gfrα1	Renal agenesis due to absence of UB emergence	(Cacalano et al., 1998) (Enomoto et al., 1998)
	ETV4/5	Abortive UB emergence due to downregulation of genes involved in cell motility	(Lu et al., 2009)
	Sall1	Renal agenesis due to abortive UB emergence	(Nishinakamura et al., 2001)
	Gremlin	Renal agenesis due to absence of UB emergence (lack of Bmp inhibition)	(Nie et al., 2011)
	Fgf10	Secondary role in activation of UB emergence	(Michos et al., 2010)
Restriction of bud emergence	**Foxc1/Foxc2**	Ventralisation of MM and ectopic UB emergences	(Kume et al., 2000)
	Slit2	Expansion of MM and ectopic UB emergences	(Grieshammer et al., 2004)
	Bmp4	Antreriorisation of MM domain and ectopic UB emergences	(Schuchardt et al., 1994)
	Cer1	Aberrant UB emergence pattern	(Chi et al., 2011)
	Gata3	Ectopic emergences of the UB along the Wolffian duct	(Grote et al., 2008)
	Sprouty1	Ectopic emergences of the UB along the Wolffian duct	(Basson et al., 2005) (Basson et al., 2006)

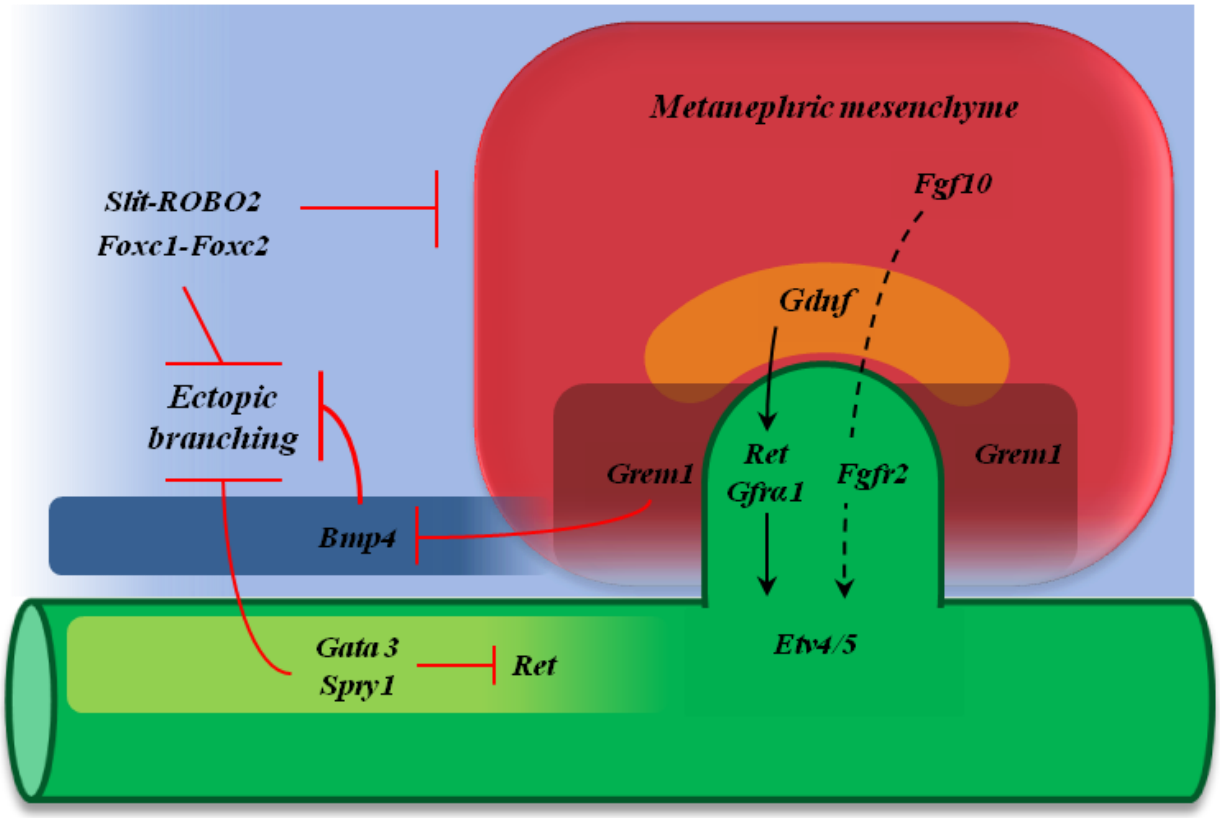

Figure 16. Schematic representation of molecular mechanisms involved in the ureteric bud outgrowth. The emergence of the ureteric bud from the Wolffian duct is a tightly controlled process that involves inductive (black arrows) and inhibitory (red lines) signals. The correct position of the metanephric mesenchyme is required for the interaction between the Wolffian duct (expressing the receptor RET) and the metanephric mesenchyme sending the GDNF signaling.

Branching induction and regulation.

In mouse, the invasion of the ureteric bud in the metanephric mesenchyme is followed by a series of 9-10 successive branching events that will give rise to the collecting duct system in the adult kidney. The ureteric bud is composed by two different cell types: the cells forming the "stalk" and the cells composing the "tip". During the branching events, the cells in the tip proliferate and increase the size of terminal ampulla before it remodels and forms two new distinct tips (Watanabe and Costantini, 2004), (Pepicelli et al., 1997). The cellular component of the ureteric tip has been shown to have a "self-renewal" property (Michael and Davies, 2004), (Karner et al., 2011). The cells in the stalk of the ureteric bud proliferate also but to a lesser extent. In parallel, they start their differentiation program to become collecting duct cells.

Every new tip derived from a branching event shares the same mechanisms that are involved in the outgrowth of the ureteric bud (figure 17). GDNF is the principal signal sent from the mesenchyme that keeps the tip proliferating and elongating via *Etv4-5*, *Ret* and *Wnt11* expression in the ureteric bud. Additional mechanisms, such as the balanced expression of *Bmp4-Grem1*or *Gdnf-Ret-Spry1*, are necessary for the correct branching of the ureteric bud (Miyazaki et al., 2000), (Michos et al., 2010). Recent studies have shown the importance of the *Slit2-Robo2* pathway in the branching events: ROBO2 is specifically expressed in the metanephric mesenchyme, whereas its ligand is produced by ureteric bud cells. Over expression of the receptor ROBO2 in metanephroi culture reduce the total number of branching events. This branching defect is due to a decreased number of condensing cells around the ureteric bud tip. The fact that ROBO has a chemiorepellent function in other tissues leads to hypothesize that the over expression of this gene affects the cell condensation around the tip. This decreased cell population is not able any longer to interact with the ureteric bud and maintain the successive branching rounds (Ji et al., 2012). Besides these actors, other genes play a role in the ureteric branching after it emerges from the Wolffian duct. For example, *Fgf7*, a member of the Fgfs family, is expressed in the metanephric mesenchyme in combination with *Fgf10*. The inactivation of *Fgf7* leads to smaller kidney with a reduced number of collecting ducts (Qiao et al., 1999), comparable with what has been described in *Fgf10* mutant animals (Michos et al., 2010). These two Fgf ligands interact both with the isoform IIIb of the receptor Fgfr2. Fgfr2IIIb, a high affinity receptor, is strongly

expressed in the tip of the ureteric bud. Perturbation in its expression or signaling leads to a defect in the total number of nephrons (Qiao et al., 1999). *Pax2* is expressed in the nephric duct and also in the ureteric bud all along kidney development. As described above, it is crucial for the specification and elongation of the nephric duct. Later on, it plays a crucial role in the ureteric bud outgrowth (Brophy et al., 2001). Heterozygous compound mutation of $Pax2^{+/-}$ $Pax8^{+/-}$ does not affect the invasion of the ureteric bud in the metanephric mesenchyme, but leads to a defective branching pattern and a reduction in the number of nephrons (Narlis et al., 2007). Clinical studies carried in patients affected by *Pax2(1Neu)* mutation showed renal hypoplasia, malformation due to a defective branching of the ureteric bud. Animals carrying the same mutation showed an aberrant branching pattern, due to an increased apoptosis of the ureteric bud (Porteous et al., 2000).

Another transcription factor, SRY-box containing gene 9 (*Sox9*), in combination with its close homologous factor Sox8, has an important role during the ureteric bud branching. Double inactivation of these two transcription factors leads to kidney defects characterized by different degrees of severity, ranging from hypoplasia to renal agenesis. *Sox9* and *Sox8* have been shown to activate important genes downstream of the RET cascade, including *Spry1* and *Etv5*. Inactivation of *Sox8* alone does not affect the ureteric bud branching, but the concomitant inactivation of one copy of *Sox9* in a *Sox8* deficient background ($Sox8^{-/-}$ $Sox9^{+/}$) leads to severe branching defects. The ureteric bud normally invades the metanephric mesenchyme, but it stops after the first round of branching, probably due to a defective GNDF/RET signaling (Reginensi et al., 2011). *Sox9* inactivation leads to dilated ureteric bud tips surrounded by ectopic cell aggregates. Expression of *Lhx1*, *Wnt4* and *Fgf8* in these structures suggests that they are early nephron precursors. The induction of these ectopic condensates is due to the loss of ureteric bud tip identity. A dramatic reduction of tip specific markers like *Ret* and *Wnt11* is coupled with an expansion of *Wnt9b* territory in the tip, where it is normally excluded (Reginensi et al., 2011).

Alk3 plays also a specific role in the ureteric bud branching besides its important role in metanephric mesenchyme determination I have described above. Specific inactivation of this receptor in the nephric duct and ureteric bud leads to extra numerary branches during the first and second round of branching. Paradoxically, after birth the mutants show a reduced number of branches. *Alk3* deficient ureteric buds show a reduction of phospho *Smad1*, an

effector of BMP-Alk3 signaling. It has been shown that *Alk3* mediates the BMP2 signaling and the initial surnumerary early branches can be ascribed to the absence of this inhibitory signal (Hartwig et al., 2008).

The transcription factor *Empty Spiracles2* (*Emx2*) is expressed in the nephric duct. Its homozygous inactivation leads to the complete absence of branching events after the emergence of the ureteric bud and its invasion in the mesenchyme (Miyamoto et al., 1997). In *Emx2* mutants, the ureteric bud is unable to branch, and it degenerates and disappears around E13.5. This event is associated with increased apoptosis of the metanephric mesenchyme. *Emx2* is crucial for the first branching but not for the emergence of the ureteric bud (Miyamoto et al., 1997), in opposition with the previous genes that play a role both in the emergence and in the control of the successive brunching of the ureteric bud.

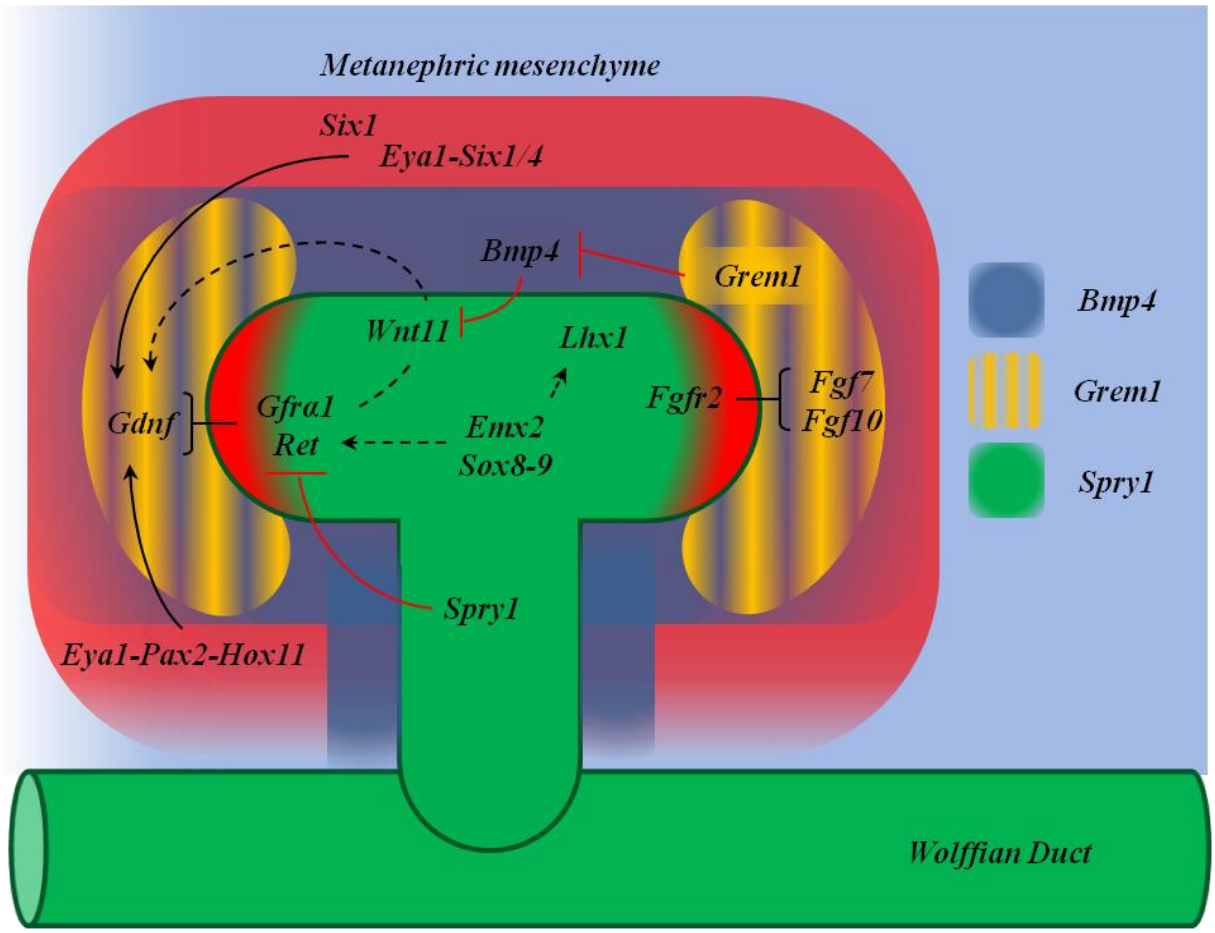

Figure 17. Scheme of epistatic interactions during the branching of the ureteric bud tip. The branching occurs in the ureteric bud tip (light red territory). GDNF-RET signaling is active in this specific part of the ureteric bud**.** *Bmp4* function is antagonized by the co-expression of *Grem1*in the mesenchyme surrounding the tip. *Spry1*, an inhibitor of the RET signaling, is expressed in the ureteric bud but is selectively excluded from its tip.

Metanephric mesenchyme condensation.

Immediately after the emergence of the ureteric bud, the metanephric mesenchyme begins to condensate around the tip (figure 18). Cells forming the cap mesenchyme are a defined subpopulation of the mesenchyme. These cells, expressing *Six2*/*Cited1*, represent a nephrogenic progenitor pool of cells that will sustain the nephron formation during all the process of kidney morphogenesis (Kobayashi et al., 2008). This fundamental role implicates a self renewal property of this pool. In this context, *Six2* is the principal gene responsible for maintaining the self-renewing of the cap mesenchymal cells via inhibition of their differentiation. The absence of *Six2* is responsible for ectopic nephron formation scattered in the mesenchyme surounding the ureteric bud. In this case, the pool of cap mesenchymal cells, having lost their self-renewal property, rapidly disappears after the formation of few nephrons, leading to severe hypoplasia. On the other hand, over expression of *Six2* inhibits further differentiation of the cap mesenchyme (the mesenchymal-to-epithelial conversion) (Kobayashi et al., 2008), (Self et al., 2006). Cells forming the condensate ($Six2^+$ $Cited1^+$) are committed to the nephron fate, but they are still multipotent, participating to all the segments of the mature nephron, without any particular localization (Boyle et al., 2008).

The survival of the differentiated metanephric mesenchyme is crucial to maintain the self-renewing cell population. Indeed the mesenchyme appears to be programmed to undergo apoptosis in the absence of proper survival signals. The cap mesenchyme cells not yet engaged in nephrogenic process express a set of genes that is indispensable for their survival and maintenance, such as *Wt1*, *Bmp7*, and *Fgf2* (table 4). Abnormalities in their expression lead to a drastic degeneration of the metanephric cap cells. In particular, lack of *Wt1* expression in the metanephric mesenchyme leads to massive apoptosis, in a ureteric bud independent way (Kreidberg et al., 1993), (Donovan et al., 1999). *Bmp7* mutants mice are affected by hypoplasia due to an arrest in the kidney development at E14.5 coupled with massive apoptosis in the mesenchyme. *Bmp7* has been also demonstrated to be crucial for metanephric mesenchyme survival in collaboration with *Fgf2* (Simic and Vukicevic, 2005), (Dudley et al., 1999). Recent experiments have elucidated a key role for two Fgf members in the maintenance of the self renewing stem cells population in the metanephric mesenchyme condensate. *Fgf9* is mainly secreted by the ureteric bud and acts redundantly with *Fgf20* that is expressed in the cap condensate. The concomitant inactivation of both genes leads to hypoplastic kidneys characterized by a drastic reduction of nephrogenic cortical zone. This

defect is due to the premature differentiation of the pool of cap condensate cells that loses its self renewing properties. Fgf20 mutation has been described in human patients affected by renal agenesis (Barak et al., 2012).

Mesenchyme derived structure formation. After the condensation around the ureteric bud tip, a subpopulation of cap mesenchyme cells enters the nephrogenic process: they become sensitive to signals from the ureteric bud, silence *Cited1* expression and start to express *Wnt4*. The condensates, via mesenchymal to epithelial transition, give rise to preaggregates that will develop in the first epithelial structure: the renal vesicle (figure 18). This nephron precursor, via proliferation and cell rearrangement will develop in canonical shaped bodies known as "*Comma shaped body"*, "*Sigma shaped body"* and finally to the mature nephron. Many studies have been carried out to understand the complex process of nephron formation and I will resume here the main steps.

Pre-Aggregates and Renal Vesicle formation. After the extinction of *Cited1* expression, the induced mesenchymal cells begin the mesenchymal-to-epithelial transition process (figure 18) (table 4). This process has been shown to involve some of the members of the secreted Wnt family glycoproteins. Wnt signaling during the mesenchymal to epithelial transition seems to involve the canonical Wnt/β-catenin pathway, whereas later epithelial differentiation involves the non canonical Wnt/PCP (planar cell polarity) pathway, reviewed in (Carroll and Das, 2011). The principal Wnt members implicated in the first steps of epithelialization are *Wnt9b* and *Wnt4*: *Wnt9b* is secreted from the ureteric bud epithelium, whereas *Wnt4* is expressed in pre-tubular aggregates. In response to *Wnt9b,* few condensate cells begin to stabilize the β-catenin, stop to express *Cited1* (Six2 is still expressed) and start to form *pre-aggregates* (Carroll et al., 2005). Preaggregates cells are positioned below the ureteric bud tip, whereas the cells above the tip remain undifferentiated. This is probably due to an interaction between *Wnt9b* and *Six2* to counteract β-catenin stabilization in order to maintain the self-renewal property (Park et al., 2007), (Karner et al., 2011). Inactivation of *Wnt9b* or *Wnt4* leads to the absence of mesenchymal to epithelial transition and mutant embryos lack totally the first steps of nephrogenesis (Carroll et al., 2005), (Stark et al., 1994). Direct implication of canonical β-catenin pathway in *Wnt4* signaling has been demonstrated by β-catenin stabilization experiments in condensed metanephric mesenchyme lacking *Wnt4* . Stabilization of β-catenin in this context is able to restore *Wnt4* downstream genes expression, including *Lhx1* (Park et al., 2007).

Fgf8 is a member of the fibroblast growth factors expressed in the condensed metanephric mesenchyme. The inactivation of *Fgf8* in the metanephric mesenchyme leads to the stop of nephrogenesis at the vesicle stage. This defect is correlated with the downregulation of *Wnt4* and *Lhx1* in the pre-aggregates and it is characterized by an increase of cell apoptosis. Hypomorph expression of *Fgf8* allows the development of the first steps of nephrogenesis until the S-shaped bodies, but these nephron precursors degenerate and undergoes apoptosis (Grieshammer et al., 2005).

Besides its expression in the ureteric bud, *LIM homeo box protein1* (*Lhx1*) starts to be expressed in the distal vesicle under the regulation of *Wnt4* and *FgF8* signaling. Its expression persists during nephron formation and it remains faintly expressed in the adult distal tubule (Karavanov et al., 1998). Conditional inactivation (Rarb2-Cre) of *Lhx1* leads to a premature stop of nephrogenesis at the vesicle step. In this model, vesicles develop, express *Wnt4*, *Fgf8* and *Pax8*, but lack markers of polarization, such as *Brn1* and *Dll1*, (Kobayashi et al., 2005).

Another important gene involved in the mesenchymal to epithelial transition is the transcriptional factor *Emx2*, expressed in the ureteric bud as we see above. In addition its important role in the branching of the ureteric bud, *Emx2* plays also a role in the mesenchymal to epithelial transition. Co-culture experiments of mutant ureteric bud and wild type metanephric mesenchyme showed an absence of epithelialisation process in the mesenchyme. The combination of mutant mesenchyme and wild type ureteric bud did not display any morphogenetic abnormalities, suggesting that the defective mesenchymal to epithelial transistion is due to the absence of *Emx2* in the ureteric bud (Miyamoto et al., 1997).

Table 4. Summary of the major genes playing a role in metanephric condensation and first steps of epithelialization.

Functions	Genes	Malformations	Ref .
Metanephric condensation	***WT1***	- Decreased survival of metanephric mesenchyme	(Kreidberg et al., 1993)
	BMP7	- Stop in nephrogenesis after condensation	(Dudley et al., 1999)
	BMP7* and *Fgf2	- Survival of metanephric mesenchyme	(Simic and Vukicevic, 2005)
	Fgf9* and *Fgf20	- Premature differentiation of cap condensate cells	(Barak et al., 2012)
First steps of metanephric mesenchyme epithelialization	***Wnt4***	- Absence of mesenchymal to epithelial transition	(Park et al., 2007)
	Wnt9b	- Absence of mesenchymal to epithelial transition	(Carroll et al., 2005)
	Fgf8	- Absence of vesicle formation	(Grieshammer et al., 2005)
	Lhx1	- Absence of vesicle formation	(Kobayashi et al., 2005)
	Emx2	- Absence of mesenchymal to epithelial transition	(Miyamoto et al., 1997)

Once the pre-aggregates are formed, committed cells compact and form the *renal vesicle* that can be defined as the first epithelial step in nephrogenesis (figure 18). This spherical structure is enveloped by a basal membrane, and cells of the vesicle have a typical apico-basal polarization. All these rearrangements lead to the formation of the lumen that will, eventually, connect to the ureteric bud lumen during later stages of vesicle development. The fusion of the two lumens involves the disaggregation of the basal membrane and the invasion of vesicle cells in the ureteric bud tip (Georgas et al., 2009). The vesicle can be divided in two distinct domains along a proximo-distal axis. The distal part contains already all the precursors that will give rise to the proximal tubules, Henle's loop and distal tubules, whereas the proximal domain will form the components of the glomerular structure, i.e. the podocytes and the Bowman's capsule cells.

Recent experiments identified around 100 genes differentially expressed in the proximal and distal domains of the vesicle (Mugford et al., 2009), (Brunskill et al., 2008), (Georgas et al., 2009). Some important genes, crucial for later nephron differentiation start to be expressed specifically in the distal segment of the vesicule and they will be described in detail later. In particular, the distal portion of the vesicle expresses *Delta-like ligand1* (*Dll1*) and *Jagged1* (*Jag1*), ligands involved in the Notch pathway; *Pou3f3* (*POU domain, class 3, transcription factor 3 - Brn1*), involved in distal tubule specification and the BMP family member *Bmp2*, probably involved in the fusion with the ureteric bud. The proximal domain of the vesicle, responsible for glomerulus development, is characterized by the expression of the transcription factor *Wilm's tumor suppressor 1* (*Wt1*) and *Transmembrane protein 100 (Tmem100)* (Georgas et al., 2009).

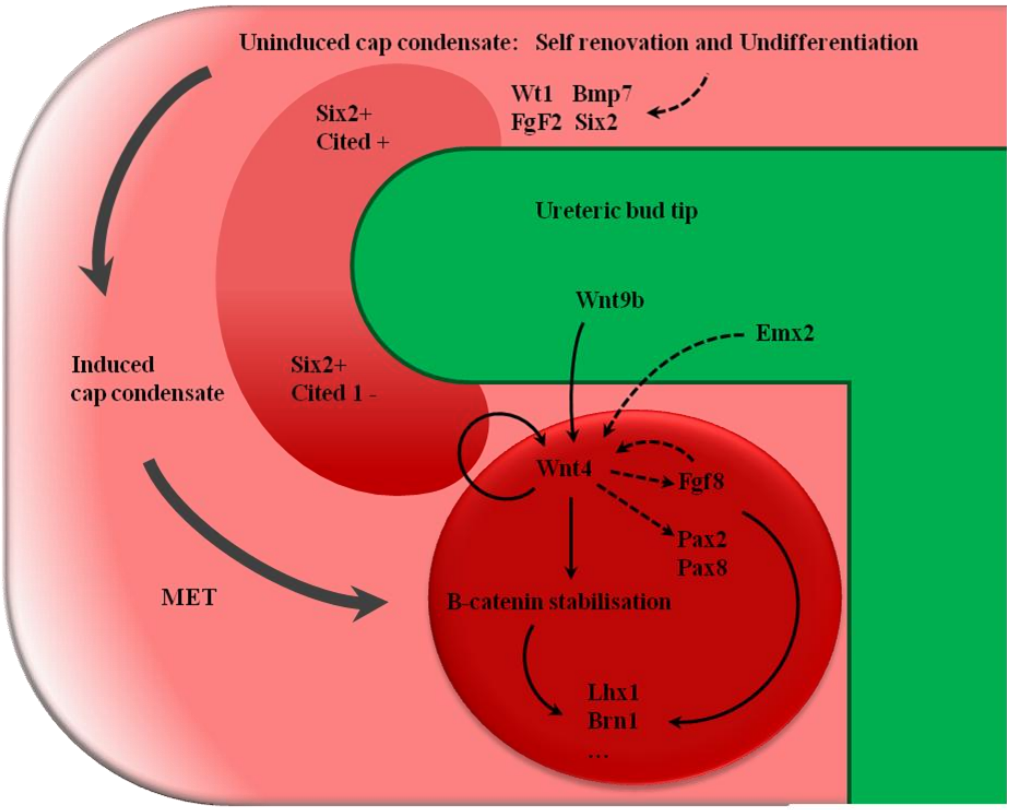

Figure 18. Scheme of mesenchymal to epithelial transition. The mesenchymal to epithelial transition starts when the induced cap mesenchyme looses its self-renewal function. These cells enter the nephrogenic differentiation program, silence Cited1 and become sensible to Wnt9b driven β-catenin stabilization. Once the pre-aggregate is formed, epithelialisation program starts and a basal membrane is formed at the vesicle step. The vesicle starts then to express spatially polarized markers in response to ureteric bud signaling.

Comma-shaped body development. After maturation, the renal vesicles have acquired a proximal-distal polarization and their internal lumen has fused with the ureteric bud. The vesicle begins, then, morphological movements that lead to the formation of the comma shaped body, a transient, short lived, step in the early nephrogenesis between the vesicle and the *Sigma shaped* body. A major morphological rearrangement leads to the formation of a first slit, physically separating the proximal part from the distal part of the vesicle (figure 19B and 19C). Cells located at the junction between proximal and distal domains rearrange their cytoskeleton and move their nucleus from the basal to the apical side. In addition their basal membrane begins to invaginate and forms the origin of the first slit. This slit will further invaginate, separating the podocytes and Bowman's capsule precursors on the lower layer (proximal limb) from the tubular precursors in the upper layer (distal limb).

Expression of angiogenic factors by podocyte precursors will attract endothelial cells that will participate to the formation of the vascular tuft (Jokelainen, 1963).

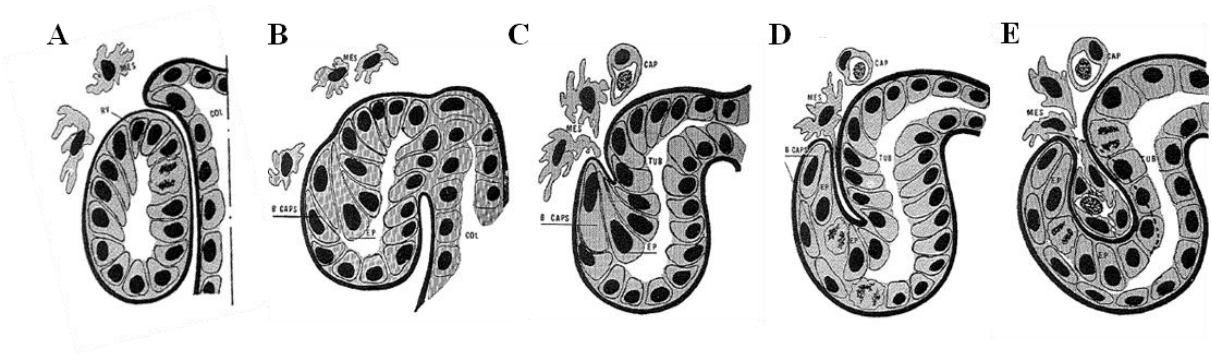

Figure 19. Morphologic rearrangements leading to the formation of Comma-shaped body. The vesicle (A) undergoes several morphological movements: initially, few cells begin to move their nuclei to the apical surface (B). This modification causes cytoskeletal rearrangement that begin to pull the basal membrane (C) forming the invagination that will attract and host the vascular and mesenchymal cells precursors in charge of forming the vascular part of the nephron (D and E), adapted from (Jokelainen, 1963).

Sigma shaped body development. The remodeling of the comma-shaped body leads to the formation of a second "slit" , secondary to the bending of the future tubular part, on the opposite side of the first one (Jokelainen, 1963). This new conformation gives rise to the S-shaped bodies. In this structure, three distinct domains can be discerned: starting from the connection with the collecting duct we have the distal limb followed by the middle and the proximal limbs. Each limb contains the precursors committed to form specific portions of the nephron. The distal limb will give rise to the convoluted distal tubule (Georgas et al., 2009), the middle limb is at the origin of Henle's loop and proximal tubules, and the proximal limb will give rise to the glomerular part of the nephron.

The mature nephron morphogenesis. Sigma shaped bodies represent a relatively well characterized step of nephron precursors. Its further development will give rise to the mature nephron, via elongation of its prospective tubular component and differentiation of its proximal part into the glomerulus.

1. Formation of the glomerulus

I will briefly describe the morphological modifications that will lead to the formation of the different component of the glomerulus (Quaggin and Kreidberg, 2008). The glomerulus is a complex structure that performs, in tight interaction with the vascular system, the filtration function of the nephron. At the S-shaped body stage, the proximal limb is composed by a relatively flattened and curved tubular structure with columnar epithelial cells. The lumen of this structure delimitates the prospective urinary space. The lower layer of this proximal part will give rise to the Bowman's capsule whereas the upper layer will give rise to the future podocytes. These podocytes precursors start to secrete the vascular endothelial growth factor A (*Vegfa)* (Eremina and Quaggin, 2004) and platelet-derived growth factors (PDGFs) (Bjarnegard et al., 2004). These growth factors have a chemioattractant and angiogenetic role on mesenchymal and endothelial cells, respectively. Both cell types invade the vascular cleft facing the podocyte precursors and endothelial cells start to form a first capillary loop (Robert et al., 1998). Later on, two parallel events occur: on one side, the first capillary loop divides in several capillaries, giving rise to a complex network (Potter, 1965). On the other hand, the upper layer, still in a form of an epithelium called the "podocyte crown" or "plate" starts a morphogenetic movement, based on the basal constriction of these epithelial cells. This will generate the bending that will envelop the capillaries and the mesangial cells that have

invaded the vascular cleft. After this invagination, podocytes begin a morphological transformation, which will lead to their final phenotypical characteristics. Starting from a columnar layer of epithelial cells, they will start to lose their cellular contacts, migrate in order to cover the network of capillaries and form their typical foot processes. In parallel, endothelial and podocyte basal lamina fuse to form a thick basement membrane, known as the glomerular basement membrane. The glomerular filtration process starts with the fenestration of endothelial cells. This process allows the passage of fluid and low molecular weight molecules through the filtration barrier composed by the fenestrated capillaries, the glomerular basal membrane and slit diaphragms (figure 20). In parallel, parietal epithelium, which emanates from the lower layer of the proximal limb, has followed the invagination of the inner visceral layer and acquire a "flattened" morphology. In addition to endothelial cells and podocytes, the glomerular tuft is composed by mesangial cells, specialized mesenchymal cells characterized by contractile functions that can modify the surface of filtration.

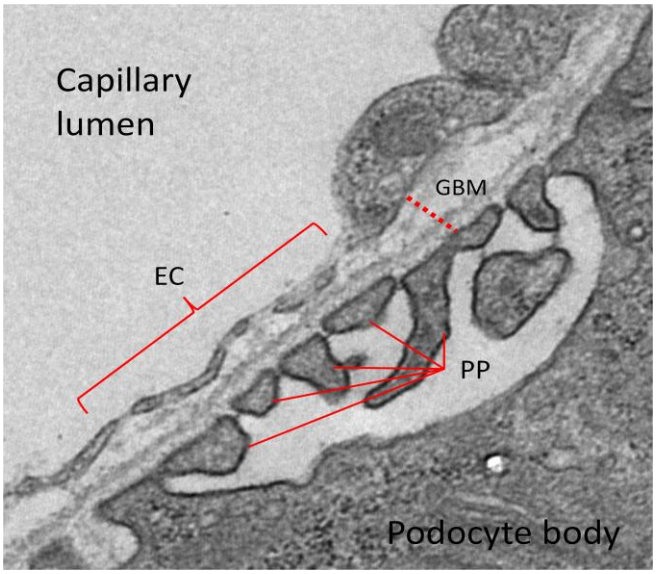

Figure 20. The glomerular filtration barrier. Electron microscopy picture showing the three layers composing the glomerular filtration barrier. EC: fenestrated Endothelial Cells; GMB: glomerular basal membrane; PP: Podocyte Foot processes

During the invagination movement of the podocyte crown, the vascular pole becomes progressively more restricted via its interaction with the extraglomerular mesangium. On the other hand, the urinary pole, joining the proximal tubular compartment, is remodeled and slides to reach the opposite side of the glomerulus.

A few genes have been show to play a crucial role in the glomerular formation and I will briefly describe some of them. Wilm' tumor suppressor *Wt1* is one of the major actor of the glomerulus development. This zinc finger transcription factor is expressed in all the condensate cells and its localisation becomes progressively restricted to the proximal portion of the renal vesicle. Wt1 is finally expressed in the proximal limb of S-shaped body, at high level in the podocyte precursors and at much lower level in the Bowman's capsule precursors. Inactivation of *Wt1* leads to agenesis of the kidney due to a massive apoptosis of the uninduced metanephric mesenchyme (Kreidberg et al., 1993). The vascular endothelial growth factor a (*Vegfa)* has been shown to be crucial for endothelial cells integration in the glomerulus. Podocyte-specific inactivation of this gene leads to the absence of filtration barrier formation, due to a defective migration and survival of endothelial cells (Eremina et al., 2003). Inactivation of *Pod1*, a transcription factor expressed during podocytes differentiation, leads to a single capillary loop and defective podocytes differentiation, characterized by immature columnar shaped cells without any foot processes (Quaggin et al., 1999). The Pax3-Cre driven inactivation of *Notch2*, a receptor involved in Notch signaling, leads to the absence of proximal tubules and glomeruli formation (Cheng et al., 2007).

2. Tubular maturation

The tubular structures of nephron are generated by the middle and distal limbs of the S-shaped body through a complex maturation process. During this process, there is an extremely intense proliferation that leads to the elongation of tubules. At the end of this elongation process, the global tubular component of nephrons is more than 300 times longer than the average width of tubules. Having its origin in the middle and distal limbs of the S-shaped body, the tubular component of the nephron undergoes a maturation process to reach its definitive organization. This elongation is accompanied by a peculiar patterning of different tubular segments that are going to acquire specific molecular signatures. Surprisingly, in comparison with the large number of genes known to play a role in the early steps of nephrogenesis, not much is known about the actors involved in the expansion and maturation of tubular structures.

One of the rare pathways known to be involved in tubular maturation is the Notch signaling. As described above, this signaling pathway plays a crucial role in glomerulus differentiation and in proximal tubule formation (Cheng et al., 2007). Several components of the Notch signaling are expressed during early steps of nephrogenesis. Among them, *Delta like1* (*Dll1*), *Jagged1* (*Jag1*), and the downstream effector of the *Hairy/Enhancer of split* family *Hes5* start to be expressed in the distal portion of the vesicule. Later on, these Notch components, in combination with the receptors Notch1/*Notch2* are specifically expressed in a peculiar sub domain of the S-shaped body, at the origin of the proximal tubules and the Henle's loops. This domain is represented by an epithelial bulge, at the junction of the proximal and the middle limb. Interestingly, this segment specifically expresses two ligands *Delta like1* (*Dll1*) and *Jagged1* (*Jag1*), the receptors *Notch1/Notch2* and the downstream effector of the *Hairy/Enhancer of split* family *Hes5* (Chen and Al-Awqati, 2005). As described above, Pax3-Cre driven inactivation of *Notch2* leads to severe kidney defects, including the absence of proximal tubules (Cheng et al., 2007). Interestingly, inactivation of *Notch2* in the cap condensates (Six2-cre inactivation model) does not affect nephron development. However, in this context, the inactivation of one copy of *Notch1* in a *Notch2*-deficient background elicits a drastic defect in nephron number (Surendran et al., 2010). The ligand *Dll1* plays an important role in the activation of *Notch2* signaling in the middle limb: an hypomorph allele of this ligand is sufficient to give a drastic defect in proximal tubular development coupled with a normal nephron number (Cheng et al., 2007). Conversely, the overexpression of constitutively active Notch1 intracellular domain (N1-ICD) in the metanephric mesenchyme (Six2-Cre) can promote and force proximal fate (Cheng et al., 2007). In addition, in the *Xenopus*, ectopic expression of downstream target of Notch, the *Hairy/Enhancer of split*, can induce more proximal fate in developing pronephros (Taelman et al., 2006).

Wnt/β-catenin canonical signaling has been demonstrated to be important in early nephron development through the role of *Wnt4* and *Wnt9b* (Lyons et al., 2004), (Carroll et al., 2005), whereas the non canonical/PCP Wnt signaling is involved in later tubular development and elongation (Fischer et al., 2006), (Saburi et al., 2008), (Simons et al., 2005), (Carroll et al., 2005). Recent evidences on *Xenopus* and Zebrafish models have suggested the possible role of the planar cell polarity pathways also in the tubular fate and specification. *Daam1* is a protein implicated in the non canonical Wnt signaling pathway. Its knockdown in *Xenopus* and *Zebrafish* reduced pronephric tubulogenesis without any particular defect in glomerular

development (Miller et al., 2011). In addition, knockdown of its interacting partner, Rho-GEF (WGEF) give rise to the same phenotype (Miller et al., 2011). Inversin (Invs, Nphp2) is known to play a key role in the switch between canonical/non canonical Wnt signaling (Simons et al., 2005). In *Xenopus*, injection of antisense morpholino against Inversin decreases the elongation of the intermediate segment of pronephric tubules (Lienkamp et al., 2010). Interestingly, deficiency of *Frizzled8* in *Xenopus*, the receptor upstream the activation of Inversin and Daam1 in the PCP pathway shows the same defective elongation in pronephros tubule (Satow et al., 2004).

Another example of genes involved in tubular maturation is the transcription factor *Brn1* (*Pou3f3*). Brn1, a class III POU protein starts to be expressed in the distal portion of the vesicle. In the S-shape body, this factor is expressed specifically in the distal limb and part of the middle limb. In mouse, its inactivation leads to an early postnatal lethality (Nakai et al., 2003). Mutant mice die during the first 24 hours after birth, due to a drastic defect in the development of Henle's loops, macula densa and distal tubules. Henle's loops emerge from the S-shape body but stop their maturation program soon after, ending with short and immature loops that do not expand in the medulla. This defect is correlated with the absence of Henle's loop differentiation markers. Similar defects affect also the macula densa and the convoluted distal tubules that lack the expression of markers, such as nitric oxide synthase gene (*Nos1*) or *Ptger3* for the macula densa and the thiazide-sensitive Na/Cl co-transporter (*NCC*, *Slc12a3*) for the convoluted distal tubules. All these results show that Brn1 is a crucial gene for the expansion of the distal tubular part of the nephron, but its absence does not affect the proximal tubules and the glomeruli (Nakai et al., 2003).

Recent studies have identified specific sub domains in the middle and distal limb of the S-shape body, characterized by the expression of a peculiar set of markers. Among them, *Irx1* and *Osr2* start to be expressed during mouse kidney development in a restricted segment of the middle limb of S-shape body. Their expression is quite mutually exclusive: *Irx1* is expressed in the more distal part of the middle limb, whereas *Osr2* is expressed more proximally in the middle segments (Yu et al., 2012b). The importance of these genes in tubular sub segments specification has been highlighted by studies in *Xenopus* and *Zebrafish*. In *Xenopus laevis*, members of Iroquios genes family, *Irx1* and *Irx3*, are essential for early steps of formation of the nephrogenic territory. Later on, knock down experiments of these genes showed a defective development of the corresponding proximal tubules, Henle's loop and distal collecting ducts of the nephron (Alarcon et al., 2008). In the same way, Odd-

skipped genes *Osr1* and *Osr2* have been shown to play crucial roles during nephron development and in the differentiation/expansion of the corresponding proximal tubule in *Xenopus* and *Zebrafish*. On the other hand, overexpression of these two genes in Xenopus leads to expansion of the nephrogenic territory and the formation of surnumerary tubules (Tena et al., 2007).

Another gene important for tubular specification and formation is *Hnf1b*. Studies performed during my thesis have highlighted the role of *Hnf1b* in the initiation of tubule development, and I will describe in details my results obtained with different time and space inactivation strategies. Previous studies had already described the role of *Hnf1b* in the maintenance of tubular diameter during elongation (Fischer et al., 2006).

Besides this transcription factor, a vast set of genes have been identified, whose mutations or inactivation leads to the loss of normal tubular diameter during development, and to cyst formation. Polycystic kidney disease (PKD) is one of the most frequent genetic disease, reviewed in (Igarashi and Somlo, 2002). Renal cysts are typically found in several human syndromes, such as Bardet-Biedl syndrome (BBS) (table 5), Meckel syndrome, and nephronophthisis (NPHP) (table 6). Interestingly, most of proteins encoded by genes involved in these syndromes are localized in the primary cilium (figure 21). This cilium is an immotile organelle that allows the cell to sense its extracellular environment. The scaffold of cilia is represented by nine microtubule doublets. This organelle needs for its generation and maintenance complex intraflagellar transport (IFT) machinery. At the base of cilia is the basal body, composed by the two centrioles tightly connected with the cytoskeleton. Several mouse models have been created to study the different ciliopathies observed in human (table 7).

The vast majority of patients suffering from Autosomal Dominant Polycystic Kidney Disease (ADPKD) develop renal cysts (normally after 30 years of age) because they carry mutations in cystic genes such as PKD1 or PKD2. Renal cysts may derive from different nephron tubular segments (and often also from glomeruli) due to a complex set of events including cellular proliferation, defective cell size control, apoptosis, fluid secretion, disorganized oriented cell division and defective convergent extension. The basic principle is that a cyst can be often considered as a tubule that has lost its cylindrical shape and has become either a spherical cavity or a wide fusiform structure filled with fluid. In general, ADPKD patients carry mutations in cystic genes at the heterozygous state. Interestingly, mouse models carrying mutations in either *Pkd1* or *Pkd2* at the homozygous state, show

(among other drastic phenotypes) dramatic developmental defects affecting nephrons. *Pkd1* germline inactivation does not affect the early stage of nephrogenesis, and mutant embryos at E14.5 show normal early developing bodies (vesicles, commas- and S-shaped bodies). Cysts start to develop from the cortical proximal tubules only around E15.5, during tubular expansion. The pattern of cyst formation is modified during development, to finally affect all tubular structures in later embryonic stages (Lu et al., 1997). Similarly to *Pkd1* inactivation, *Pkd2* mutants show a normal development of nephron precursors. Cysts develop after E15.5, and are initially derived from the Bowman's capsule and only in lower proportion from the tubules (Wu et al., 2000). Finally, cysts affect predominantly the distal part of the tubular component later on. In the same way, inactivation of *Pkhd1* in mouse model can recapitulate the corresponding autosomal recessive form of Polycystic Kideny Disease (AR-PKD) described in human. The absence of the protein fibrocystin/polyductin (FPC) encoded by *Pkhd1* gene is responsible for cysts formation in already differentiated, but still elongating tubules.

As previously discussed, polycystins and polyductin are localized in the primary cilium. This organelle plays a crucial role in the maintenance of tubular diameter during tubular elongation. This role has been illustrated by the formation of cysts in animal models lacking the expression of proteins involved in primary cilium structure and/or function, including *Kif3a* and *Polaris* (also known as *Tg737*) (Lin et al., 2003), (Lehman et al., 2008).

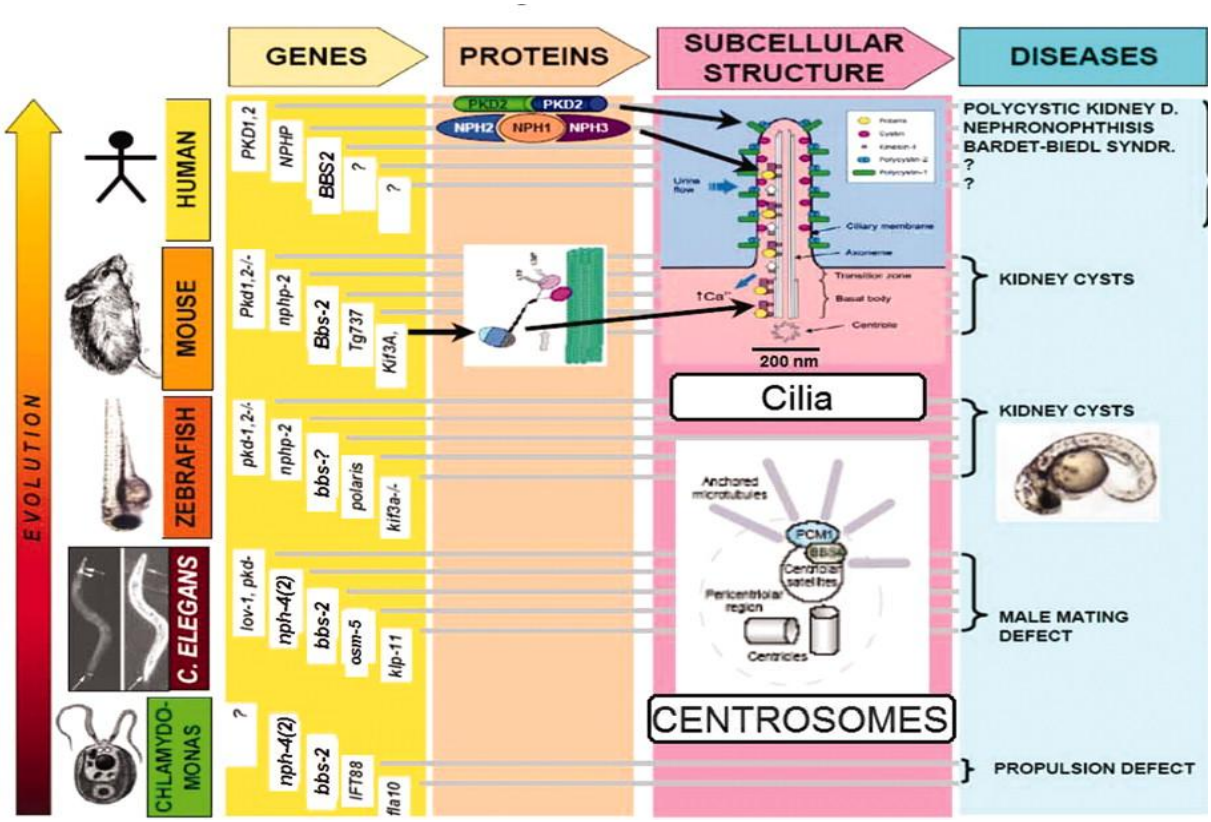

Figure 21. Schematic representation of some proteins localized in the cilium/basal body and involved in renal cystic disease. The scheme summarizes some of the proteins involved in cystic pathologies that are related to cilium signaling or structural disorders. Evolutionary conserved genes, such as Pkd, Nphp and Bbs genes, are involved in the expression of protein related to the ciliary function. These genes are linked to ciliopathies when defectively expressed (adapted from (Hildebrandt and Zhou, 2007)).

Maintenance of tubular diameter during tubular elongation is tightly regulated by a large number of signaling pathways. Among them, Wnt signaling is known to control tubular caliber, via its role in cell proliferation and planar cell polarity (canonical and non canonical pathways) (McNeill, 2009). For example, overexpression of beta-catenin in mouse leads to cyst formation, via an excessive cell proliferation in tubular cells. Non canonical Wnt pathway is involved in oriented cell division and loss of this orientation has been shown to participate to cysts formation in several animal models (Jonassen et al., 2008) ,(Fischer et al., 2006). In addition, defective convergent extension has also been shown to be involved in the control of tubular diameter.

Recently, the role of the Hippo pathway has been highlighted in cyst formation. The Hippo pathway was first discovered in *Drosophila*, and it consists in a kinase cascade activation, presumably by cell-cell contact sensing, that finally controls cycle progression, growth, and development via activation of the transcription factors YAP and TAZ (Badouel et al., 2009) (figure 22). Inactivation of *Taz* in mouse has been carried out by different groups (Hossain et al., 2007), (Tian et al., 2007), and all the animals lacking this transcription factor are affected by cyst formation and defect in kidney development. The renal cysts originate principally from the Bowman's capsule and the proximal tubules. Interestingly, analyses carried out in young animals lacking *Taz* showed no difference in the expression of *Pkd1*, *Pkd2* and *Pkhd1* genes, whereas in adult mice the lack of *Taz* leads to the downregulation of the ciliary genes *Tg737*, *Kif3a* and *Pkhd1* (Hossain et al., 2007) and the overexpression of *Pkd2* due to defective ubiquitination (Tian et al., 2007). These differences can suggest a distinct role played by this transcription factor during kidney development and later on in renal tubular maintenance.

The other Hippo pathway component, YAP, has been shown to play a role in animals lacking *Pkd1* (Happe et al., 2011). In a wild type contest, the activation of cell cycling by injury elicits the expression and the migration of YAP in the nucleus during the repairing process. Once the regeneration of the tissue is achieved, the proliferation stops and the expression of *Yap* drops. This protein is released from the nucleus to the cytoplasm and rapidly degraded. In a conditional mutant model of *Pkd1*, the protein YAP persists in the nucleus even after the regeneration of the tissue. This persistent signaling leads to increased and abnormal cell proliferation and contributes to the formation of cysts (Happe et al., 2011). Analysis of human cystic samples confirmed the presence of nuclear YAP only in cystic

tissues and not in the normal or pre-dilation tubules. In addition, YAP downstream targets related to cell proliferation are upregulated in the cystic tissue.

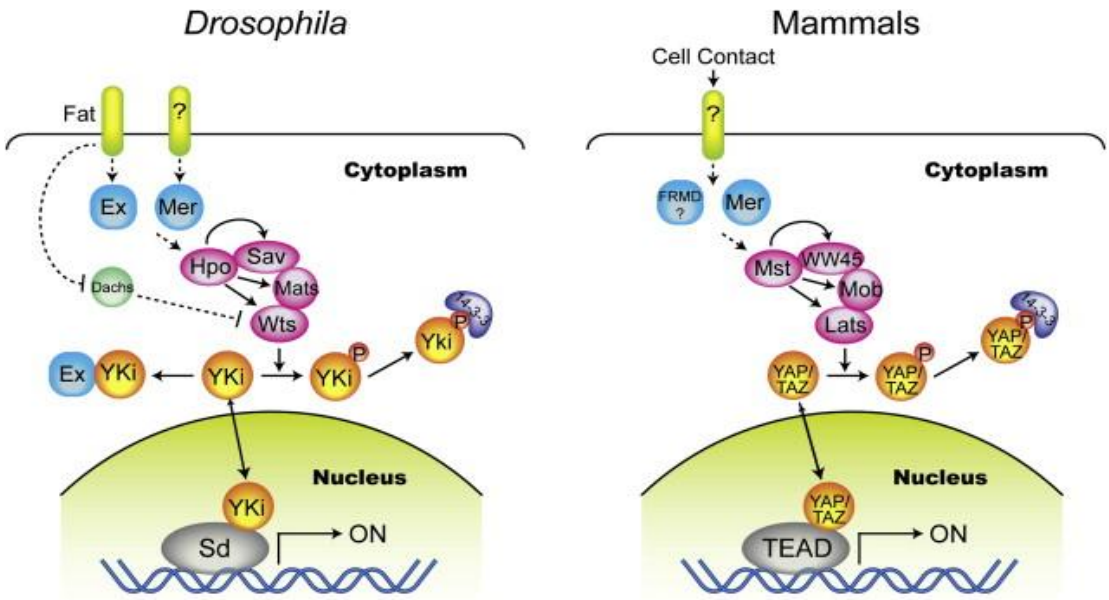

Figure 22. Schematic representation of the Hippo pathway. The Hippo pathway was first characterized in the *Drosophila* and later on in the mammals. The correspondent actors between fly and mammals are shown in the same color. Dashed lines indicates biochemical mechanisms still elusive or not well elucidated (Zhao et al., 2009)

Table 5. Genes identified in Bardet-Biedl syndrome (adapted from (Tobin and Beales, 2007))

Gene	Genic location	Cellular localisaiton	Domains	Putative function
BBS1	11q13	Basal body/cilium	None	Cilia function
BBS2	16q21	Basal body/cilium	None	Cilia function/flagellum formation
BBS3/ARL6	3p12-q13	Basal body/cilium	GTP-binding	Vesicle trafficking
BBS4	15q23	Pericentriolar/basal body	TPR/PilF	Microtubule transport
BBS5	2q31	Basal body/cilium	DM16 DUF1448	Cilia function/flagellum formation
BBS6/MKKS	20p12	Basal body/cilium	TCP1 chaperonin	Cilia function/flagellum formation
BBS7	4q32	Basal body/cilium	TPR/PilF	Intra flagellar transport particle assembly
BBS8/TTC8	14q31	Basal body/cilium	TPR/PilF	Intra flagellar transport particle assembly
BBS9/B1	7p14.3	Unknown	COG1361 membrane biogenesis	Unknown—expressed in bone cells
BBS10 BBS11/	12q21.2	Unknown	TCP1 chaperonin	Unknown
TRIM32	9q31-34.1	Unknown	RING WD40 NHL Barmotin B-Box	E3 ubiquitin ligase
BBS12	4q27	Unknown		Type II chaperonin

Table 6. Genes whose mutations are responsible for nephronophthisis (Hurd and Hildebrandt, 2011)

Locus	Gene	Genetic location	Protein	Mutation frequency	Extrarenal features
NPHP1	*NPHP1*	2q13	Nephrocystin-1	23%	SLS, JS,
NPHP2	*INV*	9q31	Inversin	1-2%	SLS, HF VSD, situs inversus
NPHP3	*NPHP3*	3q22.1	Nephrocystin-3	<1%	SLS, HF, MKS, situs inversus
NPHP4	*NPHP4*	1p36.22	Nephrocystin-4 or nephroretinin	2-3%	SLS
NPHP5	*IQCB1*	3q21.1	Nephrocystin-5 or IQ motif containing B1	3-4%	SLS
NPHP6	*CEP290*	12q21.32	Centrosomal protein 290	1%	LCA, SLS, JS, MKS, BBS
NPHP7	*GLIS2*	16p13.3	GLI similar 2	<0.5%	
NPHP8	*RPGRIP1L*	16q12.2	RPGRIP1-like	0.5%	SLS, JS, MKS
NPHP9	*NEK8*	17q11.1	NIMA-related kinase 8	<0.5%	SLS
NPHP10	*SDCCAG8*	1q44	Serologically defined colon cancer antigen 8	<0.5%	SLS, BBS-like
NPHP11	*TMEM67*	8q22.1	Transmembrane protein 67	<0.5%	JS, HF, MKS
NPHPL1	*XPNPEP3*	22q13	X-prolyl aminopeptidase 3	<0.5%	cardiomyopathy, seizures
	TTC21B	2q24.3	Intraflagellar transport protein 139	<1%	JS, MKS, BBS, JATD

BBS: Bardet-Biedl syndrome; **HF**: hepatic fibrosis; **JATD**: Jeune asphyxiating thoracic dystrophy; **JS**: Joubert syndrome; **LCA**: Leber's congenital amaurosis; **MKS**: Meckel-Gruber syndrome; **SLS**: Senior-Loken syndrome; **VSD**: ventricular septal defect

Table 7. Genes whose mutations are responsible for ciliopathies (Hurd and Hildebrandt, 2011)

Locus (protein)	Mutants	Type	Viability	Key references
Alström				
Alms1 (Alms1)	*Alms1*^{foz}	Spontaneous	AV	Arsov et al., 2006b
	Alms1^{L2131X}	ENU – truncation at exon 10	AV	Li et al., 2007
	Alms1$^{Gt(XH152)Byg}$	Gene trap – hypomorphic	AV	Collin et al., 2005
BBS				
Bbs1 (Bbs1)	*Bbs1*^{GT1NK}	Gene trap – probably null	EL, AV	Kulaga et al., 2004
	Bbs1^{tm1Vcs} (M390R)	Targeted knock-in	AV	Davis et al., 2007
Bbs2 (Bbs2)	*Bbs2*^{tm1Vcs}	Targeted – null	AV	Nishimura et al., 2004
Bbs3 (Arl6)	*Arl6*^{tm1Vcs}	Targeted deletion – transcript specific	AV	Pretorius et al., 2010
Bbs4 (Bbs4)	*Bbs4*^{Gt1NK}	Gene trap	EL, birth, AV	Kulaga et al., 2004
	Bbs4^{tm1Vsc}	Targeted – null	EL, birth, AV	Mykytyn et al., 2004
Bbs5 (Bbs5)	None			
Bbs6 (Mkks)	*Mkks*$^{Gt(OST367255)Lex}$	Gene trap	EL, AV	Ross et al., 2005
	Mkks^{tm1Vcs}	Targeted – null	EL, AV	Fath et al., 2005
Bbs7 (Bbs7)	*Bbs7* null[a]	Targeted	ND	Zhang et al., 2012
Bbs8 (Tct8)	*Tct8*^{tm1Reed}	Targeted reporter – null	AV	Tadenev et al., 2011
Bbs9 (Bbs9)	None			
Bbs10 (Bbs10)	None			
Bbs11 (Trim32)	*Trim32*$^{Gt(BGA355)Byg}$	Gene trap – probably null	AV	Kudryashova et al., 2009
	Trim32^{tm1Spc}	Targeted knock-in – hyopmorphic	AV	Kudryashova et al., 2011
Bbs12 (Bbs12)	None			
Bbs13 (Mks1)	*Mks1*^{krc}	ENU – probably null	EL	Weatherbee et al., 2009
	Mks1$^{del64-323}$	ENU – possible dominant negative	EL	Cui et al., 2011
Bbs14 (*Cep290*)	*Cep290*^{rd16}	Spontaneous	AV	Chang et al., 2006
	Cep290^{tm1Jgg}	Targeted – null	AV	Lancaster et al., 2011
Bbs15 (Wdpcp)	None			
Bbs16 (Sdccag8)	None			
JBTS				
Jbts1 (Inpp5e)	*Inpp5e*$^{tm1.1Ssch}$	Targeted conditional – null	EL (global KO)	Jacoby et al., 2009
Jbts2 (Tmem216 and Tmem138)	None			
Jbts3 (Jouberin)	*Ahi1*^{tm1Jgg}	Targeted – null	PNL (80%)	Lancaster et al., 2009; Lancaster et al., 2011
	Ahi1^{tm1Ruif}	Targeted reporter – null	ND	Hsiao et al., 2009; Westfall et al., 2010
Jbts4 (Nphp1)	*Nphp1*$^{tm1.1Hung}$	Targeted – null	AV	Jiang et al., 2008
	Nphp1^{tm1Jgg}	Targeted – null	AV	Louie et al., 2010
Jbts5 (Cep290)	*Cep290*^{rd16}	Spontaneous	AV	Chang et al., 2006
	Cep290^{tm1Jgg}	Targeted – null	AV	Lancaster et al., 2011
Jbts6 (Tmem67)	*Tmem67*^{tm1Dgen}	Targeted reporter	PNL	Garcia-Gonzalo et al., 2011
Jbts7 (Rpgrip1l)	*Rpgrip1l*^{tmUrt}	Targeted – null	Birth	Vierkotten et al., 2007
Jbts8 (Arl13b)	*Arl13b*^{hnn}	ENU – null	EL	Caspary et al., 2007
Jbts9 (Cc2d2a)	*Cc2d2a*$^{Gt(AA0274)Wtsi}$	Gene trap – null	EL	Garcia-Gonzalo et al., 2011
Jbts10 (Ofd1)	*Ofd1*$^{tm2.1Bfra}$	Targeted conditional – null	Male: EL; female: birth	Ferrante et al., 2006
Jbts11 (Ttc21b)	*Ttc21b*^{aln}	ENU – probably null	EL	Tran et al., 2008
Jbts12 (Kif7)	*Kif7*$^{tm1.2Hui}$	Targeted – null	Birth	Cheung et al., 2009
	Kif7^{zmaki}	ENU	EL (late)	Liem et al., 2009
Jbts13 (Tctn1)	*Tctn1*$^{Gt(KST296)Byg}$	Gene trap – null	EL	Reiter and Skarnes, 2006
Jbts14 (Tmem237)	None			
Jbts15 (Cep41)	*Tsga14*$^{Gt(AW0157)Wtsi}$	Gene trap – null	EL	Lee et al., 2012

Locus (protein)	Mutants	Type	Viability	Key references
Jeune				
Atd1 (Atd1)	None			
Atd2 (IFT180)	*Ift80*$^{Gt(AN0245)Wtsi}$	Gene trap – strong hypomorph	Mostly EL; some AV	Rix et al., 2011
Atd3 (Dync2h1)	*Dync2h1*$^{Gt(RRM278)Byg}$	Gene trap	EL	Garcia-Garcia et al., 2005
	Dync2h1^{lln}	ENU	EL	Huangfu and Anderson, 2005
Atd4 (Ttc21b)	*Ttc21b*^{aln}	ENU – probably null	EL	Tran et al., 2008
Atd5 (Wdr19)	*Ift144*^{twt}	ENU – hypomorph	EL	Ashe et al., 2012
MKS				
Mks1 (Mks1)	*Mks1*$^{del64-323}$	ENU – dominant negative	EL	Cui et al., 2011
	Mks1^{krc}	ENU – probably null	EL	Weatherbee et al., 2009
Mks2 (Tmem216)	None			
Mks3 (Tmem67)	*Tmem67*^{tm1Dgen}	Targeted reporter	PNL	Garcia-Gonzalo et al., 2011
Mks4 (Cep290)	*Cep290*^{rd16}	Spontaneous	AV	Chang et al., 2006
	Cep290^{tm1Jgg}	Targeted – null	AV	Lancaster et al., 2011
Mks5 (Rpgrip1l)	*Rpgrip1l*^{tm1Urt}	Targeted – null	Birth	Vierkotten et al., 2007
Mks6 (Cc2d2a)	*Cc2d2a*$^{Gt(AA0274)Wtsi}$	Gene trap – null	EL	Garcia-Gonzalo et al., 2011
Mks7 (Nphp3)	*Nphp3*^{pcy}	Hypomorphic	AV	Olbrich et al., 2003
	Nphp3^{tm1Cbe}	Targeted – null	EL	Bergmann et al., 2008
Mks8 (Tctn2)	*Tctn2*$^{tm1.1Reit}$	Targeted – null	EL	Garcia-Gonzalo et al., 2011; Sang et al., 2011
Mks9 (B9d1)	*B9d1*$^{tm1a(EUCOMM)Wtsi}$	Gene trap – null	EL	Dowdle et al., 2011
Mks10 (B9d2)	*B9d2/Tgfb1*^{tm1Flv} *(Stumpy)*	Targeted deletion	ND	Town et al., 2008
NPHP				
Nphp1 (Nphp1)	*Nphp1*$^{tm1.1Hung}$	Targeted – null	AV	Jiang et al., 2008
	Nphp1^{tm1Jgg}	Targeted – null	AV	Louie et al., 2010
Nphp2 (Invs)	*Invs*^{Inv}	Random insertion	AV	Yokoyama et al., 1993
Nphp3 (Nphp3)	*Nphp3*^{pcy}	Hypomorphic	AV	Olbrich et al., 2003
	Nphp3^{tm1Cbe}	Targeted – null	EL	Bergmann et al., 2008
Nphp4 (Nphp4)	*Nphp4*^{nmf192}	ENU	AV	Won et al., 2011
Nphp5 (Iqcb1)	None			
Nphp6 (Cep290)	*Cep290*^{rd16}	Spontaneous	AV	Chang et al., 2006
	Cep290^{tm1Jgg}	Targeted – null	AV	Lancaster et al., 2011
Nphp7 (Glis2)	*Glis2*^{tm1Amj}	Targeted – null	AV	Kim et al., 2008
	Glis2^{tm1Tre}	Targeted reporter	AV	Attanasio et al., 2007
Nphp8 (Rpgrip1l)	*Rpgrip1l*^{tm1Urt}	Targeted – null	Birth	Vierkotten et al., 2007
Nphp9 (Nek8)	*Nek8*^{jck}	Possible hypomorph	AV	Liu et al., 2002
Nphp10 (Sdccag8)	None			
Nphp11 (Tmem67)	*Tmem67*^{tm1Dgen}	Targeted reporter	PNL	Garcia-Gonzalo et al., 2011
Nphp12 (Ttc21b)	*Ttc21b*^{aln}	ENU – probably null	EL	Tran et al., 2008
OFD				
Ofd1 (Ofd1)	*Ofd1*$^{tm2.1Bfra}$	Targeted conditional – null	Male: EL Female: birth	Ferrante et al., 2006

Introduction IV

IV. Transcription factors and genes expression

Cell differentiation and organ morphogenesis are controlled by a complex set of events that define accurate patterns of gene expression in time and space. It is well known that transcriptional regulation of gene expression plays an important role during this process. In this respect, regulation is mediated through the integrated action of many *cis*-regulatory elements including core promoters and more distal cis-acting elements that are crucial in the modulation of the expression of genes.

Transcription factors can be subdivided in two principal classes: General Transcription Factors (GTFs) and Specific Transcription Factors (STFs). GTFs and STFs can bind to specific DNA sequences present in the promoter region next to the transcription start site. The preinitiation complex (PIC) is a large complex of proteins that is necessary for the transcription of protein-coding genes (figure 23). The preinitiation complex plays a crucial role in positioning RNA polymerase II over gene transcription start sites. During these steps it denatures the DNA and helps RNA polymerase II to start active transcription of template DNA from a specific start site. Typically the PIC contains six general transcription factors: TFIIA, TFIIB, TFIID, TFIIE, TFIIF, and TFIIH (Roeder, 1996). GTFs usually recognize common consensus sequences located in the promoter region: the most common example is the TATA consensus sequence (T/A)AA(G/A), located at -31/-26 base pairs from the transcription starting site, that provides the anchoring for the TATA binding proteins (TBP) and the successive assembling of the pre-initiating complex (PIC). Gene transcription is then started by the RNA polymerase II and its modulation is controlled by STFs. This latter class of transcription factors is much more variable than the GTFs: they are expressed (and therefore active) according to a precise pattern and they can have repressor/activator effect on gene transcription (reviewed in (Maston et al., 2006)). STFs bind specific short DNA sequences known as transcription factor binding sites (TFBS). These sequences are not necessary close to the promoter region of the gene, but they can also be located hundreds of kilobases upstream or downstream the transcription starting site and they are able to interact with the proximal located GTFs thanks to the flexibility of DNA.

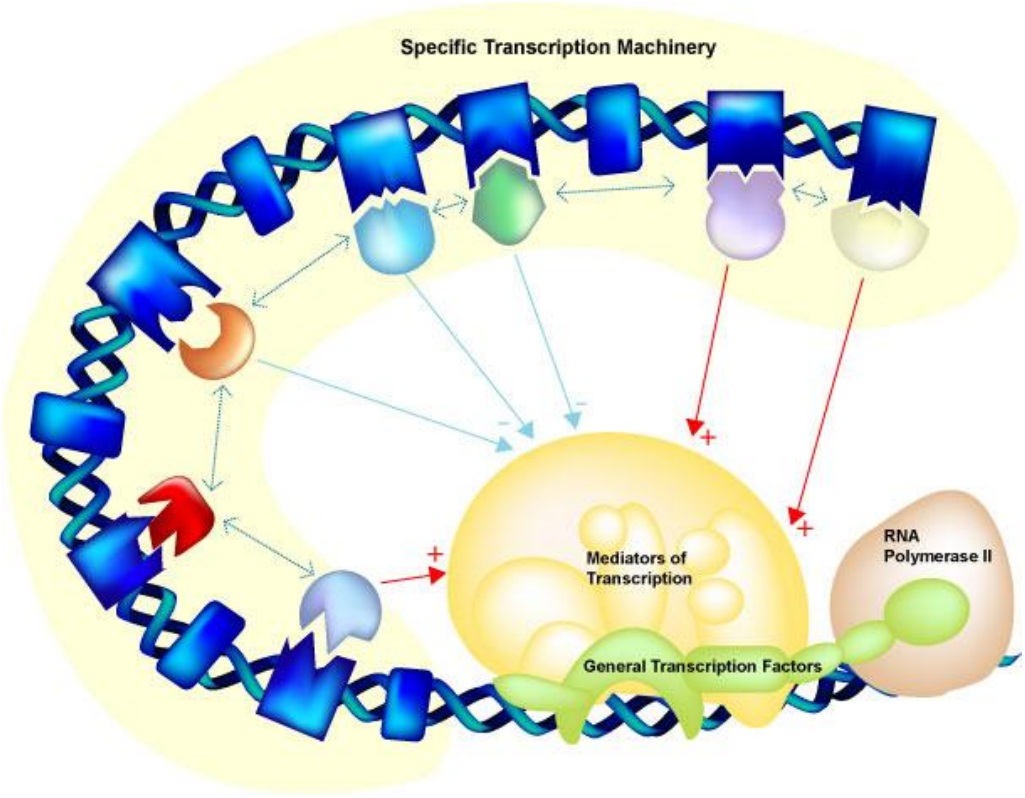

Figure 23. Different configurations of STFs and GTFs during gene expression. GTFs normally sit close to the starting point of transcription and interact directly with the RNA polymerase II . GTF are common to all genomes. The STFs are spread in the regulatory regions (close or relatively far from the TSS). Image adapted from http://legacy.genwaybio.com/gw_file.php?fid=2081

In the nucleus, the huge length of higher eukaryote chromosomal DNA is highly compacted due to the presence of protein complexes that together with DNA constitute the chromatin. The basic repeat element of chromatin is the nucleosome, composed by a globular octamer complex formed by histones (2 dimers of histone H3/H4 and 2 dimers of histones H2A/H2B). DNA can wrap around this core structure with two turns for a global length of 147 bp. Together with the inter nucleosomal DNA (linker DNA) of an approximative length of 60 nt these structures can form a fiber of approximately 10 nm width that is typically called "beads on a string" fiber. The conformation of chromatin has a very crucial effect of the possibility for a gene to be transcriptionally activated. The packaging of chromatin in highly condensed structures (heterochromatin) makes DNA inaccessible to the factors that are required for gene transcription. Post-translational modifications of histones are capable of inducing drastic changes to chromatin accessibility and therefore gene expression. The transcription of genes can be activated in the euchromatin conformation where the chromatin presents a relaxed conformation accessible to transcription factors (Hahn, 2004).

The balance between eu- and heterochromatin may be controlled by specific events: for example specific posttranslational modification such as acetylation of histones at specific residues (K9 or K27) or methylation of histone H3 in position K4 are known to be correlated with open euchromatin conformation. On the other hand, methylation on the position K9 and K27 of the histone H3 are correlated with a closed heterochromatin conformation. The enzymes responsible of the chromatin modification belong to distinct protein complexes (reviewed in (Suzuki and Bird, 2008), (Wang et al., 2004)). In addition, specific ATP-dependent chromatin remodeling machineries (Li and Greene, 2007) play a crucial role in the control of chromatin accessibility. Chromatin remodeling leads to transient unwrapping of the end DNA from histone octamers, moving nucleosomes to different translational positions (sliding), or forming DNA loops. All these modifications change the accessibility of nucleosomal DNA to transcription factors, allowing them to recognize their specific binding sites (reviewed in (Li et al., 2007)). Another crucial effect is generated by DNA modification via the specific methylation of cytosines located in CpG dinucleotides. This modification in mammalian cells is strictly correlated with transcriptionally inactive close heterochromatin configuration. This methylation can be inherited by daughter cells after mitosis (reviewed in (Suzuki and Bird, 2008)). Chromatin modifications are often responsible for a net change in the global electric charge of the nucleosome which, in turn, may loosen inter- or intranucleosomal interactions. This effect is evidenced by the observation that, after

acetylation, via histone acetyltransferase enzymes (HAT), histones are easier to displace from DNA. This gives access to the binding sites of transcription factors (Reinke and Horz, 2003).

Gene expression is finally the result of a concerted action of different control mechanisms. Chromatin conformation is structurally able to modulate the accessibility of transcriptional factors and transcriptional complex to their consensus sites on the DNA (figure 24). On the other hand, transcriptional factors themselves can interact and modify the chromatin conformation in order to modify silent heterochromatin into euchromatin which is typically in a transcriptionally active conformation. My studies focused on the role of a particular transcription factor, called HNF1beta. This protein has been shown to play a crucial role in differentiation and morphogenesis of several organs.

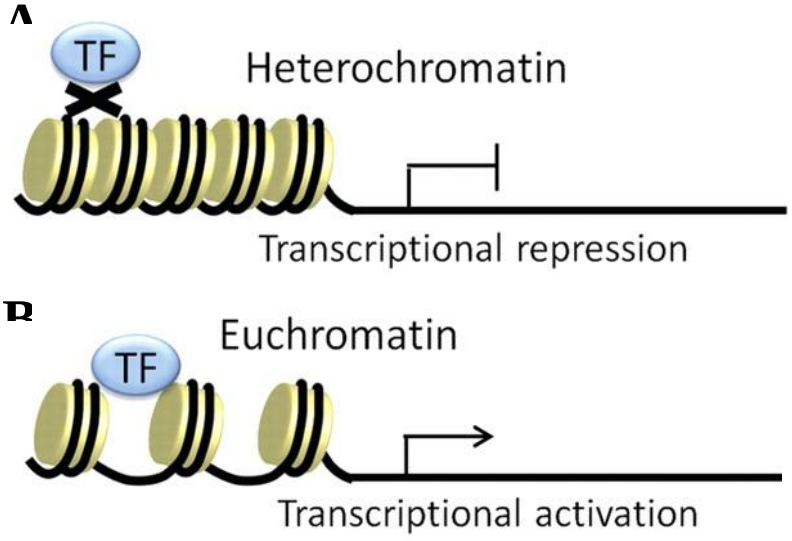

Figure 24. Chromatin conformation and control of transcription. The condensed (heterochromatin) or relaxed (euchromatin) chromatin conformation differently interact with the transcription factors. (**A**) A compacted chromatin conformation around the histones is not accessible to the transcription factors with a consequent transcription silencing. (**B**) Relaxation of the chromatin and the eventual dissociation of histones allow the transcription factors to reach their binding sites and activate the gene transcription (adapted from (Ohtani and Dimmeler, 2011)).

IV. 1 Structure of transcription factors and their specificity

Transcription factors specifically recognize and bind relatively short DNA sequences. The specificity for DNA binding is provided by a specialized protein domain called DNA binding domain. The vast majority of these domains recognize the consensus sequences by interacting with bases in the major groove of the DNA double helix. Some transcription factors can bind the DNA in a dimeric conformation. In most cases, this provides a significant increase in the specificity of DNA recognition. According to the protein structure of their binding domains, transcription factors can be classified in a small number of groups: the helix-turn-helix transcription factors family (that includes also the homeobox and the POU transcription factors), the zinc-finger motifs family, the basic leucin zipper family and the helix-loop-helix motif family. These different families differ in their structure and the way they interact with the DNA sequences.

The helix-turn-helix motif is one of the simplest DNA binding domains: it is formed by two α-helices connected together and held in a fix angle by a short chain of amino acids that constitutes the "turn". Some transcription factors are usually active in homo- or heterodimer configuration and bind symmetric (palindromic) consensus sites. Homeobox proteins are a special class of the helix-turn-helix transcription factors, characterized by a domain composed of 60 amino acids in which three α helices are connected by short loops. The C-terminal helix contains conserved hydrophobic residues that stabilize the structure and is responsible for the interaction with the major groove of DNA. This helix generally recognizes the typical homeobox target ATTA sequences. On the other hand, the other two shorter N-terminal helices are too far from the DNA to interact with it. The C-terminal helix and the loops between the other helices can form hydrogen bonds with the DNA backbone via the abundant arginine and lysine residues. The homeobox domain is also present in the POU proteins family. The name of this family derives from the first transcription factors that were described to contain the POU domain (Pit1, Oct1-2 and the Unc86 in the nematodes). The POU domain is a bipartite domain composed by two separate subunits connected by a variable and often flexible region. The N-terminal functional subunit is known as the POU-specific (POUs) domain, while the C-terminal subunit is a homeobox domain. The DNA binding specificity of these transcription factors is the net product of both the DNA binding of the POU domain and the homeobox (Phillips and Luisi, 2000). The paired box proteins (PAX) form another group of nine transcription factors that contains a paired-type homeodomain or,

in some members, a partial homeobox composed by only the first α-helix (PAX2, PAX5 and PAX8). These transcription factors contain also additional conserved motifs such as the conserved optapeptide (all except PAX6 and PAX4). The typical structure of PAX proteins is composed by N-terminal and C-terminal regions of the paired domain that are in contact with two successive major DNA grooves (Czerny et al., 1993).

Contrary to the helix-turn-helix motifs that are composed only by aminoacidic sequence, the Zinc finger DNA binding motif uses one or more zinc ions in coordination with structural components represented by cysteine, histidine, and occasionally aspartate sidechains. The presence of the zinc ion stabilizes the thermal stability of the conformation. Initially, this class of protein was named "zinc finger". One of the most recurrent classical motif binds zinc ion via a couple of histidine and cysteine (C2H2 Zn finger) and is composed by an α-helix and a β-hairpin structure. Zinc fingers motifs have the ability of creating multimers, increasing DNA binding specificity. At least 14 classes of Zinc finger containing transcription factors have been identified: these proteins share the presence of Zinc structural bindings, but differ for their conformation. Interestingly, specific class of zinc fingers are able to mediate the interaction of proteins with other molecules, including lipids, DNA/RNA and other proteins (Matthews and Sunde, 2002).

Another class of DNA binding proteins domain motifs are characterized by the presence of basic amino acids, (mostly arginine and lysine) in direct contact with the major groove of the DNA. This class of transcription factors includes the basic Leucine Zipper Domain and the basic Helix-loop-Helix Domain. The leucine zipper (also known as leucine scissors) is a super-secondary structure formed by a dimer of parallel α-helices: each helix contains several leucine residues regularly spaced at the distance of seven residues. These leucins form the core for lateral hydrophobic side. This conformation allows the zipper structure to dimerize with the corresponding leucines of the second helix, forming a coiled coil that is finally able to bind the major groove of the DNA (Landschulz et al., 1988). The basic Helix-Loop-Helix (bHLH) domain is structurally different and not related with the Helix-Turn-Helix DNA binding domains previously described: bHLH it is composed of two α-helices of different size, connected by a flexible loop. Usually, all transcription factors that contain a helix-loop-helix motif are dimeric. Each of them contains a DNA binding domain characterized by the presence of basic amino acid residues that provide the interaction interface with the major groove of the DNA. DNA binding region is provided by the bigger α-helix, whereas the smaller one is able to fold and allow the dimerisation with a second

transcription factor containing the same bHLH motif. This family of DNA binding motif recognize a specific sequence called E-box (5'CANNTG 3').

IV. 2 The Hepatocyte Nuclear Factor 1 family

The Hepatocyte Nuclear Factors 1 (HNF1s) family is a small family of transcription factors, composed by two members: HNF1α and HNF1β. They are encoded by the genes *HNF1A* and *HNF1B* in human and *Hnf1a* and *Hnf1b* in mouse. Historically, the HNF1 family members have been first identified as liver specific transcription factors, able to induce the expression of particular genes in hepatocytes in cell culture (Courtois et al., 1987). These two genes were cloned for the first time in the early 90s (Frain et al., 1989) ,(Rey-Campos et al., 1991), (Bach et al., 1992). Considering the high percentage of homology they share, they probably derive from the duplication of a common ancestral gene.

HNF1α and HNF1β are dimeric transcription factors, which can form both homo- and heterodimers. Each transcription factor is composed by three different functional domains (figure 25). The first domain is the dimerisation domain at the N-terminal part of the protein: the two transcription factors share 72% of homology in this portion and this characteristic allows them to form either homo- (α/α; β/β) or heterodimers (α/β) through the formation of four helix bundles structures. The strongest homology between HNF1α and HNF1β is observed in the DNA binding domain (91% of identity). This high level of identity explains the fact that both transcription factors can bind the same DNA consensus sequence 5'-GTTAATNATTAAC-3' (figure 26). The DNA binding region is composed by a homeodomain and 5 alpha helices structure: these domains are common with the transcription factors belonging to the POU family (for *Pit1*, *Oct1* and *Unc1*) (Tomei et al., 1992).The transactivation domain is located in the C-terminal part of the proteins. This domain is responsible for the interaction with co-regulator elements (Sourdive et al., 1993), (Tomei et al., 1992). Interestingly, HNF1α and HNF1β shared only 47% of identity/ homology in this portion. This low level of homology (Mendel and Crabtree, 1991) (figure 25), together with the distinct although overlapping pattern of expression in some tissues, could participate to the specificity of HNF1α and HNF1β (see below).

During early steps of embryogenesis, *Hnf1a* is not essential for normal mouse development. Its germline inactivation leads to hepatic, pancreatic and renal defects shortly after birth (Pontoglio et al., 1996). Conversely, *Hnf1b* germline inactivation leads to embryonic lethality at E7.5, due to a defective extraembryonic visceral endoderm differentiation (Coffinier et al., 1999b), (Barbacci et al., 1999). In order to circumvent this early lethality and to study the role of *Hnf1b* during organogenesis, chimeric tetraploid complementation strategy (Haumaitre et al., 2005) or mice carrying a *Hnf1b* floxed allele (Coffinier et al., 2002), allowing a Cre-LoxP strategy (Abremski and Hoess, 1984), have been generated.

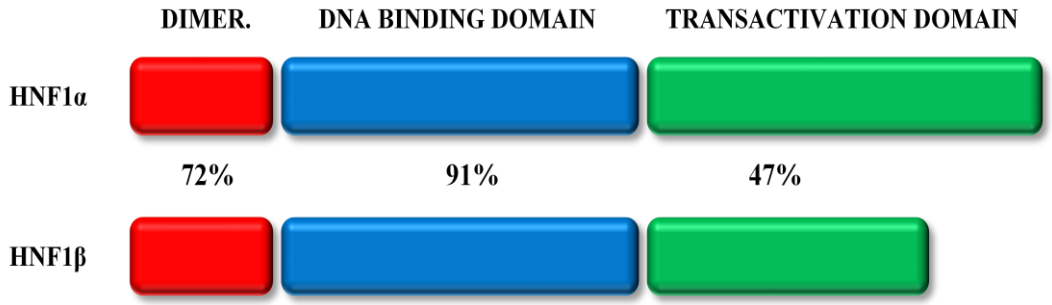

Figure 25 . Schematic representation of the two HNF1 family members and their relative homology. HNF1α and HNF1β share a high homology in the dimerization (72%) and DNA binding (91%) domains. The diversification in transactivation domain (only 47%) could participate to the different characteristics of the two factors.

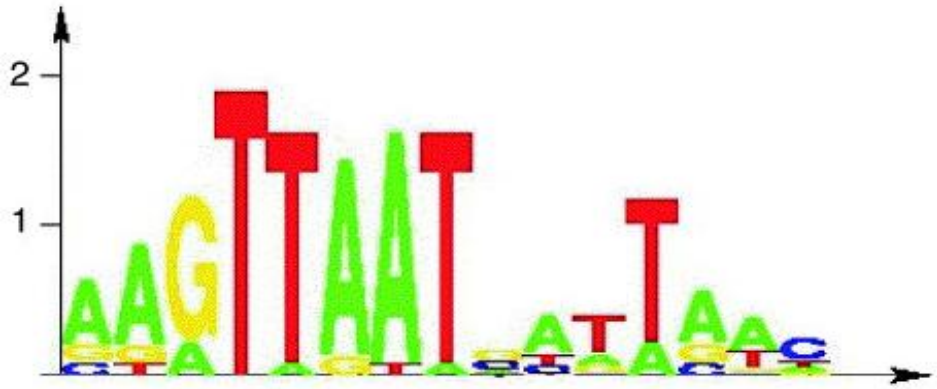

Figure 26 . Graphic representation of the palindromic HNF1 consensus sequence. On the horizontal axis are represented the different nucleic acids present in different known binding sites. Their frequency is plotted on the vertical axis (from (Krivan and Wasserman, 2001)).

HNF1α and HNF1β are both expressed in epithelial structures of several organs such as liver, kidney, pancreas and intestine (Pontoglio et al., 1996), (Coffinier et al., 1999a). I will briefly describe the role played by *Hnf1a* and *Hnf1b* in the different organs (table 8) and focus on the specific role of *Hnf1b* in the kidney and its implication in human renal diseases.

As we said before, the two transcription factors, HNF1α and HNF1β (known also as HNF1 and vHNF1 respectively), were initially characterized as two closely related homeoproteins that activate the transcription of liver specific genes (Rey-Campos et al., 1991). In this organ, the two transcription factors have a different expression pattern. *Hnf1b* is expressed early during liver morphogenesis and it is mostly restricted to the biliary ducts and only slightly expressed in the periportal hepatocytes, whereas *Hnf1a* is expressed later and more diffusely in both hepatocytes and colangiocytes (Coffinier et al., 2002), (Pontoglio et al., 1996). In early steps of liver specification, the endoderm activates the expression of early liver specific genes such as albumin (*Alb*), transthyretin (*Ttr*) and alpha fetoprotein (*Afp*): these genes characterize the nascent bipotential precursors of hepatoblast population from which the hepatocytes and biliary cells are derived (Lemaigre and Zaret, 2004).

Tetraploid/diploid compounds experiments rescued the early lethality of *Hnf1b* inactivation. In this model, extraembryonic tissues develop normally, whereas the epiblast derives exclusively from *Hnf1b* deficient ES cells. This technique allowed obtaining embryos that develop until E15-16.5. Analysis of these embryos showed that the absence of *Hnf1b* in embryonic tissues results in a drastic defect of liver differentiation from the ventral mesoderm and the absence of liver bud emergence. These defects are due to the severe downregulation of specific transcription factors that are in charge of starting the hepatic developing program (including *Foxa2, Hnf4, Hnf1a, Hnf6* and *Gata6*). These results showed that *Hnf1b* controls the expression of crucial transcription factors at the origin of hepatic differentiation (Lokmane et al., 2008). Inactivation of *Hnf1b* in the liver after these first developmental steps has been obtained with the use of an AlfpCre mouse strain (AlfP-CRE, (Kellendonk et al., 2000)), expressing the Cre under the control of regulatory sequences present in albumin and α-fetoprotein. This strategy allows the recombination of the floxed *Hnf1b* alleles in hepatoblasts that will give rise to both hepatocytes and biliary cells. With this model of inactivation, mutant animals survive few weeks after birth and suffer from a severe defect in intrahepatic biliary ducts development and metabolic dysfunctions: mice affected by *Hnf1b* AlfpCre

deletion suffer from defective biliary ducts branching and dysplastic glad bladder that leads to bile accumulation in the serum (hyperbilubinemia). This defect is probably a consequence of drastic downregulation, in absence of *Hnf1b,* of a sodium-independent transporter *Oatp1 (Slc21a1)* (Coffinier et al., 2002). The other *Hnf1* family member, *Hnf1a*, is expressed later during liver development and diffusely in all hepatocytes and cholangiocytes: lack of *Hnf1a* is correlated to hepatomegaly and leads to hyperphenylalaninemia (Pontoglio et al., 1996). The phenylalanine hydroxylation is an obligatory step for the metabolic conversion of this essential amino acid and it is carried out by the phenylalanine hydroxylase (PAH). *Hnf1a* has been reported to directly bind a PAH enhancer sequence and mice lacking *Hnf1a* suffer from an absence of expression of this gene (Pontoglio et al., 1996). The inactivation of *Hnf1a* impairs the chromatin opening and causes hypermethylation of transcription control sequence upstream phenylalanine hydroxylase promoter. These defects leave the chromatin in a closed conformation, preventing the gene to be expressed (Pontoglio et al., 1997).

Besides liver development and function, *Hnf1* family transcription factors are very important during the development of other organs including the gastro intestinal tract. In particular, they are expressed during the organogenesis of pancreas and intestine. *Hnf1b* is expressed in the very early stage of organ cell type's specification, whereas *Hnf1a* begins to be expressed later in already differentiated structures (Ott et al., 1991), (Coffinier et al., 1999a). The pancreas emerges from the foregut-midgut junction as ventral and dorsal outgrowth that lately fuse to form a complex organ, composed by two different compartments (reviewed in (Jorgensen et al., 2007)). The exocrine compartment of the pancreas is composed by the pancreatic acini and produces the digestive enzymes. These enzymes are used by the digestive tract to further break down carbohydrates, proteins and lipids. The endocrine function is provided by the islets of Langerhans: these spherical structures are composed by different specific cell types that secrete hormones to regulate, mainly, the glucose homeostasis. More in particular, in these islets, α cells produce glucagon, β cells produce insulin, δ cells are responsible for somatostatin secretion, and finally γ cells synthetize the pancreatic polypeptide. During pancreas morphogenesis, *Hnf1b* has very important roles in the primordial structure formation and fate acquisition (Haumaitre et al., 2005). The pancreatic differentiation, that takes place at the junction mid-foregut, is tightly regulated by the restricted balance between the signalling molecule *Sonic Hedghog* (*Shh*) and the homeobox gene *Ipf1* (or *Pdx1*): the expression domains of these two genes are mutually exclusive and *Ipf1* is necessary to establish the pancreatic primordium territory in a place

where *Shh* is not expressed (Ahlgren et al., 1997). *Hnf1b* early inactivation in the embryonic development leads to pancreatic agenesis. This agenesis is a consequence of the direct downregulation of *Ipf1* and the expansion of *Shh* territory that does not allow the gut to acquire the pancreatic fate (Haumaitre et al., 2005). *Hnf1a*, in the other hand, is not necessary for the first steps of pancreatic development but it has an important role in the control of genes expressed in endocrine cells. Homozygous germline inactivation of *Hnf1a* in mouse leads to diabetes, due to defective insulin secretion. Analysis of these animals has shown alterations in the pathways that regulate β cell responses to glucose and arginine (Pontoglio et al., 1998). Gene expression studies of *Hnf1a*-deficient mice identified a wide spectrum of *Hnf1a* direct targets. Some of these genes are specifically expressed in the pancreas and their defective expression is responsible for defective nutrient metabolism and hormone production-secretion (Servitja et al., 2009), (Shih et al., 2001).

The development of the intestine is an example of redundancy between *Hnf1a* and *Hnf1b*: single inactivation of either *Hnf1a* or *Hnf1b* does not lead to defects, whereas combined germline inactivation of *Hnf1a* and *Hnf1b* specific Cre-driven inactivation in the intestine (Villin-cre Ert2) leads to severe defect in intestinal epithelial cells development (D'Angelo et al., 2010). The double mutant animals died from dehydration shortly after gene inactivation: the lethality is due to downregulation of *Slc26a3* expression, a gene encoding for an anion exchanger involved in intestinal water absorption (D'Angelo et al., 2010). The absence of *Hnf1a* and *Hnf1b* also affects the final differentiation of both the secretory and absorptive cell population: *Hnf1* factors inactivation have been shown to affect *Atoh1* expression and the Notch signaling (via direct downregulation of the receptor *Notch2* and its ligand *Jag1*). These two binary alternative fates are responsible for the specification of secretory (paneth or goblet cells) and absorptive (enterocytes) lineage differentiation, respectively. The double mutant mice showed a significant increase of committed goblet cells that however were lacking the final differentiated markers: this unbalanced higher commitment of secretory respect to the absorptive lineage is possibly due to the downregulation of Notch signaling in absence of *Hnf1a* and *Hnf1b* (D'Angelo et al., 2010).

Table 8. Role of Hnf1a and Hnf1b in different organs

Organ	***Hnf1a* inactivation**		***Hnf1b* inactivation**	
	Malformations	Models (Ref)	Malformations	Models (Ref)
Liver	Hepatomegaly Hyperphenyl-alaninemia	Germline Inactivation (Pontoglio et al., 1996)	Drastic defect in liver specification	Tetrapliod compound (Lokmane et al., 2008) Epiblast inactivation (unpublished)
			Severe defect in intrahepatic biliary duct formation	AlfpCre inactivation (Coffinier et al., 2002)
Pancreas	Diabetes due to a defective insulin secretion	Germline inactivation (Pontoglio et al., 1996) (Pontoglio et al., 1998)	Pancreas agenesis	Tetraploid compound (Haumaitre et al., 2006)
Intestine	No phenotype	Germline inactivation (D'Angelo et al., 2010)	No phenotype	Villin Cre inactivation (D'Angelo et al., 2010)
	Defective differentiation of secretory and absorptive cell population	Germline inactivation and Villin Cre inactivation of Hnf1b (D'Angelo et al., 2010)	Defective differentiation of secretory and absorptive cell population	Germline inactivation and Villin Cre inactivation of Hnf1b (D'Angelo et al., 2010)

IV. 3 The Hepatocyte Nuclear Factors 1 in the kidney

The Hnf1 family members are also important for kidney development and function. As discussed before, *Hnf1a* is not necessary for the morphogenesis of the kidney, but its inactivation leads to severe functional defects (Pontoglio et al., 1996). *Hnf1a* is selectively expressed in proximal tubules: this tubular segment is responsible for massive reabsorption of water and small low molecular weight molecules that can pass through the glomerular filtration barrier such as glucose, phosphates and aminoacids.

Homozygous inactivation of *Hnf1a* leads to the loss of several of these molecules in the urine: the mutant animals suffer, just after birth, from polyuria, glucosuria, phosphaturia and aminaciduria (Pontoglio et al., 1996) that are characteristic features of the renal Fanconi's syndrome in human. The defective reabsorption of these components has been related to defective expression of proximal tubules membrane transporters and co-transporters. During primary urine processing, glucose is mainly reabsorbed via the sodium-dependent co-transporter *Slc5a2 (SGLT2)*, a low affinity co-transporter expressed in the brush border membrane of S1 and S2 proximal tubular cells. Its expression level is strongly decreased in absence of *Hnf1a* (Pontoglio et al., 1996). In a similar manner, most of phosphates are reabsorbed via sodium/phosphate transporters (*Npts*). In *Hnf1a* mutants affected by phosphaturia, the expression of a specific Npt transporter, *Npt1*, in proximal tubules is drastically decreased (Cheret et al., 2002).

MODY5/HNF1B patients suffer from renal developmental malformations. However, the molecular mechanism of this phenotype is still poorly understood. The study of mouse models helped to elucidate some of the roles of *Hnf1b* during kidney morphogenesis (table 9). *Hnf1b* is expressed since the first step of kidney morphogenesis. Its expression is detectable in the nephric duct (the Wolffian duct) and in the ureteric bud as soon as it emerges from the Wolffian duct. *Hnf1b* is not expressed in the uninduced metanephric mesenchyme. However, it is turned on in the first step of epithelial derivates, starting from the renal vesicle stage. The expression of this factor is maintained in the adult kidney, where it is expressed in the collecting duct system (derived from the branching of ureteric bud) and in the tubular part of the nephron (derived from the mesenchymal-to-epithelial transition of the metanephric mesenchyme) (Coffinier et al., 1999a).

The morphogenesis of kidney starts with the invasion of the ureteric bud in the metanephric mesenchyme where it undergoes a serial of dichotomic branches: at this stage, *Hnf1b* is expressed in the Wolffian duct and in the branching ureteric bud (Coffinier et al., 1999a). To avoid the early lethality linked to the essential roles of *Hnf1b* in the extraembryonic tissue, chimeric compounds driven studies have made use of tetra- and diploid embryonic stem cells in order to allow the extraembryonic tissues to develop normally. The mutants obtained showed that the absence of *Hnf1b* leads to severe defects in early steps of kidney development (Lokmane et al., 2010): *Hnf1b* inactivation affects the ureteric bud development, leading to abortive branching. The few branches are characterized by a *Wnt11* downregulation and a delayed expression of the GDNF receptor *Ret*, underlining a defective ureteric bud tip patterning (Lokmane et al., 2010). This defect in the ureteric bud impairs the crosstalk between ureteric bud tip and metanephric mesenchyme: the mesenchyme, in the absence of proper stimuli from the ureteric bud, is no longer able to begin the mesenchymal-to-epithelial transition and the subsequent nephrogenesis. It has been shown that this malformation seems to be linked to the direct downregulation of key genes expressed in the ureteric bud (Lokmane et al., 2010), known to be crucial in epithelial to mesenchymal transition, such as *Wnt9b* (Carroll et al., 2005).

The production of mice carrying *Hnf1b* floxed alleles (Coffinier et al., 2002) enabled its inactivation in selective tissue and/or at different time points. Specific inactivation of *Hnf1b* has been carried out in elongating collecting ducts and Henle's loop with a mouse strain expressing the Cre-recombinase under the control of *Cadherin 6* (Ksp) promoter (Gresh et al., 2004), (Fischer et al., 2006), (Verdeguer et al., 2010). In this model, the absence of *Hnf1b* resulted in dilation of tubules already at birth that form cysts few days after (Gresh et al., 2004). This study, carried out in our laboratory, showed that *Hnf1b* is able to directly regulate the expression of several genes known to be mutated in cystic human renal pathologies. In particular, it has been described a drastic downregulation of Polyductin1/Fibrocystin (Pkhd1), Polycystin2 (Pkd2), Uromodulin (Umod), and Nphp1 (Gresh et al., 2004). Interestingly, Pkhd1 and Pkd2 gene products are located in a specialized cell organelle, the primary cilium. The primary cilium is considered as a sensor of the extracellular environment and plays a key role in cyst formation (Pazour et al., 2002), (Yoder, 2007). Pkd2 has been shown to modulate proliferation. To determine if an abnormal cell proliferation was at the basis of cyst formation in this model, the pattern of proliferation was investigated, during the tubular elongation process. During tubular maturation, tubular cells

begin an intense but controlled proliferation in order to elongate tubules until they have reached their final length. This tubular elongation is characterized by an oriented cell division (OCD)/planar cell polarization, which participates in the maintenance of a constant tubular diameter. This peculiar OCD is lost in *Hnf1b*-deficient tubules, participating to tubular dilation (Fischer et al., 2006).

By using a transgenic mouse strain that express an inducible Cre (Mx-Cre, (Kuhn et al., 1995)), it has been possible to inactivate *Hnf1b* at different time points after birth (Verdeguer et al., 2010). In this way, our laboratory indentified a cystogenic competence window that lasted approximately until post natal day 10 (P10). Inactivation of *Hnf1b* after this period did not cause any phenotype unless tubular cells were forced to proliferate. During the cystogenic competence period, massive cell proliferation still occurs in elongating renal tubules, whereas after this period, cell proliferation is progressively shut down. Tubular cell proliferation can be reinduced in adult animals by performing an ischemia-reperfusion injury. Interestingly, by doing such an injury, cyst formation is again observed in *Hnf1b*-deficent tubules (Verdeguer et al., 2010). In this context our group has shown that when *Hnf1b* is inactivated in quiescent cells, most of its target genes continue to be expressed. However, when cells proliferate the expression of most of them (such as *Pkhd1*, *Pkd2*, *Kif12*, *Crb3*, *Tcfap2b*, *Tmem* and *Bicc1*) is eventually turned off. Our laboratory has shown that HNF1β acts as a chromatin bookmarking factor that is required for postmitotic gene expression reprogramming (Verdeguer et al., 2010).

All these studies improved our knowledge about the molecular mechanisms of gene exrpression controlled by *Hnf1b*. As discussed before, *Hnf1b* is expressed in nephron tubular precursors that give rise to all tubular segments of the nephrons. Morphogenesis and specification of the different nephron segments are tightly controlled processes. The aim of my project is to elucidate the role of this transcription factor in the very early steps of nephrogenesis, making use of different inactivation strategies.

Table 9. Role of Hnf1b in kidney

***Hnf1b* inactivation in kidney**	
Malformations	**Models**
Drastic defect in kidney morphogenesis	- Tetraploid compound (Lokmane et al., 2010) - Epiblast inactivation (unpublished data)
Polycystic disease	- Ksp-Cre inactivation during tubular elongation (Gresh et al., 2004) -Mx-Cre inactivation during tubular elongation (Verdeguer et al., 2010)
No phenotype	- Mx-Cre inactivation in mature kidney (Verdeguer et al., 2010)
Absence of tubular specification and expansion	- Six2-Cre inactivation (Unpublished data)
Tubular dysmorphogenesis and cyst formation	- Rarb2-Cre inactivation (Unpublished data)

Introduction V

V. Hnf1 transcription factors and human diseases (MODY syndrome)

The liver-enriched transcription factors HNF1A and HNF1B were first discovered in studies designed to identify proteins responsible for the tissue-specific regulation of gene expression in the liver. Subsequent studies have shown that these two factors are expressed in other organs, including the pancreas, the kidneys, and genital apparatus. Mutations in these two genes are involved in Maturity Onset Diabetes of the Young (MODY) syndrome: the term refers to monogenic form of diabetes that appears before 25 years of age. In fact, the appearance of clinical symptoms occurs within the first three decades of life in the majority of the patients, but few can live the entire life with a non-diagnosed MODY syndrome. Mutations in several different genes have been currently identified in MODY patients (table 10). In particular, the glucokinase gene encodes an enzyme of the glycolytic pathway and mutations in this gene are involved in MODY type 2 diabetes, whereas some other genes encode nuclear proteins that control the appropriate expression of pancreatic β-cell genes. Mutations in the transcription factors HNF1A and HNF1B are the cause of MODY type 3 and type 5 onsets, respectively. Mutations in IPF1 (Insulin Promoter Factor-1), encoding a homeodomain-containing protein, are found in MODY type 4 patients, whereas mutations in HNF4A, that encodes a steroid nuclear receptor family member, cause MODY type 1. More recently, new and rare MODYs diseases have been identified: the majority of them do not affect directly the glucose metabolism, except for MODY10 that is characterized by mutation in the Insulin gene. Mutations in NeuroD1 (Neurogenic Differentiation-1, a basic helix-loop-helix transcription factor) have been described in MODY6 patients. MODY7 is associated with mutation in the Kruppel-like factor 11 (KLF11), whereas MODY9 is related to mutation in the transcription factor PAX4. The last described is MODY10, associated with mutations in the B-lymphocyte tyrosine kinase.

Table 10. Genes involved in Maturity onset diabetes of the young (MODY)

Type	OMIM	Gene (protein) involved / chromosome location	Incidence
MODY 1	125850	**Hepatocyte nuclear factor 4α** (HNF4A) / Chrom:20q12-q13.1	5%
MODY 2	125851	**Glucokinase** (GKC) / Chrom: 7p15-p13	22%
MODY 3	600496	**Hepatocyte nuclear factor 1α** (HNF1A) / Chrom: 12q24.2	58%
MODY 4	606392	**Insulin promoter factor-1** (IPF1) / Chrom: 13q12.1	rare
MODY 5	137920	**Hepatocyte nuclear factor 1β** (HNF1B) / Chrom: 17cen-q21.3	2%
MODY 6	606394	**Neurogenic differentiation 1** (Neuro D1) / Chrom: 2q32	rare
MODY7	610508	**Kruppel-like factor 11** (Klf11) / Chrom: 2p25.1	rare
MODY8	609812	**Bile salt dependent lipase** (Cel) / Chrom : 9q34.2	rare
MODY9	612225	**Pax4** / Chrom 7q32.1	rare
MODY10	613370	**Insulin** (Ins) / Chrom 11p15.5	rare
MODY11	613375	**B-lymphocyte tyrosine kinase** (Blk) /Chrom: 8p23-p22	rare

V. 1 Pancreatic defects correlated to MODY syndrome

MODY type 3, due to HNF1A mutations, is the most common type of MODY in populations with European ancestry. It is responsible for about 70% of all MODY cases in Europe (Yamagata et al., 1996). A wide spectrum of mutations in HNF1A has been identified in MODY3 patient families: mutations can span all over the three domains of the protein, but they are frequently identified in a hot-spot present on the exon 4 (Kaisaki et al., 1997). In addition, mutations in the promoter region have been reported to decrease the transcriptional activity of the gene (Godart et al., 2000). The abnormal glucose homeostasis affecting the patients carrying HNF1A mutations is due to a severe defect in insulin secretion due to abnormal glucose sensing of β cells in pancreatic Langerhans islets. Interestingly, studies carried on transcriptional cascades in the pancreas suggested a reciprocal control between HNF1A and HNF4A, a nuclear receptor whose mutations are involved in MODY type 1 (Stoffel and Duncan, 1997), (Duncan et al., 1998). Maturity onset diabetes of the young type 5 is correlated with HNF1B mutations. The first mutation in HNF1B was reported in a MODY5 patient described in 1997 (Horikawa et al., 1997): subsequent analyses discovered a wide range of mutations affecting different domains of the gene, including missense, nonsense, frame-shift, splice site mutations and single exon deletion/duplication/translocation.

In addition, whole HNF1B gene deletion seems to be the most common mutational mechanism (Bellanne-Chantelot et al., 2005). The incidence of HNF1B mutations among the total diabetic patients is however modest and attends only 2% of MODY patients (Fajans and Bell, 2011).

V. 2 Renal defects correlated to MODY syndrome

MODY3 and MODY5 patients are characterized by a variable severity of kidney pathologies. As we described before, HNF1A is expressed in renal proximal tubules, where massive reabsorption of glucose and water takes place. MODY3 patients carrying HNF1A mutations suffer from defective renal reabsorption of glucose: this loss of glucose in the urine participates to "maintain" normal level of glycemia (glucosuria normo-glycemic) (Menzel et al., 1998). In mouse, germline inactivation of *Hnf1a* leads to glucose reabsorption defect very similar to the one observed in human patients affected by MODY3. This defective glucose reabsorption is due to a defective expression of Slc5a2 (SGLT2), a gene whose expression is controlled by HNF1α (Pontoglio, 2000). This low affinity, high capacity glucose transporter expressed in the proximal tubule, is responsible for most of the renal reabsorption of glucose. The inactivation of *Hnf1a* leads affects also the phosphate transporter *Npt1* and *Npt4 expression* via direct control of several phosphate cotransporteur (Cheret et al., 2002).

Much more severe and complex are the renal defects observed in MODY5 patients. Recent studies have consolidated the idea that the first trait of patients carrying HNF1B mutations is represented by renal malformations, compared to the relative low incidence of diabetes mellitus. Almost all the patients carrying HNF1B mutations present with renal structural abnormalities, whereas glycemia defects are present only in around half of the patients (around 58%). For all these reasons, MODY5 disease has been proposed as Renal Cysts and Diabetes (RCAD) due to the higher incidence of cystic kidney phenotype compared to the one of the diabetic traits (Rizzoni et al., 1982). The renal cystic malformations involve mostly cysts derived from the tubular compartment of the nephrons but hypoplastic familiar glomerular cystic kidney disease (FGCKD) has also been reported (Bingham et al., 2001), (Lindner et al., 1999). Experimental studies in animal models showed a direct implication of *Hnf1b* in the expression of genes that, if mutated in the human, give rise to renal cystic phenotypes: in particular *Hnf1b* has been demonstrated to directly regulate the expression of

Pkhd1 (responsible for autosomal recessive polycystic disease, ARPKD) and *Pkd2* (autosomal dominant polycystic kidney disease, ADPKD) (Gresh et al., 2004), (Hiesberger et al., 2004).

Besides the presence of cysts, that represent the more constant renal abnormality, MODY5 patients present with a large variety of renal pathological traits, concerning mostly developmental abnormalities that I will describe in details later. The variability of the phenotype could be explained by the wide range of mutations described in families affected by MODY5. Recent clinical studies have shown more than 60 different heterozygous mutations all over the HNF1B locus, causing missense, frameshift, non sense and splice site defects. Interestingly, occurrence of mutations in the DNA binding domain, composed by exons 2-3 and part of the exon 4, has been described in around 70% of patients (Chen et al., 2010). Besides point mutation, genomic rearrangements include duplications, inversion or single exon deletion (frequently concerning the exon 5) has been described. Interestingly, large genomic rearrangements are also very frequent: whole-gene deletion of the HNF1B locus is considered as the most common genotype leading to malformation (Bellanne-Chantelot et al., 2005). This large genomic deletion pointed out a possible under estimation of MODY5 incidence in the population due to the apparent absence of mutation (Bellanne-Chantelot et al., 2004). In humans, one other characteristic of the majority of HNF1B mutations is represented by de novo mutations, predominantly represented by large genomic deletions. The intrinsic genomic instability of the HNF1B locus is linked to the presence of large (>70Kbp) genomic segmental duplications that surround the locus at the distance of more than 1 Mbp (Bellanne-Chantelot et al., 2004), (Carette et al., 2007). This observation suggest the idea that this gene has a particularly fragile structure easily prone to the occurrence of unequal crossing over between these segmental duplications that might account for the genomic rearrangements at this locus (Bellanne-Chantelot et al., 2004), (Carette et al., 2007).

Recent studies on pediatric cohorts have shown that renal malformations are detected by ultrasound imaging in approximatively 20-30% of young patients/fetuses carrying HNF1B mutations. These defects are part of the Congenital Abnormalities of the Kidney and Urinary Tract (CAKUT) (Ulinski et al., 2006). CAKUT syndrome represents 20-30% of prenatal abnormalities and it occurs in 1 out of 500 or 1 out of 1000 births. CAKUT are responsible for about 40% of cases of chronic kidney disease in children (Neild, 2011). Although some forms

of CAKUT are part of multisystemic syndromes or are associated with family history, most of the renal anomalies are sporadic and concern only the kidney and/or the urinary tract. CAKUT syndrome includes a wide range of structural and functional malformations that can affect the kidney (renal hypo-dysplasia, hydronephrosis) or the urinary tract such as megaureter in collecting system, ureterocele and vesicoureteral reflux (reviewed in (Song and Yosypiv, 2011)).

CAKUT represents a developmental pathology, due to a defective program of kidney morphogenesis (Cain et al., 2010), (Schedl, 2007) (table 11). It has been shown that defective function of a considerable number of transcription factors is involved in this pathology, among which HNF1B mutations. Mutations in *HNF1B* are the most common genetic cause leading to CAKUT (Song and Yosypiv, 2011). The use of animal models has provided a deep insight on the role played by these genes during renal morphogenesis. These studies have help to build the genetic networks at the base normal development of the kidney (reviewed in (Song and Yosypiv, 2011)). Concerted inductive interactions of many genes, expressed in the different compartments during the development, are required for normal morphogenesis of the kidney and lower urinary tract: monogenic mutations might affect kidney development at multiple steps and cause a broad phenotypic spectrum of CAKUT that ranges from cysts formation to total renal agenesis, according to the specific compartment affected during the development and the different penetrance of the phenotype.

In this context, *HNF1B* is expressed during all the step of kidney morphogenesis. In human, it has been well described that mutations of its sequence can lead to severe malformation of the kidney. Nevertheless, the precise role of *HNF1B* at different timing and in different compartments has not been yet completely elucidated.

Table 11. Non-syndromic human congenital anomalies in the kidney and urinary tract CAKUT (adapted from (Song and Yosypiv, 2011))

Type of malformation	Cause	Anatomical malformations	Genes involved
Renal agenesis	No interaction between the MM and the UB	- Absence of ureter and kidney	Ret/GDNF
Renal hypoplasia	Aberrant interactions among the UB and MM or stroma	- Reduced number of UB branches –Reduced nephrons formed - small kidney size	Pax2 Sall1 Six2 BMP4 **HNF1β** UMOD
Renal dysplasia	Aberrant interactions among the UB and MM or stroma	- Reduced number of UB branches and nephrons - Presence of undifferentiated stromal and mesenchymal cells, cysts and cartilage - Frequently associated with kidney hypoplasia	Pax2 **HNF1β** UMOD Nphp1 BMP4 Six2
Polycystic kidneys	Abnormal tubular and collecting duct patterning	- Cysts in tubules and collecting duct - Normally formed glomeruli	PKDH1 PKD2 **HNF1β**
Multicystic dysplastic kidneys	Aberrant interactions among the UB and MM or stroma	- Absence of glomeruli and tubules - Presence of large cysts Aberrant patterning Poorly formed atreic ureters	**HNF1β** UPIIIA
Medullary cystic kidneys	Aberrant interactions among the UB and MM or stroma	- Tubular atrophy, interstitial fibrosis, Cysts in distal tubules and medullary collecting ducts	UMOD
Duplex ureter	Supernumerary UB budding from the Wolffian duct	- Duplex ureters and kidneys or duplex ureters and collecting ducts - Vesicoureteral reflux or obstruction in presence of ectopic UB emergence	ROBO2 FOXC1-C2 BMP4
Horseshoe kidney	Defect in renal capsule	- Kidney are fused at inferior lobes and located lower than usual	**HNF1β**

Project Design

Project Design

Congenital Abnormalities of Kidney and urinary Tract (CAKUT), a genetic disorder that affects 1 out 500 newborns is characterized by a wide spectrum of renal malformations of different degrees of severity (Neild, 2011), (Chen et al., 2010). CAKUT are present already at birth and they have as origin a defect in the renal development program. CAKUT-related malformations are one of the major features in a monogenic diabetic syndrome with early onset, the Maturity Onset Diabetes of the Young (MODY) type 5. This syndrome is due to mutations of HNF1B (Horikawa et al., 1997), a transcription factor belonging to the hepatocyte nuclear factor-1 family. Several studies have described a large set of mutations occurring in the sequence of HNF1B, ranging from point mutations to large scale genomic rearrangements. Another trait of MODY5 patients is a high variability in the renal phenotype in presence of the same mutation. The spectrum of malformations is principally composed by cysts, but patients can also present with renal hypo-dysplasia to total renal agenesis in the most severe cases (Chen et al., 2010), (Heidet et al., 2010), (Ulinski et al., 2006).

Hnf1b is expressed in all the epithelial tubular structures of the kidney both during the renal morphology and adult kidney. Analysis of animals carrying inactivation of *Hnf1b* (germline or tissue specific) has partially elucidated the different important roles of this gene during embryogenesis or organ development and maturation. These models have shown that different phenotypes can be observed depending on the time and place of *Hnf1b* inactivation. For instance, *Hnf1b* germline inactivation leads to early embryonic lethality (Barbacci et al., 1999), (Coffinier et al., 1999a), whereas later inactivations are responsible for kidney malformations often characterized by cysts (Gresh et al., 2004), (Hiesberger et al., 2004), (Verdeguer et al., 2010), (Fischer et al., 2006). The early lethality of *Hnf1b* germline inactivation can be circumvent by a strategy based on chimeric compounds made by wild type extraembryonic tissues and mutant epiblastic cells. These embryos develop until E15.5 and suffer from a complex set of dysfunctions including a drastic defect in kidney morphogenesis. This severe renal defect affects the ureteric bud branching and prevents the formation of nephron (Lokmane et al., 2010). Specific inactivation of *Hnf1b* in already formed nephrons (Ksp-Cre mediated inactivation) demonstrated that *Hnf1b* regulates the tubular caliber during elongation through the direct control of several genes expressed in the cilium. In particular, *Hnf1b* can regulate the expression of several genes whose mutations in human is linked to cystic kidney diseases, such as *PKHD1*, *PKD2* and *UMOD* (Gresh et al., 2004), (Fischer et

al., 2006). A peculiar role of *Hnf1b* has been elucidated during cell proliferation. Recently, the concept of "bookmarking" function has been introduced concerning the intrinsic function of some transcription factors to remain bound to the chromatin during mitosis. This property has been demonstrated for *Hnf1b* (Verdeguer et al., 2010), suggesting a key role of this factor in restoring the expression of some target genes just after mitosis.

As we saw before, during the development, the kidney components derive from two distinct compartments that are in tight communication: the renal collecting system derives from the branching process that occurs in the ureteric bud, whereas the nephrons derive from the condensation and epithelialisation of the cap metanephric mesenchyme (reviewed in (Little et al., 2010)). *Hnf1b* is expressed since the early formation of the nephric duct (Wolffian duct) and its expression persists in the ureteric bud during all the branching process. This factor is not expressed in the metanephric mesenchyme, but its expression is switched on in the epithelial structures derived from the mesenchyme during nephron development. *Hnf1b* is expressed from the stage of vesicle, only in a restricted domain (Coffinier et al., 1999a) and its expression persists all along the successive steps of nephron formation and in the tubular part of the mature nephron.

Various renal phenotypes are observed in MODY5 patients, including hypoplasia due to a defective ureteric branching, and dysplasia, a consequence of defective nephron formation. These observations suggest that *Hnf1b* could play different roles during nephrogenesis, regulating both collecting duct system and nephron formation. To elucidate these roles, we designed animal models at different time of inactivation, and in different compartments of the developing kidney. In the first part of my work, I have used a Cre recombinase expressed under the control of promoter of genes expressed in the epiblast (Mox2, (Tallquist and Soriano, 2000), and Sox2, (Hayashi et al., 2002)). This approach allowed us to inactivate *Hnf1b* floxed alleles ($Hnf1b^{f/f}$ or $Hnf1b^{LacZ/f}$) (Coffinier et al., 1999b) exclusively in the embryonic tissues, rescuing the lethal phenotype due to extraembryonic tissue differentiation described in the germline inactivation (Barbacci et al., 1999), (Coffinier et al., 1999a). This inactivation leads to severe defect in the early steps of metanephric development and allowed us to study the role played by *Hnf1b* specifically in ureteric bud branching. In the second part of the project, we have inactivated *Hnf1b* specifically in the metanephric mesenchyme, in a context where the ureteric bud remains wild-type. For this purpose, we used mouse lines expressing the Cre recombinase specifically in the metanephric mesenchyme (Six2- and Rarb2- driven Cre recombinase) (Kobayashi et al., 2005),

(Kobayashi et al., 2008). This strategy allowed us to circumvent the drastic developmental block due to defective ureteric bud lacking *Hnf1b*. In this way we could study the role of Hnf1b specifically in the metanephric mesenchyme derived structures in presence of a correct induction signaling from the ureteric bud (figure26).

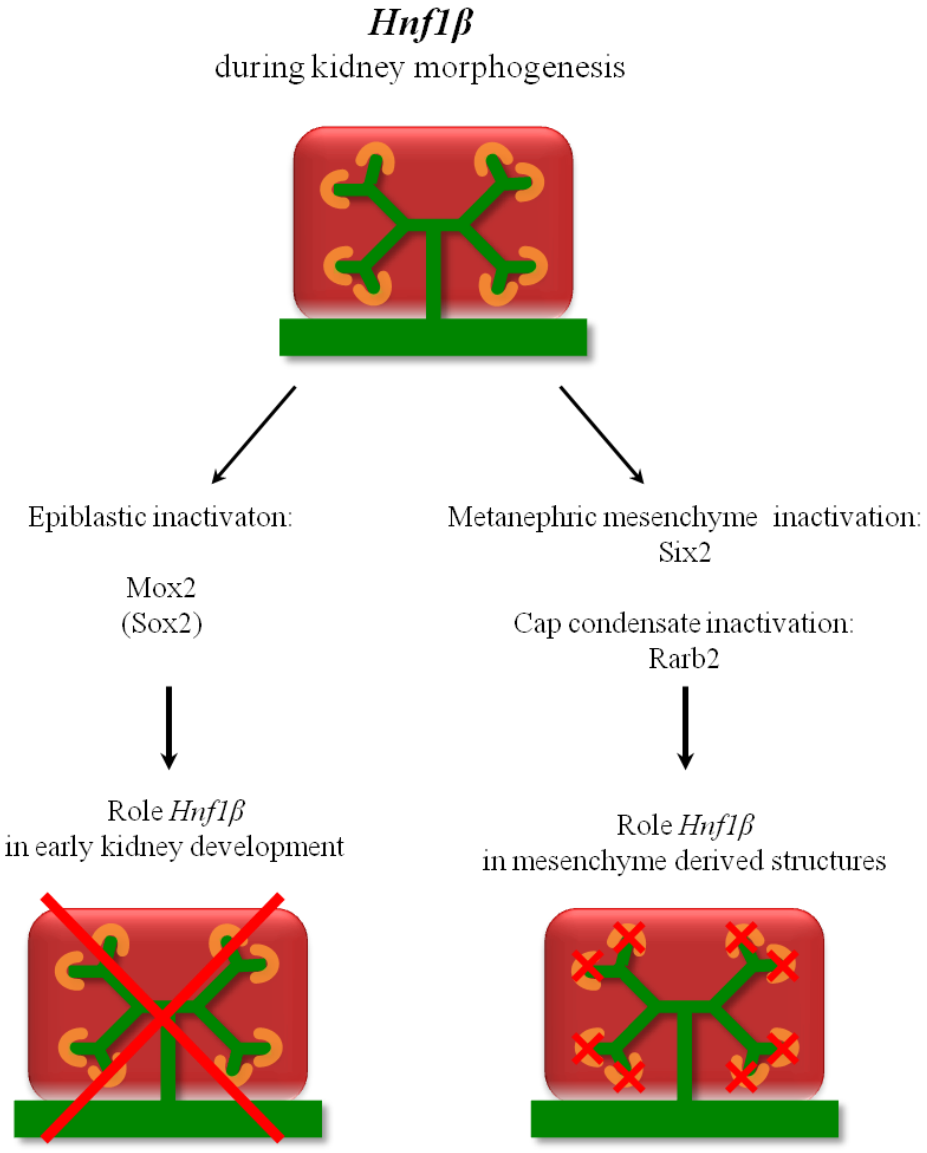

Figure 26. Schematic representation of project design

Materials and methods

Material and Methods

Animals

Tissue- specific inactivation of HNF1b was obtained using a Cre-LoxP strategy. Mox2Cre mice were kindly provided by P. Soriano (Tallquist and Soriano, 2000). Sox2Cre (Hayashi et al., 2002), Rarb2 Cre (Kobayashi et al., 2005), Six2::Cre (Kobayashi et al., 2008), Hnf1b $^{LacZ/+}$ (Coffinier et al., 1999a) and Hnf1b$^{f/f}$ (Coffinier et al., 2002) mice were previously described. Since *Cre*; *Hnf1b* $^{flox/+}$ or *Cre*; *Hnf1b*$^{LacZ/+}$mice were indistinguishable from wild-type mice, all these animals were used as controls (indicated here as "control" in the figures). Animals were maintained in two animal facilities each of which is licensed by the Ministry of Agriculture (Agreement A 75-14-02, dated April 24, 2007). All experiments were conforming to the relevant regulatory standards.

Histological and Immunohistochemical analysis

Human fetal renal specimens as well as tissue for DNA isolation were collected after obtaining informed consent from the parents. The pregnancy had been interrupted during the third trimester because of cystic kidneys, after parents requested and acceptation by the prenatal diagnosis center of Lyon (France). Genomic DNA was isolated by standard methods. Mutation screening was performed as in (Heidet et al., 2010). Images from histological section from MODY5 patient carrying a c0232G>T, p.Glu78X mutation were provided by professor Laurent Daniel, CHU Timone, Marseille, France.

Mouse kidneys have been dissected from embryos at different embryonic stages (E12.5, E13.5, E14.5, E16.5 and E18.5 days of gestation) and from newborn pups (at P0), fixed in 4% PFA for 24-48 hours and embedded in paraffin. For histological analysis, 5µm paraffin sections were stained with hematoxylin and eosin. Paraffin sections for immunohistochemical analyses were treated with the MOM Kit (Vector lab, ref BMK-2202) according the manufacturor instructions. Briefly, antigen demasking was performed in citrate buffer (Dako, ref. S2369). Sections were then incubated with blocking medium for one hour and incubated with the following antibodies: mouse anti-WT1 (Dako, ref. M356101 dilution 1:100), rabbit anti-laminin (Sigma, ref L9393 dilution 1:200), rabbit anti-Jagged1 (SantaCruz, ref SC-8303 dilution 1:200), Lotus Tetranogolobus Lectin-LTL (Vector, ref B-1325, dilution 1:200), Dolichos Biflorus Agglutinin (Vector, ref B-1035 dilution 1:200), homemade 3.12

mouse anit-HNF1β (Chouard et al., 1997) (dilution 1:100) and rabbit anti-Hnf4α (FRHNF4, 1:200). After several washes, secondary antibodies Alexa Fluor (Invitrogen) against rabbit or mouse and coupled with different fluorochromes were incubated for 1 hour at RT (dilution 1:500). The slides were mounted in liquid mounting medium VectaShield (Vector, ref H1000) and analyzed under bright field microscope or spinning disk confocal microscope. All the pictures taken have been analyzed with ImageJ (http://rsbweb.nih.gov/ij/) and mounted with Adobe Illustrator.

In situ Hybridization

Subcloned PCR products or PCR templates obtained from E17.5 cDNA have been transcribed to generate the in situ hybridization probes**,** using DIG RNA Labeling Kit (ROCHE, ref 11 175 025 910). In situ hybridization experiment have been carried on according laboratory protocol: briefly, after dewaxing, 6µm paraffin kidney sections were post fixed in PFA 4% for 10 minutes, treated with Proteinase K (10 minutes of PK 20µg/ml in pre-warmed PBS 37°C), fixed for 5 minutes in PFA4%. Slides were acetylated (10 minutes in 0.02M HCl, 0.1M Triethanolamine, 0.25% Acetic Anhydride) and permeabilized (30 minutes in PBS-Triton 0.5%) before incubation with Hybridization Buffer (SSC 5X, Yeast RNA 100µg/ml, Dendhardt's 1X, Formamide deionized 50%) 2-3 hours at RT. Probes were then added to the slides for an overnight hybridization at 67°C. The slides have then been washed in MABT and incubated with anti-DIG antibody ON in MABT-goat serum 10%-blocking reagent (Roche) at RT. Revelation has been carried out with BM purple for 24-72 hours. The slides were eventually stained with Laminin antibody and revealed in visible Immunohistochemestry using DAB. The following probes have been tested: Wnt9b, Dll1, Pax2, Osr2, Irx1, Lhx1, Emx2, Wnt11, c-Ret, Spry1. The probe for Wnt9b have been kindly provided by Thomas J. Carroll (University of Texas, Dallas, USA)

Probe templates Primers

Osr2	rev	GCTGCAGCTCACCAATTACTCC	***Lhx1***	rev	ACAAATGGTTCCCGTAGCTG
	for	ACTTTGCCGCACTGCTCGCAGC		for	CAACATGCGTGTTATCCAGG
Irx1	rev	ACCCTCACACAGGTCTCCAC	***PvAlb***	rev	CTGGAGAACCTGTTCGCTTC
	for	GGAAAGATCGCATGTTCAGCA		ford	CAGAGGCATCTCTCACCACA
Dll1	rev	CTAGAACACTCTGGGAGCGG	***Slc12a1***	rev	CTGGTATGGTGAAGGCAGGT
	for	GTCTTCAAAGACCCAGGGATG		for	CAAACCAAAAGCAAGCCATT
Spry1	rev	GAGGCCGAGGATTTCAGATG	***Wnt11***	rev	CCGCCACCATCAGTCACACCAT
	for	GCCACACTGTTCGCAGATGA		for	GACGTAGCGCTCCACCGTGC

Quantitative RT-PCR

cDNA have been obtained from total RNA of E13.5, E14.5 and P0 kidneys from wild type and mutant animals, using the kit SuperScript® III Reverse Transcriptase (Invitrogen, ref 18080-051). Gene expression was analyzed by qPCR with Stratagene Mx3000P™ real-time PCR system using SYBR Green-Rox (Roche). Primers were designed using Primer3 online software. All these genes have been tested for 3 wild type and mutant animals at E13.5 and P0 age and 5 wild type and mutant animals at E14.5.

qRT-PCR Primers

Vil1	rev	GCGAGACTTTCCGGAGCTACT	***Hey1***	rev	CCGACGAGACCGAATCAATAAC
	for	CCCCTTTCCGGATCACAAG		for	TCAGGTGATCCACAGTCATCTG
Hnf4α	rev	ATCACCTGGCAGATGATCGAA	***Cdh6***	rev	CTAGTGGCTTCCCAGCAAAG
	for	AGGTTGTCAATCTTGGCCATG		for	CTGATAATCGGATCCCGTGT
Slc12a1	rev	CTGGCCTCATATGCGCTTATT	***Brn1***	rev	CAGCCTACAGCTGGAAAAGG
	for	AGATTTGGCATACGAGGCATG		for	GGTACCCACCTGCGAGTAGA
Slc12a3	rev	GGCCTACGAACACTATGCTAAC	***Hnf1α***	rev	AACCACCCTCTCTCCCAGTAA
	for	AGTCAGCTCACGACCTTGC		for	GCCGCAGACACTGTGACTAA
PvAlb	rev	CAGACTCCTTCGACCACAAAAA	***OSR2***	rev	CCACGGACTGTACACCTGTC
	for	AACCCCAATCTTGCCGTCC		for	GAAAGATCGCATGTTCAGCA
Dll1	rev	GAACAACCTAGCCAATTGCCA	***Irx1***	rev	ATTCACGAGAGGACCCACAC
	for	GCCCCAATGATGCTAACAGAA		for	TCCTTTCCCACACTCCTGAC
Jag1	rev	ACTCGGAAGTGGAGGAGGATG	***Pax2***	rev	CAAAGTTCAGCAGCCTTTCC
	for	AGCGGACTTTCTGCTGGTGT		for	GTTAGAGGCGCTGGAAACAG
Jag2	rev	CAATGCTGAGCCTGACCAATAC	***Lhx1***	rev	TGCGTCCAGTGCTGTGAAT
	for	GACGGACAGTGGCATTCAAA		for	AACCAGATCGCTTGGAGAGAT
Notch2	rev	CCCTGATCATCGTGGTGCT	***WT1***	rev	GGTTTTCTCGCTCAGACCAG
	for	AATGCGCAAGTTGGTGTGG		for	GGTGTGGGTCTTCAGATGGT
Hes5	rev	TCAACAGCAGCATAGAGCAGC	***Wnt9b***	rev	GTGAGGTCCTGACACCCTTC
	for	TCCAGGATGTCGGCCTTCT		for	GCCTGGACAGCTTCAGTAGG

Chromatin Immuno-Precipitation

Nuclei have been purified from pooled embryonic kidneys (8 kidneys from E17.5 embryos or 10 kidneys from P0) as previously described (Verdeguer et al., 2010). Briefly: kidneys wild type animals were homogenized in 5ml SHB buffer (1.9M sucrose, 15mM HEPES pH 7.9, 15mM KCl, 0.5mM DTT, 0.5mM Spermine, 0.5mM Spermidine, with protease inhibitors Complete Roche and phenylmethylsulphonyl fluoride 0.5mM). The suspension was ultracentrifugated through another cushion (8.5ml) of SHB for 1 hour at 25000rpm at 4°C and the pellet of purified nuclei was gently resuspended in 300µl of SucC buffer (0.34mM sucrose, 15mM HEPES pH7.9, 60mM KCl, 15mM NaCl, 15mM beta-mercaptoethanol, 2mM $MgCl_2$, with protease inhibitor Complete Roche and phenylmethylsulphonyl fluoride 0.5mM). The Nuclei were crosslinked in 1% formaldehyde at 30°C for 13 minutes: the reaction was stopped adding glycine at the concentration of 0.125M. Nuclei were then layered on 3ml cushion of 0.9M sucrose SucC buffer and centrifuged 4000rpm for 15 minutes to eliminate formaldehyde and glycine. The pellet of nuclei was resuspended in 600ml The sonication has been performed in Bioruptor sonicator in SBAR buffer (50 mM HEPES, 140 mM NaCl, 1 mM EDTA, 1% Triton, 0.1% sodium deoxycholate and 0.1% SDS with protease inhibitors Complete Roche and phenylmethylsulphonyl fluoride 0.5 mM). The quantity of chromatin recovered has been estimated after decrosslink of an aliquot 10 minutes in boiling water, RNAse treatment, PK treatment and Phenol-Clorophorm precipitation. The equivalent of 8-10µg of chromatin has been used for the CHIP two different aliquots have been directly incubated during 2 hours with Dynadbeads rocking at 4°C (pre-clearing) in order to eliminate the aspecific binding of the beads that were discarded immediately after. The precleared aliquots have been then incubated ON at 4°C, one with the HNF-1β antibody (Santa Cruz, sc22840) and the second with IgG as a control. Quantification of the precipitated specific DNA fragments was carried out with qPCR in triplicates.

Relative fold enrichment of DNA fragments was calculated using the following formula:

$$\text{Fold enrichment} = \frac{\text{ChIP HNF1}\beta}{\text{ChIP IgG}}$$

Quantitative PCR Primers for HNF1β conserved binding sites

Gene	Sites	Primers
Dll1	17_15515811_HsRnCfDrXtBtMdEcPa_3.6 chr17:15515812-15515826	AGGGTCTGAGCTATGCTTGC GCTGTGTCCAACAGGGACTT
	17_15212029_HsGgRnBtMdEcPa_8.0 chr17:15212030-15212044	AAGAGCGGCCTCAGTCATTA CAGACCATAGCCACAGGACA
Pax2	19_44816081_HsGgRnCfXtBtMdAcEcPa_9.5 chr19:44816082-44816096	GCGGAAGCAGATTAACATGCA AGACAGACTCGAGCCGATCG
	19_44817159_HsRnCfBtMdAcEcPa_4.4 chr19:44817160-44817174	TTTCAGCCTCCGCTCCATC CAACTGGAAGCATTGGAGTGG
	19_44825430_HsRnCfBtEcPa_9.6 chr19:44825431-44825445	TCTCTTTTCGGTGGTCTCAGC AGAGGTGAAAAACGAGGACTCAA
	19_44841343_HsGgRnCfBtMdAcEcPa_4.2 chr19:44841344-44841358	GGAAATGGACAACACAACAGTTC GGCTAATTCCCCTTGTGGC
Emx2	19_59530330_HsRnCfBtEc_7.2 chr19:59530331-59530345	GGAGGCGGCTGATGAATAGA GCGCTGCTCTCTGTTTATTGG
	19_59531898_HsRnCfBtOaMdEc_4.5 chr19:59531899-59531913	CAAGCTGGACTTGAATGCCC AACCACACTGACCAGCAGAGG
Wnt9b	11_103596962_HsRnCfBtMdEcPa_7.6 chr11:103596963-103596977	TCCCCTCCCAGACACAGAGA CCCCCTGATTAATGTTTAACGG
Lhx1	11_84346920_HsRnCfOaMdEcPa_4.5 chr11:84346921-84346935	CTGACACCGGAAGGCGATT TTGCTCTCTCCATTCTCCCTG
Hnf1b	11_83610899_HsRnCfXtBtMdEcPa_3.7 chr11:83610900-83610914	CCAGGAGTTGCTGAACCAAAA CAGTGGAGACTCTTTCGCCC
	11_83633472_HsRnCfBtMdEc_9.8 chr11:83633473-83633487	TTAAACCCAGCGTCGGTGAG TCACCCCAAGGAAGCCTCT
	11_83654480_HsRnPa_7.9 chr11:83654481-83654495	GCACAGTGGCCCATGACATA GCACCCATTCCTGGTATTGGT
	11_83666366_HsGgRnCfXtBtTrTnMdEcPaGa_3.5 chr11:83666367-83666381	GATCACTTGCCGGTCCTCTC CGCTTGGCTCCTTGGATAATT
	11_83694946_HsGgRnCfBtOaMdEcPa_4.4 chr11:83694947-83694961	AGCACACACCTGACTCCCAGT AAGATACCCTGCTCCCGAGAG
	11_83698772_HsRnCfBtEcPa_5.2 chr11:83698773-83698787	CCAAGACAGCACACCTCGGT CCCTGCAAACAAACTTCCAGA
Spry1	3_37551569_HsRnBtEc_4.5 chr3:37551570-37551584	AGCGAGGTGAGTTCTCGCTG GACGAAACGGTCCTCAGGAG

Assessment of proliferation and apoptosis extent

To evaluate the index of proliferation and apoptosis, freshly dissected kidneys have been fixed in PFA 4% for 30 minutes included in Agarose 4%. 80µm thick sections with Vibratome sections were then postfixed for 10 minutes at RT and incubated with Peanut Agglutinin (rhodamine coupled, Vector, ref RL-1072) and anti-Histone H3 tri methyl K9, phospho S10 (Abcam, ref Ab5819) or anti-Cleaved Caspase3 ASP 175 (Cell Signaling, ref 9661S) antibodies for 48h in PBS-Sodium Azide 0.1%-Triton 0.01%. After the incubation and 3 washes of 8 hours in total, the sections have been incubated with appropriated secondary antibodies and DAPI for 12 hours.

Electron microscopy

Kidneys were cut in small pieces of around 1mm3, fixed 1 hour in glutaraldehyde 3% and postfixed in Osmium Oxyde 1%. 70nm EPON resin embedded sections were obtained with an Ultramicrotome Reichert Ultracut S. The samples were analyzed with Electron Microscope JEOL 1011.

Thick sections and 3D reconstruction

Freshly dissected kidney from wild type and mutant embryos at different embryonic stages were fixed in 4% PFA for 10-15 minutes and embedded in 4% agarose. Thick sections (90-100 µm) were cut with Vibratome (Leika), post fixed 5 minutes and incubated with ati-laminin antibody and DBA lectin. After 24h wash in PBS-Sodium Azide 0,1%, secondary antibody was incubated for 48h, washed and mounted in liquid mounting medium Vectashield (Vector) and analyzed with Spinning disk confocal microscope. Stack images were taken and analyzed with ImageJ. Three dimensional (3D) models were created on the base of confocal stacks using the software IMOD (http://bio3d.colorado.edu/imod/).

In silico analysis of HNF1 binding sites

To analyze the molecular mechanisms and the targets involved in the phenotypes we observed, we made use of an in silico approach developed in the laboratory to determine if these genes might be possibly under the direct control of HNF1β. HNF1 binding sites were selected based on a collection of several criteria similarly to what has been described in (D'Angelo et al., 2010), (Vallania et al., 2009). Briefly, the first criterion was the Hidden Markov Model (HMM) score of the putative sequence, a parameter that takes into account the resemblance to the canonical putative nucleotide sequence consensus. In particular, we selected putative binding sites with HMM ≥4. The second parameter was the degree of conservation (the sequence had to be conserved in at least 4 distinct species out of 12). The identification of conserved sites was carried out by considering couple of orthologous genes between the mouse genome and each of the 11 other species. The species that were considered (besides the mouse) were *Homo sapiens, Gallus gallus, Canis familiaris, Danio rerio, Xenopus tropicalis, Takufugu rubripes, Tetraodon nigroviridis, Bos taurus, Rattus norvegicus, Sus scrofa, Equus caballus*. For the comparison, for each species we extracted the HNF1 binding sites in 100 kb around any given gene. For each putative binding site (BS) we extracted a sequence of 100 nucleotides centered on each BS for a given mouse gene as well as for the corresponding one-to-one orthologous gene for a given species. In a second step, we identified the putative pairs of conserved BSs between the 2 sets of sequences by using BLAST, verifying that the 100 nucleotides alignment proposed by BLAST actually involved the HNF1-BS. The standalone BLASTN parameters were K 7, G 3, E 1, q 1, W 7, r 2, z 1, e 0.01, a 1, F F and a blast score of 60. The set of putative pairs of orthologous conserved sites were then evaluated for colinearity of the genomic homologous regions extracted from the Compara multispecies database of the Ensembl project (gapped alignments information). The boundaries of the homologous regions (connections) were sorted (decreasing order) according to their alignment score and considered (placed, or conserved) one after the other only if their connection did not intercross an already placed one (colinearity rule). Then, the potential pairs of conserved sites were sorted according to their decreasing blast score and their chromosomal positions were considered (orthologous) only if they did not intercross the collinear connections or the already ‘‘placed’’ sites between the 2 genomic regions.

Results Part I

Role of Hnf1b in early step of kidney development and ureteric bud branching.

(Paper in preparation)

The presence of CAKUT in patients carrying *HNF1B* mutations and the early expression of Hnf1b during metanephros development suggested a crucial role of this transcription factor in the very first steps of renal morphogenesis. As we discussed above, the epithelial components of the kidney derive from two different compartments. The collecting duct system derives from the ureteric bud branching process, whereas the nephron development itself starts from the mesenchymal-to-epithelial transition of the metanephric blastema around the ureteric bud tip.

In the first part of my work, I focused my attention on the role that *Hnf1b* plays in the early steps of the kidney development. To study the role of *Hnf1b* in this context, we made use of specific Cre inactivation that does not recombine this gene in the extra-embryonic tissues: the experiments were carried out using a strain in which the Mox2 promoter drives the Cre recombinase, that efficiently inactive the gene exclusively in the epiblastic tissues (MORE) (Tallquist and Soriano, 2000). The MORE model showed some chimerism in the inactivation pattern, therefore we also confirmed our results using a second Cre epiblast specific recombinase, the Sox2-Cre (Hayashi et al., 2002), slightly more efficient that MORE. Using this strategy of inactivation, the mutant embryos are able to develop until E15.5-E16.5 but they die at this age due to hepatic defects, as described also in (Lokmane et al., 2008). These embryos lacking *Hnf1b* showed a severe defect in kidney morphogenesis. At the macroscopic level, mutant embryos have only rudimentary metanephros. The ureteric bud emerges from the Wollfian duct but does not branch correctly. The abortive ureteric bud development is coupled with the absence of mesenchymal-to-epithelial transition induction. The mutant ureteric bud is able to invade the metanephric mesenchyme and branch once, but it is unable to branch further and it is also unable to induce the epithelialisation of the surrounding blastema. The markers of cap condensation (the protein NCAM) and of the first step of vesicles epithelialisation (the Wnt family member *Wnt4*) are absent in the mutant embryos. Histological analysis of mutant rudimentary kidneys shows disorganized clusters of cells around the ureteric bud tips compared with the columnar well ordered layer of cells in control embryos.

Our work and other results (Lokmane et al., 2010) showed that these malformations are due to a drastic downregulation of key genes involved in kidney morphogenesis. In particular, we showed that *Hnf1b* can bind in vivo the promoter region of *Wnt9b, Emx2*, *Pax2* and *Lhx1,* which expression is aborted in the mutant embryos. Former experiments have shown that the absence of these genes have been related to severe kidney defects (Carroll et al., 2005), (Torres et al., 1995), (Kobayashi et al., 2005), (Miyamoto et al., 1997).

In addition to the results obtained by Lokmane et al, we have also observed in our mouse models the presence of misplaced and extranumerary ureteric buds along the Wolffian duct, suggesting an additional role of *Hnf1b* in the control of the unique ureteric bud outgrowth. The balance between inductive and repressive signals is crucial to restrain the ureteric bud emergence to a unique position. Missregulation of genes in charge of repressing ectopic emergences are correlated with severe renal abnormalities including the presence of multiple ureters and duplex kidneys.

Three dimensional analysis of whole mount Wolffian duct and metanephros shows the presence of extranumerary ectopic buddings spreading all along the Wolffian duct and in the stalk of the ureteric bud. This phenotype was even more penetrant when we used a more efficient recombination strategy (Sox2Cre). Analysis of the molecular mechanism at the basis of this phenotype shows that in absence of *Hnf1b,* key genes involved in the restriction of the ureteric bud emergence in a unique place are downregulated. In particular, we observed a drastic downregulation of *Sprouty1 (Spry1). Spry1* is a membrane-associated inhibitor of the c-Ret kinase activity and lays downstream of the GDNF/RET signaling. *Spry1* is expressed mainly in the nephric duct and more faintly in the surrounding mesenchyme (Mason et al., 2006). Inactivation of *Spry1* leads to ectopic emergence of several buds in the Wolffian duct and in the stalk of the ureteric bud. In silico analysis identified one HNF1 binding site in the region surrounding the gene promoter of *Spry1* and chromatin immuno-precipitation experiments confirmed that this site is bound by *Hnf1b* in vivo. In addition we observed a minor downregulation of *Slit2* expression. *Slit2,* a ligand of ROBO that is expressed in the nephric duct and in the ureteric bud trunk. As described previously, the Slit2/ROBO signalling is necessary for the inhibition of ectopic emergence along the Wolffian duct during kidney development. The absence of one of these two components leads to abnormal rostral metanephric mesenchyme expansion that leads to extra numerary buddings (Grieshammer et al., 2004).

We have also observed that the X-gal staining (reflecting the expression of a LacZ cassette under the control of the *Hnf1b* promoter) is patchy in the Wolffian duct. By in silico analysis, we have found several HNF1 binding consensus sequences surrounding *Hnf1b* promoter region. CHiP experiments confirmed the binding of this transcription factor on its own promoter in vivo. These results suggest that HNF1β, via a positive loop, controls its own expression. This hypothesis could explain the X-gal staining pattern observed in the nephric duct. The initial activation of *Hnf1b* expression is carried out by not yet identified actors, and could be maintained via a direct and positive transcriptional feedback loop. In absence of HNF1β, this positive loop is absent and the X-gal staining progressively fades away in cells during Wolffian duct migration.

In this first part of my study, we described a crucial dual role of *Hnf1b* expression in the ureteric bud: on one side, *Hnf1b* is essential for the correct expression of key genes (such as *Emx2*, *Pax2* and *Lhx1*) involved in the ureteric bud branching and in the mesenchymal to epithelial transition (*Wnt9b*). In the other hand, *Hnf1b* is also crucial to restrict the emergence of the ureteric bud at a unique position, probably via the regulation of *Spry1*, an important gene in charge of inhibiting extra numerary ectopic buddings along the Wolffian duct and the ureteric bud stalk.

Classification: Biological Sciences/Developmental Biology

HNF1β controls a crucial transcriptional network in kidney development

Filippo M Massa[§], Francisco Verdeguer, Serge Garbay, Jacqueline Barra, Evelyne Fischer[*,§], and Marco Pontoglio[*]

Current Address: Institut Cochin, Université Paris Descartes, CNRS (UMR 8104). Inserm, U567 France. 24 rue du faubourg Saint Jacques, Paris 75014, France

* Corresponding authors marco.pontoglio@inserm.fr, evelyne.fischer@inserm.fr

§ Equal contribution.

Abstract

Renal morphogenesis is a highly coordinated process that requires reciprocal inductive interactions between the ureteric bud (UB) and the metanephric blastema. Depending on the timing and nature of the affected compartment, disruption of this morphogenetic process may lead to developmental defects ranging from renal agenesis to urinary tract malformations. Hepatocyte Nuclear Factor 1β (HNF1β) is a homeoprotein expressed in renal epithelia from the early steps of kidney morphogenesis. This gene is frequently mutated in children with renal hypodysplasia but the cellular and molecular mechanisms responsible for this developmental defect are not fully understood.

With the use of a mouse model for HNF1β-deficiency, we showed that the lack of *HNF1β* leads to a drastic kidney developmental defect that recapitulates several of the traits observed in patients carrying *HNF1β* mutations. Similarly to what has been previously shown, metanephros of mutant mouse embryos were characterized by abnormal branching of the UB and lack of mesenchymal to epithelial transition. We demonstrated that HNF1β is required for the UB-specific expression of several key genes including *Pax2, Lhx1, Emx2* and *Wnt9b.* Chromatin immunoprecipitation experiments demonstrated a direct transcriptional hierarchy between *HNF1β* and all these crucial genes, known to play essential roles in nephrogenesis. In addition, *HNF1β* controls the expression of *Sprouty1* a crucial gene involved in the restriction of ureteric bud outgrowth to a unique place. The defective expression of these direct target genes could be responsible for the observed abortive branching events in the Wollfian duct and the ureteric bud. Our findings shed a light on the molecular mechanisms responsible for renal developmental defects that are typically observed in patients carrying mutations in *HNF1β.*

Keywords: nephrogenesis/ureteric bud morphogenesis/branching/MODY5

Introduction

Kidney organogenesis in vertebrates is a notable example of a highly coordinated morphogenetic process where different structural components reciprocally interact (Dressler, 2006) (Schedl, 2007). This process starts with the outgrowth of the Ureteric Bud (UB), an epithelial structure that grows out from the caudal part of the Wolffian duct (nephric duct) and invades the metanephric mesenchyme. Signalling from the mesenchyme induces the UB to growth and branch (Costantini and Shakya, 2006; Nigam and Shah, 2009). The outgrowth of the ureteric bud from a single specific point of the Wollfian duct is tightly regulated by the balance between inductive and inhibiting signals. The inductive signalling is mainly represented by expression and secretion of GDNF from the metanephric mesenchyme. This diffusible protein interacts with its receptor c-Ret on the surface of the Wolffian duct cells to initiate the outgrowth of the ureteric bud. The restriction of the outgrowth at a unique place is regulated by a complex inhibitory system that prevents ectopic ureteric bud outgrowth along the Wolffian duct. Among them, Sprouty1 (Spry1) is an inhibitor of the c-RET kinase activity. In the absence of Spry1, the GDNF/RET signalling is not constrained to a restricted domain of the Wolffian duct, leading to ectopic and supernumerary ureteric bud outgrowth (Basson et al., 2005). Once the outgrowth has properly occurred, the successive branching process contributes to the definitive architecture of the kidney by giving rise to the collecting duct tree system. At the same time, the UB induces the mesenchyme to initiate mesenchymal to epithelial transition. Cells from the metanephric blastema condensate around the UB tips and form the first cellular condensates. These condensates develop into nephron precursors that ultimately will give rise to the tubular epithelial component of the nephrons. Defects in this highly coordinated program may lead to a variety of Congenital Abnormalities of the Kidney and Urinary Tract (CAKUT) (Schedl, 2007; Song and Yosypiv, 2011). Depending on the timing and nature of the affected compartment, abnormalities in the differentiation program can lead to defects ranging from kidney agenesis to urinary tract malformations. Defective branching of the UB may lead to renal hypoplasia, whereas the defective mesenchymal differentiation can give rise to renal dysplasia. It is worth noting that these defects (renal hypodysplasia) represent the most common cause of end-stage renal disease in the pediatric population (Sanna-Cherchi et al., 2009). Despite its obvious clinical importance, little is known about the molecular mechanisms at the basis of CAKUT.

The complex set of events that organize the structure of the future metanephros is based on specific signalling pathways that are selectively activated in the UB and in the mesenchymal compartment. This program is coordinated by the concerted action of transcription factors that trigger the expression of crucial effectors in the right place and at the right moment (Costantini and Shakya, 2006; Ribes et al., 2003). Among them, the Wnt signalling pathway has been shown to play a crucial role in renal development (Bridgewater et al., 2008; Park et al., 2007; Schmidt-Ott and Barasch, 2008). In particular, it has been shown that renal vesicle formation is due to Wnt4 expression (Stark et al., 1994). Once activated, its expression is maintained by a positive feedback mechanism that drives the differentiation towards the epithelial conversion. Recently, Wnt9b has been shown to be essential for the initiation of the first events of Mesenchymal to Epithelial Transition (MET) in metanephric mesenchyme (Carroll et al., 2005). During metanephros development, *Wnt9b* is exclusively expressed in the UB. By diffusing in the surrounding mesenchyme, this glycoprotein triggers the activation of the β-catenin signalling pathways that eventually will induce the expression of Wnt4. The molecular mechanisms, and in particular the transcriptional cascades that initiate and regulate the expression of crucial effectors responsible for UB morphogenesis and differentiation are still poorly understood (Costantini and Shakya, 2006; Shah et al., 2004).

HNF1β is an atypical homeodomain-containing transcription factor that binds DNA and activate transcription as homodimer or heterodimer with a closely related factor called HNF1α (Cereghini, 1996). *HNF1β* is expressed during kidney development since the first morphogenetic steps and its expression is maintained in adulthood in all the tubular epithelial cells of the kidney (Cereghini et al., 1992; Coffinier et al., 1999a; Lazzaro et al., 1992; Ott et al., 1991).

The important role played by HNF1β is documented by the phenotype of patients carrying heterozygous mutations in this gene. Autosomal dominant mutations in the *HNF1B* gene are associated with a particular form of diabetes mellitus called Maturity Onset Diabetes of the Young type 5 (MODY5) (Horikawa et al., 1997). MODY5 patients are often characterized by the presence of renal cysts (Bingham et al., 2001). We have recently shown that cyst formation in *HNF1β*-deficient tubules is due to the defective expression of several polycystic kidney disease genes (Gresh et al., 2004; Hiesberger et al., 2004; Verdeguer et al., 2010). This defect leads to the loss of oriented cell division during the proliferative renal tubular elongation (Fischer et al., 2006).

Recent studies have also shown that in pediatric patients or fetuses, the occurrence of hypodysplasia is frequently associated with *HNF1β* mutations (Decramer et al., 2007; Ulinski et al., 2006). Evidences that HNF1β is playing an important role in kidney organogenesis and cyst formation has been provided by frog and zebrafish studies (Bohn et al., 2003; Sun and Hopkins, 2001).

To assess the roles of HNF1β during early nephrogenesis, we carried out a Cre mediated deletion of the *HNF1β* gene from the very first steps of embryogenesis and specifically in the epiblast using the Mox2Cre mouse strain (Tallquist and Soriano, 2000). This strategy circumvented the early lethality observed in germ-line *HNF1β*-deficient embryos (Barbacci et al., 1999; Coffinier et al., 1999b). In agreement with recent studies using tetraploid chimeric embryos (Lokmane et al., 2010), we showed that Mox2Cre specific inactivation of *HNF1β* leads to a drastic defect in kidney development. Our studies showed that HNF1β plays several roles: it first regulates the branching of the UB and subsequently the initiation of mesenchyme to epithelium conversion via the direct transcriptional activation of crucial actors of nephrogenesis. In addition, HNF1β controls crucial genes involved in the restriction of ureteric bud outgrowth to a unique place.

Results

Kidney agenesis after early conditional *HNF1β* inactivation

It has been previously shown that a germ-line inactivation of *HNF1β* leads to early death of the embryos due to a defect in extra-embryonic visceral endoderm differentiation (Barbacci et al., 1999; Coffinier et al., 1999b). To circumvent this problem we adopted a tissue restricted inactivation of *HNF1β* by crossing mice carrying a floxed allele with a Mox2Cre strain (Tallquist and Soriano, 2000) expressing the Cre recombinase selectively in the epiblast and not in the extraembryonic tissues. This strategy led to an extensive inactivation of *HNF1β* in all embryonic tissues without compromising the differentiation of the extraembryonic compartment. As previously shown, inactivation of *HNF1β* by the replacement of the first exon with a β-galactosidase cassette (heterozygous inactivation) has no effect on murine embryonic development in heterozygous embryos (Coffinier et al., 1999a). In contrast, homozygous *HNF1β*-deficient embryos inactivated with this strategy, died around E15.5 and presented with developmental defects in pancreas, liver and kidney as described with the use of tetraploid aggregation (Haumaitre et al., 2005; Lokmane et al., 2008; Lokmane et al., 2010)). Mutant embryos at E14.5 had a rudimentary metanephros (Fig. 1*B* vs *A*), indicating that HNF1β must play a crucial role in renal morphogenesis. In addition, mutant embryos had a marked defect in mesonephric tubulogenesis (Fig. 1*B* vs *A*).

Expression pattern of HNF1β during nephrogenesis

In order to unravel the role of HNF1β in kidney morphogenesis, it was important to monitor the expression pattern of this factor during the early steps of nephrogenesis. The use of an nls-lacZ cassette under the transcriptional control of the endogenous *HNF1β* promoter has shown that HNF1β is expressed in the mesonephros (Wolffian duct and mesonephric tubules), in the emerging UB and during the subsequent steps of UB branching (Coffinier et al., 1999a). Interestingly, we could show that the uninduced metanephric mesenchyme did not express HNF1β (Fig. 2). When mesenchymal cells start to condense around the UB tip they form a mass called the cap condensate. Some of these condensed cells give rise to preaggregates that progressively evolve into the formation of renal vesicles. These structures subsequently form nephrons via the formation of intermediates represented by comma and sigma-shaped bodies. With the use of immunohistochemistry and X-gal staining, we could

show that HNF1β was not expressed in the cap condensates and preaggregates (Fig. 2*A* and *C*) but was turned on as soon as renal vesicles were formed (Fig. 2*B* and *C*). Interestingly, the expression of HNF1β in renal vesicle was characterized by an asymmetrical pattern. Only few cells in close contact with the UB epithelium clearly expressed HNF1β (Fig. 2*B* and *C*). In all subsequent stages, HNF1β expression remained specifically restricted to the prospective tubular compartment whereas the prospective podocytes were negative for both immunoreactivity against HNF1β protein and for the highly sensitive X-gal staining (Fig. 2*D*). These data indicated that HNF1β expression during nephrogenesis is activated early in the UB compartment but relatively late during the mesenchymal to epithelial conversion process since it is activated only in already formed epithelial structures.

Branching morphogenesis defects in *HNF1β* deficiency

The rudimentary kidney that is formed in the absence of HNF1β was characterized by a drastically defective branching morphogenesis. In control embryos, the UB emerges from the Wolffian duct and undergoes a first branching (Fig. 3*A*). The branched arms give rise to the classically stereotyped T-shaped structure where the perpendicular branched arms are parallel with the Wolffian duct (Fig. 3*A*). In mutant embryos, the UB outgrowth from the Wolffian duct occurred at a slightly more rostral position (Fig. 3*B*). Later on, mutant UB gave rise to a first branching event that, however, was aberrantly shaped (Fig. 3*B*). The mutant branched structures were shorter and characterized by a Y-shaped structure where the arms were no longer parallel with the Wollfian duct. Subsequent branching events tended to be delayed and rare (Fig. 3*D-F*). In most cases, they were characterized by an erratic and disorganized pattern that gave rise to atypical structures (Fig. 3*F*). In some cases, we observed ombrella-like structures, with multiple branches from a unique primary node of the UB (Fig. 1*B* or Fig. 3*F* as an example). These observations underline the crucial role of HNF1β in early UB morphogenesis.

Mesonephric phenotypes

Interestingly, in the nephric duct of mutant embryos the expression of β-galactosidase, under the control of the endogenous *HNF1β* promoter, was highly patchy, particularly in the caudal part of the Wolffian duct (right panels on Fig. 3). This is in sharp contrast with the uniform and strong expression of the β-galactosidase in heterozygous embryos all along the entire Wolffian duct (left panels on Fig. 3). This observation may underlay the presence of a

positive feedback loop where HNF1β may activate its own expression (see below). In addition, the morphogenesis of the mesonephros was drastically compromized. Mutant embryos displayed an abnormal shaped Wolffian duct and mesonephric tubules did not form (Fig. 4A). It is known that during development, the common nephric duct undergoes a progressive remodeling that eventually connects the ureter directly to the bladder (Batourina et al., 2005; Chi et al., 2009). In mutant embryos the common nephric duct did not undergo this process leading to an aberrantly organized junction where the UB remained joined to the Wolffian duct at E12.5 (Fig. S1*B* vs *A*).

Ectopic ureteric bud outgrowth in *HNF1β* deficiency embryos

In wild type embryos, the outgrowth of the ureteric bud is specifically restricted to a unique place facing the metanephric mesenchyme that expresses *Gdnf*. In mutants, we observed several extranumerary ureteric bud outgrowth, both in the Wolffian duct and the ureteric bud stalk (Fig. 4A-B). This defect was more penetrant in Sox2-Cre driven recombination, where the degree of Hnf1b deletion is fully achieved compared to the chimeric MORE driven deletion. (Fig. 4C). Several inhibitory signals are responsible for the restriction of the ureteric bud outgrowth. Our results showed a drastic reduction of *Sprouty1* (*Spry1*) expression in the ureteric bud (Fig. 4D). Interestingly, Spry1 gene has a highly conserved HNF1 binding site at +8.2k bp from the transcription starting point. ChIP experiments showed that HNF1β bound to this site in vivo (Fig.E). All together these results suggest a direct role of HNF1β in the control of the expression of *Spry1*.

Lack of mesenchymal to epithelial conversion in *HNF1β*-deficient kidney

In mutant embryos, the drastic defect of UB branching was accompanied by the absence of any clear polarized epithelial structures (Fig. 5). In mutant embryos, next to UB tips, we could observe some condensed cells. However, these structures looked less organized and polarized than what was observed in control embryos (Fig. 5*A* and *B*). Noteworthy, no subsequent stages of nephron differentiation could be observed in mutant embryos. In order to characterize in more details the developmental block from the molecular point of view, we monitored the expression of specific markers sequentially activated during nephrogenesis. In wild-type embryos, N-CAM expression is activated in the multilayered structure that corresponds to the cap condensates and is maintained in the subsequent steps of nephron differentiation and early tubules (Abbate et al., 1999). In mutant embryos no clear N-CAM

positive condensates were visible around the UB tips. Generally, only few non condensed cells scattered throughout the mesenchyme expressed this protein (Fig. 5*C* and *D*). *Wnt4* is first expressed in the ventral portion of the cap condensate and, later on, in aggregates and renal vesicles. This marker was never expressed in *HNF1β*-deficient embryos (Fig. 5*E* and *F*). This observation correlates with the absence of the typical developmental intermediates (aggregates and vesicles) in mutant embryos. Moreover, the absence of *Wnt4* or defective N-CAM expression indicated that the mesenchyme of mutant embryos could not activate the genetic program of mesenchymal to epithelial conversion typical of the first nephrogenic events.

In a previous study, we showed that the inactivation of *HNF1β* with another Cre recombinase that is expressed in the UB during nephrogenesis (KspCre) (Shao et al., 2002) did not dramatically interfere with nephrogenesis and instead induced polycystic kidney disease (Gresh et al., 2004). This difference is actually due to the specific expression pattern of the KspCre that was not expressed at the terminal portion of the UB (Fig. S2).

The absence of HNF1β leads to defective transcription of key factors involved in renal morphogenesis

Our results indicate that the inactivation of *HNF1β* prevented the development of nephron precursors in the mesenchymal compartment. However, in the mesenchyme, *HNF1β* is supposed to be expressed only in renal vesicles, structures that are never formed in mutant embryos. Hence, the observed developmental defect must rely on a non-cell autonomous mechanism. The only structure that is supposed to expressed *HNF1β* at the time when the developmental defect is observed is the UB. We therefore supposed that this phenotype could be due to a defective heterotypic induction of the UB on the mesenchyme, caused by the loss of expression of *HNF1β* in the UB.

During nephrogenesis, the UB is characterized by a stereotyped patterned expression of genes. Some of them are specifically expressed only at the very tip, whereas others are expressed throughout the whole length or specifically in the stalk (Bridgewater and Rosenblum, 2009). Given the clear involvement of the UB in the defective nephrogenesis of *HNF1β*-deficient embryos, we monitored the expression pattern of a certain number of UB genes. Our results showed that the cells at the tip of the UB normally express the specific set of UB tip genes including *c-Ret*, and *Wnt11* (Fig. S3). This indicated that defective

nephrogenesis could not be simply ascribed to a generalized defect of gene expression patterning in the UB.

Since HNF1β is a transcription factor, we could reasonably suppose that the observed defective signalling of the UB could be ascribed to the defective expression of one or more genes under the direct transcriptional control of *HNF1β*. To verify this possibility we took advantage of a recently developed *in silico* approach (using a Hidden Markov Model based on 59 known HNF1 binding sites, that allows the identification of putative HNF1 binding sites conserved in a relative large number of species (Tronche et al., 1997) (MP and SG, unpublished results). To restrict our search we focused on typical UB genes whose defective expression could explain the observed phenotype. This approach led us to identify a number of genes with a particular high enrichment for evolutionary conserved HNF1 binding sites including *Wnt9b*, *Lhx1*, *Emx2* and *Pax2*. Interestingly, *Pax2* expression in normal embryos occurs both in the UB and in the metanephric mesenchyme. In *HNF1β*-deficient embryos the mesenchymal expression of *Pax2* was maintained to a rather normal level (Fig. 6*A*, *B*, and Fig. S4). However, in the UB epithelium its expression was dramatically compromised (Fig. 6*A*, *B*, and Fig. S4). In a similar way, *Wnt9b*, *Lhx1* and *Emx2* had a significant drop in their expression in the UB at the time when the defective renal development was observed (Fig. 6*C-H*). These results indicate that kidney rudiments in *HNF1β*-deficient embryos were characterized by the decreased expression of a number of crucial genes involved in renal morphogenesis.

Direct targets involved in the defects

To investigate whether the affected genes were directly controlled by *HNF1β*, we verified with the use of chromatin immunoprecipitation (ChIP) if the sites located next to the affected genes were actually bound *in vivo*. We particularly focused our attention on the best conserved and scored HNF1 binding sites. Our results showed that the highly conserved sites that we identified via our *in silico* approach next to *Wnt9b*, *Lhx1*, *Emx2* and *Pax2* genes, were actually bound by HNF1β *in vivo* (Fig. 7). These results suggest a direct transcriptional cascade of *HNF1β* on several key genes playing an essential role during kidney development.

It is worth to note that a previous study identified an important cis-acting transcriptional control region that was required for enhancement of the expression of *Pax2*, specifically in the Wolffian duct and the ureter. Our results have shown here that this region

harbors a highly conserved HNF1 site located at -6.5 Kb that is bound *in vivo* by HNF1β (Kuschert et al., 2001).

The patchy expression of β-galactosidase in mutant nephric ducts (Fig. 3) suggested a potential positive control of HNF1β on its own expression. Our results indicated that the *HNF1β* genomic region contained a surprisingly high number of HNF1 binding sites that were highly conserved in a large number of species. Most of these sites were bound *in vivo* by HNF1β (Fig. 7) suggesting a direct and positive transcriptional feedback loop.

Discussion

Our current studies demonstrated that HNF1β plays a key role in organogenesis of the kidney. The embryonic deletion of *HNF1β* leads to drastic defects in metanephric morphogenesis, including defective UB branching pattern and remodelling of the common nephric duct and absence of mesenchymal to epithelial transition. In addition to these defects, we showed that HNF1β plays an essential role in the restriction of the ureteric bud outgrowth to a unique site.

Absence of mesenchymal to epithelial conversion

We demonstrated that the inactivation of *HNF1β* is responsible for the disruption of the inductive signal from the UB that activates the tubulogenic program in the mesenchyme. When the UB invaded the metanephric mesenchyme, in mutant embryos, some mesenchymal cells tried to condense and cap the first UB branching event. However, they failed to activate the expression of Wnt4. The failure of metanephric mesenchyme induction does not seem to be a consequence of a defective patterning of the UB gene expression since the expression of specific markers of UB morphological differentiation, including *c-Ret* or *Wnt11*, was maintained in the tip.

Since the initial experiments carried out in the 50s the UB was shown to be the source of a diffusible factor, able to activate the Mesenchymal to Epithelial Transition (MET) of the surrounding metanephric blastema (Grobstein, 1953). Recently, Wnt9b has been shown to play a essential role in this induction. This protein acts as a paracrine signal from the UB to the metanephric mesenchyme to initiate a tubulogenic program through the activation of *Pax8, Fgf8* and *Wnt4* expression (Carroll et al., 2005). Once activated, this program is maintained by a positive feedback loop where Wnt4 seems to play a major role (Stark et al., 1994). In *HNF1β*-deficient embryos, *Wnt9b* expression was strongly downregulated in the UB and chromatin immunoprecipitation experiments showed that HNF1β directly binds to an evolutionary conserved site in this gene *in vivo*. These results suggest a hierarchical relationship between *HNF1β* and the gene encoding for this crucial diffusible factor. This transcriptional cascade could explain the lack of renal epithelial derivatives in *HNF1β* mutant embryos. Paradoxically, the inactivation of *Wnt9b* with a Cre recombinase under the control of the *Ksp* promoter does not prevent MET but leads to a cystic phenotype (Karner et al., 2009). In a similar way, KspCre specific inactivation of *HNF1β* does not cause defective

nephrogenesis, but instead, gives rise to dramatic polycystic kidney disease (Gresh et al., 2004). The differences between the phenotypes induced by the Ksp and Mox2 driven Cre are due to the lack of activity of the transgenic Ksp promoter in the terminal part of the UB. These results suggest that this part of the UB is sufficient to induce the MET program in the mesenchyme.

UB-specific transcriptional defects

The results described above suggest that *Pax2, Lhx1* and *Emx2* expression lay downstream of HNF1β in the molecular cascade that regulate kidney development. However, it is worth to note that the lack of HNF1β does not perfectly phenocopy the germ line homozygous mutation of these targets. In fact, *Pax2*, *Lhx1* or *Emx2* homozygous mutant embryos, suffer from either the complete defective outgrowth of the UB (Shawlot and Behringer, 1995; Torres et al., 1995) or its first branching (Miyamoto et al., 1997). Interestingly, in Mox2Cre *HNF1β*-deficient embryos the renal developmental defect is significantly less severe. In our model, the ureteric bud emerges from the Wolffian duct to invade the metanephric mesenchyme and it is able to branch a few times. This paradox can be explained by the fact that in our mutant embryos the defective expression of these targets specifically concerns the UB and not the intermediate mesoderm and the metanephric blastema before MET. These structures express *Lhx1*, *Emx2* and *Pax2* but not *HNF1β.* Since these targets maintain their expression in these HNF1β negative compartments, we must deduce that these genes must rely on two independent transcriptional activation mechanisms: the first is HNF1β-dependent, specifically in the UB, whereas the second is HNF1β-independent in both the intermediate mesoderm and the metanephric blastema. In *HNF1β*–deficient embryos the residual normal expression of *Pax2* in the metanephric mesenchyme could activate *Gdnf* expression and signaling necessary for the outgrowth of the UB from the Wolffian duct. The role of *Pax2* in UB morphogenesis was already suggested by the analysis of the phenotype of the compound *Pax2/Pax8* heterozygous (Narlis et al., 2007). Kidneys from these double heterozygous animals are more severely hypodysplastic and characterized by a reduction in ureter tips and nephron number in comparison with wild-type or *Pax2* heterozygous kidneys. In addition, in human, mutations of *PAX2* are linked to vesico-ureteric reflux and are associated with a subgroup of CAKUT, the renal-coloboma syndrome (Sanyanusin et al., 1995), characterized by a renal hypodysplasia. In a similar way, it has been

already shown that the selective inactivation of *Lhx1* in the Wolffian duct and in its derivates leads to a much milder phenotype with outgrowth of UB but defective branching (Kobayashi et al., 2005; Pedersen et al., 2005) *vs.* a complete renal agenesis in the case of a *Lhx1* germ-line mutation (Shawlot and Behringer, 1995; Torres et al., 1995). Interestingly, we revealed a positive feedback loop of HNF1β on its own expression. Since *HNF1β* seems to be a crucial regulator of multiple pathways activated in the UB, this feedback loop could be a way to warrant the robustness of the cell differentiation program activated by *HNF1β*. In addition to the defective ureteric bud branching, mutant embryos showed ectopic ureteric bud outgrowth that could be linked to the observed dowregulation of *Spry1* in the Wolffian duct and ureteric bud stalk.

Sequential roles of HNF1β in kidney.

We have previously shown that the phenotypical consequences of the inactivation of *HNF1β* in the kidney may dramatically depend on the context. When *HNF1β* is inactivated from the very first steps of nephrogenesis there are drastic UB branching and nephrogenesis defects. However, when *HNF1β* is inactivated in newly formed elongating tubules, a severe polycystic phenotype was observed (Gresh et al., 2004). Interestingly, both of these aspects, the defective differentiation and morphogenesis (hypodysplasia and cysts) can be found in MODY5 patients (Bellanne-Chantelot et al., 2004; Decramer et al., 2007; Ulinski et al., 2006). One of the feature of MODY5 is the lack of any clear genotype-phenotype correlation. A critical parameter that could determine the extent and the type of dysfunction could be the variable onset of somatic mutations. The unusually high proportion of *de novo* *HNF1β* mutations suggests an intrinsic instability of the *TCF2* locus (Bellanne-Chantelot et al., 2005; Mefford et al., 2007). Somatic genomic rearrangement could give rise to a loss of heterozygosity and play a crucial role in the heterogeneity of the observed phenotype. Depending on the time and place where they take place, they could results in embryonic kidney abnormalities or cystic disease contributing to the variability of the phenotype observed in patients.

In conclusion, all these considerations highlight the multifaceted aspect of gene function when we consider the multiple and diverse temporal and spatial action domain during kidney development. Our study shed a light on the molecular mechanisms leading to renal hypodysplasia, a developmental abnormality that may lead to severe kidney failure.

Methods

Mouse strains

HNF1β^{lacZ} and *HNF1β*^{flox} alleles were previously described (Coffinier et al., 1999a; Coffinier et al., 2002). Mox2Cre and ROSA26R mice were provided by P. Soriano (Soriano, 1999; Tallquist and Soriano, 2000). The KspCre strain was previously described (Shao et al., 2002). Since *HNF1β*$^{lacZ/+}$ and *Cre*; *HNF1β*$^{flox/+}$ mice were indistinguishable from wild-type mice, both genotypes were used as controls (indicated here as "control"). Animals protocols were approved by our institutional review committee.

Histological analysis, immunohistochemistry and X-gal staining

Whole mount X-gal stainings were performed as described (Pontoglio et al., 1996). For histological analysis and immunohistochemistry, embryos were fixed in PFA 4% overnight and embedded in paraffin. For immunostaining, sections were boiled 10 minutes in 10 mM citric acid pH6. HNF1β and N-CAM immunodetection were performed with a mouse monoclonal (TC 3-12) anti-rat HNF1β antibody (1/100) (Chouard et al., 1997) and an anti-mouse N-CAM (1/100) (Sigma C9672), respectively. Sections were processed with an M.O.M.^{TM} kit (PK-2200, Vector), according to manufacturer's procedures. Peroxidase activity was revealed with 3,3-diaminobenzidine tetrahydrochloride (D-0426, Sigma).

In situ hybridization

Subcloned PCR products or PCR templates obtained from E17.5 cDNA have been transcribed to generate the in situ hybridization probes**,** using DIG RNA Labeling Kit (ROCHE, ref 11 175 025 910). In situ hybridization experiment have been carried on according laboratory protocol: briefly, after dewaxing, 6µm paraffin kidney sections were post fixed in PFA 4% for 10 minutes, treated with Proteinase K (10 minutes of PK 20µg/ml in pre-warmed PBS 37°C), fixed for 5 minutes in PFA4%. Slides were acetylated (10 minutes in 0.02M HCl, 0.1M Triethanolamine, 0.25% Acetic Anhydride) and permeabilized (30 minutes in PBS-Triton 0.5%) before incubation with Hybridization Buffer (SSC 5X, Yeast RNA 100µg/ml, Dendhardt's 1X, Formamide deionized 50%) 2-3 hours at RT. Probes were then added to the

slides for an overnight hybridization at 67°C. The slides have then been washed in MABT and incubated with anti-DIG antibody ON in MABT-goat serum 10%-blocking reagent (Roche) at RT. Revelation has been carried out with BM purple for 24-72 hours. The following probes have been tested: Wnt9b, Pax2, Lhx1, Emx2, Wnt11, c-Ret, Spry1. The probe for Wnt9b have been kindly provided by Thomas J. Carroll (University of Texas, Dallas, USA)

Probe templates Primers

Wnt11	rev	CCGCCACCATCAGTCACACCAT
	for	GACGTAGCGCTCCACCGTGC
Lhx1	rev	ACAAATGGTTCCCGTAGCTG
	for	CAACATGCGTGTTATCCAGG
*Spry**1***	rev	GAGGCCGAGGATTTCAGATG
	for	GCCACACTGTTCGCAGATGA

Chromatin Immuno-Precipitation

Nuclei have been purified from pooled embryonic kidneys (8 kidneys from E17.5 embryos or 10 kidneys from P0) as previously described {Verdeguer, 2010 #2546}. Briefly: kidneys wild type animals were homogenized in 5ml SHB buffer (1.9M sucrose, 15mM HEPES pH 7.9, 15mM KCl, 0.5mM DTT, 0.5mM Spermine, 0.5mM Spermidine, with protease inhibitors Complete Roche and phenylmethylsulphonyl fluoride 0.5mM). The suspension was ultracentrifugated through another cushion (8.5ml) of SHB for 1 hour at 25000rpm at 4°C and the pellet of purified nuclei was gently resuspended in 300µl of SucC buffer (0.34mM sucrose, 15mM HEPES pH7.9, 60mM KCl, 15mM NaCl, 15mM beta-mercaptoethanol, 2mM $MgCl_2$, with protease inhibitor Complete Roche and phenylmethylsulphonyl fluoride 0.5mM). The Nuclei were crosslinked in 1% formaldehyde at 30°C for 13 minutes: the reaction was stopped adding glycine at the concentration of 0.125M. Nuclei were then layered on 3ml cushion of 0.9M sucrose SucC buffer and centrifuged 4000rpm for 15 minutes to eliminate formaldehyde and glycine. The pellet of nuclei was resuspended in 600ml The sonication has been performed in Bioruptor sonicator in SBAR buffer (50 mM HEPES, 140 mM NaCl, 1 mM EDTA, 1% Triton, 0.1% sodium deoxycholate and 0.1% SDS with protease inhibitors Complete Roche and phenylmethylsulphonyl fluoride 0.5 mM). The quantity of chromatin recovered has been estimated after decrosslink of an

aliquot 10 minutes in boiling water, RNAse treatment, PK treatment and Phenol-Clorophorm precipitation. The equivalent of 8-10µg of chromatin has been used for the CHIP two different aliquots have been directly incubated during 2 hours with Dynadbeads rocking at 4°C (pre-clearing) in order to eliminate the aspecific binding of the beads that were discarded immediately after. The precleared aliquots have been then incubated ON at 4°C, one with the HNF-1β antibody (Santa Cruz, sc22840) and the second with IgG as a control. Quantification of the precipitated specific DNA fragments was carried out with qPCR in triplicates.

Relative fold enrichment of DNA fragments was calculated using the following formula:

$$\text{Fold enrichment} = \frac{\text{ChIP HNF1}\beta}{\text{ChIP IgG}}$$

Quantitative PCR Primers for HNF1β conserved binding sites

Gene	Sites	Primers
Pax2	19_44816081_HsGgRnCfXtBtMdAcEcPa_9.5 chr19:44816082-44816096	GCGGAAGCAGATTAACATGCA AGACAGACTCGAGCCGATCG
	19_44817159_HsRnCfBtMdAcEcPa_4.4 chr19:44817160-44817174	TTTCAGCCTCCGCTCCATC CAACTGGAAGCATTGGAGTGG
	19_44825430_HsRnCfBtEcPa_9.6 chr19:44825431-44825445	TCTCTTTTCGGTGGTCTCAGC AGAGGTGAAAAACGAGGACTCAA
	19_44841343_HsGgRnCfBtMdAcEcPa_4.2 chr19:44841344-44841358	GGAAATGGACAACACAACAGTTC GGCTAATTCCCCTTGTGGC
Emx2	19_59530330_HsRnCfBtEc_7.2 chr19:59530331-59530345	GGAGGCGGCTGATGAATAGA GCGCTGCTCTCTGTTTATTGG
	19_59531898_HsRnCfBtOaMdEc_4.5 chr19:59531899-59531913	CAAGCTGGACTTGAATGCCC AACCACACTGACCAGCAGAGG
Wnt9b	11_103596962_HsRnCfBtMdEcPa_7.6 chr11:103596963-103596977	TCCCCTCCCAGACACAGAGA CCCCCTGATTAATGTTTAACGG
Lhx1	11_84346920_HsRnCfOaMdEcPa_4.5 chr11:84346921-84346935	CTGACACCGGAAGGCGATT TTGCTCTCTCCATTCTCCCTG
Hnf1b	11_83610899_HsRnCfXtBtMdEcPa_3.7 chr11:83610900-83610914	CCAGGAGTTGCTGAACCAAAA CAGTGGAGACTCTTTCGCCC
	11_83633472_HsRnCfBtMdEc_9.8 chr11:83633473-83633487	TTAAACCCAGCGTCGGTGAG TCACCCCAAGGAAGCCTCT
	11_83654480_HsRnPa_7.9 chr11:83654481-83654495	GCACAGTGGCCCATGACATA GCACCCATTCCTGGTATTGGT
	11_83666366_HsGgRnCfXtBtTrTnMdEcPaGa_3.5 chr11:83666367-83666381	GATCACTTGCCGGTCCTCTC CGCTTGGCTCCTTGGATAATT
	11_83694946_HsGgRnCfBtOaMdEcPa_4.4 chr11:83694947-83694961	AGCACACACCTGACTCCCAGT AAGATACCCTGCTCCCGAGAG
	11_83698772_HsRnCfBtEcPa_5.2 chr11:83698773-83698787	CCAAGACAGCACACCTCGGT CCCTGCAAACAAACTTCCAGA
Spry1	3_37551569_HsRnBtEc_4.5 chr3:37551570-37551584	AGCGAGGTGAGTTCTCGCTG GACGAAACGGTCCTCAGGAG

Acknowledgements

We thank Tom Caroll for the Wnt9b probe. We are grateful to Michel Leibovici and Moshe Yaniv for critical reading our manuscript. FM and FV were supported by the Société Française de Néphrologie. This work was supported by the « Société de Néphrologie », the « Agence Nationale Recherche » and the « Fondation de la Recherche Medicale ».

References

Abbate, M., Brown, D., and Bonventre, J.V. (1999). Expression of NCAM recapitulates tubulogenic development in kidneys recovering from acute ischemia. Am J Physiol *277*, F454-463.

Barbacci, E., Reber, M., Ott, M.O., Breillat, C., Huetz, F., and Cereghini, S. (1999). Variant hepatocyte nuclear factor 1 is required for visceral endoderm specification. Development *126*, 4795-4805.

Basson, M.A., Akbulut, S., Watson-Johnson, J., Simon, R., Carroll, T.J., Shakya, R., Gross, I., Martin, G.R., Lufkin, T., McMahon, A.P., *et al.* (2005). Sprouty1 is a critical regulator of GDNF/RET-mediated kidney induction. Dev Cell *8*, 229-239.

Batourina, E., Tsai, S., Lambert, S., Sprenkle, P., Viana, R., Dutta, S., Hensle, T., Wang, F., Niederreither, K., McMahon, A.P., *et al.* (2005). Apoptosis induced by vitamin A signaling is crucial for connecting the ureters to the bladder. Nat Genet *37*, 1082-1089.

Bellanne-Chantelot, C., Chauveau, D., Gautier, J.F., Dubois-Laforgue, D., Clauin, S., Beaufils, S., Wilhelm, J.M., Boitard, C., Noel, L.H., Velho, G., *et al.* (2004). Clinical spectrum associated with hepatocyte nuclear factor-1beta mutations. Ann Intern Med *140*, 510-517.

Bellanne-Chantelot, C., Clauin, S., Chauveau, D., Collin, P., Daumont, M., Douillard, C., Dubois-Laforgue, D., Dusselier, L., Gautier, J.F., Jadoul, M., *et al.* (2005). Large genomic rearrangements in the hepatocyte nuclear factor-1beta (TCF2) gene are the most frequent cause of maturity-onset diabetes of the young type 5. Diabetes *54*, 3126-3132.

Bingham, C., Bulman, M.P., Ellard, S., Allen, L.I., Lipkin, G.W., Hoff, W.G., Woolf, A.S., Rizzoni, G., Novelli, G., Nicholls, A.J., *et al.* (2001). Mutations in the hepatocyte nuclear factor-1beta gene are associated with familial hypoplastic glomerulocystic kidney disease. Am J Hum Genet *68*, 219-224.

Bohn, S., Thomas, H., Turan, G., Ellard, S., Bingham, C., Hattersley, A.T., and Ryffel, G.U. (2003). Distinct molecular and morphogenetic properties of mutations in the human HNF1beta gene that lead to defective kidney development. J Am Soc Nephrol *14*, 2033-2041.

Bridgewater, D., Cox, B., Cain, J., Lau, A., Athaide, V., Gill, P.S., Kuure, S., Sainio, K., and Rosenblum, N.D. (2008). Canonical WNT/beta-catenin signaling is required for ureteric branching. Dev Biol *317*, 83-94.

Bridgewater, D., and Rosenblum, N.D. (2009). Stimulatory and inhibitory signaling molecules that regulate renal branching morphogenesis. Pediatric nephrology (Berlin, Germany) *24*, 1611-1619.

Carroll, T.J., Park, J.S., Hayashi, S., Majumdar, A., and McMahon, A.P. (2005). Wnt9b plays a central role in the regulation of mesenchymal to epithelial transitions underlying organogenesis of the mammalian urogenital system. Dev Cell *9*, 283-292.

Cereghini, S. (1996). Liver-enriched transcription factors and hepatocyte differentiation. Faseb J *10*, 267-282.

Cereghini, S., Ott, M.O., Power, S., and Maury, M. (1992). Expression patterns of vHNF1 and HNF1 homeoproteins in early postimplantation embryos suggest distinct and sequential developmental roles. Development *116*, 783-797.

Chi, X., Michos, O., Shakya, R., Riccio, P., Enomoto, H., Licht, J.D., Asai, N., Takahashi, M., Ohgami, N., Kato, M., *et al.* (2009). Ret-dependent cell rearrangements in the Wolffian duct epithelium initiate ureteric bud morphogenesis. Dev Cell *17*, 199-209.

Chouard, T., Jeannequin, O., Rey-Campos, J., Yaniv, M., and Traincard, F. (1997). A set of polyclonal and monoclonal antibodies reveals major differences in post-translational modification of the rat HNF1 and vHNF1 homeoproteins. Biochimie *79*, 707-715.

Coffinier, C., Barra, J., Babinet, C., and Yaniv, M. (1999a). Expression of the vHNF1/HNF1beta homeoprotein gene during mouse organogenesis. Mech Dev *89*, 211-213.

Coffinier, C., Gresh, L., Fiette, L., Tronche, F., Schutz, G., Babinet, C., Pontoglio, M., Yaniv, M., and Barra, J. (2002). Bile system morphogenesis defects and liver dysfunction upon targeted deletion of HNF1beta. Development *129*, 1829-1838.

Coffinier, C., Thepot, D., Babinet, C., Yaniv, M., and Barra, J. (1999b). Essential role for the homeoprotein vHNF1/HNF1beta in visceral endoderm differentiation. Development *126*, 4785-4794.

Costantini, F., and Shakya, R. (2006). GDNF/Ret signaling and the development of the kidney. Bioessays *28*, 117-127.

Decramer, S., Parant, O., Beaufils, S., Clauin, S., Guillou, C., Kessler, S., Aziza, J., Bandin, F., Schanstra, J.P., and Bellanne-Chantelot, C. (2007). Anomalies of the TCF2 gene are the main cause of fetal bilateral hyperechogenic kidneys. J Am Soc Nephrol *18*, 923-933.

Dressler, G.R. (2006). The cellular basis of kidney development. Annu Rev Cell Dev Biol *22*, 509-529.

Fischer, E., Legue, E., Doyen, A., Nato, F., Nicolas, J.F., Torres, V., Yaniv, M., and Pontoglio, M. (2006). Defective planar cell polarity in polycystic kidney disease. Nat Genet *38*, 21-23.

Gresh, L., Fischer, E., Reimann, A., Tanguy, M., Garbay, S., Shao, X., Hiesberger, T., Fiette, L., Igarashi, P., Yaniv, M., *et al.* (2004). A transcriptional network in polycystic kidney disease. The EMBO journal *23*, 1657-1668.

Grieshammer, U., Le, M., Plump, A.S., Wang, F., Tessier-Lavigne, M., and Martin, G.R. (2004). SLIT2-mediated ROBO2 signaling restricts kidney induction to a single site. Dev Cell *6*, 709-717.

Grobstein, C. (1953). Inductive epitheliomesenchymal interaction in cultured organ rudiments of the mouse. Science *118*, 52-55.

Haumaitre, C., Barbacci, E., Jenny, M., Ott, M.O., Gradwohl, G., and Cereghini, S. (2005). Lack of TCF2/vHNF1 in mice leads to pancreas agenesis. Proc Natl Acad Sci U S A *102*, 1490-1495.

Hiesberger, T., Bai, Y., Shao, X., McNally, B.T., Sinclair, A.M., Tian, X., Somlo, S., and Igarashi, P. (2004). Mutation of hepatocyte nuclear factor-1beta inhibits Pkhd1 gene expression and produces renal cysts in mice. J Clin Invest *113*, 814-825.

Horikawa, Y., Iwasaki, N., Hara, M., Furuta, H., Hinokio, Y., Cockburn, B.N., Lindner, T., Yamagata, K., Ogata, M., Tomonaga, O., *et al.* (1997). Mutation in hepatocyte nuclear factor-1 beta gene (TCF2) associated with MODY. Nat Genet *17*, 384-385.

Karner, C.M., Chirumamilla, R., Aoki, S., Igarashi, P., Wallingford, J.B., and Carroll, T.J. (2009). Wnt9b signaling regulates planar cell polarity and kidney tubule morphogenesis. Nat Genet.

Kobayashi, A., Kwan, K.M., Carroll, T.J., McMahon, A.P., Mendelsohn, C.L., and Behringer, R.R. (2005). Distinct and sequential tissue-specific activities of the LIM-class homeobox gene Lim1 for tubular morphogenesis during kidney development. Development *132*, 2809-2823.

Kuschert, S., Rowitch, D.H., Haenig, B., McMahon, A.P., and Kispert, A. (2001). Characterization of Pax-2 regulatory sequences that direct transgene expression in the Wolffian duct and its derivatives. Dev Biol *229*, 128-140.

Lazzaro, D., De Simone, V., De Magistris, L., Lehtonen, E., and Cortese, R. (1992). LFB1 and LFB3 homeoproteins are sequentially expressed during kidney development. Development *114*, 469-479.

Lokmane, L., Haumaitre, C., Garcia-Villalba, P., Anselme, I., Schneider-Maunoury, S., and Cereghini, S. (2008). Crucial role of vHNF1 in vertebrate hepatic specification. Development *135*, 2777-2786.

Lokmane, L., Heliot, C., Garcia-Villalba, P., Fabre, M., and Cereghini, S. (2010). vHNF1 functions in distinct regulatory circuits to control ureteric bud branching and early nephrogenesis. Development *137*, 347-357.

Mefford, H.C., Clauin, S., Sharp, A.J., Moller, R.S., Ullmann, R., Kapur, R., Pinkel, D., Cooper, G.M., Ventura, M., Ropers, H.H., *et al.* (2007). Recurrent reciprocal genomic rearrangements of 17q12 are associated with renal disease, diabetes, and epilepsy. Am J Hum Genet *81*, 1057-1069.

Miyamoto, N., Yoshida, M., Kuratani, S., Matsuo, I., and Aizawa, S. (1997). Defects of urogenital development in mice lacking Emx2. Development *124*, 1653-1664.

Narlis, M., Grote, D., Gaitan, Y., Boualia, S.K., and Bouchard, M. (2007). Pax2 and Pax8 Regulate Branching Morphogenesis and Nephron Differentiation in the Developing Kidney. J Am Soc Nephrol *18*, 1121-1129.

Nigam, S.K., and Shah, M.M. (2009). How does the ureteric bud branch? J Am Soc Nephrol *20*, 1465-1469.

Ott, M.O., Rey-Campos, J., Cereghini, S., and Yaniv, M. (1991). vHNF1 is expressed in epithelial cells of distinct embryonic origin during development and precedes HNF1 expression. Mech Dev *36*, 47-58.

Park, J.S., Valerius, M.T., and McMahon, A.P. (2007). Wnt/beta-catenin signaling regulates nephron induction during mouse kidney development. Development *134*, 2533-2539.

Pedersen, A., Skjong, C., and Shawlot, W. (2005). Lim 1 is required for nephric duct extension and ureteric bud morphogenesis. Dev Biol *288*, 571-581.

Pontoglio, M., Barra, J., Hadchouel, M., Doyen, A., Kress, C., Bach, J.P., Babinet, C., and Yaniv, M. (1996). Hepatocyte nuclear factor 1 inactivation results in hepatic dysfunction, phenylketonuria, and renal Fanconi syndrome. Cell *84*, 575-585.

Ribes, D., Fischer, E., Calmont, A., and Rossert, J. (2003). Transcriptional control of epithelial differentiation during kidney development. J Am Soc Nephrol *14 Suppl 1*, S9-15.

Sanna-Cherchi, S., Ravani, P., Corbani, V., Parodi, S., Haupt, R., Piaggio, G., Innocenti, M.L., Somenzi, D., Trivelli, A., Caridi, G., *et al.* (2009). Renal outcome in patients with congenital anomalies of the kidney and urinary tract. Kidney Int *76*, 528-533.

Sanyanusin, P., Schimmenti, L.A., McNoe, L.A., Ward, T.A., Pierpont, M.E., Sullivan, M.J., Dobyns, W.B., and Eccles, M.R. (1995). Mutation of the PAX2 gene in a family with optic nerve colobomas, renal anomalies and vesicoureteral reflux. Nat Genet *9*, 358-364.

Schedl, A. (2007). Renal abnormalities and their developmental origin. Nat Rev Genet *8*, 791-802.

Schmidt-Ott, K.M., and Barasch, J. (2008). WNT/beta-catenin signaling in nephron progenitors and their epithelial progeny. Kidney Int *74*, 1004-1008.

Schuchardt, A., D'Agati, V., Larsson-Blomberg, L., Costantini, F., and Pachnis, V. (1994). Defects in the kidney and enteric nervous system of mice lacking the tyrosine kinase receptor Ret. Nature *367*, 380-383.

Shah, M.M., Sampogna, R.V., Sakurai, H., Bush, K.T., and Nigam, S.K. (2004). Branching morphogenesis and kidney disease. Development *131*, 1449-1462.
Shao, X., Somlo, S., and Igarashi, P. (2002). Epithelial-specific Cre/lox recombination in the developing kidney and genitourinary tract. J Am Soc Nephrol *13*, 1837-1846.
Shawlot, W., and Behringer, R.R. (1995). Requirement for Lim1 in head-organizer function. Nature *374*, 425-430.
Song, R., and Yosypiv, I.V. (2011). Genetics of congenital anomalies of the kidney and urinary tract. Pediatric nephrology (Berlin, Germany) *26*, 353-364.
Soriano, P. (1999). Generalized lacZ expression with the ROSA26 Cre reporter strain. Nat Genet *21*, 70-71.
Stark, K., Vainio, S., Vassileva, G., and McMahon, A.P. (1994). Epithelial transformation of metanephric mesenchyme in the developing kidney regulated by Wnt-4. Nature *372*, 679-683.
Sun, Z., and Hopkins, N. (2001). vhnf1, the MODY5 and familial GCKD-associated gene, regulates regional specification of the zebrafish gut, pronephros, and hindbrain. Genes Dev *15*, 3217-3229.

Tallquist, M.D., and Soriano, P. (2000). Epiblast-restricted Cre expression in MORE mice: a tool to distinguish embryonic vs. extra-embryonic gene function. Genesis *26*, 113-115.

Torres, M., Gomez-Pardo, E., Dressler, G.R., and Gruss, P. (1995). Pax-2 controls multiple steps of urogenital development. Development *121*, 4057-4065.

Tronche, F., Ringeisen, F., Blumenfeld, M., Yaniv, M., and Pontoglio, M. (1997). Analysis of the distribution of binding sites for a tissue-specific transcription factor in the vertebrate genome. J Mol Biol *266*, 231-245.

Ulinski, T., Lescure, S., Beaufils, S., Guigonis, V., Decramer, S., Morin, D., Clauin, S., Deschenes, G., Bouissou, F., Bensman, A., *et al.* (2006). Renal phenotypes related to hepatocyte nuclear factor-1beta (TCF2) mutations in a pediatric cohort. J Am Soc Nephrol *17*, 497-503.

Verdeguer, F., Le Corre, S., Fischer, E., Callens, C., Garbay, S., Doyen, A., Igarashi, P., Terzi, F., and Pontoglio, M. (2010). A mitotic transcriptional switch in polycystic kidney disease. Nat Med *16*, 106-110.

Figure Legends

Fig. 1. Defective nephrogenesis in *HNF1β* deficiency. X-gal staining of control *HNF1β* $^{flox/lacZ}$ (*A*) and *HNF1β*-deficient embryos (*B*) where *HNF1β* gene is inactivated by a Mox2Cre recombinase *(Mox2Cre;HNF1β* $^{flox/lacZ}$) at E14.5. In mutant embryos, the ureteric bud (UB) had only branched few times (black arrowheads). No mesonephric tubules were visible in mutant embryos (black arrows).

Fig. 2. HNF1β expression during kidney development. Immunohistochemistry (*A* and *B*) and X-gal staining (*C* and *D*) on kidney sections from *HNF1β* $^{flox/lacZ}$ embryos. HNF1β protein expression and X-gal staining were detectable along the entire UB (*A-D*). *HNF1β* protein and X-gal staining were not detected in the uninduced metanephric mesenchyme and in the initial stages of nephrogenesis: cap condensates (arrows in *A* and *C*) and preaggregates (arrow in *B*). *HNF1β* protein and transcription were detectable in vesicles only in cells facing the UB (arrowheads in *B* and *C*). In comma-shaped and sigma-shaped bodies (*D*) X-gal staining was restricted to the prospective tubular structures (arrow in *D*) whereas no staining was observed in the prospective podocytes (arrowheads in *D*).

Fig. 3. Nephric duct and early ureteric bud abnormal morphogenesis in mutant embryos. Whole mount X-gal staining on control (*Mox2Cre; HNF1β* $^{+/lacZ}$*)* and *HNF1β*-deficient (*Mox2Cre; HNF1β* $^{flox/lacZ}$*)* embryos at E11.5 (*A* and *B*), E12.5 (*C* and *D*), E13.5 (*E* and *F*). In mutant embryos, the UB emerges from a slightly more rostral position compared to control embryos (compare arrows in *B* vs *A*). The mutant UB produced an abnormal Y-shaped branching event compared to the T-shaped branching observed in control at E11.5 (compare arrowheads in *B* vs *A*). Later on, UB branching was delayed and rare, giving rise to a rudimentary structure (compare *D* vs *C* and *F* vs *E*). In mutants, the caudal part of the nephric duct (arrowheads on panel *D*) had a faint and mottled X-gal staining compared to the homogenous staining in control embryos. No mesonephric tubules developed in mutant embryos (compare arrowheads in *F* and *E*).

Fig. 4. The absence of HNF1β leads to ectopic ureteric bud outgrowth. (A-B) At E13.5, mesonephric tubules do not form in mutant embryos (arrowhead in A). Note the presence of ectopic outgrowth of buds both from the Wolffian duct (asterisks in A) and the ureteric bud stalk (asterick in B) in mutant embryos. (C) X-Gal staining for LacZ cassette under control of *HNF1β* promoter shows a second ectopic outgrowth of the ureteric bud

(arrow) in the metanephric mesenchyme in the mutant kidney. The phenotype is worsened with a a more efficient Cre inactivation (Sox2-Cre) compared with MORE inactivation strategy. (D) *In situ* hybridisation shows a drastic reduction of Spouty1 expression in the mutant kidney compared with the control. (E) Chromatin immunoprecipitation experiment shows that HNF1β is bound *in vivo* to an HNF1 binding site in the gene Spry1.

Fig. 5. *HNF1β* embryonic inactivation results in absence of mesenchymal to epithelial conversion. Resin (*A* and *B*) and paraffin sections (*C-F*) from control (left panels) and mutant (right panels) embryos. (*A* and *B)* Few cells were organized around the UB tip, but in mutants embryos they did not form the cap condensates (compare arrows in *B* vs *A*). (*C* and *D*) Immunohistochemistry with an anti-N-CAM antibody. In wild-type embryos, the UB was surrounded by multilayered N-CAM positive cells (arrows in *C*), whereas in mutants, only few disorganized cells expressed N-CAM (arrows in *D*). (*E* and *F*) In wild-type *Wnt4* was expressed in condensates and in renal vesicles (arrows in *E*). These structures did not form in mutants and *Wnt4* mRNA was not detected (*F*). (*C-F*) The UB epithelium is illustrated by dashed lines.

Fig. 6. *HNF1β* embryonic inactivation leads to a marked decrease of *Pax2*, *Lhx1*, *Emx2* and *Wnt9b* mRNA in the UB. *In situ* hybridization on paraffin sections for *Pax2* (*A* and *B*), *Lhx1* (*C* and *D*), *Emx2* (*E* and *F*), and *Wnt9b* (*G* and *H*) in mutant (right panels) and control (left panels) E12,5 embryos. (*A* and *B*) In mutants, *Pax2* mRNA was not detected in the UB (compare arrows in *B* vs *A*) whereas its expression was maintained in the mesenchyme (arrowheads). (*C-H*) The UB expression of *Lhx1*, *Emx2* and *Wnt9b* was strongly decreased in mutants. The UB epithelium is illustrated by dashed lines.

Fig. 7 . *In vivo* binding of HNF1 protein to their chromatin target sites in genes known to be involved in kidney development. Predicted *in silico* HNF1 binding sites (red vertical bars) within *Pax2, Emx2, Wnt9b, Lhx1* and *HNF1β* genes**.** The relative fold enrichment for each DNA fragment upon chromatin immunoprecipitation of HNF1β is illustrated as histograms. Red histograms represent HNF1 binding sites with significant fold enrichments (grey histograms represent the fold enrichment with negative control IgG). Non significant binding is represented by black histograms. PCR experiments were performed in triplicate. Close to *Pax2* gene, more than 20 sites were identified in a window of 100 kb around the transcriptional start site. Three of them, highly conserved were significantly bound (positioned at -22,6kb, -15,8kb and -6,5kb respectively). Two sites detected close to the *Emx2*

gene (at -1,3kb and -2.8kb with respect to the putative transcriptional start site) were significantly bound by HNF1β in vivo. *Wnt9b* and *Lhx1* genes contain each one HNF1 binding site, localized at around +14kb and -8kb respectively from the transcription start site. Both sites were bound *in vivo*. Several HNF1 binding sites were identified close to *HNF1β* transcription start site. Four sites highly conserved in a large number of species (positioned at -54kb, -31kb, +2kb and +34kb from the transcriptional start site, respectively) were strongly bound in vivo by HNF1β. Red vertical bars stand for non tested predicted binding sites. All given site positions are based on the Ensembl Release 53 (Mouse assembly mm9). Species abbreviation: Hs: Homo sapiens, Mm:Mus musculus, Rn: Rattus norvegicus, Cf:Canis familiaris, Xt: Xenopus tropicalis, Bt: Bos Taurus, Md: Monodelphis domestica, Gg: Gallus gallus, Tr: Takifugu rubripes, Tn: Tetraodon nigroviridis, Pa: Pongo pygmaeus abelii, Ga: Gasterosteus aculeatus, Ec: Equus caballus, Oa: Ornithorhynchus anatinus.

Supplementary Figure Legends

Fig. S1. Absence of remodeling in the common nephric duct in *HNF1β*-deficient embryos. X-gal staining on kidney of control (*Mox2Cre HNF1β*$^{+/lacZ}$) and mutant *(Mox2Cre HNF1β*$^{flox/lacZ}$) embryos at E12.5. β-galactosidase activity is an indicator of the endogenous *HNF1β* promoter activity. (*A*) In control embryos, the Wolffian duct and the UB were already directly connected to the urogenital sinus (arrow). (*B*) In mutants, the common nephric duct was abnormally long and the UB is still directly connected with the Wolffian duct (arrow).

Fig. S2. Persistent residual expression of HNF1β in the ureteric bud tips of KspCre *HNF1β* mutant mice. (*A* and *B*) HNF1β immunostaining (in black) on paraffin section of control *HNF1β* $^{flox/+}$ (*A*) and mutant (*KspCre; HNF1β* $^{flox/lacZ}$)(*B*) embryos at E17.5. HNF1β protein was expressed in the tip of the ureteric bud (compare arrowheads in *B* vs *A*) but was not detected in the UB stalk (arrows in *B* vs *A*). (*C* and *D*) Whole mount X-gal staining on kidney of *HNF1β* $^{flox/lacZ}$ (*C*) and *KspCre; ROSA26R* (*D*) mice at E15.5. β-galactosidase reflects the activity of the endogenous *HNF1β* promoter activity in panel (*C)* whereas in the panel (*D)* the β-galactosidase is an indicator of KspCre-driven recombination on the *ROSA26R* locus. X-gal staining was not observed in the most superficial cortical region of *KspCre;ROSA26R* embryonic kidneys, where the UB tips were localized (compare arrows in *C* and *D*).

Fig. S3. Normal ureteric bud tip gene expression patterning in HNF1β -deficient embryos. *In situ* hybridization on paraffin sections of control (left panels) and mutant (right panels) E12,5 embryos for *c-Ret* (*A* and *B*) and *Wnt11* (*C* and *D*). (*A-D*) In both control and mutant embryos, *c-Ret* and *Wnt11* were specifically expressed in UB tips and not in UB trunk. UB epithelium is highlighted by a dashed contour.

Fig. S4. Downregulation of *Pax2* in Mox2Cre *HNF1β*-deficient embryos. Whole mount *in situ* hybridization of *Pax2* in control *HNF1β* $^{flox/lacZ}$ (*A*) and mutant *Mox2Cre; HNF1β* $^{flox/lacZ}$ (*B*) embryos at E10.5. In mutant embryos, only a residual expression of *Pax2* could be detected in the Wolffian duct (compare *B* vs *A*; arrows), whereas this mRNA was expressed at normal level in the uninduced metanephric mesenchyme (compare *B* vs *A*; arrowheads).

Fig. S5. *In vivo* binding of HNF1 protein to chromatin target sites in genes known to be involved in kidney development. Predicted *in silico* HNF1 binding sites (red vertical bars) within *Pax2, Emx2, Wnt9b, Lhx1* and *HNF1β* genes**.** The relative fold enrichment for each DNA fragment upon chromatin immunoprecipitation of HNF1β is illustrated as histograms. Red histograms represent HNF1 binding sites with significant fold enrichment (grey histograms represent the fold enrichment with negative control IgG). Non significant binding is represented by black histograms. Close to *Pax2* gene three highly conserved sites were significantly bound (positioned at -15.8.kb, -14.5kb and -6.5kb respectively). Two sites detected close to the *Emx2* gene (at -1,3kb and -2.8 kb with respect to the putative transcriptional start site) were significantly bound by HNF1β *in vivo*. *Wnt9b* and *Lhx1* genes contain each one HNF1 binding site, localized at around +14kb and -8kb respectively from the transcription start site. Both of these sites were bound *in vivo*. Several HNF1 binding sites were identified next to *HNF1β* gene. Five sites highly conserved in a large number of species (positioned at -54kb, -31kb, -10kb, +2kb and +34kb from the transcriptional start site, respectively) were strongly bound *in vivo* by HNF1β. All site positions are based on the Ensembl Release 53 (Mouse assembly mm9). Species abbreviation: Hs: Homo sapiens, Mm: Mus musculus, Rn: Rattus norvegicus, Cf: Canis familiaris, Xt: Xenopus tropicalis, Bt: Bos taurus, Md: Monodelphis domestica, Gg: Gallus gallus, Tr: Takifugu rubripes, Tn: Tetraodon nigroviridis, Pa: Pongo pygmaeus abelii, Ga: Gasterosteus aculeatus, Ec: Equus caballus, Oa: Ornithorhynchus anatinus.

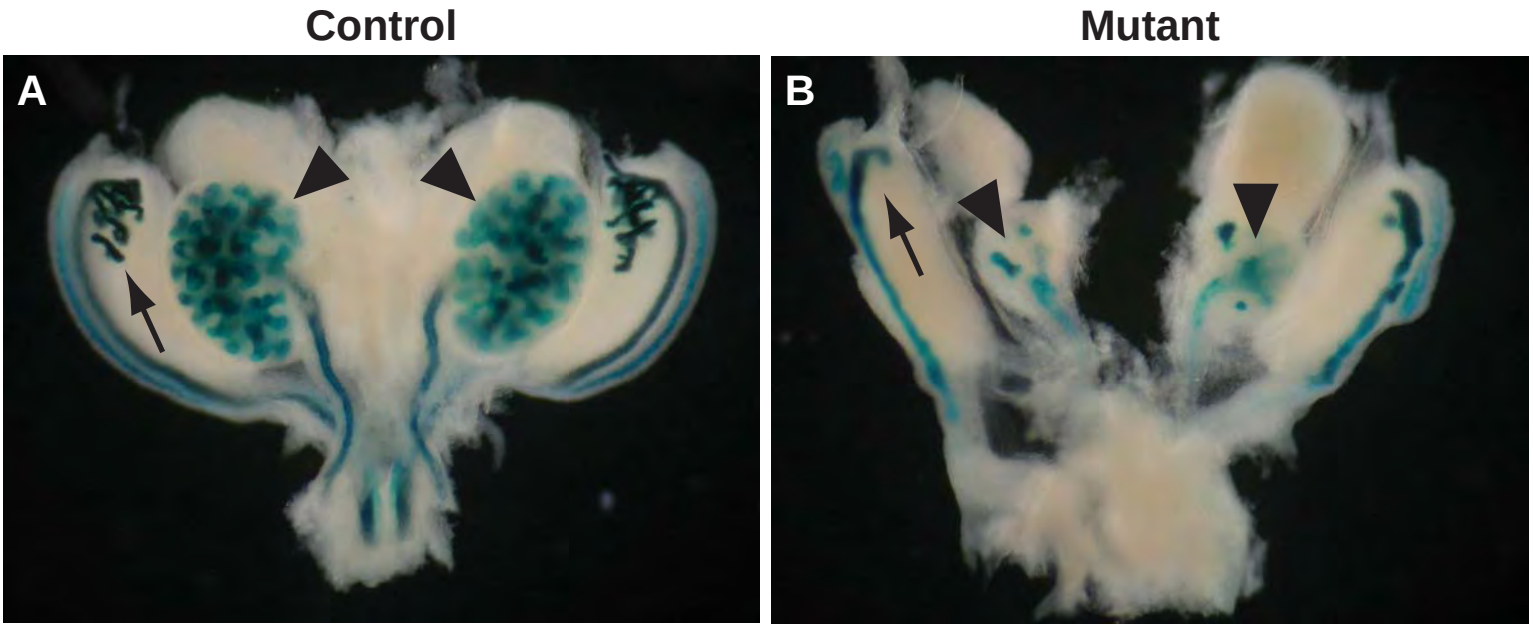

Figure 1

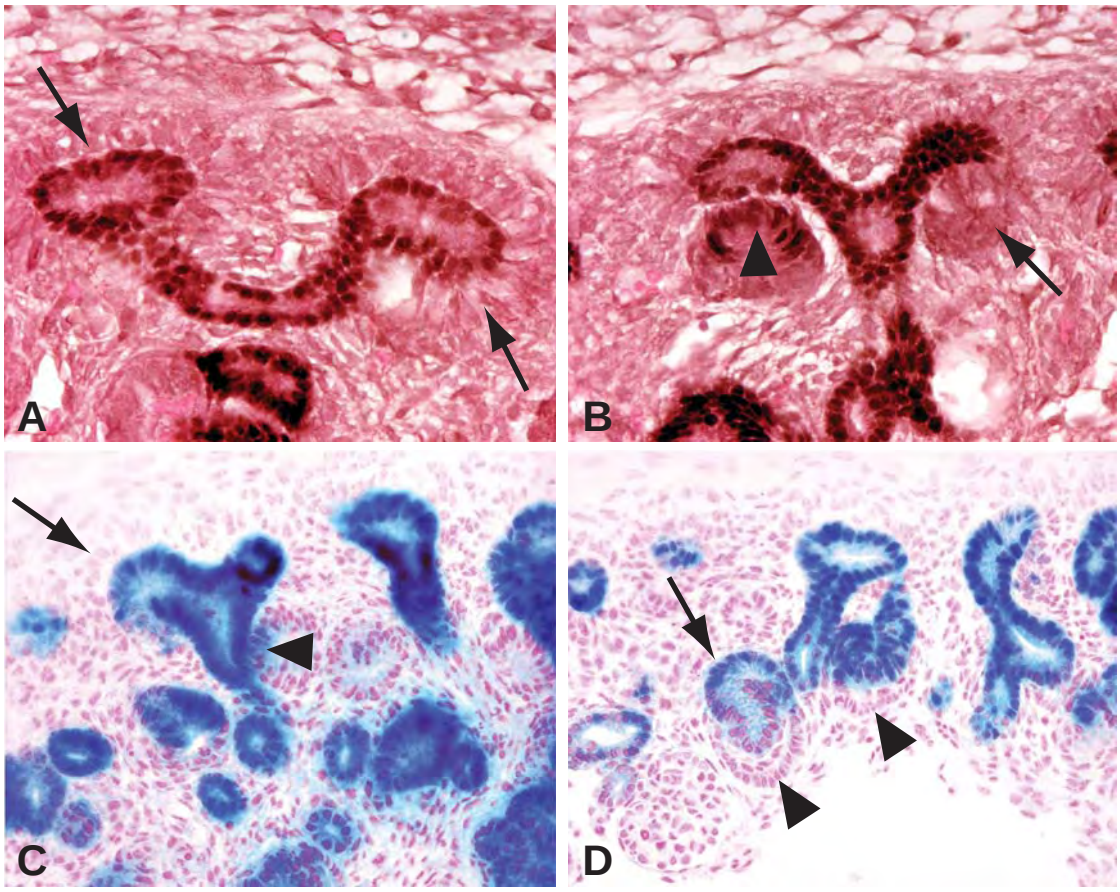

Figure 2

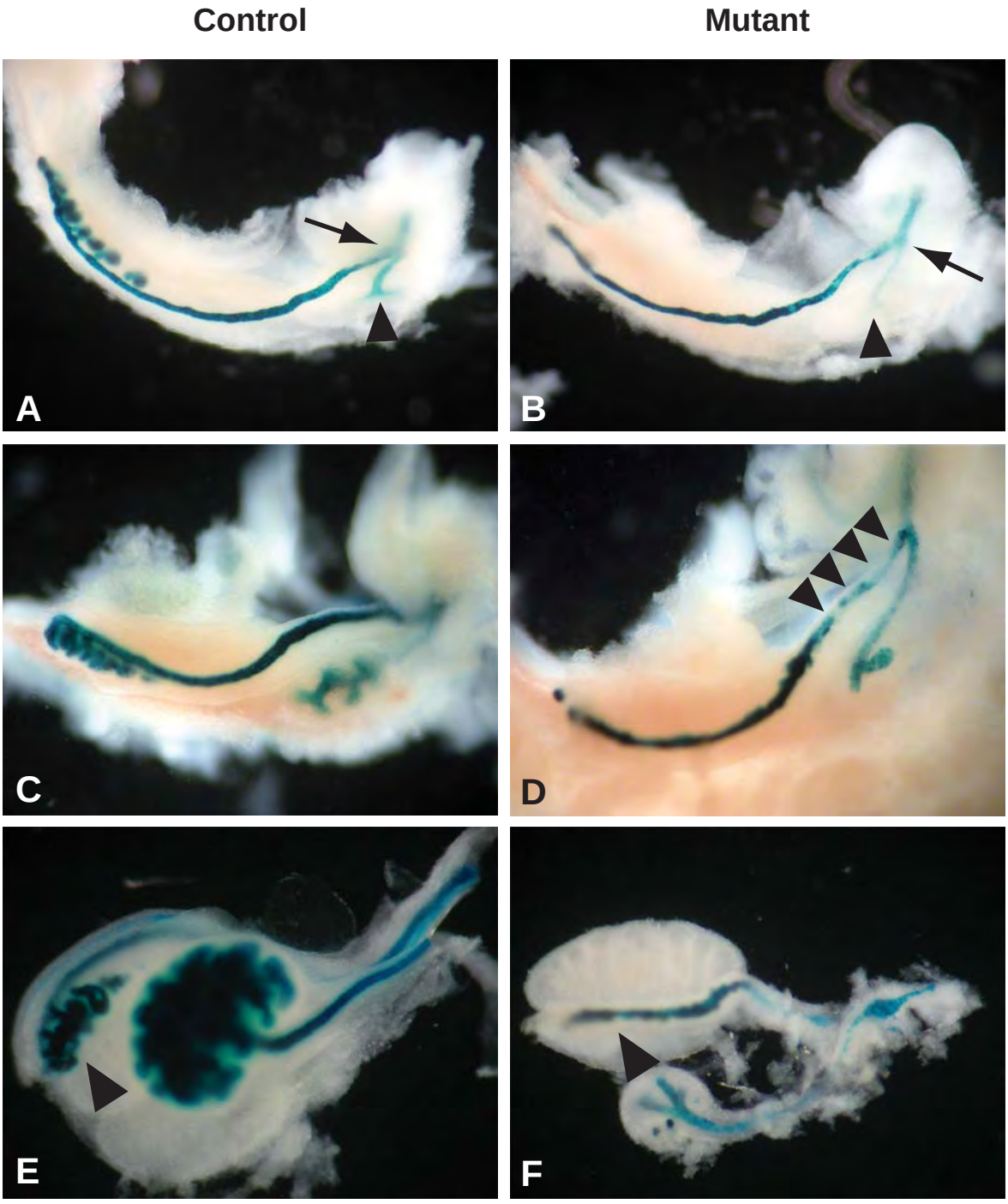

Figure 3

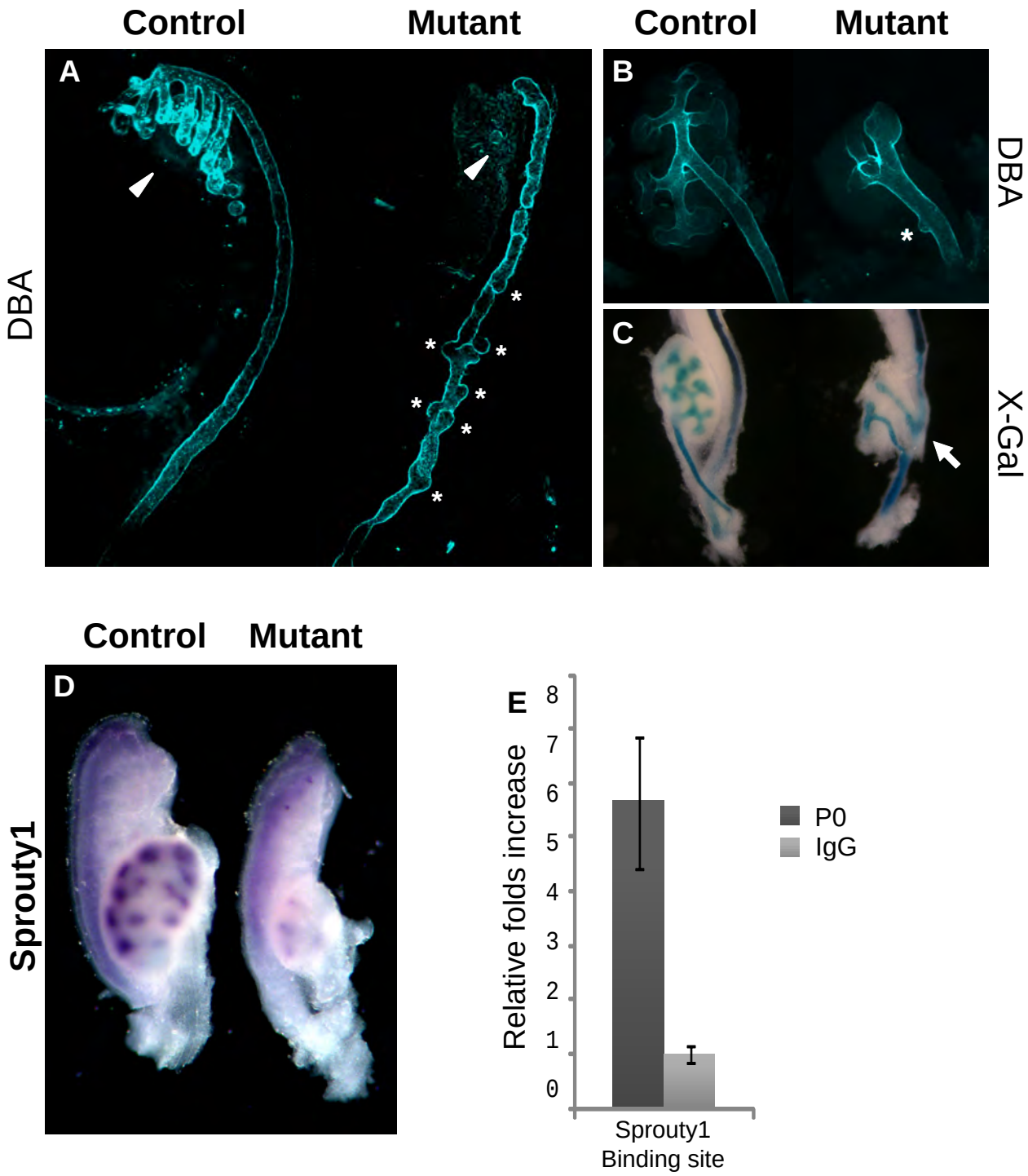
Control
Mutant
Control
Mutant
A
B
C
DBA
DBA
X-Gal
Control
Mutant
D
Sprouty1
Relative folds increase
8
7
6
5
4
3
2
1
0
P0
IgG
Sprouty1
Binding site

Figure 4

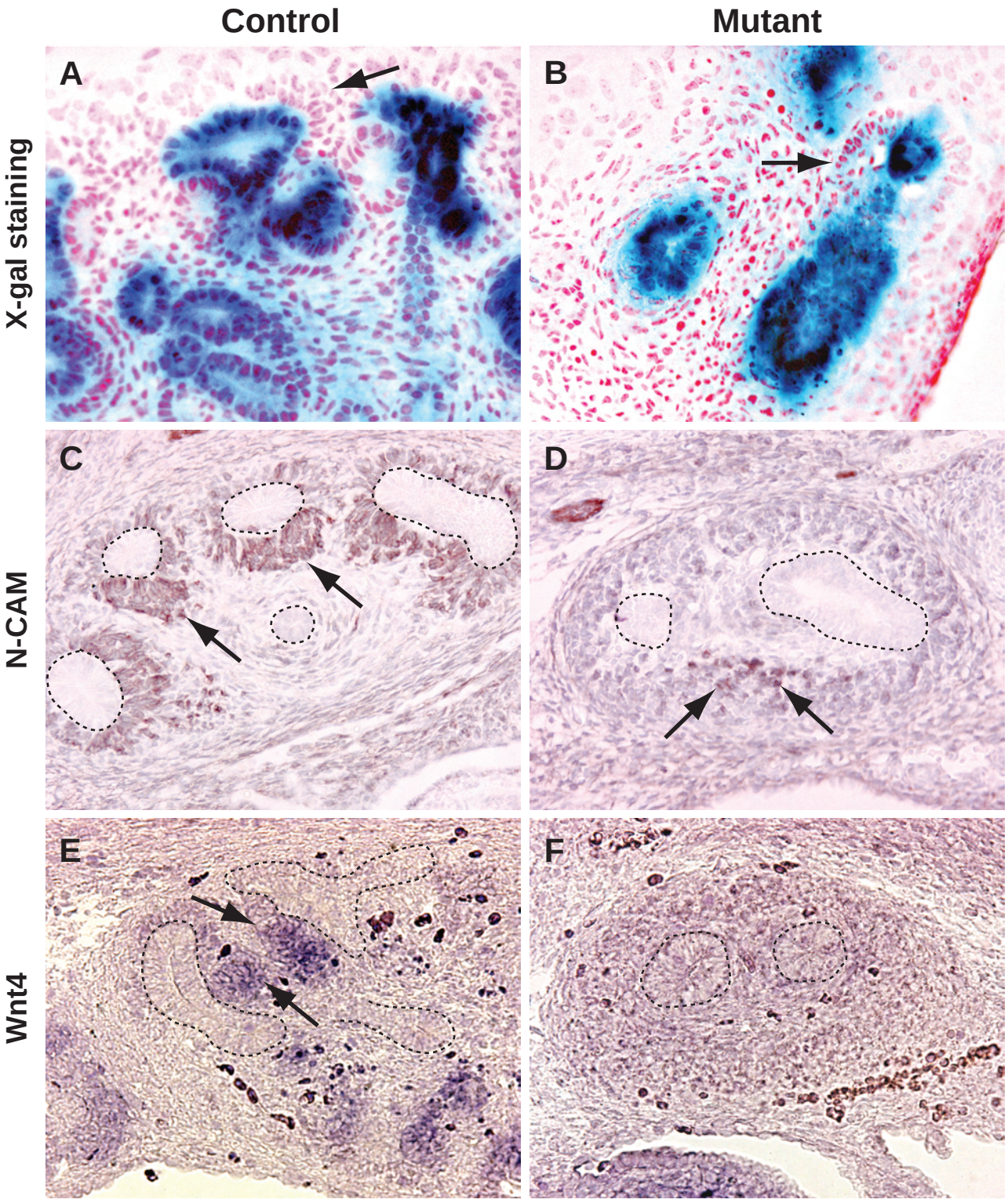

Figure 5

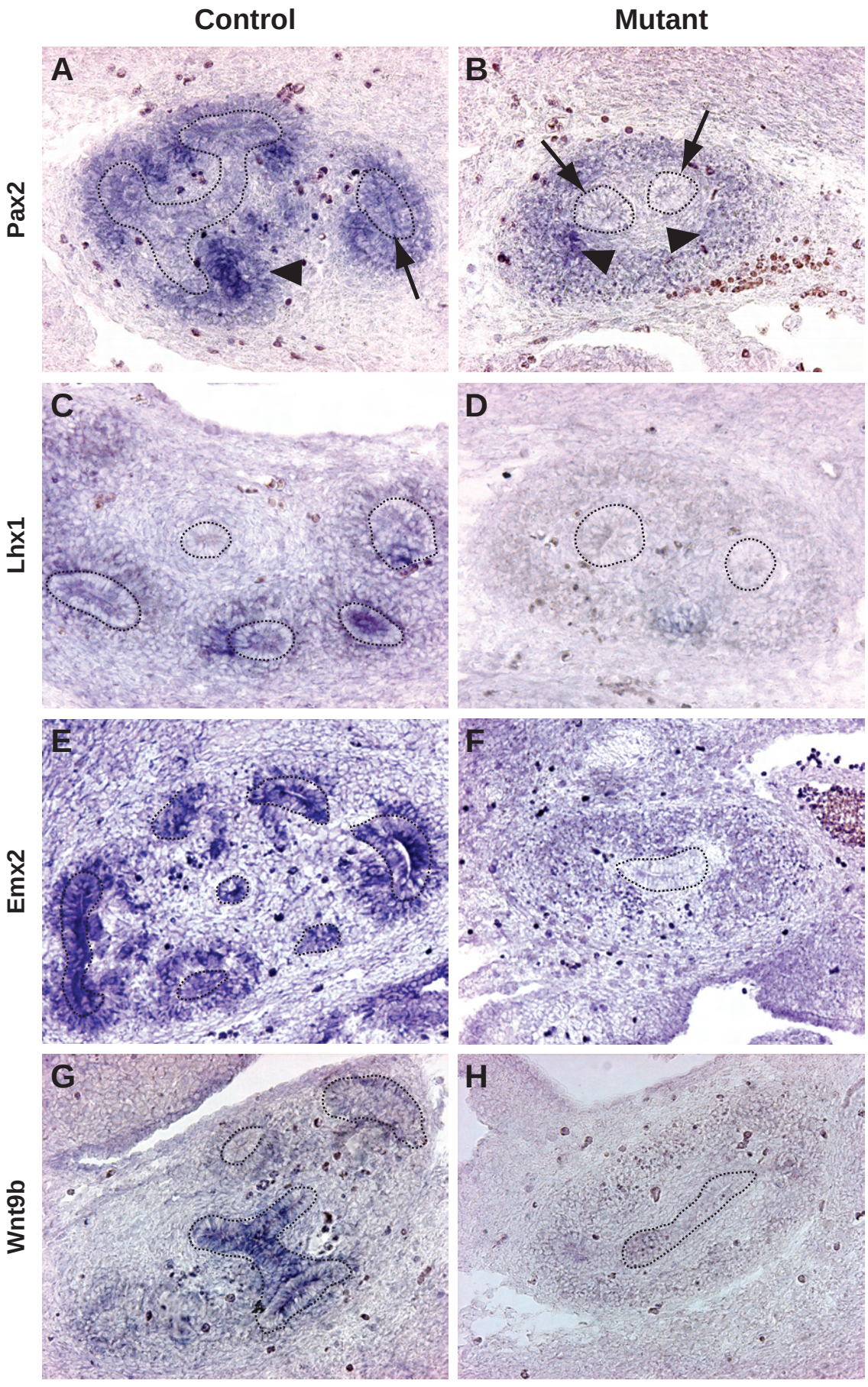

Figure 6

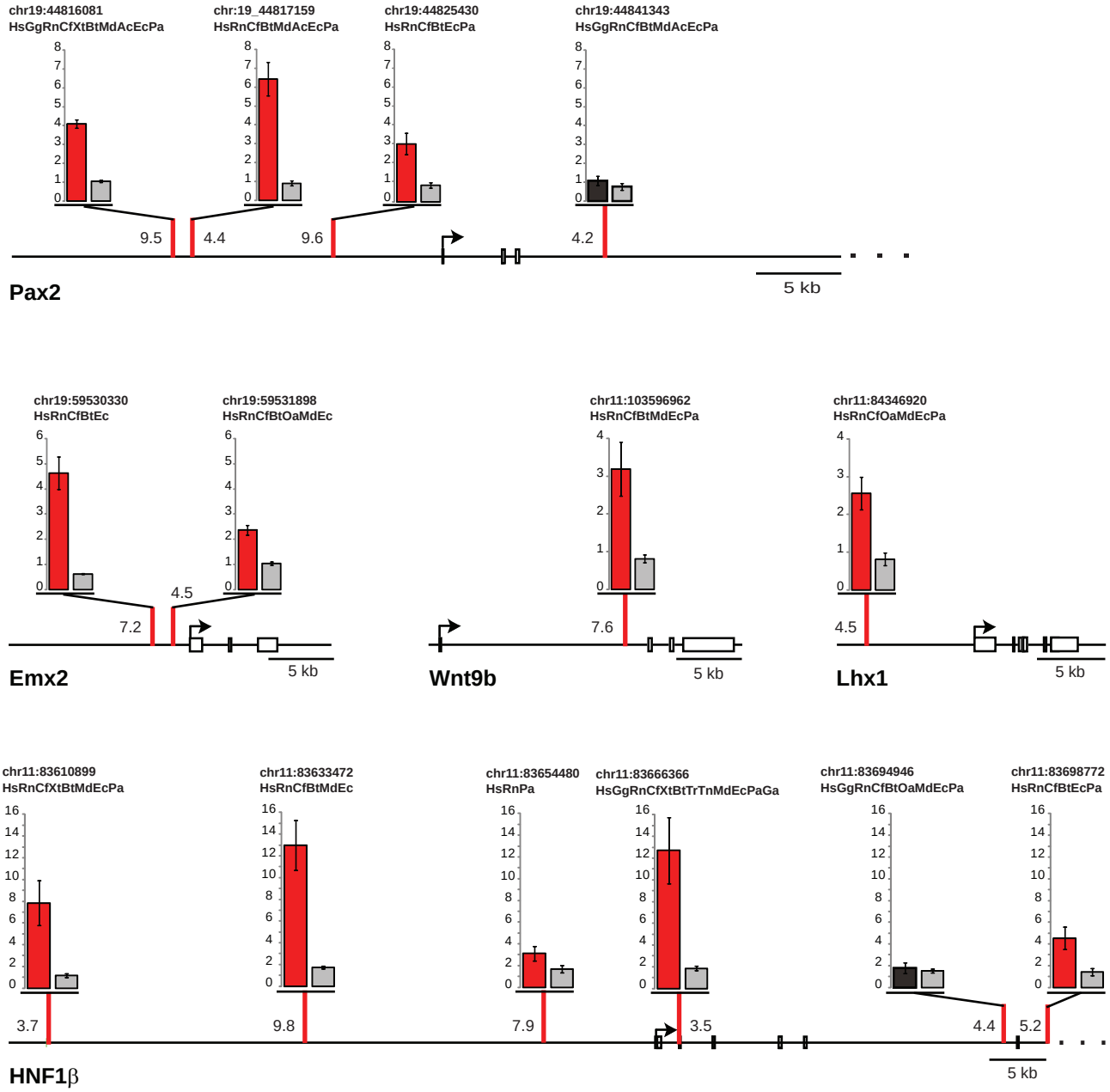
chr19:44816081
HsGgRnCfXtBtMdAcEcPa
chr:19_44817159
HsRnCfBtMdAcEcPa
chr19:44825430
HsRnCfBtEcPa
chr19:44841343
HsGgRnCfBtMdAcEcPa
9.5
4.4
9.6
4.2
5 kb
Pax2
chr19:59530330
HsRnCfBtEc
chr19:59531898
HsRnCfBtOaMdEc
4.5
7.2
5 kb
Emx2
chr11:103596962
HsRnCfBtMdEcPa
7.6
5 kb
Wnt9b
chr11:84346920
HsRnCfOaMdEcPa
4.5
5 kb
Lhx1
chr11:83610899
HsRnCfXtBtMdEcPa
chr11:83633472
HsRnCfBtMdEc
chr11:83654480
HsRnPa
chr11:83666366
HsGgRnCfXtBtTrTnMdEcPaGa
chr11:83694946
HsGgRnCfBtOaMdEcPa
chr11:83698772
HsRnCfBtEcPa
3.7
9.8
7.9
3.5
4.4
5.2
5 kb
HNF1β
chr11:84346920 , chromosomal coordinates (mouse genome mm9)
HsRnCfOaMdEcPa , conserved species list
Relative fold enrichment
Binding of HNF1β
Binding of IgG
5.7
Conserved binding site with HMM score
Significant/non significant binding of HNF1β
Non significant binding of IgG
Transcription start site
Exon

Figure 7

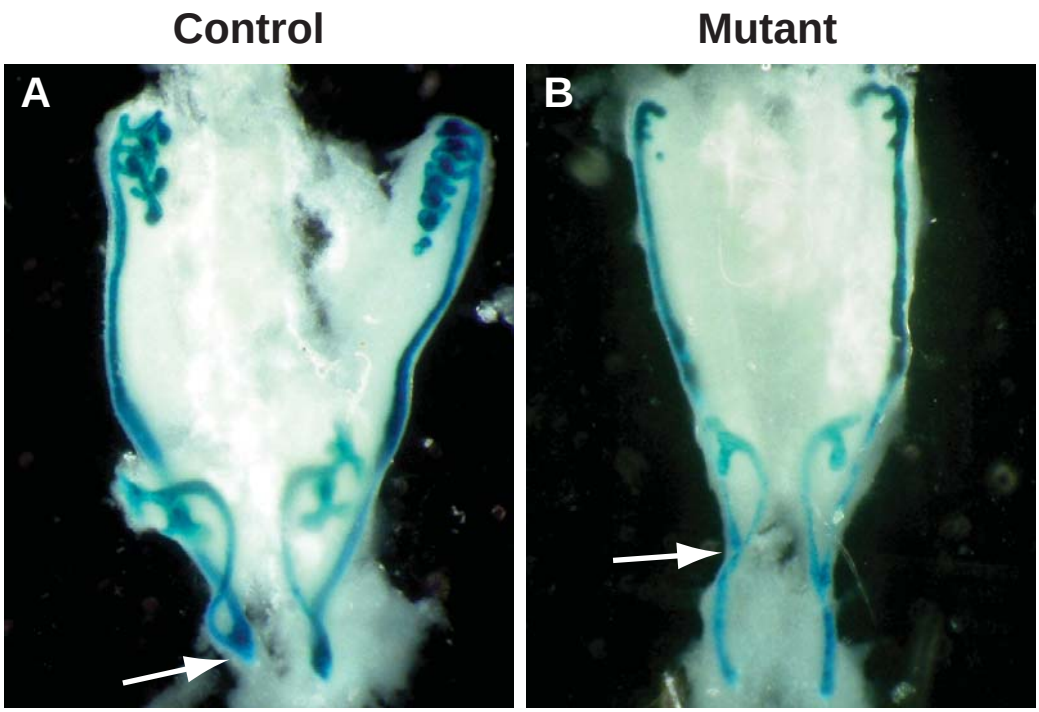

Figure S1

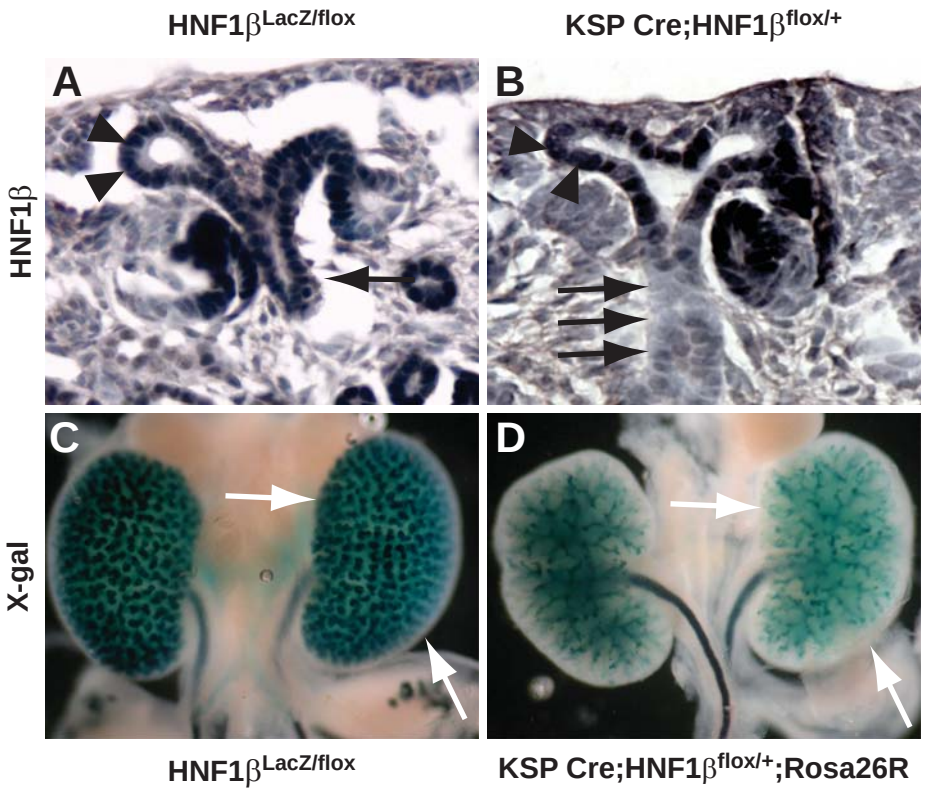
HNF1β LacZ/flox
KSP Cre;HNF1β flox/+
A
B
HNF1β
C
D
X-gal
HNF1β LacZ/flox
KSP Cre;HNF1β flox/+;Rosa26R

Figure S2

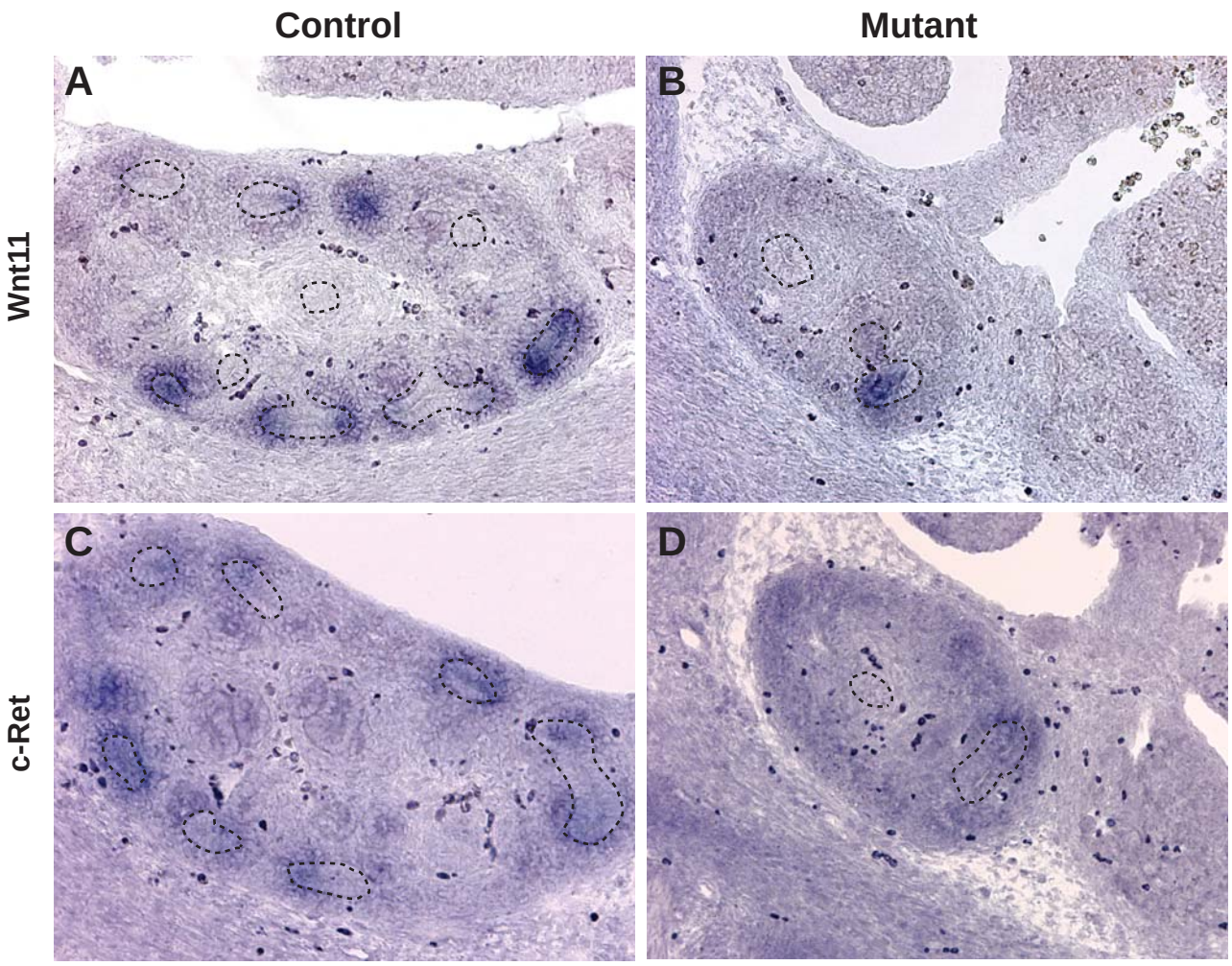

Figure S3

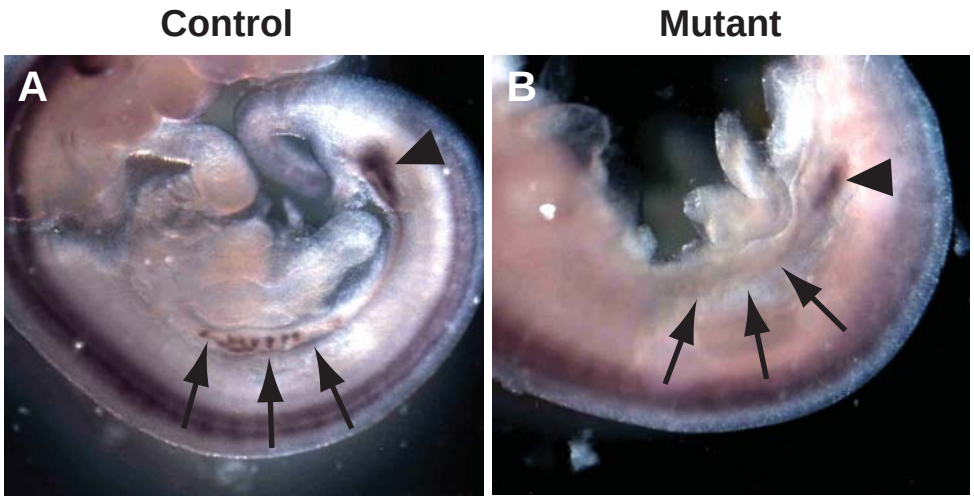

Figure S4

Results Part II

Role of Hnf1b in tubulogenesis

(Paper submitted)

In the first part of my work, I assessed the role of *Hnf1b* in the ureteric bud, but the model we used did not allow us to study the role of *Hnf1b* in the structures derived from the metanephric mesenchyme. The defective development of the ureteric bud totally prevented the mesenchymal to epithelial transition. Renal vesicles, the first epithelial structure derived from the mesenchyme where *Hnf1b* is expressed, never formed in this model. The aim of this second part of my study is to elucidate the role of *Hnf1b* in nephron precursors.

In order to avoid the drastic defect described for the inactivation of *Hnf1b* in the epiblast, we used a specific Cre recombinase under the control of *Six2* gene promoter. This Cre recombinase is expressed only in the cap condensate cells and, thus, will affect only mesenchyme derived structures and not the ureteric bud (Kobayashi et al., 2008). Mutant embryos develop until birth with an expected Mendelian ratio. Interestingly, none of the mutant newborns survived more than 24 hours after birth.

To assess the cause of this early post natal lethality we first analyzed macroscopically the urinary system of newborn mutant. In these animals, kidneys were 30% smaller than the controls and the production of urine was almost not-detectable (empty bladders) suggesting a severe renal failure.

The histological analysis performed on paraffin embedded samples showed that the specific inactivation of *Hnf1b* in the metanephric mesenchyme prevented the development of the tubular part of the nephrons. Apparently normal glomeruli were directly connected to the collecting duct via short tubules. We analyzed in newborn animals the expression of several markers specific for the different tubular segments: LTL (a lectin specific for proximal tubule), *Slc12a2* (a Na/K/Cl cotransporter expressed in the Henle's loop), Parvalbumin (*PvAlb*, specifically expressed in the convoluted collecting duct). Both immunohistochemistry and RT-qPCR analyses showed the absence of these specific tubular markers in mutants. In this model, the collecting duct is not affected by *Hnf1b* inactivation and the expression of its marker, the lectin DBA, is not affected. *Wt1* expression in podocytes is not modified compared to controls.

Further analyses of mutant animals showed that the lack of the tubular part of the nephron is due to the absence of the presumptive precursors of Henle's loop and proximal tubule at the S-shape body stage. In this developping nephron, tubular precursors are present in a peculiar region of the most proximal part of the middle limb (that we identify as "bulge"). In wild type embryos, the first expression of proximal tubules differentiating markers (*villin1* and *Hnf1a*) occurs at the stage of E14.5 when the bulge starts massive increase of size and length. This event never occurs in mutants and the bulge, reduced to a small structure unable to starts the differentiation program, undergoes massive apoptosis.

The aberrant morphology of the S-shaped body is the first evident malformation in the mutants. To better understand when the nephron developing program begins to be affected by *Hnf1b* inactivation, we analyzed early steps of nephrogenesis (vesicle, commas and early S-shape bodies). In these early nephron precursors the phenotype is not yet set and the mutant structures and controls are identical. One of the most studied pathway responsible for the determination of the nephron proximal fate is the Notch signalling pathway: in fact, it has been shown that the inactivation of the receptor *Notch2* is responsible for defective development of proximal tubules and glomeruli (Cheng et al., 2007). In addition, it has also been shown that hypomorphic expression of *Dll1*, a Notch ligand, leads to the reduction of proximal tubules length (Cheng et al., 2007). Therefore, we analyzed the expression of several components of the Notch pathway at E13.5, a time point where the differentiation of the first tubular structures did not have occurred yet. Interestingly, we found a significant decrease specifically in the expression of *Dll1* and *Hes5*, a downstream effector of Notch, whereas all the others components of the pathway maintained a comparable expression level between mutant and controls. By in situ hybridization we showed that in control animals, *Dll1* is normally expressed starting from the distal part of the vesicle and remains expressed in the bulge of S-shaped body. Mutant animals showed, instead, an evident decrease of its expression already in the vesicule, a stage precceding the observed phenotype. This results and the downregulation of the Notch effector *Hes5* (although it is not involved in renal malformation when inactivated in mouse model (Chen and Al-Awqati, 2005) suggest that the decrease activation of the Notch pathway is probably at the basis of the nephric defective specification observed in *Hnf1b* mutant animals.

The absence of *Hnf1b* also affects the expression of other genes important for the nephron development. In particular, we observed a downregulation of *Osr2*, *Irx1*, and *Pou3f3 (Brn1)*. *Osr2* and *Irx1* are two genes involved in the tubulogenesis in *Zebrafish* and *Xenopus*

models (Alarcon et al., 2008), (Tena et al., 2007). *Osr2* and *Irx1* are specifically expressed in restricted portion of the middle limb in the S-shaped body. In mutants, their expression is strongly downregulated. Chromatin immuno precipitation experiments on wildtype animals showed that *Hnf1b* is able *in vivo* to bind consensus sequence on their promoter regions, suggesting a direct control of *Hnf1b* on *Irx1* and *Osr2* expression. *Brn1* is a class III POU protein that starts to be expressed in the distal domain of vesicle. In mouse, this transcription factor is important for the expansion of distal collecting tubules and Henle's loops (Nakai et al., 2003). Our study showed a drastic reduction of Pou3f3 expression already in E13.5 mutant kidneys compared with the controls.

In conclusion, our studies have demonstrated that *Hnf1b* plays an essential role for the generation of renal tubules. In particular, *Hnf1b* is required for the formation of a specific mid-limb sub-compartment (epithelial bulge) of S-shaped body, which is probably at the origin of the expansion of proximal tubules and Henle's loops via the activation of the Notch pathway.

A novel transcriptional cascade in nephron tubular development

Filippo Massa[1], Serge Garbay[1], Raymonde Bouvier[2], Marie-Claire Gubler[3], Laurence Heidet[4], Marco Pontoglio[1*] and Evelyne Fischer[1*]

1) « Expression Génique, Développement et Maladies » (EGDM) Team / INSERM U1016/ CNRS UMR 8104 / Université Paris-Descartes Institut Cochin Dpt. Génétique et Développement, 75014 Paris, France
2) Hospices civils de Lyon, Centre de pathologie Est, 69677 Bron Cedex, France
3) INSERM U983, Hôpital Necker-Enfants Malades, Paris, France
4) AP-HP, Centre de Référence MARHEA, Service de Néphrologie Pédiatrique, Hôpital Necker-Enfants Malades, 149 rue de Sèvres, 75743 Paris Cedex 15, France

* Co-last and corresponding authors: marco.pontoglio@inserm.fr, evelyne.fischer@inserm.fr

Keywords: **HNF1β** / **MODY5** / **Notch pathway** / **Kidney development**

Summary

Nephron morphogenesis is a complex process that generates blood-filtration units (glomeruli) connected to extremely long and patterned tubular structures. The molecular and cellular mechanisms that control this developmental process are still largely unknown. Hepatocyte Nuclear Factor 1β (HNF1β) is a divergent homeobox transcription factor that is expressed in kidney since the first steps of nephrogenesis. Mutations in this gene (HNF1B/MODY5; OMIM #137920) are frequently found in patients who suffer from developmental renal pathologies, whose mechanisms have not been completely elucidated. Here we show that the inactivation of *Hnf1b*, in the murine metanephric mesenchyme, leads to a drastic tubular defect characterized by the absence of proximal, distal and Henle's loop segments. Nephrons were eventually characterized by dilated glomeruli directly connected to collecting ducts via a primitive and short tubule. We demonstrate that early nephron precursors, in the absence of HNF1β gave rise to deformed S-shaped bodies, characterized by the absence of the typical bulge of epithelial cells at the bend between mid- and lower segments. The absence of this bulge eventually leads to the complete absence of proximal tubules and Henle's loops. This defect is linked to a decreased expression of *Dll1*, a direct target of HNF1β, and the consequent defective activation of Notch in the prospective tubular compartment of comma and S-shaped bodies. Our results disclose a novel hierarchical relationship between HNF1β and key genes involved in renal development. In addition, these studies define a novel structural and functional component of S-shaped bodies, at the origin of tubular formation.

INTRODUCTION

Kidney development is a tightly regulated morphogenic process based on the crosstalk between the Metanephric Mesenchyme (MM) and Ureteric Bud (UB) (Dressler, 2009). Any dysfunction in this process may lead to a variety of Congenital Abnormalities of the Kidney and Urinary Tract (CAKUT) (Rumballe et al., 2010). Depending on the nature of the affected compartment, abnormalities in the differentiation program can lead to defects ranging from kidney agenesis to urinary tract malformations. Defective branching of the UB leads to renal hypoplasia, whereas defective mesenchymal differentiation can give rise to renal dysplasia. Remarkably, CAKUT represent overall 20-30% of prenatal anomalies and are responsible for about 40% of cases of chronic kidney disease in children (Neild, 2009).

One of the most prevalent genetic defects responsible for this complex pathology is represented by mutations in the gene encoding for Hepatocyte Nuclear Factor-1β (*HNF1B*), a divergent homeobox transcription factor. *HNF1B* mutations are detected in approximately 20 - 30 % of patients or fetuses that suffer from renal developmental anomalies predominantly including renal cysts, hyperechogenicity, hypoplasia, or single kidneys (Ulinski et al., 2006; Decramer et al., 2007; Heidet et al., 2010). Even though mutations in *HNF1B* are known to be responsible for Maturity-Onset Diabetes of the Young (MODY) type 5 (Lindner et al., 1999), several studies have consolidated the idea that one of first traits of pediatric patients and fetuses carrying *HNF1B* mutations is rather represented by the occurrence of renal malformations (Ulinski et al., 2006; Decramer et al., 2007; Heidet et al., 2010). The study of animal models for the deficiency of *Hnf1b* in renal development and maturation has helped to understand some of the functions exerted by HNF1β (Bohn et al., 2003; Gresh et al., 2004; Hiesberger et al., 2004; Sun et al., 2004; Wu et al., 2004; Lokmane et al., 2010; Verdeguer et al., 2010). It has been demonstrated that the phenotype of mice lacking *Hnf1b* depends very much on when (developmental timing) and where (what tissues compartment) exactly the inactivation of this gene is generated. For instance, it has been shown that the germ-line inactivation of the *Hnf1b* gene is embryonic lethal (E7.5) due to defective differentiation of the extra-embryonic visceral endoderm (Barbacci et al., 1999; Coffinier et al., 1999a). During kidney development the lack of this gene in the UB leads to defective UB branching and to the absence of mesenchymal to epithelial transition due to a defective expression of key genes including *Wnt9b* ((Lokmane et al., 2010) and unpublished observations). In parallel, it has

been shown that the deletion of *Hnf1b* in already formed, still elongating, tubular segments leads to a severe polycystic kidney phenotype (Gresh et al., 2004; Verdeguer et al., 2010). In this context, it has been demonstrated that HNF1β is a chromatin bookmarking factor that is required for the postmitotic reprogramming of the expression of a number of genes whose mutations are frequently associated with cystic kidney disease (Verdeguer et al., 2010). In addition, we have shown that the elongation of normal nephrons, during their post natal maturation, is due to the peculiar alignment of mitotic spindles with the tubular axis. This mitotic alignment is lost in the renal cystic epithelium of *Hnf1b* mutant mice (Fischer et al., 2006).

In the last years a considerable number of studies have clarified the key molecular mechanisms involved in the very first steps of nephron morphogenesis (Boyle et al.; Stark et al., 1994; Carroll et al., 2005; Cheng et al., 2007; Dressler, 2009). However, the signaling pathways and the actors that specify and determine the identity of the tubular nephron component and its expansion in nephron precursors are still mostly unknown. Recent studies have highlighted the critical role of the Notch signaling pathway in tubular segmentation and glomerular formation. Canonical Notch signaling pathway involves the binding of specific ligand (Jagged or Delta like) to Notch receptors. This binding is responsible for proteolytic cleavages of the receptor that lead the intracellular domain of Notch (NICD) to translocate to the nucleus. NICD then can bind to RBP-J and activate the expression of a number of target genes including the Hes and Hey families of transcription factors (Kopan and Ilagan, 2009). The inactivation of *Notch2*, one of the Notch receptors, in renal mesenchyme, is responsible for the absence of both proximal tubular formation and glomerulogenesis. In addition, a hypomorphic allele of one of its ligands, Delta-like1 (Dll1), is responsible for a drastic defect in tubular formation and a reduction of the number of nephrons (Kiernan et al., 2005; Cheng et al., 2007).

Nephron tubular compartments are generated by a proliferative expansion of presumptive tubular cells that emerge from S-shaped bodies. At the morphological level, these nephron precursors are composed by three distinct segments: the upper limb, which will give rise to the Distal Convoluted Tubule (DCT), the mid-limb, which is at the origin of Henle's Loop (HL) and Proximal Tubules (PT), and the lower limb that will form the blood filtration unit of the nephron, the glomerulus. Recently, the analysis of the expression pattern of specific developmental genes has shown that the mid-limb can be further subdivided in

specific domains (Thiagarajan et al., 2011; Yu et al., 2012). However, the biological significance of this fine-tuned, patterned genes expression, along with the actual developmental functions of these domains remains still poorly explored.

In the present study, we demonstrated that the lack of HNF1β, in the metanephric mesenchyme, leads to the formation aberrant nephrons with dilated glomeruli and the absence their typical tubular components, Henle loops, distal and proximal tubules. Mutant S-shaped bodies were characterized by the absence of a bulge of epithelial cells in the mid-limb. We have shown that this phenotype was linked to the defective expression of *Dll1* and lack of Notch signalling pathway activation.

MATERIAL AND METHODS

Mice. Specific inactivation of *Hnf1b* in the metanephric mesenchyme was obtained using a Cre-LoxP strategy. Six2-Cre (Kobayashi et al., 2008), *Hnf1b* $^{LacZ/+}$, *Hnf1b*$^{f/f}$ mice were previously described (Coffinier et al., 1999b; Coffinier et al., 2002). Since *Six2-Cre*; *Hnf1b*$^{f/+}$ or *Six2-Cre*; *Hnf1b* $^{LacZ/+}$ mice were indistinguishable from wild type mice, all these animals were used as controls (indicated in this study as "control"). Animals were maintained in two animal facilities each of which is licensed by the French Ministry of Agriculture (agreement A 75-14-02, dated April 24, 2007). All experiments were conforming to the relevant regulatory standards.

Tissue samples preparation and immunohistochemistry. Fetal renal specimen as well as fetal tissue for DNA isolation was collected after obtaining informed consent from the parents. The pregnancy had been interrupted during the third trimester because of cystic kidneys, after parents request and acceptation by the prenatal diagnosis center of Lyon (France). Genomic DNA was isolated by standard methods. Mutation screening was performed as in (Heidet et al., 2010). Images from histological sections from a MODY5 patient carrying a c.232G>T, p.Glu78X mutation were provided by Professor Laurent Daniel, CHU Timone, Marseille, France.

Mouse kidneys have been dissected from embryos at E13.5, E14.5, E16.5 and E18.5 days of gestation and from newborn pups (at P0), fixed in 4% PFA for 24 hours and embedded in paraffin. For histological analysis, 5µm paraffin sections were stained with Hematoxylin Eosin. Immunohistochemical analysis were performed on 5µm paraffin sections. After antigen retrieval in boiling citrate buffer (Dako, ref. S2369) for 15 minutes, sections were treated with the MOM Kit (Vector lab, ref BMK-2202) according the manufacturer instructions and incubated with the antibodies for 1 hour at room temperature or at 4°C overnight. For the list and dilution of antibodies, refer to Supplementary Material and Methods. After several washes in PBS 1X Tween 0.1% (PBST), secondary antibodies Alexa Fluor (Invitrogen) against rabbit or mouse and coupled with different fluorochromes were incubated for one hour at RT (1:500). The slides were mounted in VectaShield (Vector, ref H1000) and analyzed with bright field microscope or spinning disk confocal microscope.

Images were analyzed with ImageJ (http://rsbweb.nih.gov/ij/) and assembled with Adobe Illustrator.

In situ hybridization (ISH). cDNA of genes of interest were obtained by RT-PCR using specific primers (For the list of the primers, see Supplementary Material and Methods, Table S1). The templates were either subcloned in pGEM7Z or used directly as templates with a specific SP6 or T7 tail to generate digoxigenin-labelled RNA probes with the Digoxigenin RNA Labeling Kit (ROCHE). ISH experiments have been carried out according to the protocol described in Supplementary Material and Methods.

Real time PCR analysis. cDNA have been obtained from total RNA from E13.5, E14.5 and P0 kidneys from control and mutant animals, using the kit SuperScript® III Reverse Transcriptase (Invitrogen, ref 18080-051). Gene expression was analyzed by qPCR with Stratagene Mx3000P™ real-time PCR system using SYBR Green-Rox (Roche ref 04 913 914 001) in triplicates. Primers were designed using Primer3 software. Expression levels in mutants are indicated relative to controls. Results were normalized with GAPDH expression level. Error bars represent standard error of the mean (n=3 for control and mutant at E13.5 and P0, and n=5 for control and mutant at E14.5). For the list of the primers, see Table S2 in Supplementary Material and Methods.

Chromatin Immuno-Precipitation (ChIP). Nuclei have been purified from pooled wild type embryonic kidneys. Chromatin preparation and ChIP were performed as previously described (Verdeguer et al., 2010) (for detailed protocol for chromatin purification and ChIP, refer to Supplementary Material and Methods). The equivalent of 10µg of chromatin (calculated in term of DNA content) has been used for ChIP: aliquots were pre-cleared 2 hour rocking at 4°C and incubated overnight at 4°C with 3µg of HNF1β antibody (Santa Cruz) or with IgG as a control. Quantification of precipitated specific DNA fragments was carried out with qRT-PCR in triplicates. Relative fold-enrichment of DNA fragments was calculated using the following formula: (ChIP HNF1β /ChIP IgG). Primers were designed using Primer3 software. For the list of the primers, see Table S3 in Supplementary Material and Methods.

Assessment of the extent of proliferation and apoptosis. To evaluate proliferation and apoptosis, freshly dissected kidney from E17.5 control and mutant embryos have been fixed in 4% PFA for 30 min and embedded in Agarose 4%. 80µm thick vibratome sections were then postfixed 10 minutes in PFA4% at RT and incubated with Peanut Agglutinin (Vector, ref RL-1072) and anti-cleaved caspase-3 antibody (R&D system, ref AF835) or anti-Phosphorylated Histone H3 antibody (Abcam, ref Ab5819) for 48h in PBS-Sodium Azide 0.1%-Triton 0.01%. After several washes, sections have been incubated with appropriate secondary antibodies and DAPI for 12 hours. Slides were analyzed with spinning disk confocal microscope.

Electron microscopy. Kidneys were cut in small slices of 1 mm^3, fixed 1 hour in glutaraldehyde 3 % and postfixed in Osmium Oxyde 1 %. EPON resin embedded samples were then cut (ultra thin 70 nm sections) with an Ultramicrotome Reichert Ultracut S and analyzed with Electron Microscope JEOL 1011.

RESULTS

HNF1β deficiency, in the metanephric mesenchyme, results in early postnatal lethality.

In order to analyze the role that HNF1β plays in mesenchymally derived nephron precursor structures, we used a Cre recombinase mouse strain that selectively inactivates *Hnf1b* in nephron progenitor mesenchymal cells, before the onset of its expression. Six2 is a transcription factor that is specifically expressed in mesenchymal stem cells that gives rise to all nephron epithelial cells (Kobayashi et al., 2008). It has been shown that BAC transgenic animals that expressed the Cre recombinase under the control of *Six2* promoter regions, target this stem cell compartment without affecting the UB (Humphreys et al., 2008). With this strategy, embryos carrying a $Hnf1b^{flox/flox}$; Six2-Cre germ-line genotype should maintain the expression of HNF1β in the UB, that in turn should provide the mesenchyme for all the signaling stimuli necessary for the mesenchymal to epithelial transition (MET), at the origin of nephrogenesis.

Our results showed that MM-specific Six2-Cre-driven *Hnf1b*-deleted embryos (indicated here as "mutant" embryos) did not suffer from any prenatal lethality and were delivered with a normal Mendelian ratio. Newborns, in their first day of life, had an almost normal appearance and could feed. However, they died between the first and second day after birth (Table1) with a lifespan compatible with a severe congenital kidney failure. Macroscopic examination showed that kidneys from mutant newborns were smaller in size with a length approximately 70% of that of control littermates (Fig. 1A,B). Consistently, the bladder of mutant embryos was smaller suggesting that pups were probably unable to produce normal urine levels (Fig. 1C,D). In addition, 15 % of newborn pups showed hydroureter and hydronephrosis (data not shown).

The expression of HNF1β in nephron precursors is essential for the development of tubules.

At birth, the nephrogenic zone, localized in the more external part of the cortex, had similar thickness in both mutant and control kidneys. However, the typical convoluted tubular epithelial structures, that are normally visible in the cortex of control animals, were absent in mutant kidneys (Fig. 1E,F). In order to characterize the identity of the missing tubular segments, we performed immunostaining and in situ hybridization (ISH) on renal histological

sections. Our results showed that at birth mutant pups lacked most of the tubular nephron segments that are typically produced by the nephrogenic mesenchyme. In particular, mutant embryos showed very drastically reduced production of Proximal Tubules (PT), Henle's loops (HL) and Distal Convoluted Tubules (DCT). The use of Lotus Tetragonolobus lectin showed only rare, scattered PTs (Fig. 1G,H). In a similar way, only very rare HLs and DCTs were detected, as shown by the almost complete lack of NKCC2 (*Slc12a1*) and Parvalbumin (*Pvalb*) expression (Fig. 1I-L). In addition, quantitative RT-PCR (qRT-PCR) demonstrated that at P0 mutant pups had a dramatic decrease in the expression of several mRNA normally expressed in PT, HL and DCT (Fig. 1M). In agreement with the absence of the expression of the Cre recombinase in the UB, the collecting ducts were not affected, as demonstrated by the presence of the typical medullar tubular rays, visible in mutant newborn pups (Fig. 1E,F). In addition, immunochemistry, immunofluorescence and qRT-PCR experiments showed that all these tubules were positive for typical markers of collecting ducts (CD) such as Dolicho biflorus aglutinin (DBA) (Supplementary material Fig. S1A,B) and *Wnt9b* (Supplementary material Fig. S1E) and remained positive for the expression of HNF1β (Fig. 2). Interestingly, the absence of HNF1β did not impair the differentiation of glomeruli. Renal corpuscles, regularly dispersed in the cortex, were present in a number comparable to that of controls animals. Consistent with these findings, podocytes expressed normal levels of *Wt1* (Supplementary material Fig. S1C,D). Nevertheless, these glomeruli presented with abnormal shape (see below), and several of them had visible dilation of their Bowman's capsule (inset in Fig. 1E,F). Taken together, these observations demonstrated that in the absence of HNF1β, nephron precursors were somehow able to form glomerular structures but were not competent to generate and expand their typical tubular nephron components.

Drastic distortion of nephron precursors in mesenchymal deleted *Hnf1b* kidneys.

In order to characterize the mechanisms of the observed phenotypes we decided to identify the first detectable abnormalities that led to these drastic developmental defects. In agreement with previous studies (McMahon et al., 2008; Lokmane et al., 2010; Harding et al., 2011), immunofluoresence experiments showed that HNF1β was not expressed in cap mesenchyme (arrow in Fig. 2A). This protein started to be detected only in renal vesicles with a clear polarized distal pattern in a limited number of cells adjacent to the UB, in the prospective tubular compartment (Fig. 2A). We showed that the first steps of mesenchymal to epithelial conversion were completely preserved in kidney from embryos carrying a Six2-Cre

driven *Hnf1b* deletion (Fig. 2B). In addition, the peculiar mutually exclusive distal/proximal expression pattern of specific genes was preserved. In both control and mutant embryos, vesicles were characterized by a polarized expression of *Jag1* in the distal portion of the vesicle, whereas *Wt1* expression was restricted to the proximal compartment (Fig. 2C,D). In mutant embryos, comma-shaped bodies did not display any detectable morphological abnormalities, whereas on the contrary, the structure of S-shaped bodies was significantly altered. HNF1β, in control embryos, was expressed at high levels in the prospective tubular segments of comma- and S-shaped bodies (Fig. 2E,G). Noteworthy, HNF1β was expressed in the prominent and protruding bulge of epithelial cells that forms the first bend between the mid and the lower limb, clearly visible in sagittal sections. In the absence of HNF1β, this typical structure did not form (Fig. 2G,H and K-N). In coronal sections of S-shaped bodies of control embryonic kidneys we could observe the mid-limb cut in a perpendicular orientation, almost circularly shaped. This structure is typically positioned over a concentric, concave layer of *Wt1* highly positive columnar epithelial cells (that gives rise to the typical podocyte precursor smiling crown) (Fig. 2I). In mutant embryos this stereotypical "smiling" structure was replaced by a "mustached" configuration (Fig. 2J). Mutant embryonic "S-shaped" structures were characterized by the presence of a mid-limb that was directly connected to the prospective urinary space in the lower limb compartment. In spite of this drastic defect, the most proximal part of the S-shaped body (lower limb) developed normally, giving rise to precursors of podocytes and Bowman capsule epithelial cells, as illustrated by the expression of *Wt1* (Fig. 2L). The unaltered structure of lower limb in mutant embryos correlated with the complete absence of expression of HNF1β in podocytes and their precursors (Fig. 2G). In summary, all these results showed that the absence of HNF1β in nephron precursors prevented the formation of the prominent and protruding bulge of epithelial cells at the bend between the mid and lower limbs.

The lack of HNF1β prevents the initiation of tubular differentiation.

It is known that the emergence, the expansion and first differentiation of proximal tubules and Henle loops begins in the more advanced and mature S-shaped bodies already at E14.5.With the use of qRT-PCR assays on cDNA, prepared from total kidneys of control embryos, we could detect the expression of typical tubular markers (*Hnf1a*, *Hnf4a*, *Vil1* and *Slc12a1*) already at this stage. Their expression further increased to higher levels just before

birth (Fig. 3A and data not shown). In agreement with the defective tubule formation and expansion, visible in newborns, the expression of all these markers was drastically decreased in mutant embryos already at E14.5 (Fig. 3B). Most of these genes are known to contain several HNF1 binding sites in their transcriptional control regions (Tronche et al., 1997), MP and SG, unpublished results). The defective expression of these genes could be have been ascribed to a potential direct transcriptional activation effect of HNF1β. The concomitant loss of expression of all these genes could have contributed to play a role in the formation and expansion of nephron tubular components. However, in agreement with previous observations (McMahon et al., 2008; Harding et al., 2011), our inspection clearly revealed that S-shaped bodies, in wild type embryos, were still devoid of a significant expression of the protein or mRNA of these genes. *Hnf1a*, *Hnf4a* and *Vil1* were expressed only at later developmental steps of differentiation and specifically when PT have already emerged from S-shaped bodies (Fig. 3C and data not shown). Since mutant embryos "S-shaped" never expanded these tubular structures, we concluded that the defective expression of all these genes was simply the consequence and not the origin of the developmental defect. All together, these experiments indicated that the absence of tubular components, observed in our mutant newborn animals, is not due to a progressive loss of normally differentiated tubules. Our results indicated that in the absence of *Hnf1b*, the process of tubular expansion and differentiation was completely impaired.

The effect of the deficiency of *Hnf1b* on proliferation and apoptosis.

The aberrant conformation of mutant S-shaped structures could have been ascribed to a defective proliferation/apoptotic balance in the precursors of S-shaped bodies (vesicle or comma-shaped bodies). To evaluate this possibility we monitored and compared the occurrence of proliferative and apoptotic events by counting the number of H3PS10 and cleaved caspase-3 positive cells, respectively. This scoring was performed in 100 μm thick vibratome sections in order to evaluate the occurrence of proliferative and apoptotic events in structures in their whole extent. These experiments showed that S-shaped bodies had a significant decreased proliferation specifically in the upper and mid-limbs. These segments were also characterized by a significantly increased number of apoptotic events (Fig. 3D,E). In the lower limb, we could not see any difference in the average number of proliferative or apoptotic events. This observation paralleled the fact that in the lower limb, *Hnf1b* is not expressed in podocyte precursors and is expressed only at low levels in the prospective capsular cells. It is worth to note that early nephron precursors (vesicles and comma-shaped

bodies) were not affected by any defective proliferation or excessive apoptosis. Aberrations in these processes only occurred in already deformed S-shaped segments (Fig. 3D,E). This suggested that the defective proliferation and excessive apoptosis might be ascribed to late, secondary effects, possibly linked to the deformation or to the lack of differentiation induced by the absence of HNF1β.

Molecular mechanisms of defective tubule specification.

Recent studies clearly indicated that gene expression pattern in nephron precursors is more complex than what was previously thought. In particular, the use of large scale analysis of the expression of transcriptional regulatory factors, has revealed novel molecular subdomains in developing renal structures (Thiagarajan et al., 2011; Yu et al., 2012). We took advantage of these studies in order to identify the specific nature of the deformation of S-shaped structures in mutant embryos. As a first approach, based on a qRT-PCR analysis, we monitored the level of expression of genes that have been shown to be expressed in subdomains of the mid-limb including *Osr2, Pou3f3* and *Irx1* (Yu et al., 2012). Our results showed a significant down regulation of their expression already at E13.5 (Fig. 4A). In control embryos *Cadh6,* at this stage, is predominantly expressed is renal vesicles. With the progressive appearance of comma- and S-shaped bodies, *Cadh6* becomes also specifically expressed in the first prospective proximal tubule precursor cells (Cho et al., 1998; Mah et al., 2000). In mutant embryos the expression of this gene was normal at E13.5 but drastically decreased, together with *Osr2*, *Pou3f3* and *Irx1* at E14.5 (Fig. 4B).

The mid-limb of S-shaped bodies is characterized by the expression of *Pou3f3* in a relative large segment whereas the expression patterns of *Osr2* and *Irx1* tend to be more restricted in the most proximal part of the mid-limb. In situ hybridization (ISH) experiments revealed that the expression of these two genes was significantly reduced in S-shaped bodies (Fig. 4C-F). In a similar way, with an immunohistochemical approach, we were able to show that the expression of *Jag1* was also decreased in the mid-limb of the S-shaped body (data not shown). The global downregulation of all these genes is probably a direct consequence of the defective specification and formation of this territory. In parallel, we also monitored the levels of expression of *Lhx1* and *Pax2,* genes whose expression is known to be controlled by HNF1β in other kidney compartments (Lokmane et al., 2010), and that have been shown to play a role in kidney development (Dressler et al., 1993; Kobayashi et al., 2005). Our qRT-PCR analysis did not show any decreased expression of *Lhx1* or *Pax2* at E14.5 (Fig. 4K). At later steps, at E19.5, the inspection of the expression pattern of these two genes by ISH showed an aberrant

persistent high expression of these two markers in abnormal S-shaped bodies in mutant and in the rare and primitive tubular segments that were formed (Fig. 4G-J). In addition, qRT-PCR performed on newborn pups showed a clear up regulation of the expression of these two genes (Fig. 4K). The persistent expression of these genes suggests that even if mutant embryos developed some short and primitive tubular components, they did not fully differentiate and still expressed markers of earlier steps of their developmental program.

It has been shown that Notch signaling plays a crucial role in the specification and differentiation of the most proximal structures of nephrons during development. Interestingly, mice carrying a hypomorphic allele of *Dll1*, one of the ligands of the notch receptors, have a phenotype reminiscent of our mutant embryos. In fact, the defective expression of *Dll1* leads to a drastically reduced formation of proximal tubules (Cheng et al., 2007). Interestingly, *Dll1*, NICD as well as *Hes5* are detected in the epithelial cells that form the bulge at the bend between mid and lower limb of the S-shaped bodies (Piscione et al., 2004; Cheng et al., 2007). We therefore decided to investigate the potential involvement of a defective Notch signaling activation in the onset of the phenoptypes observed in *Hnf1b* mutant embryonic kidneys. We first assessed the expression of *Notch2*, a key actor that had been shown to be controlled by HNF1α and HNF1β in the intestine (D'Angelo et al., 2010). Quantitative RT-PCR experiments showed that at E13.5 the expression of *Notch2* was similar in mutant and control embryonic kidneys (Fig. 5A). This level of expression was maintained also at E14.5 with no differences between genotypes (Fig. 5B). In a similar way, *Jag1* was found to be normally expressed. On the other hand, we saw a significant down regulation of *Dll1*, accompanied by a significant down regulation of *Hes5*, one of the effector target genes of the Notch signaling (Fig. 5A,B). In agreement with previous studies, our ISH experiments showed that *Dll1* is particularly strongly expressed in the epithelial bulge of control S-shaped bodies. We showed that this expression was drastically decreased in mutants (Fig. 5C,D). The observed defective expression of *Dll1* in mutants could have been ascribed to the lack of formation of this particular segment. Interestingly, *Dll1* is known to be expressed in earlier precursors including vesicles and comma-shaped bodies, structures that were apparently normally formed in our mutant embryos. When we then assessed the expression of *Dll1* in these earlier structures we could clearly see that the expression of *Dll1* in vesicles and comma-shaped bodies was significantly down regulated in mutant embryos (Fig. 5E-H). These results indicated that HNF1β was probably required for the correct transcriptional activation of this gene in nephron precursors.

HNF1β binds to several chromatin sites of crucial kidney developmental genes.

To investigate whether *Dll1* could be directly controlled by HNF1β we decided to assess its direct binding in vivo by chromatin immunoprecipitation (ChIP) experiments on embryonic kidneys. As a first step, we identified the position of the best candidate HNF1 binding sites with a previously described in silico approach which takes into account the resemblance of the sites to the classical HNF1 consensus (HMM score) and the evolutionary conservation of sites across 14 species (Tronche et al., 1997), MP and SG, unpublished results). This led to the identification of a particularly well conserved site, 2Kb upstream the transcriptional start site of the *Dll1* gene together with a second site much farther away (302 Kb downstream). Our results showed that both sites were actually bound in vivo (Supplementary Material Fig. S2). The combination of the ISH and ChIP results suggest that the absence of the bulge formation observed in *Hnf1b*-deficient kidneys might be a direct consequence of the defective expression of *Dll1* as a direct target of HNF1β already in early nephron precursors (vesicles and comma-shaped bodies).

Our in silico approach led us to discover evolutionary well conserved binding sites also around *Osr2* and *Irx1* genes. Our ChIP results showed that one site, detected close to the *Osr2* gene (24.1Kb upstream the putative transcriptional start site) and three sites around *Irx1* (14 Kb, 65 Kb and 66 Kb with respect to the putative transcriptional start site), were significantly bound in vivo (Supplementary Material Fig. S2). These results suggest that HNF1β might participate in the trancriptional activation of *Osr2* and *Irx1* in already expanding and differentiating tubules. It is known that these two genes are transcriptionally activated starting with the formation of the bulge of the S-shaped bodies. Since these two genes are not detected in the deformed S-shaped bodies, one possibility is that their defective expression could be simply due to the absence of formation of their territory. On the other hand, we cannot rule out that the expansion of this critical territory might also be controlled by HNF1β also via the transcriptional activation of these two genes.

Glomerular differentiation is not dramatically affected by the absence of HNF1β.

After the formation of S-shaped structures, the tubular components of nephron normally proliferate and form their typical long tubules including PT, HL and DCT. In this respect, nephron spatial organization is characterized by the fact that the final portion of the HL coincides with the macula densa, a specific tubular structure that is intimately connected

with the vascular pole of the same glomerulus. The spatial organization of *Hnf1b*-deficient nephrons was characterized by a very short primitive tubule emerging from the glomerulus and directly connected to the presumptive macula densa. Normally, the connection between the urinary pole of a glomerulus is located opposite (at 180°) in respect to the vascular pole. In our mutant embryos, the absence of tubular expansion had probably led to a deformation of glomeruli such that the two poles were forced to be close each other (Fig. 6A-C). In addition, the vascular tuft, instead of showing its typical constriction at its base (by the formation of the vascular pole) was characterized by an atypical distended conformation. In spite of this alteration, the glomerular structures, at the ultrastructural level, were globally normal, with podocytes and their foot-processes surrounding capillaries with fenestrated endothelial cells (Supplementary Material Fig. S3). As previously mentioned, mutant glomeruli had dilations of their Bowman's (urinary) space, forming glomerular cysts. All together, these results showed that podocyte differentiation was not altered but the global architecture of capillary tuft was distorted.

The renal phenotype linked to human *HNF1B* deficiency.

Fetuses carrying heterozygous mutations of *HNF1B* present with a set of complex and extremely variable renal abnormalities ranging from kidney agenesis, hypodysplasia and/or cysts (Decramer et al., 2007; Heidet et al., 2010). These abnormalities can be linked to an impaired differentiation process in metanephric mesenchyme derived structures due to the defective expression of *HNF1B* and/or his target genes. To try to compare the pathological features observed in MODY5 patients with those observed in our mouse model, we analyzed paraffin sections from a MODY5 fetus (Patient 1) carrying a complete genomic deletion affecting all the exons of the gene. Histological analysis of kidney sections revealed the presence of specific focal areas characterized by clusters of glomeruli, without their typical surrounding set of cortical convoluted tubules (Fig. 6D). Immunofluorescence experiment confirmed that there were only very few LTL positive tubular sections (Fig. 6F). In addition, some of these glomerular structures were dilated and their capillary tuft was spread, similarly to what was observed in mutant mouse embryos (Fig. 6 E,G). In addition, the analysis of paraffin sections from a MODY5 child (Patient 2) carrying a c.232G>T, p.Glu78X mutation showed the presence of glomerular cysts that were one next to each other and lacked their typical surrounding tubular structures (Fig. 6H). In addition, we observed again the spreading of glomerular tufts (Fig. 6I).

DISCUSSION

It is known that patients who carry *HNF1B* mutations (MODY5 patients) suffer from complex developmental dysfunction of kidney morphogenesis ranging from kidney agenesis, dysplasia and cyst formation (Ulinski et al., 2006; Decramer et al., 2007; Heidet et al., 2010). Previous studies indicated that the expression of *Hnf1b* in the UB of mouse embryonic kidneys is absolutely required for the expression of several key genes including *Wnt9b*, an essential secreted factor for the condensation of the metanephric mesenchyme ((Lokmane et al., 2010) and unpublished observations). The absence of HNF1β in the UB leads to a complete block of nephrogenesis before the typical mesenchymal to epithelial conversion. On the other hand, very little was known on the function played by HNF1β during the first steps of nephrogenesis once this gene is programmed to be turned on in the mesenchymal derived epithelial structures. In the present study, using a Six2-Cre inactivation strategy, we showed that the expression of Hnf1β is not required for the first steps of nephron formation in mouse. The absence of this transcription factor does not perturb the typical formation and segmentation of renal vesicles and comma-shaped bodies. The first visible consequence of HNF1β deficiency becomes evident only in S-shaped bodies. In these structures, the most proximal portion of the mid-limb is deformed and the bulge of epithelial cells that probably contains the precursors of PT and HL is missing (Fig. 7). This defect could be linked to the decreased expression of *Dll1*, a gene whose hypomorphic allele can lead to defective expansion of renal tubules. We showed that *Dll1* expression is decreased in earlier nephron precursors (vesicles and comma-shaped bodies) before the appearance of any deformation (visible only in S-shaped bodies). In addition, HNF1β protein binds to the transcriptional control regions of this gene in vivo. All these considerations suggest that HNF1β might indeed play a crucial role in the activation of this gene. It is worth to note that the phenotype of our mutant overlaps only partially with that induced by the deletion of *Notch2* (Cheng et al., 2007). In fact, these mutant embryos suffer from a complete lack of the most proximal part of nephron including proximal tubule and glomeruli. These observations suggest that the activation of Notch pathway, in the most proximal part of the nephron, is HNF1β independent. In addition, HNF1β was required for the differentiation and expansion of distal convoluted tubules, a process that does not require *Notch2* (Cheng et al., 2007). All together, these considerations indicate that this transcription factor is involved in the formation of all nephron tubular components.

The analysis of the phenotype of mesenchyme specific *Hnf1b*-deficient kidneys showed that PT and HL formation seems to be generated by a specific sub-segment of S-shaped bodies. This process, promoted via the activation of the Notch signaling leads to the specification of a set of cells, probably already in comma-shaped body. The expansion of the number of these cells gives rise to a particular territory in the more proximal part of the mid-segment of the S-shaped body. This particular subdomain of the S-shaped body, organized as a protruding bulge of epithelial cells, is probably at the origin of the future expansion of the whole tubular component of the nephron between the glomerulus and the macula densa. At the molecular levels, specific markers are expressed in this peculiar domain of the S-shaped body such as Osr2 and Irx1. Interestingly, the down regulation of *Irx1* in Xenopus leads to abnormal morphogenesis of the intermediate pronephric tubules (Alarcon et al., 2008). In parallel, *Osr2* has been involved in proximal segment differentiation in Xenopus and Zebrafish (Tena et al., 2007) but its role in mammalian kidney morphogenesis is probably redundant since its inactivation, in mouse, does not lead to any renal abnormality (Lan et al., 2004). Interstingly, Osr2 been shown to act as a repressor that negatively regulates the expression of *Pax2* in Zebrafish/Xenopus (Tena et al., 2007). This property might explain the persistent high expression of *Pax2* observed in the primitive tubules of mutant embryos. Even if the defective expression of *Irx1* and *Osr2* may not necessarily play any direct causal role in our phenotype, the presence of HNF1binding sites that are bound in vivo suggest that they could constitute a direct transcription cascade under the control of HNF1β in later steps of differentiation (Fig. 7).

Interestingly, *Hnf1b*-deficient S-shaped structures can generate a glomerulus whose podocytes can reach maturity with the development of normal foot processes. This observation is somewhat compatible with the fact that HNF1β is not expressed in podocyte and their precursors. The only proximal nephron structure that expresses HNF1β is Bowman's capsule. In this respect, we observed some dilation of the Bowman's (urinary) space and the formation of glomerular cysts. This glomerulocystic phenotype is frequently observed in MODY5 patients that carry mutations in *HNF1B* at the heterozygous state (Bingham et al., 2001). Intriguingly, in mouse, the heterozygous inactivation of *Hnf1b* does not display any significant phenotype unless mice carry compound heterozygosity for both *Hnf1b* and other transcription factors (Paces-Fessy et al., 2012). On the other hand, the complete deletion of *Hnf1b* in either the UB or in the mesenchyme or in already formed tubules gives rise to the same traits that are observed MODY5 patients. This indicates that somehow, the

haploinsufficiency in MODY5 patients could reduce the protein levels below a critical threshold. This could lead to the appearance of phenotype either in the UB leading to defective branching and mesenchymal conversion (hypo-dysplasia) or to defective tubular expansion accompanied by glomerular cysts. These phenotypes are recapitulated in mouse embryo models where it has been demonstrated that HNF1β controls the expression of critical effectors of kidney morphogenesis. In conclusion, our studies have demonstrated that HNF1β plays an essential role for the generation of renal tubules. In particular, HNF1β is required for the formation of a specific mid-limb sub-compartment (epithelial bulge) of S-shaped bodies, which is probably at the origin of the expansion of proximal tubules and Henle's loops via the activation of the Notch pathway (Fig. 7).

ACKNOWLEDGMENTS

We are grateful to Moshe Yaniv for helpful discussions and critical reading of the manuscript. We are also very grateful to Professor Laurent Daniel, CHU Timone, Marseille, France for providing us with images of histological section of a kidney from a MODY5 patient. This work was supported by the "Fondation pour la Recherche Médicale" (equipe FRM) and the Fondation Bettencourt-Schueller (Prix Coup d'Elan); European Community's Seventh Framework Programme FP7/2009 [agreement no: 241955, SYSCILIA]; "Agence National pour la Recherche". We are very grateful to the platform of "Imagerie cellulaire", "Morphologie et Histologie" and the animal house facilities of the Cochin Institute. FM was supported by "Société de Néphrologie" and "Fondation pour la Recherche Médicale" fellowships.

REFERENCES

Alarcon, P., Rodriguez-Seguel, E., Fernandez-Gonzalez, A., Rubio, R. and Gomez-Skarmeta, J. L. (2008) 'A dual requirement for Iroquois genes during Xenopus kidney development', *Development* 135(19): 3197-207.

Barbacci, E., Reber, M., Ott, M. O., Breillat, C., Huetz, F. and Cereghini, S. (1999) 'Variant hepatocyte nuclear factor 1 is required for visceral endoderm specification', *Development* 126(21): 4795-805.

Bingham, C., Bulman, M. P., Ellard, S., Allen, L. I., Lipkin, G. W., Hoff, W. G., Woolf, A. S., Rizzoni, G., Novelli, G., Nicholls, A. J. et al. (2001) 'Mutations in the hepatocyte nuclear factor-1beta gene are associated with familial hypoplastic glomerulocystic kidney disease', *Am J Hum Genet* 68(1): 219-24.

Bohn, S., Thomas, H., Turan, G., Ellard, S., Bingham, C., Hattersley, A. T. and Ryffel, G. U. (2003) 'Distinct molecular and morphogenetic properties of mutations in the human HNF1beta gene that lead to defective kidney development', *J Am Soc Nephrol* 14(8): 2033-41.

Boyle, S. C., Kim, M., Valerius, M. T., McMahon, A. P. and Kopan, R. 'Notch pathway activation can replace the requirement for Wnt4 and Wnt9b in mesenchymal-to-epithelial transition of nephron stem cells', *Development* 138(19): 4245-54.

Carroll, T. J., Park, J. S., Hayashi, S., Majumdar, A. and McMahon, A. P. (2005) 'Wnt9b plays a central role in the regulation of mesenchymal to epithelial transitions underlying organogenesis of the mammalian urogenital system', *Dev Cell* 9(2): 283-92.

Cheng, H. T., Kim, M., Valerius, M. T., Surendran, K., Schuster-Gossler, K., Gossler, A., McMahon, A. P. and Kopan, R. (2007) 'Notch2, but not Notch1, is required for proximal fate acquisition in the mammalian nephron', *Development* 134(4): 801-11.

Cho, E. A., Patterson, L. T., Brookhiser, W. T., Mah, S., Kintner, C. and Dressler, G. R. (1998) 'Differential expression and function of cadherin-6 during renal epithelium development', *Development* 125(5): 803-12.

Coffinier, C., Barra, J., Babinet, C. and Yaniv, M. (1999a) 'Expression of the vHNF1/HNF1beta homeoprotein gene during mouse organogenesis', *Mech Dev* 89(1-2): 211-3.

Coffinier, C., Gresh, L., Fiette, L., Tronche, F., Schutz, G., Babinet, C., Pontoglio, M., Yaniv, M. and Barra, J. (2002) 'Bile system morphogenesis defects and liver dysfunction upon targeted deletion of HNF1beta', *Development* 129(8): 1829-38.

Coffinier, C., Thepot, D., Babinet, C., Yaniv, M. and Barra, J. (1999b) 'Essential role for the homeoprotein vHNF1/HNF1beta in visceral endoderm differentiation', *Development* 126(21): 4785-94.

D'Angelo, A., Bluteau, O., Garcia-Gonzalez, M. A., Gresh, L., Doyen, A., Garbay, S., Robine, S. and Pontoglio, M. (2010) 'Hepatocyte nuclear factor 1alpha and beta control terminal differentiation and cell fate commitment in the gut epithelium', *Development* 137(9): 1573-82.

Decramer, S., Parant, O., Beaufils, S., Clauin, S., Guillou, C., Kessler, S., Aziza, J., Bandin, F., Schanstra, J. P. and Bellanne-Chantelot, C. (2007) 'Anomalies of the TCF2 gene are the main cause of fetal bilateral hyperechogenic kidneys', *J Am Soc Nephrol* 18(3): 923-33.

Dressler, G. R. (2009) 'Advances in early kidney specification, development and patterning', *Development* 136(23): 3863-74.

Dressler, G. R., Wilkinson, J. E., Rothenpieler, U. W., Patterson, L. T., Williams-Simons, L. and Westphal, H. (1993) 'Deregulation of Pax-2 expression in transgenic mice generates severe kidney abnormalities', *Nature* 362(6415): 65-7.

Fischer, E., Legue, E., Doyen, A., Nato, F., Nicolas, J. F., Torres, V., Yaniv, M. and Pontoglio, M. (2006) 'Defective planar cell polarity in polycystic kidney disease', *Nat Genet* 38(1): 21-3.

Gresh, L., Fischer, E., Reimann, A., Tanguy, M., Garbay, S., Shao, X., Hiesberger, T., Fiette, L., Igarashi, P., Yaniv, M. et al. (2004) 'A transcriptional network in polycystic kidney disease', *Embo J* 23(7): 1657-68.

Harding, S. D., Armit, C., Armstrong, J., Brennan, J., Cheng, Y., Haggarty, B., Houghton, D., Lloyd-MacGilp, S., Pi, X., Roochun, Y. et al. (2011) 'The GUDMAP database--an online resource for genitourinary research', *Development* 138(13): 2845-53.

Heidet, L., Decramer, S., Pawtowski, A., Moriniere, V., Bandin, F., Knebelmann, B., Lebre, A. S., Faguer, S., Guigonis, V., Antignac, C. et al. (2010) 'Spectrum of HNF1B mutations in a large cohort of patients who harbor renal diseases', *Clin J Am Soc Nephrol* 5(6): 1079-90.

Hiesberger, T., Bai, Y., Shao, X., McNally, B. T., Sinclair, A. M., Tian, X., Somlo, S. and Igarashi, P. (2004) 'Mutation of hepatocyte nuclear factor-1beta inhibits Pkhd1 gene expression and produces renal cysts in mice', *J Clin Invest* 113(6): 814-25.

Humphreys, B. D., Valerius, M. T., Kobayashi, A., Mugford, J. W., Soeung, S., Duffield, J. S., McMahon, A. P. and Bonventre, J. V. (2008) 'Intrinsic epithelial cells repair the kidney after injury', *Cell Stem Cell* 2(3): 284-91.

Kiernan, A. E., Cordes, R., Kopan, R., Gossler, A. and Gridley, T. (2005) 'The Notch ligands DLL1 and JAG2 act synergistically to regulate hair cell development in the mammalian inner ear', *Development* 132(19): 4353-62.

Kobayashi, A., Kwan, K. M., Carroll, T. J., McMahon, A. P., Mendelsohn, C. L. and Behringer, R. R. (2005) 'Distinct and sequential tissue-specific activities of the LIM-class homeobox gene Lim1 for tubular morphogenesis during kidney development', *Development* 132(12): 2809-23.

Kobayashi, A., Valerius, M. T., Mugford, J. W., Carroll, T. J., Self, M., Oliver, G. and McMahon, A. P. (2008) 'Six2 defines and regulates a multipotent self-renewing nephron progenitor population throughout mammalian kidney development', *Cell Stem Cell* 3(2): 169-81.

Kopan, R. and Ilagan, M. X. (2009) 'The canonical Notch signaling pathway: unfolding the activation mechanism', *Cell* 137(2): 216-33.

Lan, Y., Ovitt, C. E., Cho, E. S., Maltby, K. M., Wang, Q. and Jiang, R. (2004) 'Odd-skipped related 2 (Osr2) encodes a key intrinsic regulator of secondary palate growth and morphogenesis', *Development* 131(13): 3207-16.

Lindner, T. H., Njolstad, P. R., Horikawa, Y., Bostad, L., Bell, G. I. and Sovik, O. (1999) 'A novel syndrome of diabetes mellitus, renal dysfunction and genital malformation associated with a partial deletion of the pseudo-POU domain of hepatocyte nuclear factor-1beta', *Hum Mol Genet* 8(11): 2001-8.

Lokmane, L., Heliot, C., Garcia-Villalba, P., Fabre, M. and Cereghini, S. (2010) 'vHNF1 functions in distinct regulatory circuits to control ureteric bud branching and early nephrogenesis', *Development* 137(2): 347-57.

Mah, S. P., Saueressig, H., Goulding, M., Kintner, C. and Dressler, G. R. (2000) 'Kidney development in cadherin-6 mutants: delayed mesenchyme-to-epithelial conversion and loss of nephrons', *Dev Biol* 223(1): 38-53.

McMahon, A. P., Aronow, B. J., Davidson, D. R., Davies, J. A., Gaido, K. W., Grimmond, S., Lessard, J. L., Little, M. H., Potter, S. S., Wilder, E. L. et al. (2008)

'GUDMAP: the genitourinary developmental molecular anatomy project', *J Am Soc Nephrol* 19(4): 667-71.

Neild, G. H. (2009) 'What do we know about chronic renal failure in young adults? II. Adult outcome of pediatric renal disease', *Pediatr Nephrol* 24(10): 1921-8.

Paces-Fessy, M., Fabre, M., Lesaulnier, C. and Cereghini, S. (2012) 'Hnf1b and Pax2 cooperate to control different pathways in kidney and ureter morphogenesis', *Hum Mol Genet* 21(14): 3143-55.

Piscione, T. D., Wu, M. Y. and Quaggin, S. E. (2004) 'Expression of Hairy/Enhancer of Split genes, Hes1 and Hes5, during murine nephron morphogenesis', *Gene Expr Patterns* 4(6): 707-11.

Rumballe, B., Georgas, K., Wilkinson, L. and Little, M. (2010) 'Molecular anatomy of the kidney: what have we learned from gene expression and functional genomics?', *Pediatr Nephrol* 25(6): 1005-16.

Stark, K., Vainio, S., Vassileva, G. and McMahon, A. P. (1994) 'Epithelial transformation of metanephric mesenchyme in the developing kidney regulated by Wnt-4', *Nature* 372(6507): 679-83.

Sun, Z., Amsterdam, A., Pazour, G. J., Cole, D. G., Miller, M. S. and Hopkins, N. (2004) 'A genetic screen in zebrafish identifies cilia genes as a principal cause of cystic kidney', *Development* 131(16): 4085-93.

Tena, J. J., Neto, A., de la Calle-Mustienes, E., Bras-Pereira, C., Casares, F. and Gomez-Skarmeta, J. L. (2007) 'Odd-skipped genes encode repressors that control kidney development', *Dev Biol* 301(2): 518-31.

Thiagarajan, R. D., Georgas, K. M., Rumballe, B. A., Lesieur, E., Chiu, H. S., Taylor, D., Tang, D. T., Grimmond, S. M. and Little, M. H. (2011) 'Identification of anchor genes during kidney development defines ontological relationships, molecular subcompartments and regulatory pathways', *PLoS One* 6(2): e17286.

Tronche, F., Ringeisen, F., Blumenfeld, M., Yaniv, M. and Pontoglio, M. (1997) 'Analysis of the distribution of binding sites for a tissue-specific transcription factor in the vertebrate genome', *J Mol Biol* 266(2): 231-45.

Ulinski, T., Lescure, S., Beaufils, S., Guigonis, V., Decramer, S., Morin, D., Clauin, S., Deschenes, G., Bouissou, F., Bensman, A. et al. (2006) 'Renal phenotypes related to hepatocyte nuclear factor-1beta (TCF2) mutations in a pediatric cohort', *J Am Soc Nephrol* 17(2): 497-503.

Verdeguer, F., Le Corre, S., Fischer, E., Callens, C., Garbay, S., Doyen, A., Igarashi, P., Terzi, F. and Pontoglio, M. (2010) 'A mitotic transcriptional switch in polycystic kidney disease', *Nat Med* 16(1): 106-10.

Wu, G., Bohn, S. and Ryffel, G. U. (2004) 'The HNF1beta transcription factor has several domains involved in nephrogenesis and partially rescues Pax8/lim1-induced kidney malformations', *Eur J Biochem* 271(18): 3715-28.

Yu, J., Valerius, M. T., Duah, M., Staser, K., Hansard, J. K., Guo, J. J., McMahon, J., Vaughan, J., Faria, D., Georgas, K. et al. (2012) 'Identification of molecular compartments and genetic circuitry in the developing mammalian kidney', *Development* 139(10): 1863-73.

LEGENDS TO FIGURES

Table 1. Early postnatal lethality in *Hnf1b* mutants. Six2-Cre mediated inactivation of *Hnf1b* does not lead to embryonic lethality: mutants and controls (wild type and *Hnf1b*$^{+/-}$ pups or embryos) were present with a normal Mendelian ratio during gestation. Newborn pups lacking *Hnf1b* in the metanephric mesenchyme survived until birth, but they died during the first 48 hours of life. *= mice found dead; ** = $P<0.01$.

Figure 1. The absence of Hnf1β in nephron precursors leads to smaller kidney and prevented the formation of tubules. (A,B) Macroscopic view of newborn kidneys showing 30% reduction in the size of *Hnf1b*-deficient kidneys. **(C,D)** Macroscopic view of the urogenital tract at P0. The bladder of mutant embryos was systematically smaller with a reduced content of urine compared to the control. (**E-L**) Histological section of newborn kidneys showing a drastic tubular defect in mutant pups. (E,F) Hematoxylin Eosin staining. Boxed areas in E and F are shown in insets and highlight the presence of cystic glomeruli in mutant. (G,H) Lotus Tetragonolobus lectin (LTL) staining (proximal tubule marker). (I,J) In situ hybridization experiments for *Slc12a1*(NKCC2), a marker of Henle's Loops and (K,L) for *Pvalb* (distal convoluted tubules marker). **(M)** Quantitative RT-PCR analysis for tubular markers at P0. Mutant pups showed a drastic decrease in the expression of markers specific for proximal tubules (*Hnf4a*, *Vill1*), Henle's Loop (NKCC2/*Slc12a1*) and distal convoluted tubules (*Pvalb* and NCC/*Slc12a3*). Scale bars: A,B 100µm; C,D 1mm; E-L 500µm.

Figure 2: The absence of Hnf1β does not affect the first steps of nephrogenesis, but is responsible for distortion of S-shaped bodies. (A,B) Detection of HNF1β in nephron precursors by immunofluorescence. A polarized (distal) expression of HNF1β is visible in vesicles (red nuclei, arrowhead in A) of control embryos whereas it is absent in vesicles of mutant embryos (arrowhead in B). Cap mesenchymal cells do not express HNF1β (arrow in A and B). **(C,D)** Mutant vesicles show a polarized expression of *Jag1* and *Wt1* that is similar to

that of control embryos. **(E,F)** Mutant comma-shaped bodies did not display any detectable abnormalities. Sporadically, chimeric residual expression of HNF1β in mesenchymal derived structures is observed in mutant embryos (see the arrow-headed nucleus in F as an example). A comparable expression of HNF1β (labeled in red) is seen in the non Six2-Cre deleted UB (stained with DBA in blue) in mutant and controls (A, B, E-H). **(G-L)** Mutant embryos suffer from a drastic deformation of S-shaped structures. (G,H) Sagittal sections of S-shaped bodies. HNF1β expression, in control embryos (G), is particularly strong in the bulge of epithelial cells that is located at the bend between the mid and lower limbs (arrow). This structure is drastically reduced in mutant embryos (H). (I-L) Coronal and sagittal sections of S-shaped bodies showing that in mutant embryos the mid-limb is inserted directly into the prospective urinary space, delimited on the top by *Wt1* highly positive (podocyte precursors labeled with red nuclei) and below by capsular cells (*Wt1* low expressing cells). **(M,N)** Hematoxylin Eosin staining of sagittal sections of S-shaped bodies. The arrow in M points to the bulge that is missing in mutants. Scale bars = 25µm.

Figure 3: The absence of tubule formation is not linked to a primary defect of proliferation or apoptosis in early nephron precursors. (A-B) Quantitative RT- PCR showing that in control embryos, markers of tubular differentiation program start to be expressed at low level around E14.5. (B) In mutant kidneys already at this stage, the expression of *Vil1*, *Hnf1a* and *Hnf4a* for the proximal tubule and NKCC2/*Slc12a1* for Henle's loop was drastically decreased. **=P<0.01. **(C)** Immunofluorescence with an anti-HNF4α antibody on wild type kidney section. HNF4α expression could not be detected in S-shaped bodies (white contour) and is only detected in already differentiated proximal tubules (arrow). **(D,E)** Proliferation/apoptosis balance in specific segments of nephron precursors. Semi-quantitative analysis of the number of mitotic (Histone H3PS10 positive) cells or apoptotic events (cleaved caspase-3 positive cells) relative to their location in sub domain of developing nephron. Vesicles and comma-shaped bodies were divided in distal and proximal part (Dist Ves = distal vesicles; Prox Ves = proximal vesicles; Dist CSB= distal comma-shaped bodies; Prox CSB = proximal comma-shaped bodies). S-shaped bodies were subdivided in proximal, mid and distal domains (Dist SSB = Distal (upper limb) of S-shaped bodies; Mid SSB = mid-limb of S-shaped bodies; Prox SSB = proximal (lower limb) of S-shaped bodies. Error bars represent standard errors. **=P < 0.01. For proliferation: $vesicles^{control}$ n=11 and $vesicles^{mutant}$ n=18, $CSB^{control}$ n=25 and CSB^{mutant} n=21, $SSB^{control}$ n=23 and SSB^{mutant} n=26. For apoptosis,

vesicles^{control} n=17 and vesicles^{mutant} n=11, CSB^{control} n=18 and CSB^{mutant} n=19, SSB^{control} and SSB^{mutant} n=30. **(F)** Immunofluorescence with an anti-cleaved caspase-3 antibody. Representative pictures of apoptotic events in S-shaped bodies in control and mutant. Scale bars: 25µm.

Figure 4: **Altered expression of markers of specific subdomains in nephron precursors in mutants. (A, B)** Quantitative RT-PCR analysis of genes with peculiar pattern of expression in the mid-limb of S-shaped bodies. Significant downregulation of *Irx1, Osr2* and *Pou3f3* expression in mutants at E13.5 and E14.5. *Cadh6* was significantly downregulated only at E 14.5. **(C-J)** In situ hybridization on paraffin sections double labelled with an anti-laminin antibody. C-F: In mutant, *Osr2* and *Irx1* are downregulated in S-shaped bodies (compare C and D, E and F). G-J: High level of expression of *Pax2* and *Lhx1* in late nephron precursors was still detectable in mutant compared to control. **(K)** Quantitative RT-PCR analysis of expression of *Pax2* and *Lhx1* showing a similar expression level at E14.5 between mutant and control but an upregulation of their expression at P0 in mutant. *=P<0.05; **=P<0.01. Scale bars: 25µm.

Figure 5: Notch pathway is affected by the absence of HNF1β in the metanephric mesenchyme. (A,B) Quantitative RT-PCR analysis of genes involved in Notch signaling pathway at E13.5 and E14.5. Significant downregulation of *Dll1* and *Hes5* in mutants at both stages. (**C-H**) *Dll1* in situ hybridization on paraffin sections double labeled with an anti-laminin antibody. The typical expression of *Dll1* in subdomains of nephron precursors is downregulated in vesicle, comma-shaped body and S-shaped body in mutant. *=P<0.05; **=P<0.01. Scale bars: 25µm.

Figure 6: The abnormal nephron conformation in mutant mouse embryos is reminiscent of the abnormalities in MODY5 patients. (A-C) Immunofluorescence of glomeruli on paraffin sections showing abnormal distended vascular tuft and glomerular cysts in mutant (B,C) compared to control (A). Note that in mutant glomeruli, the urinary pole (Star) is in close connection with the vascular pole, compared to its opposite localization in control (Star in A). (**D-I**) Histological analysis (D,E,H,I) and immunoflorescence (F,G) of

paraffin kidney sections from a MODY5 fetus (D-G) and from a MODY5 child (H,I) (Courtesy Professor Laurent Daniel, CHU Timone, Marseille, France). A consistent number of glomeruli are visible on these sections, accompanied by very few LTL positive tubular sections (F). Note the glomerular cysts, with a spread capillary tuft (arrow in E,G-I). (*=P<0.05; **=P<0.01). Scale bars: A-C 50µm, D-I 100µm.

Figure 7: Models depicting the function of HNF1β on nephron tubule formation. **(A)** HNF1β directly controls the expression of *Dll1* in early nephron precursors. *Dll1*, through Notch signaling, activates the specification of the epithelial bulge at the junction between mid and lower limbs in S-shaped bodies. This peculiar territory will express a set of markers that might participate to the further steps of tubular expansion and differentiation. Genes that have been shown to be modulated in their expression in the absence of *Hnf1b* in metanephric mesenchyme are indicated with a red arrow. **(B)** Schematic structure of wild type and mutant S-shaped bodies. The bulge of epithelial cells (arrow) that is present in wild type at the junction of the mid and lower limbs does not emerge in mutant.

Age	Controls	Mutants	Total
E14.5-16.5	75	24	99
E17.5-18.5	47	20	67
P0	22	8	30
P1	51	19	70
P2	46	10*	56
P>2	48	0**	48

Table 1

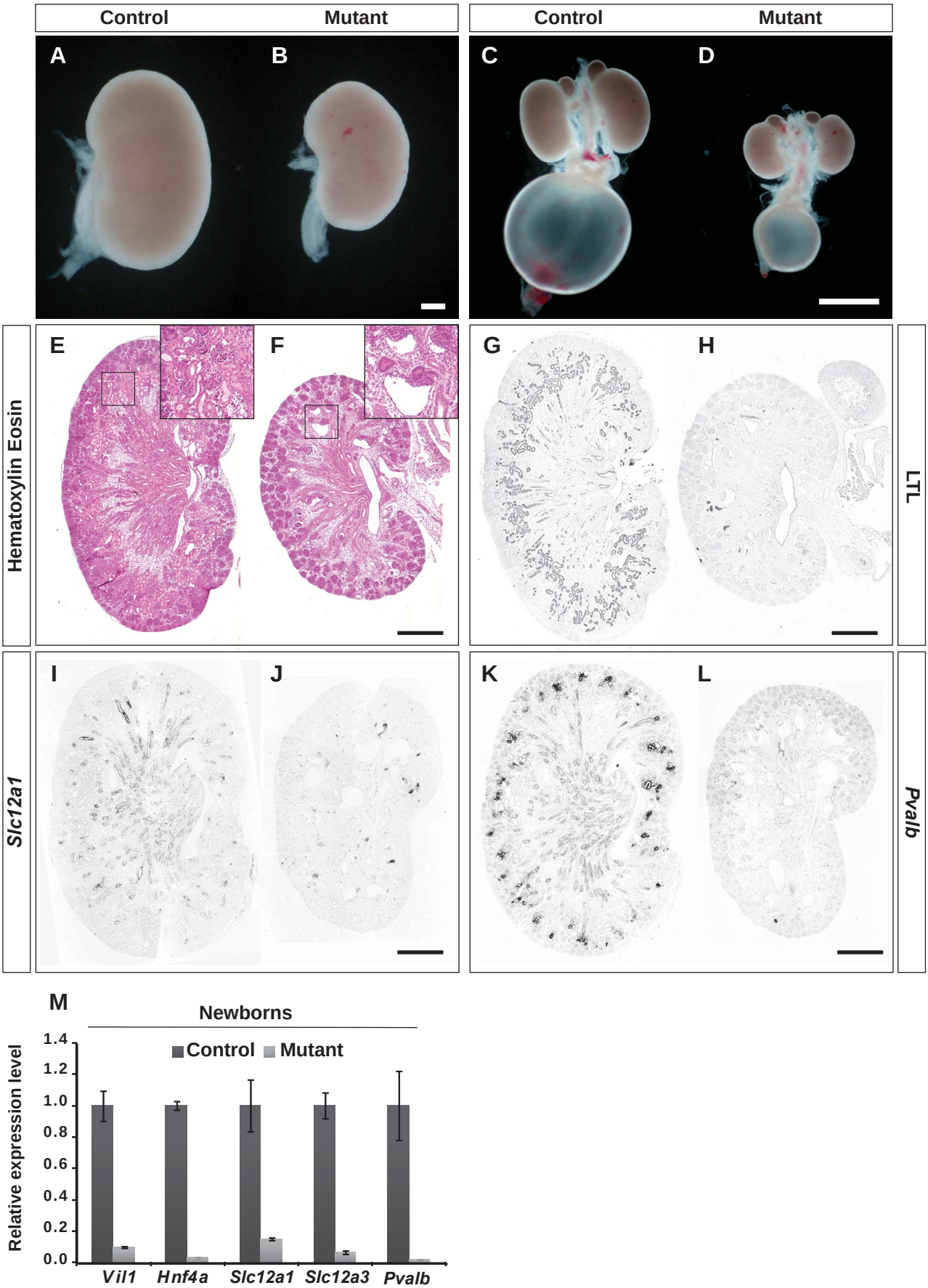
Control
Mutant
Control
Mutant
A
B
C
D
Hematoxylin Eosin
E
F
G
H
LTL
Slc12a1
I
J
K
L
Pvalb
M
Newborns
Control
Mutant
Relative expression level
1.4
1.2
1.0
0.8
0.6
0.4
0.2
0.0
Vil1
Hnf4a
Slc12a1
Slc12a3
Pvalb

Figure 1

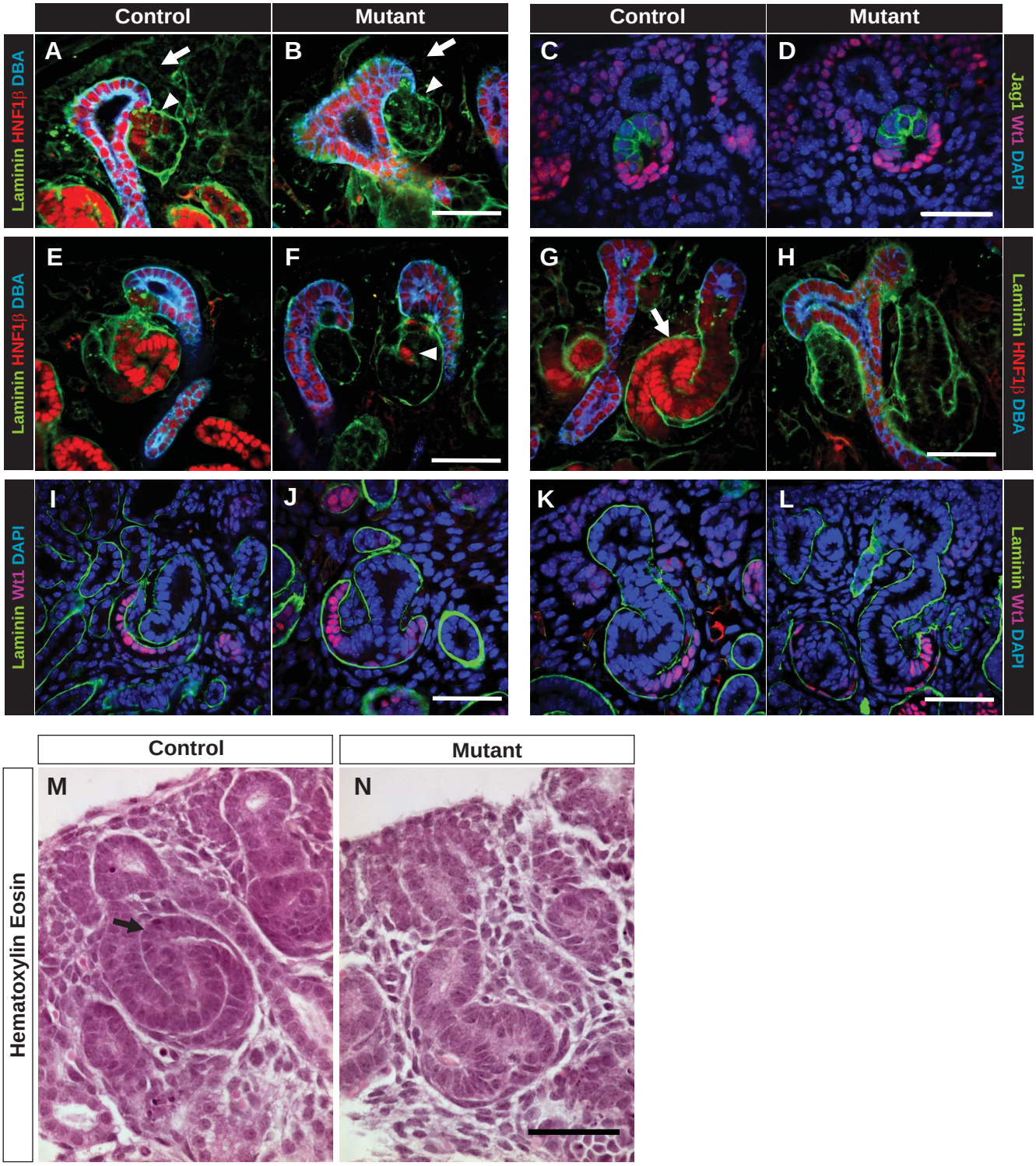
Control
Mutant
Control
Mutant
A
B
C
D
Laminin HNF1β DBA
Jag1 Wt1 DAPI
E
F
G
H
Laminin HNF1β DBA
Laminin HNF1β DBA
I
J
K
L
Laminin Wt1 DAPI
Laminin Wt1 DAPI
Control
Mutant
Hematoxylin Eosin
M
N

Figure 2

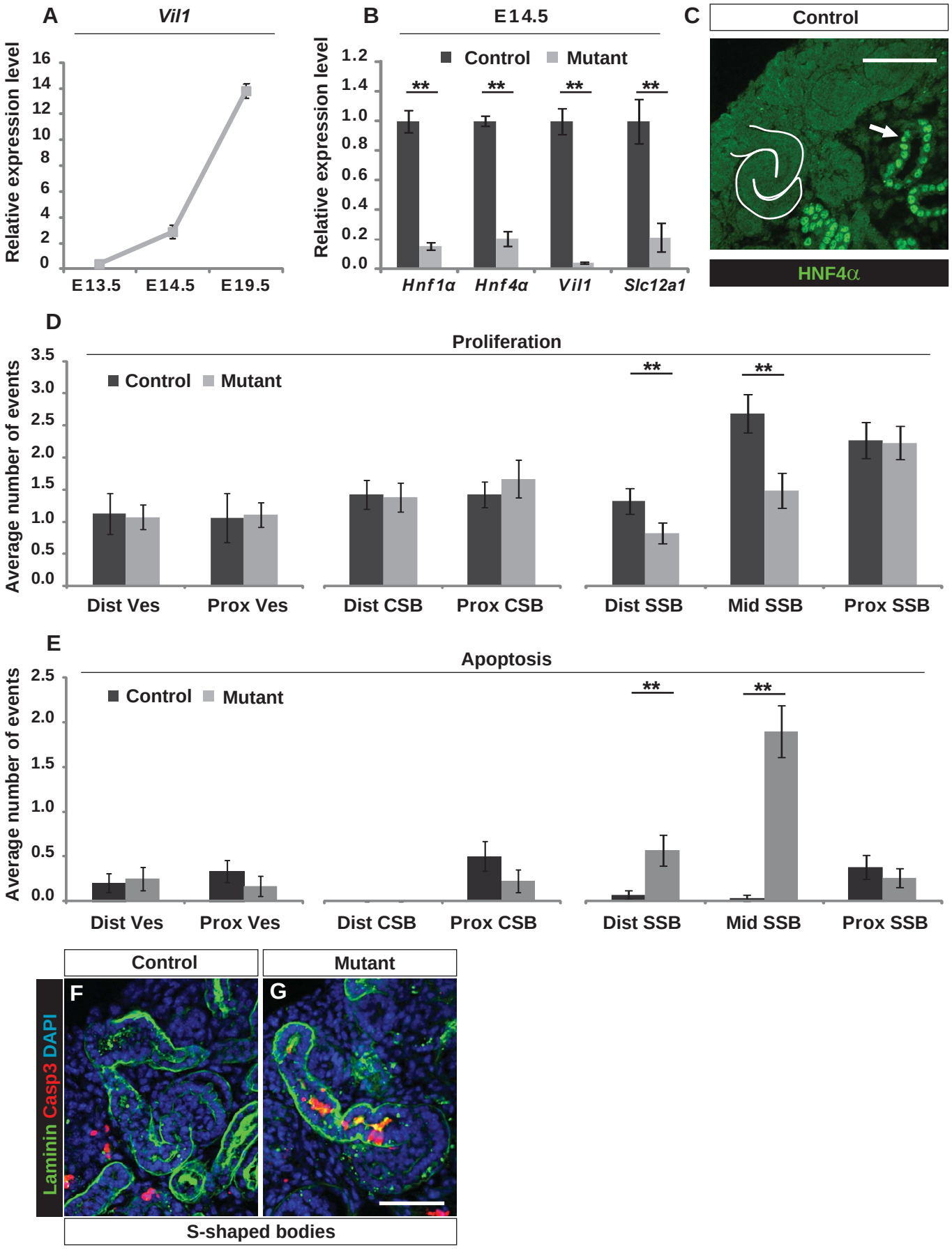
A
Vil1
Relative expression level
16
14
12
10
8
6
4
2
0
E13.5
E14.5
E19.5
B
E14.5
Control
Mutant
Relative expression level
1.2
1.4
1.0
0.8
0.6
0.4
0.2
0.0
**
**
**
**
Hnf1α
Hnf4α
Vil1
Slc12a1
C
Control
HNF4α
D
Proliferation
Average number of events
3.5
3.0
2.5
2.0
1.5
1.0
0.5
0.0
Control
Mutant
**
**
Dist Ves
Prox Ves
Dist CSB
Prox CSB
Dist SSB
Mid SSB
Prox SSB
E
Apoptosis
Average number of events
2.5
2.0
1.5
1.0
0.5
0.0
Control
Mutant
**
**
Dist Ves
Prox Ves
Dist CSB
Prox CSB
Dist SSB
Mid SSB
Prox SSB
Control
Mutant
Laminin Casp3 DAPI
F
G
S-shaped bodies

Figure 3

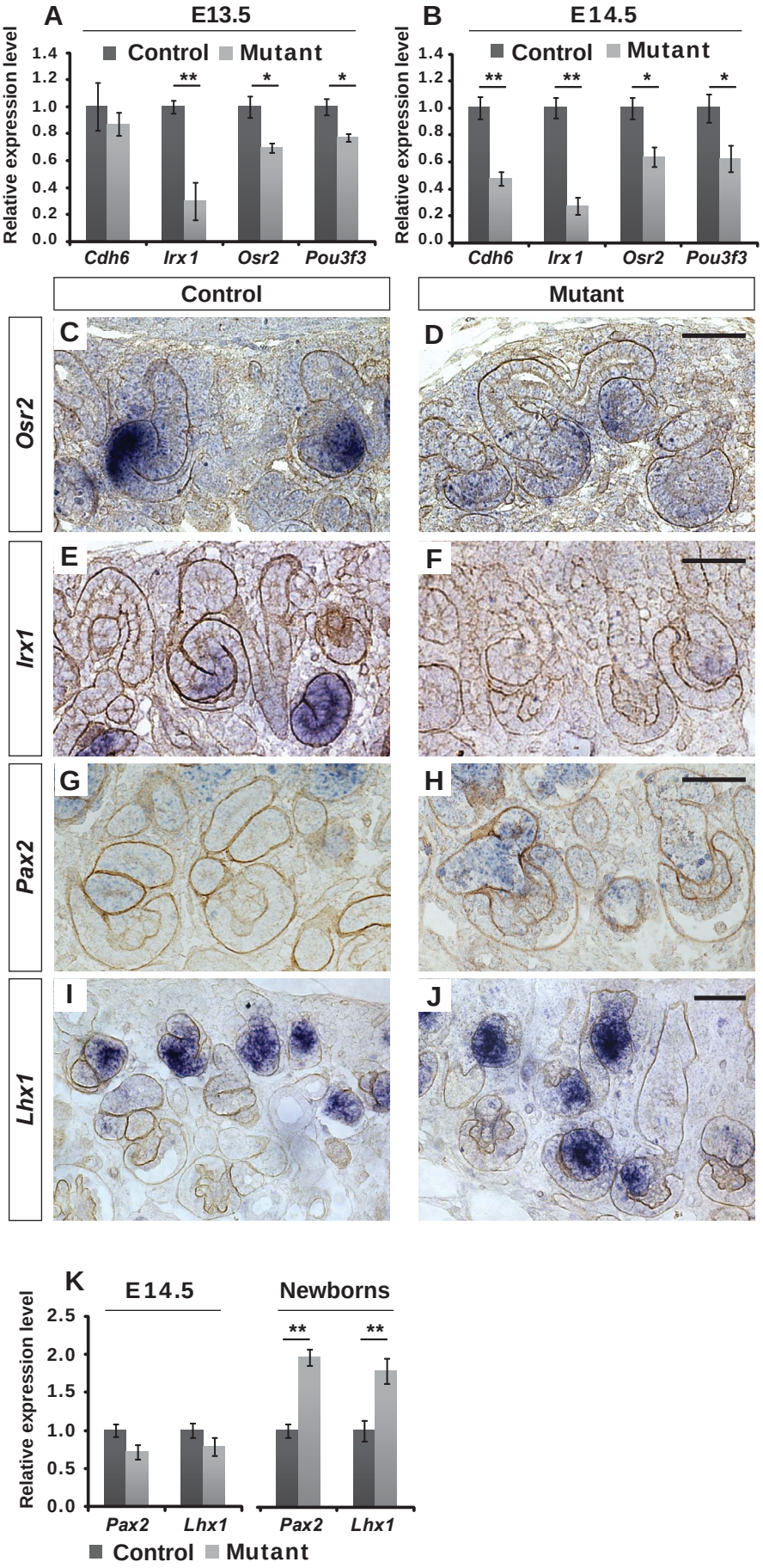
A
E13.5
Control
Mutant
Relative expression level
1.4
1.2
1.0
0.8
0.6
0.4
0.2
0.0
**
*
*
Cdh6
Irx1
Osr2
Pou3f3
B
E14.5
Control
Mutant
Relative expression level
**
**
*
*
Cdh6
Irx1
Osr2
Pou3f3
Control
Mutant
Osr2
Irx1
Pax2
Lhx1
C
D
E
F
G
H
I
J
K
E14.5
Newborns
Relative expression level
2.5
2.0
1.5
1.0
0.5
0.0
**
**
Pax2
Lhx1
Pax2
Lhx1
Control
Mutant

Figure 4

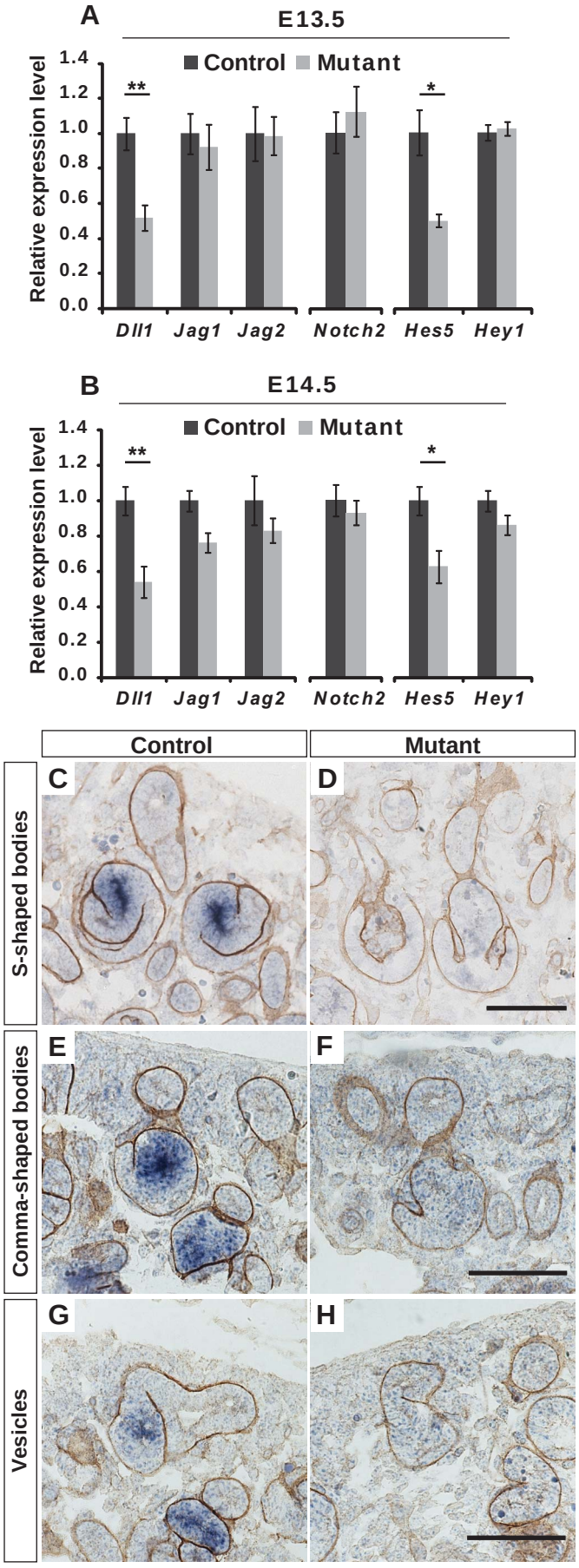
A
E13.5
Control
Mutant
Relative expression level
1.4
1.2
1.0
0.8
0.6
0.4
0.2
0.0
**
*
Dll1
Jag1
Jag2
Notch2
Hes5
Hey1
B
E14.5
Control
Mutant
Relative expression level
1.4
1.2
1.0
0.8
0.6
0.4
0.2
0.0
**
*
Dll1
Jag1
Jag2
Notch2
Hes5
Hey1
Control
Mutant
S-shaped bodies
Comma-shaped bodies
Vesicles
C
D
E
F
G
H

Figure 5

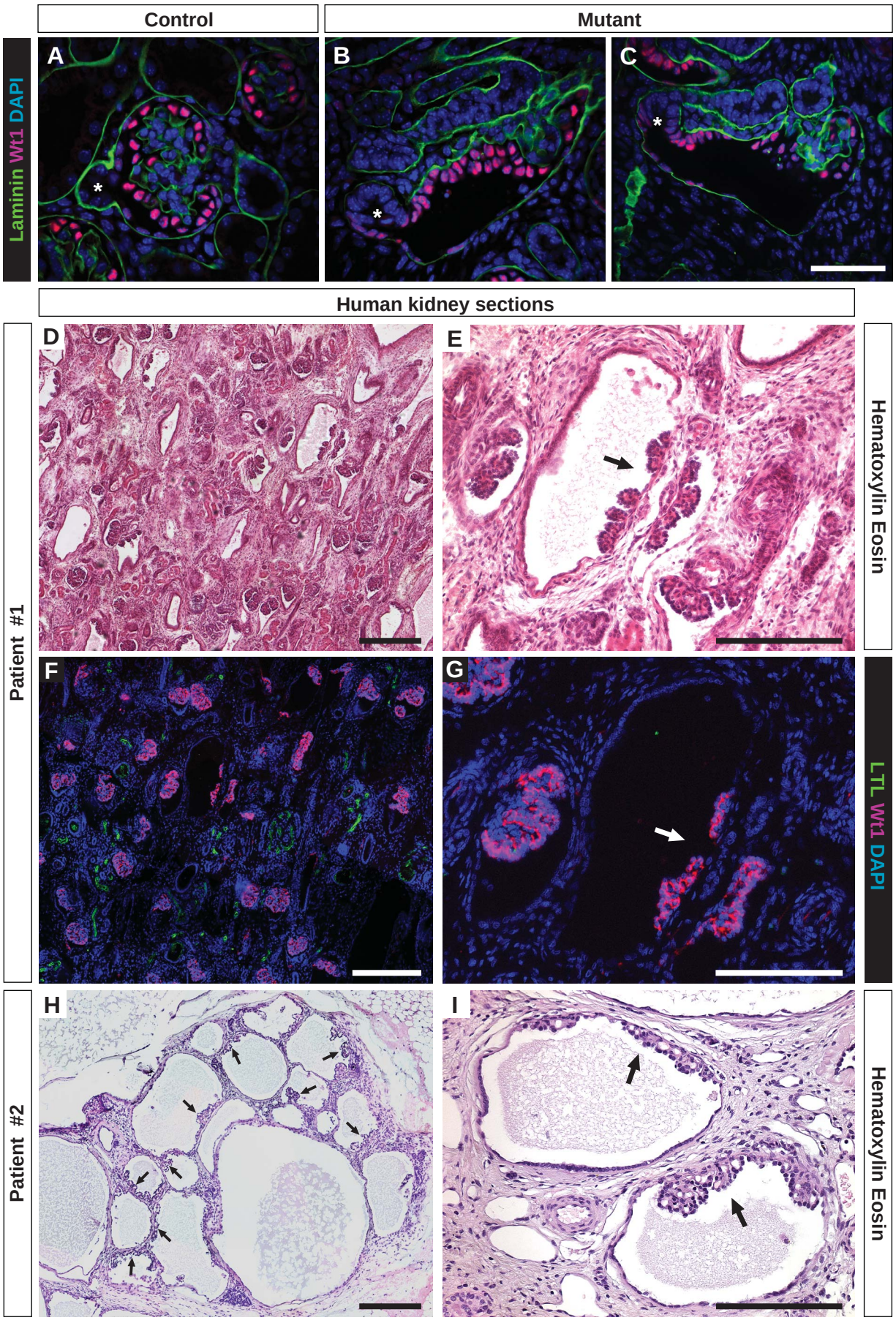
Control
Mutant
A
B
C
Laminin Wt1 DAPI
Human kidney sections
Patient #1
D
E
Hematoxylin Eosin
F
G
LTL Wt1 DAPI
Patient #2
H
I
Hematoxylin Eosin

Figure 6

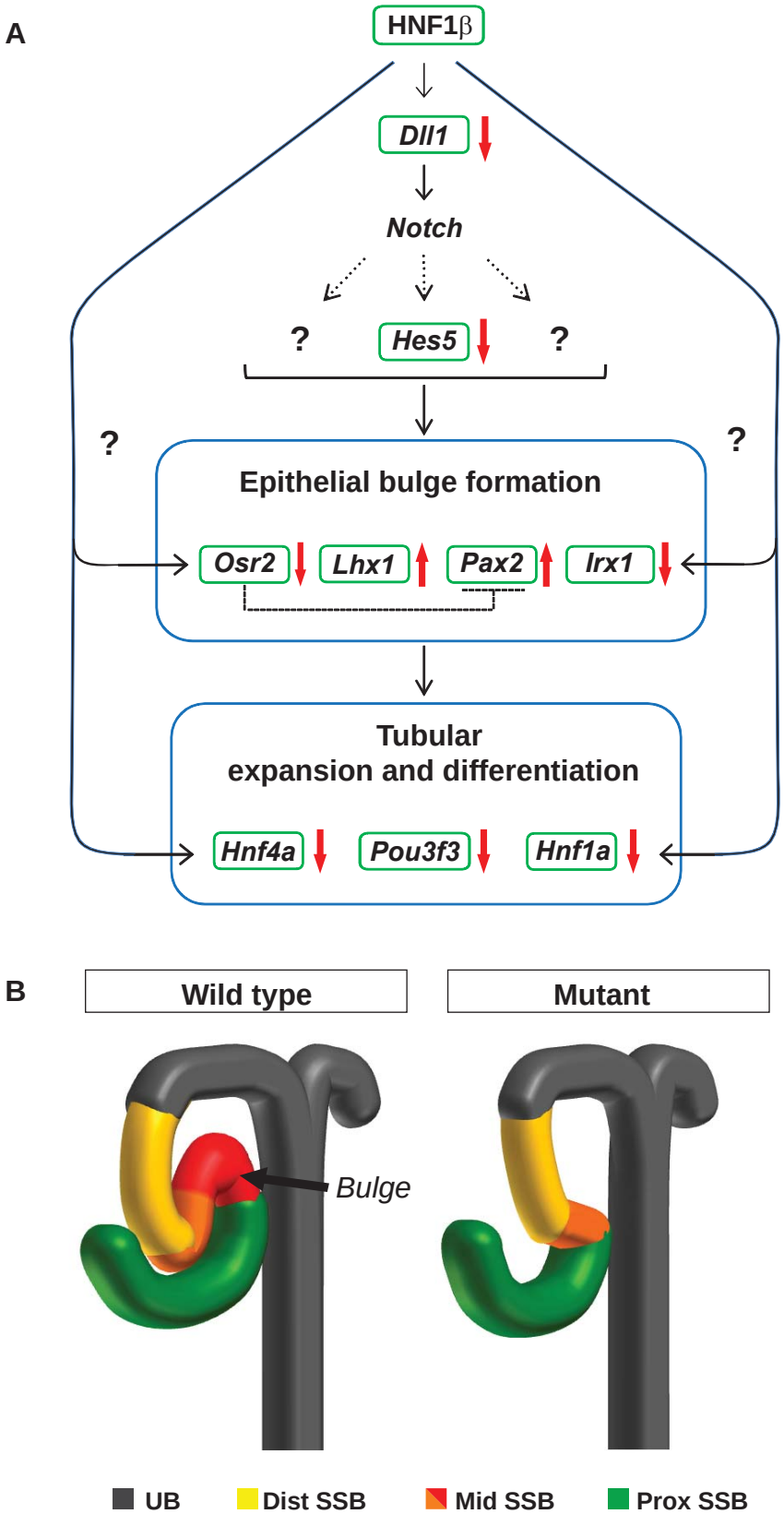
A
HNF1β
Dll1
Notch
?
Hes5
?
?
?
Epithelial bulge formation
Osr2
Lhx1
Pax2
Irx1
Tubular
expansion and differentiation
Hnf4a
Pou3f3
Hnf1a
B
Wild type
Mutant
Bulge
UB
Dist SSB
Mid SSB
Prox SSB

Figure 7

Supplementary Material

Figure S1: The absence of HNF1β in metanephric mesenchyme does not affect UB branching and podocytes differentiation. (A,B) Kidney sections of new born from control and mutant showed a similar staining for collecting ducts with Dolicho biflorus agglutinin (DBA). **(C,D)** Mutant pups had a comparable number of glomeruli at birth (*Wt1*)**. (E)** Quantitative RT-PCR analysis of specific markers of collecting ducts (*Wnt9b*) and podocytes (*Wt1*) did not show any difference between control and mutant kidneys at E14.5. Scale bar: 500µm.

Figure S2: In vivo binding of HNF1β to its chromatin target sites in genes involved in tubular differentiation. Predicted in silico HNF1 binding sites (vertical bars) in *Dll1*, *Osr2*, and *Irx1* genes were tested in ChIP experiments for in vivo HNF1β binding. The relative enrichment for each DNA fragment upon immunoprecipitation of HNF1β is illustrated as histograms. Colored bars represent HNF1 binding sites with enrichments significantly higher than background (gray bars). PCR experiments were performed in triplicate and the standard errors of these quantifications are shown as error bars. Species list of conserved sites: Ac, Anolis carolinensis; Bt, Bos taurus; Cf, Canis familiaris; Dr, Danio rerio; Ec, Equus caballus; Gg, Gallus gallus; Hs, Homo sapiens; Md, Monodelphis domestica; Oa, Ornithorhynchus anatinus; Pa, Pongo pygmaeus abelii; Rn, Rattus norvegicus; Xt, Xenopus tropicalis.

Figure S3: Podocytes develop normally in the absence of HNF1β. (**A,B**) Transmission electron microscopy of glomerular sections showing similar extent of foot processes differentiation in podocytes of control (A) and mutant (B) newborn pups.

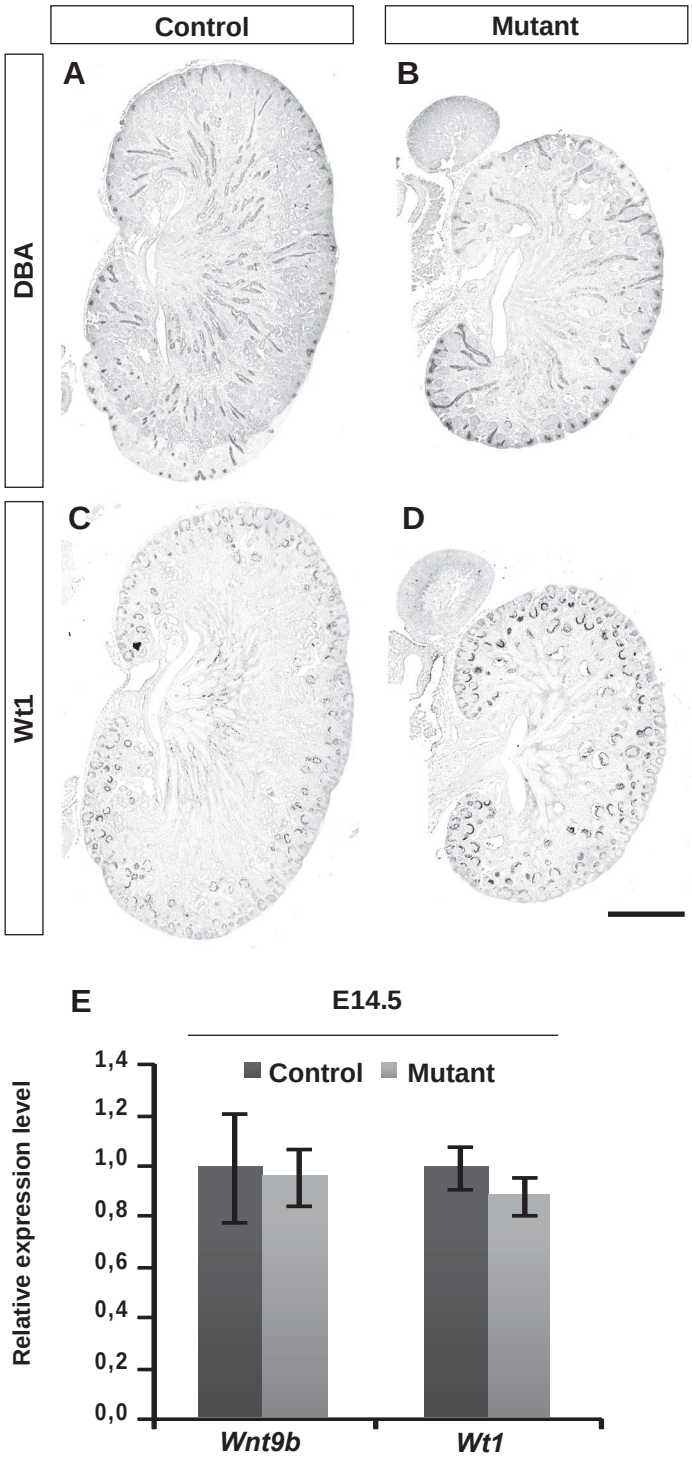
Control
Mutant
A
B
DBA
C
D
Wt1
E
E14.5
Control
Mutant
Relative expression level
1,4
1,2
1,0
0,8
0,6
0,4
0,2
0,0
Wnt9b
Wt1

Figure S1

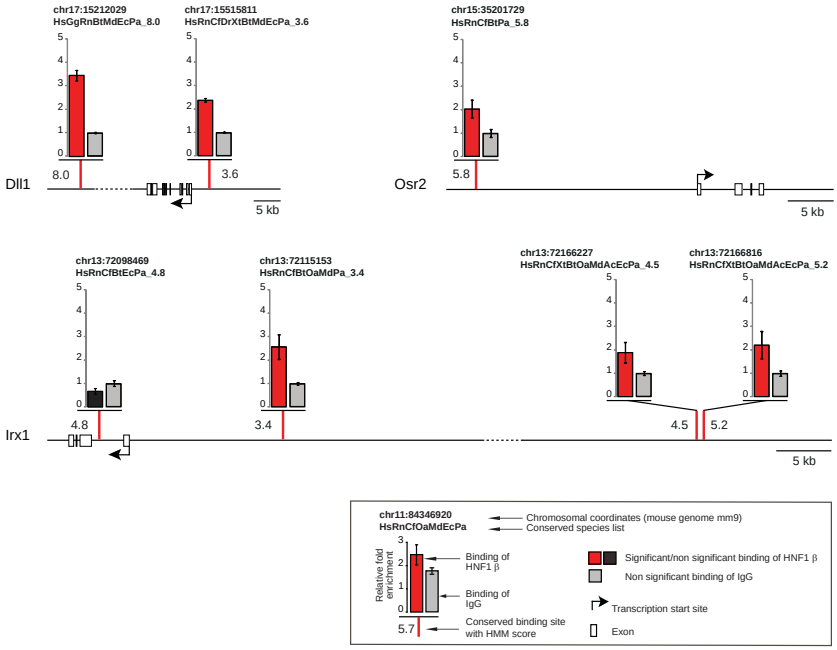
chr17:15212029
HsGgRnBtMdEcPa_8.0
chr17:15515811
HsRnCfDrXtBtMdEcPa_3.6
Dll1
8.0
3.6
5 kb
chr15:35201729
HsRnCfBtPa_5.8
Osr2
5.8
5 kb
chr13:72098469
HsRnCfBtEcPa_4.8
chr13:72115153
HsRnCfBtOaMdPa_3.4
chr13:72166227
HsRnCfXtBtOaMdAcEcPa_4.5
chr13:72166816
HsRnCfXtBtOaMdAcEcPa_5.2
Irx1
4.8
3.4
4.5
5.2
5 kb
chr11:84346920
HsRnCfOaMdEcPa
Chromosomal coordinates (mouse genome mm9)
Conserved species list
Relative fold enrichment
Binding of HNF1 β
Binding of IgG
5.7
Conserved binding site with HMM score
Significant/non significant binding of HNF1 β
Non significant binding of IgG
Transcription start site
Exon

Figure S2

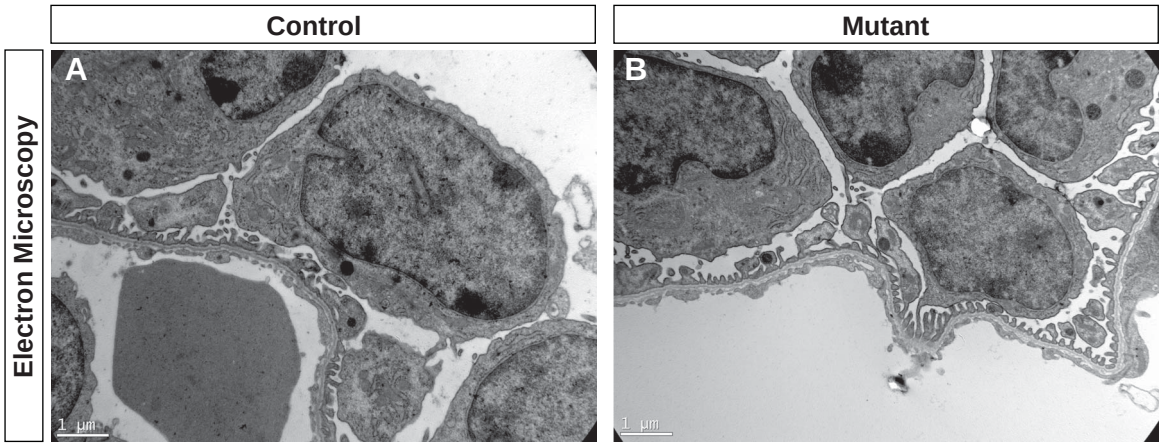

Figure S3

Supplementary Material and Methods

Chromatin Purification.

Chromatin was prepared as previously described with slight modifications (Gresh et al., 2004; Verdeguer et al., 2010). Briefly : Kidneys from 8 E17.5 wild type embryos were homogenized in 5 ml of SHB buffer (1.9M sucrose, 15mM HEPES pH 7.9, 15mM KCl, 0.5mM DTT, 0.5mM Spermine, 0.5mM Spermidine, with protease inhibitors Complete Roche and phenylmethylsulphonyl fluoride 0.5 mM). The suspension was then ultracentrifugated through another cushion (8.5 ml) of SHB for 1 hour at 25000rpm at 4°C and the pellet of purified nuclei was gently resuspended in 400µl of SucC buffer (0.34M Sucrose, 15mM HEPES pH 7.9, 60mM KCl, 15mM NaCl0, 15mM beta-Mercaptoethanol, 2mM MgCl2 with protease inhibitors Complete Roche and phenylmethylsulphonyl fluoride 0.5 mM). Nuclei were then crosslinked with 1% formaldehyde at 30°C for 13 minutes: the reaction was stopped by adding Glycine to final concentration of 0.125mM. Nuclei were then layered on a 3ml cushion of 0.9M Sucrose SucC buffer and centrifuged 4000 rpm for 15 minutes at 4°C. Nuclei were resuspended in 600µl of SBAR buffer (50 mM HEPES pH7.9, 140mM NaCl, 1mM EDTA, 1 % Triton X-100, 0.1 % Na-Deoxycholate, 0.3 % SDS with protease inhibitors Complete Roche and phenylmethylsulphonyl fluoride 0.5 mM). Chromatin fragmentation was carried out in aliquots of 300µl in Bioruptor Sonicator with 3 cycles of 5 minutes (30 seconds off, 30 seconds on).

In Situ Hybridisation (ISH)

Paraffin sections (6 µm thick) were dried overnight at 40°C. The slides were then dewaxed and rehydrated and post fixed in paraformaldehyde (PFA) 4% for 10 minutes at RT. Proteinase K treatment (10 minutes of PK 10µg/ml in pre-warmed PBS 37°C) was followed by fixation for 5 minutes in PFA 4 % and then acetylated 10 minutes (0.02M HCl, 0.1M Triethanolamine, 0.25% Acetic Anhydride). Permeabilization was carried out at RT for 30 minutes in PBS-Triton 0.5%. After several washes in 1X PBS and 2 hours of preincubation in Hybridization Buffer (SSC 5X, Yeast RNA 100µg/ml, Denhardt's 1X, deionized formamide 50%), sections were incubated with 200 ng/ml probes in 80 µl of hybrization buffer overnight

at 67°C. The next day, slides were washed 2 times 5 minutes in SSC 5X at 67°C, followed by 2 washes of 30 minutes in SSC 0.2 X at 67°C and 2 washes in MABT (Maleic Acid 10mM, NaCl 150mM, Tween-20 0.1%, pH 7.5) 5 minutes at RT. Incubation with anti-DIG antibody diluted 1:2000 was performed overnight in MABT-goat serum 10%-blocking reagent (Roche) at RT. Revelation was carried out with BM purple for 24-72 hours (Roche). Slides were labeled with anti-laminin antibody and revealed with Diamino Benzidine (EnVision Kit, DAKO).

Antibodies

In the experiments of immunohistochemistry or immunofluorescence we made use of the following antibodies: mouse anti-*Wt1* (Dako, 1:100); rabbit anti-laminin (Sigma, 1:200); home made rabbit anti-HNF4α (FRHNF4) (1:100); rabbit anti-Jagged1 (SantaCruz, 1:200), Lotus Tetragonolobus Lectin (LTL) (Vector, 1:200); Dolichos Biflorus Agglutinin (DBA) (Vector, 1:200); 3.12 mouse anti HNF1β ((Chouard et al., 1997) 1:100)

References

Chouard, T., Jeannequin, O., Rey-Campos, J., Yaniv, M. and Traincard, F. (1997) 'A set of polyclonal and monoclonal antibodies reveals major differences in post-translational modification of the rat HNF1 and vHNF1 homeoproteins', *Biochimie* 79(12): 707-15.

Gresh, L., Fischer, E., Reimann, A., Tanguy, M., Garbay, S., Shao, X., Hiesberger, T., Fiette, L., Igarashi, P., Yaniv, M. et al. (2004) 'A transcriptional network in polycystic kidney disease', *Embo J* 23(7): 1657-68.

Verdeguer, F., Le Corre, S., Fischer, E., Callens, C., Garbay, S., Doyen, A., Igarashi, P., Terzi, F. and Pontoglio, M. (2010) 'A mitotic transcriptional switch in polycystic kidney disease', *Nat Med* 16(1): 106-10.

Table S1 : Quantitative RT-PCR Primers

Vil1	reverse	GCGAGACTTTCCGGAGCTACT
	forward	CCCCTTTCCGGATCACAAG
Hnf4a	reverve	ATCACCTGGCAGATGATCGAA
	forward	AGGTTGTCAATCTTGGCCATG
Slc12a1	reverse	CTGGCCTCATATGCGCTTATT
	forward	AGATTTGGCATACGAGGCATG
Slc12a3	reverse	GGCCTACGAACACTATGCTAAC
	forward	AGTCAGCTCACGACCTTGC
Pvalb	reverse	CAGACTCCTTCGACCACAAAAA
	forward	AACCCCAATCTTGCCGTCC
Dll1	reverse	GAACAACCTAGCCAATTGCCA
	forward	GCCCCAATGATGCTAACAGAA
Jag1	reverse	ACTCGGAAGTGGAGGAGGATG
	forward	AGCGGACTTTCTGCTGGTGT
Jag2	reverse	CAATGCTGAGCCTGACCAATAC
	forward	GACGGACAGTGGCATTCAAA
Notch2	reverse	CCCTGATCATCGTGGTGCT
	forward	AATGCGCAAGTTGGTGTGG
Hes5	reverse	TCAACAGCAGCATAGAGCAGC
	forward	TCCAGGATGTCGGCCTTCT
Hey1	reverse	CCGACGAGACCGAATCAATAAC
	forward	TCAGGTGATCCACAGTCATCTG
Cdh6	reverse	CTAGTGGCTTCCCAGCAAAG
	forward	CTGATAATCGGATCCCGTGT
Pou3f3	reverse	CAGCCTACAGCTGGAAAAGG
	forward	GGTACCCACCTGCGAGTAGA
Hnf1a	reverse	AACCACCCTCTCTCCCAGTAA
	forward	GCCGCAGACACTGTGACTAA
Osr2	reverse	CCACGGACTGTACACCTGTC
	forward	GAAAGATCGCATGTTCAGCA
Irx1	reverse	ATTCACGAGAGGACCCACAC
	forward	TCCTTTCCCACACTCCTGAC
Pax2	reverse	CAAAGTTCAGCAGCCTTTCC
	forward	GTTAGAGGCGCTGGAAACAG
Lhx1	reverse	TGCGTCCAGTGCTGTGAAT
	forward	AACCAGATCGCTTGGAGAGAT
Wt1	reverse	GGTTTTCTCGCTCAGACCAG
	forward	GGTGTGGGTCTTCAGATGGT
Wnt9b	reverse	GTGAGGTCCTGACACCCTTC
	forward	GCCTGGACAGCTTCAGTAGG

Table S2: ISH Probes Primers

Osr2	reverse forward	GCTGCAGCTCACCAATTACTCC ACTTTGCCGCACTGCTCGCAGC
Irx1	reverse forward	ACCCTCACACAGGTCTCCAC GGAAAGATCGCATGTTCAGCA
Dll1	reverse forward	CTAGAACACTCTGGGAGCGG GTCTTCAAAGACCCAGGGATG
Lhx1	reverse forward	ACAAATGGTTCCCGTAGCTG CAACATGCGTGTTATCCAGG
Pvalb	reverse forward	CTGGAGAACCTGTTCGCTTC CAGAGGCATCTCTCACCACA
Slc12a1	reverse forward	CTGGTATGGTGAAGGCAGGT CAAACCAAAAGCAAGCCATT

Table S3: ChIP Primers

Gene	Sites		
Dll1	17_15515811_HsRnCfDrXtBtMdEcPa_3.6 chr17:15515812-15515826	reverse forward	AGGGTCTGAGCTATGCTTGC GCTGTGTCCAACAGGGACTT
	17_15212029_HsGgRnBtMdEcPa_8.0 chr17:15212030-15212044	reverse forward	AAGAGCGGCCTCAGTCATTA CAGACCATAGCCACAGGACA
Irx1	13_72166227_HsRnCfXtBtOaMdAcEcPa_4.5 chr13:72166228-72166242	reverse forward	ACTCATGCCTGCGATAATCC TTCCCACCAACCTCATTTTC
	13_72166816_HsRnCfXtBtOaMdAcEcPa_5.2 chr13:72166817-72166831	reverse forward	CGGCTGCTAATCCAGTGTCT GGGAGGACTTTCTCCTGTCC
	13_72115153_HsRnCfBtOaMdPa_3.4 chr13:72115154-72115168	reverse forward	ATGATGGTTCCAGGCTGTTC TGTGTGGATTGCTCATGGAT
	13_72098469_HsRnCfBtEcPa_4.8 chr13:72098470-72098484	reverse forward	TCCAGGGCACTCTTCAGTCT ACCTGTCACCGCTACAGACC
Osr2	15_35201729_HsRnCfBtPa_5.8 chr15:35201730-35201744	reverse forward	ATGCTGGCCTTTTATGTTGC TGTGGGAAAATCAGACAGCA

Project Discussion

Discussion

The role of HNF1beta during kidney morphogenesis

Patients affected by MODY5 suffer from a diverse set of renal malformations (Chen et al., 2010; Heidet et al., 2010). These malformations are part of the Congenital Abnormalities of the Kidney and Urinary Tract (CAKUT), a relatively common disease due to impaired kidney morphogenesis (Rumballe et al., 2010).

The use of mouse models of *Hnf1b* tissue specific inactivation represents a crucial tool in order to elucidate mechanisms at the basis of CAKUT malformations in MODY5 patients. The human disease is due to mutation of *HNF1B* at the heterozygous state, whereas, in mouse, the phenotypes are visible only when the tissue specific inactivation of *Hnf1b* is homozygous. This observation suggests that contrary to murine models, the haploinsufficiency of *HNF1B* in human is sufficient to reduce the protein level below a critical threshold. A second peculiarity of the human disease is the high incidence of *de novo* mutations often linked to large genomic deletions. This indicates that the human gene has an intrinsic instability. Somatic mutations could prevent *HNF1B* expression in time/place specific manner and explain part of the heterogeneity of the phenotype. Depending when and where these putative somatic mutations occur, they could differently affect kidney development program. This hypothesis suggests a different role for *Hnf1b* during kidney morphogenesis according to the time and place where it is expressed. To try to better understand and discriminate between these roles, different mouse models have been develop in order to inactivate *Hnf1b* in a time and/or specific manner.

Hnf1b is already expressed in the very early steps of kidney morphogenesis and it is maintained in all tubular structures in the adult kidney. The other HNF1 family member, *Hnf1α*, is expressed only in late stages of nephrogenesis and specifically only in proximal tubules. This difference of expression during kidney morphogenesis suggests a unique and essential role of *Hnf1b* that could not be replaced by the redundancy.

With the use of different specific Cre-recombination strategies, I inactivated *Hnf1b* in specific compartments. A previous work on chimeric compound inactivation has underlined the role of *Hnf1b* in the regulation of the ureteric bud branching and the mesenchymal to epithelial transition: this defect seems to be correlated with the inactivation of key genes implicated in

the ureteric bud branching and in the mesenchymal epithelialisation induction (Lokmane et al., 2008). In my work I took advantage of a different strategy of gene inactivation based on a LoxP/Cre system. In this way I could achieve *Hnf1b* inactivation in the whole embryo, excluding the extra embryonic tissues to avoid the germline early lethality. In agreement with previous published results, I showed that *Hnf1b* is not essential for the Wolffian duct formation and the outgrowth of the ureteric bud. However the lack of Hnf1b lead to severe defects of kidney development similar to what has been previously described (our data and (Lokmane et al., 2008)). Our model showed that the mutant ureteric bud tip still expresses specific genes, including *c-Ret*, *Wnt11* and *Sox9*, known to be involved in the crosstalk with the metanephric mesenchyme. Therefore, the presence of a normal tip, at least in the early steps of UB outgrowth, can explain the fact that the UB is still receptive to the inductive signals from the metanephric mesenchyme and to begin the invasion of the metanephric blastema. However, later on, something goes wrong immediately after this step. In fact, the ureteric bud does not branch in a dichotomic way at the end of each tip. Often, aberrant branching may occur and give rise to "umbrella like" structures. In addition, in a systematic way, there is no sign of mesenchymal to epithelial transition. *In situ* hybridization experiments on the aberrant mutant ureteric bud have shown that several key genes important for the branching events are extremely downregulated in absence of *Hnf1b*. In particular, we showed that *Wnt9b* was almost not expressed in the mutant ureteric bud. It is known that the inactivation of *Wnt9b* is sufficient to block the crosstalk between the two compartments. Interestingly, the inactivation of *Hnf1b* exclusively in the trunk of the developing ureteric bud (KSP-driven Cre recombinase) does not affect the branching pattern, but it leads to abnormal cell proliferation of this compartment that ends up with a severe cystic phenotype (Gresh et al., 2004). However, in this case it is known that the precise expression pattern of the CRE recombinase is not affecting the very tip of the UB. Therefore, it is likely that the normal branching phenotype of Ksp-CRE driven-*Hnf1b* deletion is due to the persistence of wild-type cells at the UB tip. In the UB of mox2-CRE driven *Hnf1b* deleted embryos other important genes are downregulated including *Pax2*, *Emx2* and *Lhx1*. These genes are known to produce drastic block in the kidney development when they are inactivated (Miyamoto et al., 1997) (Shawlot and Behringer, 1995),(Torres et al., 1995). In our model, the phenotype is less severe than in the germ line inactivation of any of these genes. One of the issues that we should take into account is that both *Pax2* and *Lhx1* have a wider expression pattern than *Hnf1b* in early steps of kidney morphogenesis. In particular, they are expressed in the intermediate mesoderm giving rise to the metanephric mesenchyme (Barnes et al., 1994)

(Dressler et al., 1990), a territory where *Hnf1b* is not expressed. Therefore, these genes must rely on different tissue specific transcription factor circuitries for their expression.

The lack of correct signaling between ureteric bud and metanephric mesenchyme has a second consequence: the mesenchyme is not able to start correctly the epithelialisation process that is crucial for the formation of nephron precursors.

Organotypic culture experiments have demonstrated that the absence of crosstalk between ureteric bud and metanephric mesenchyme is deleterious for both compartments: isolated metanephric mesenchyme undergoes apoptosis unless provided with a permissive stimulus from the ureteric bud and, in the other way around, the ureteric bud tissue degenerates upon separation from metanephric mesenchyme with limited or altered branching morphogenesis (Saxen and Sariola, 1987) (Kispert et al., 1996) (Sainio et al., 1997b). We demonstrate that *Hnf1b* is able to coordinate this communication between ureteric bud and metanephric mesenchyme and its absence is sufficient to block kidney development at its very early stage: our results correlate with the more severe outcomes of *HNF1B* related renal pathologies characterized by renal agenesis.

Hnf1b is also expressed in the epithelium that differentiates from the mesenchyme. In the *Hnf1b* epiblastic inactivation model, the severe phenotype prevented us from studying the function of *Hnf1b* in the tissues that derive from this mesenchyme. In order to circumvent this problem, we made use of a different inactivation model (Six2-driven Cre) to inactivate *Hnf1b* specifically in the metanephric mesenchyme in a context of wild-type ureteric bud tip. In this model, the crosstalk with the metanephric mesenchyme was maintained and the mesenchymal to epithelial transition occurred. *Hnf1b* is programmed to be expressed specifically in the distal part of vesicle, in the cells that are next to the ureteric bud. Later on, it is expressed in all the tubular epithelial structures of the nephron including the distal convoluted tubules, Henle's loop and proximal tubules. We have shown that the inactivation of *Hnf1b* is responsible for the lack of specification and expansion of the tubular part of nephrons. This drastic phenotype is linked to the defective specification of the middle limb of sigma shaped bodies. During nephron morphogenesis, this territory is able to form a bulge of cells and to further elongate and to evolve in proximal tubule and Henle's loop.

To elucidate the molecular mechanisms at the basis of the lack of tubules, we focused our investigations on the Notch signaling pathway, which has already been demonstrated to be a critical factor for the proximal fate of the nephron. We studied the expression of

canonical Notch pathway members that are expressed during early steps of kidney development including several ligands (*Dll1*, *Jag1* and *Jag2*), the receptors (*Notch1* and *Notch2*) and some downstream effectors including members of HES/HEY family. My results have shown that the expression of *Dll1* and *Hes5* is downregulated. Interestingly it has been previously shown that hypomorphic expression of Dll1 impairs Notch signaling leading to defective proximal tubular development with a normal glomerular development (Cheng et al., 2007). All these results suggest that defective Notch signaling could play a role in our phenotype. It is worth to note that the inactivation of *Hnf1b* in the mesenchyme does not completely phenocopy the inactivation of *Notch*2 in this compartment. In fact, it has been demonstrated that Pax3-Cre-driven *Notch2* deficient embryos are characterized by the absence of both proximal tubules and glomeruli. On the contrary, renal corpuscles are formed in HNF1beta-deficient embryos.

The difference of phenotypes between *Notch2* and *Hnf1b* mutants can be ascribed to the complex roles played by *Notch1* and *Notch2* receptor genes. The analysis of the phenotypes induced by the inactivation of *Notch1* and *Notch2* indicated that these receptors play overlapping roles. The phenotype of the Pax3-Cre inactivation of *Notch2* is however more drastic (missing glomeruli and proximal tubules) and leads to a blockage of nephrogenesis that is earlier than that elicited by *Hnf1b* inactivation. In fact in HNF1beta mutants we have deformed S-shaped bodies. These structures are never formed in *Notch2* mutants. It is likely that the Notch receptors, through the activation mediated by their ligands, might be required for distinct sequential roles during nephron nephrogenesis. The absence of receptors leads to a blockage of nephron morphogenesis in the initial steps of differentiation. On the other hand, the deficiency of the expression of Dll1, a Notch ligand characterized by a highly restricted expression pattern along the nephron, leads to the defective specification and expansion of tubules without affecting the normal development of glomeruli. This phenotype is similar to what I observed in kidney with a Six2-driven *Hnf1b* deficiency.

It is worth to note when *Notch2* (and not *Notch1*) is inactivated relatively early (with a Pax3-Cre, proximal tubules and glomeruli do not form. On the contrary, if *Notch2* is inactivated slightly later (with a Six2-Cre), no major phenotypes are observed apart from a variable and poorly penetrant reduction of the final number of nephrons. This observation would indicate that the critical function played by Notch2 must take place before the onset of the deletion mediated by the Six2-Cre transgene. In other words, when Six2-Cre inactivates *Notch2*, this gene has already accomplished a critical function (Surendran et al., 2010).

Therefore, Notch1 and Notch2, together, are required for nephrogenesis, at a step after the onset of Six2-Cre expression. In a *Notch2* deficient background, the loss of one copy of *Notch1* leads to a more severe reduction of nephrons, and the combined inactivation of these two genes leads to a phenotype comparable with the one observed with the Pax3-Cre deletion of *Notch2* (Surendran et al., 2010). Careful analysis of this latter phenotype shows, in fact, an early stop in the nephrogenesis process, before the formation of differentiated renal vesicle.

Our work highlighted the role of Notch signaling later during nephrons formation, in the middle limb of the S-shaped body. Inactivation of Notch signaling specifically in this subdomain leads to the lack of tubular formation.

To analyze the molecular mechanisms and the targets involved in the phenotypes we observed, we made use of an *in silico* approach developed in the laboratory to determine if these genes might be possibly under the direct control of this transcription factor. This led to the identification of a very well conserved HNF1 binding site, 2Kb upstream the transcriptional start site of the Dll1 gene together with a second site much farther away (302 Kb downstream). Our results showed that both sites were actually bound in vivo. These ChIP results suggest that the defective expression of Dll1 might be a direct consequence of the absence of HNF1beta already in early nephron precursors (vesicles and comma-shaped bodies).

At the molecular levels, other specific markers are expressed in middle limb of the S-shaped body such as *Osr2*, *Irx1* and *Brn1*. Interestingly, *Osr2* has been involved in proximal tubular differentiation in Xenopus and Zebrafish (Tena et al., 2007) but its role in mammalian kidney morphogenesis is probably redundant since its inactivation, in mouse, does not lead to any renal abnormality. The down regulation of *Irx1* in *Xenopus* leads to abnormal morphogenesis of the intermediate pronephric tubules (Alarcon et al., 2008). Interestingly, *Osr2* been shown to act as a repressor, and to regulate negatively the expression of Pax2 in *Zebrafish*/*Xenopus*. This mechanism might explain the persistent high expression of Pax2 observed in the primitive tubules of mutant embryos (Tena et al., 2007).

The silico approach that we applied led us to discover well conserved HNF1 binding sites also around Osr2 and Irx1 genes. Our ChIP results showed that these sites were significantly bound in vivo. These results suggest that HNF1beta might participate in the transcriptional activation of Osr2 and Irx1 in already expanding and differentiating tubules. Even if these genes do not play any causal role in our phenotype, we can speculate that they

could constitute a direct transcription cascade under the control of Hnf1b involved in later steps of differentiation.

The inactivation of *Hnf1b* in the mesenchyme does not lead to any gross alteration of the differentiation of podocyte precursors. In agreement with this observation is the fact that this cell type does not express *Hnf1b*. Even if podocytes are not directly affected by *Hnf1b* inactivation, the general structure of the glomerulus is deformed with an aberrant localization of the urinary and vascular poles. In mutant glomeruli the vascular and urinary poles are not in opposite position. In addition, the Bowman's capsule is also affected by severe dilatation. Analysis of renal human samples of MODY5 patients show in some area a complete lack of proximal tubules, reminiscent of what was observed in our murine model.

In conclusion, our results granted new insights in the comprehension of *Hnf1b* roles during kidney development. Depending on time/place selective inactivation of *Hnf1b* in mouse models, we can recapitulate some malformations observed in MODY5 patients. In this study, I showed that *Hnf1b* is able to control different transcription cascades involved in sequential morphologic events. We suggest that the high variability of human renal malformations correlated with MODY5 syndrome could be ascribed to different pattern of inactivation of the very same gene.

Perspectives

The work of my thesis highlighted new transcriptional networks involved in the development of the kidney. The drastic phenotype observed in *Hnf1b* epiblastic inactivation disclosed the important role of this transcription factor in the expression of several genes involved in the branching of the ureteric bud and the mesenchymal to epithelial transition, the first step of nephron morphogenesis in the blastema. In the other hand, inactivation of *Hnf1b* in the cap mesenchyme, in the presence of a wild type ureteric bud allows the first steps of epithelialisation and nephrogenesis, but the subsequent steps of tubular specification and expansion are severely affected.

We have shown that *Hnf1b* directly controls the expression of several genes known to be crucial for the ureteric bud branching and for the correct crosstalk between the ureteric bud and the blastema. Later on, in epithelial structures derived from the metanephric blastema, we have shown that *Hnf1b* controls the expression of *Dll1*, a ligand of the Notch pathway that is known to be implicated in tubular specification. The downregulation of this ligand is associated with a decreased expression of Notch downstream effector *Hes5*. Altogether, these results highlighted a novel role of Notch pathway in tubular specification and expansion.

These results I have obtained during my work elucidated some of the molecular cascades controlled by *Hnf1b* during kidney development in different compartments. I was also able to define more precisely the spatial sub-compartmentalization of the nephron precursors.

I will discuss some preliminary data and perspectives on the identification of the mechanisms leading to the formation of mature functional nephron. These future works could increase the knowledge of this fascinating and complicated process.

Future perspective

Perspective 1: Analysis of gene expression in *Hnf1b* deficient nephron precursors.

Molecular signaling pathways and transcriptional cascades involved during the development and differentiation of several organs are frequently conserved across species. This particularity allowed us to select some crucial genes already known to be involved in kidney development and to analyze their expression in our models. In addition, an in silico approach has been developed in the laboratory (Serge Garbay), based on the conservation of HNF1binding sites. By chromatin immunoprecipitation experiments, we were able to test the binding of Hnf1β on these candidates in vivo. Altogether, these results could help us to identify some crucial cascades under the direct control of *Hnf1b*, involved in tubular formation.

In order to further increase our knowledge on the mechanisms controlled by *Hnf1b*, our laboratory is carrying out a high-throughput analysis, taking advantage of the SOLEXA technology.

We will analyze the differential expression of all the genes present in early step of nephron development, in the presence or the absence of *Hnf1b*. To do this, we extracted RNA from E13.5 kidneys and we performed SOLEXA sequencing on pooled samples from control embryos and Six2-Cre-inactivated *Hnf1b* deficient embryos.

We chose this stage of the development because the tubular component of the nephron has not started yet its differentiation program (the first markers of nephric segments differentiation start to appear at E14.5). The presence of differentiating tubules could bias the comparison between the control and the mutants, in which these segments never develop.

The list of genes differentially expressed in absence of *Hnf1b* will allow us to select gene candidates whose expression pattern could suggest a key role in tubular specification and expansion. In order to identify which genes could be directly transcriptionally controlled by HNF1beta we will take advantage of the recent publication of the ENCODE project results. The idea would be to intersect HNF1binding sites that have been conserved by evolution (according to a strict criterion of conservation among different species) with the position of DNase I hypersensitive sites that the ENCODE consortium has identified in kidney tissues and in several renal cell types. In this respect, we will take into consideration genes

particularly enriched in HNF1binding sites that are localized in open and particularly accessible chromatin conformations. This strategy will allow us to identify genes that could be considered good candidates in the control of the early steps of nephron development. These genes will be analyzed in perspective to their possible involvement human renal pathologies. In collaboration with the reference center for rare diseases (Maladies Rénales Héréditaires de l'Enfant et de l'Adulte, MARHEA) directed by Laurence Heidet and Remi Salomon, we could monitor their expression in human patients to elucidate new pathways or to give a deeper explanation of the origin of renal malformation correlated to these mutations.

Perspective 2: Role of *Hnf1b* during tubular specification and elongation.

The inactivation of *Hnf1b* in the cap mesenchyme cells via Six2-Cre driven recombination resulted in complete absence of *Hnf1b* expression (> 95%) in early developing nephrons. This absence of expression resulted in the drastic absence of tubular formation. This severe defect prevented us from studying the possible role of *Hnf1b* in further steps of tubular differentiation, after they emerge from S-shaped precursors. It was previously shown by our laboratory that the inactivation of *Hnf1b* in already formed but still elongating collecting ducts and Henle's loop leads to the formation of cyst. In Six2-Cre inactivation model, we showed that the nephron precursors lacking *Hnf1b* cannot set their differentiation program and they enter partially in apoptosis. Therefore, the potential role of *Hnf1b* after the first steps of tubular specidfication remains unclear. In particular, does *Hnf1b* play a role in the differentiation of adjacent but totally different segments (such as proximal tubule and Henle's loop)?

To study the role of *Hnf1b* in this context, we used a Cre recombinase that showed a more chimeric inactivation pattern than the Six2-Cre. The inactivation of *Hnf1b* has been carried out using the RaRb2-Cre mice line (Kobayashi et al., 2005). The mutants we obtained with this model did not suffer from perinatal lethality and they survive several months after birth. However, all the animals lacking *Hnf1b* developed normoglycemic glucosuria soon after.

Histological analysis of kidneys few days after birth showed the presence of normally shaped developing nephrons in the nephrogenic region and the presence of tubular cysts. The severity of the cystic disease we observed was very variable and could be related to the different extent of *Hnf1b* inactivation observed in different pups (Preliminary results, figure 1A-C). In fact, the X-Gal staining on animals that carry both Rosa26R-lacZ cassette and the Cre showed very chimeric and variable pattern of recombination (around 10-20% of the cells in epithelial structures derived from the mesenchyme). Nevertheless, all the mice lacking *Hnf1b* were affected by tubular cyst formation. The most evident defect at the histological level, besides the cysts, was a drastic decrease of proximal tubules in the mutant kidneys compared with the wild type: we observed, in average, 50% reduction of proximal tubules section between mutant and control animals without any significant defect in the total number of nephrons. In addition, the few remaining proximal tubules were often already dilated (Preliminary results figure 1A-C). LTL immunohistological staining in mutant kidneys show a global decrease in the staining when compared to controls (Preliminary results figure 1D-E). Quantitative PCR of proximal tubules markers (*Villin1*, *Megalin* and *Cubilin*) confirmed a significant decrease in their expression, whereas the Na/Cl cotransporter of the Henle's loop (*Scl12a3*) was slightly decreased and the markers for podocytes (*Wt1*) and collecting duct (*Aquaporin2*) were not affected at all (Preliminary results figure 1F). These results are consistent with the fact that the defective glucose reabsorption could be related to an abnormally shorter proximal tubule. Nevertheless, we cannot rule out that the expression at the cellular level of some specific glucose transporter (SGLT2 and SGLT1) is affected in our model. Altogether, these results showed that the spotted inactivation of *Hnf1b* seems to affect the elongation of the tubular segments of the nephrons.

Histological analysis of cysts showed an interesting peculiarity: a high percentage of cysts present with adjacent staining of markers for proximal tubules (LTL) and thick ascendant limb of the Henle's loop (Nkcc2; Slc12a3) (Preliminary results figure 1H-I). In control kidneys, these two segments are never adjacent due to the presence in between them of the thin descendant limb of Henle's loop that do not express *Slc12a3*. This defect, never observed in any of the renal cystic mouse model described so far, suggests a possible specific role of *Hnf1b* in the patterning of different tubular segments.

Preliminary results figure1: Renal phenotype resulting from chimeric inactivation of *Hnf1b* in the metanephric mesenchyme condensate. (A-C) Histological analysis of paraffin sections of *Hnf1b* mutant kidneys show different degrees of cyst formation (B,C) compared to the controls (A), spanning from mild (B) to severe (C) cystogenesis. (D-E) Immunohistological analysis of LTL staining, specific for the proximal tubules, showed a drastic diminution of positive tubules segment in the mutant compared to the control. (F) RT-qPCR on the expression of proximal tubular genes (*Vil1*, *Meg* and *Cub*), Henle's loop marker (*Slc12a3*; *Nkcc2*) markers of podocytes (*Wt1*) and collecting ducts (*Aq2*). * $p>0.05$; ** $p>0.01$. (G-I) Immunohistological staining of Slc12a3 and LTL showed that these two tubular segments are adjacent in the mutant (G-H) compare to control (I).

Perspective 3: 3D reconstruction of nephron precursors

Our results showed that the absence of *Hnf1b* in the early step of nephrogenesis is responsible for a dramatic deformation of nephron precursors. This defect becomes visible at the stage of S-shaped body, where the bulge of the more proximal part of the middle limb territory begins to develop and differentiate into proximal tubule and Henle's loop precursors. In the absence of *Hnf1b,* this region never develops and the distal limb directly connects to the presumptive podocytes precursors of the proximal limb. To better elucidate the malformation observed in histological thin sections, we adopted a 3D approach to visualize the nature of the developing structures. The phenotype analysis based on 3D tissue reconstruction allows a better identification of the place where the defect takes place and the interaction between the different segments.

The renal tissue was processed with two different protocols according to the reactivity of the antibodies used during the experiments. In the first case, freshly dissected kidneys were included in agarose gel, directly cut in thick 90-100µm sections with a Vibratome (Leika) and incubated a long time with the antibodies to reach their complete penetrance in the tissue. The slices were then analyzed with spinning disk confocal microscope, and Z-stacks of images were collected. Three dimensional (3D) models were created on the base of confocal stacks using the software IMOD (http://bio3d.colorado.edu/imod/). A second protocol using serial thick paraffin sections was used when a demasking procedure was needed to allow the antibodies to recognize their correspondant epitopes. The slides were incubated 48 hours with

primary/secondary antibodies and analyzed with spinning disk confocal microscope. In order to reconstruct the totality of the structures, serial stacks of subsequent slides have been aligned and piled up using mathematical algorithms elaborated in the team by S. Garbay. Briefly, a translation/rotation was applied between serial stacks to achieve an optimal match between them. This technique can, theoretically, allow a complete reconstruction of the kidney… but we will focus by now on the developing nephrons.

The preliminary models we obtained showed a clear deformation of the S-shaped body in mutant animals. Further studies on this model could give a more in depth knowledge of several crucial processes that are at the basis of the kidney morphology, such as the morphogenic movements, the differentiation process, the proliferation pattern and the exact compartmentalization of the different cell precursors.

Preliminary results figure2: Three dimensionnal reconstruction of developing nephrons. 3D approach modeling the spatial conformation of S-shaped body in control (left) and mutant (right). The different colors represent in red the basal membrane labelled by anti-Laminin antibody, in green the DBA positif ureteric bud and in light blue the lumen of the tube. **A-B**: side view of S-shaped body; **C-D** front view of the structures; **E-F** structure of the luminal space of the tubules.

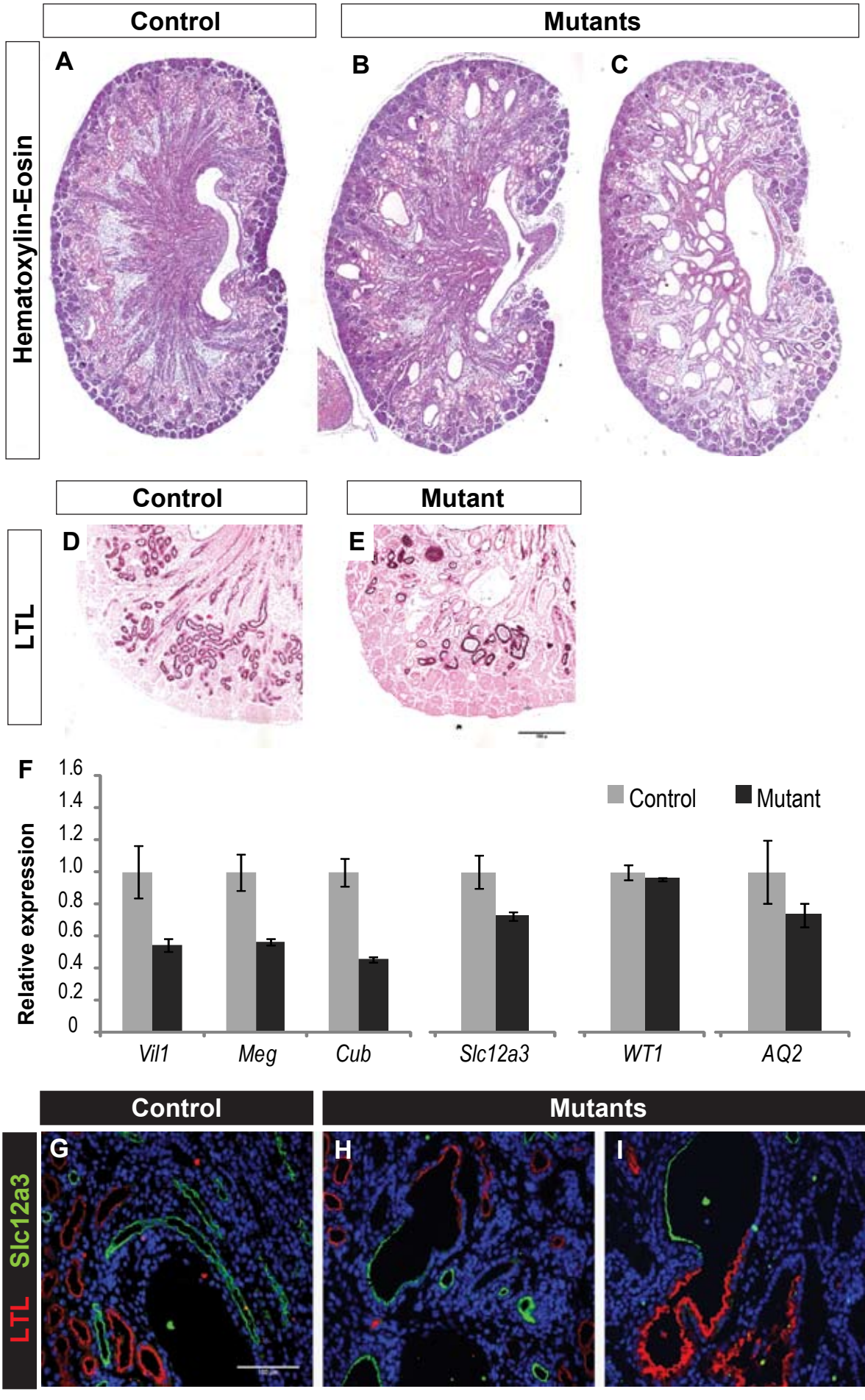

Supplementary results Figure 1

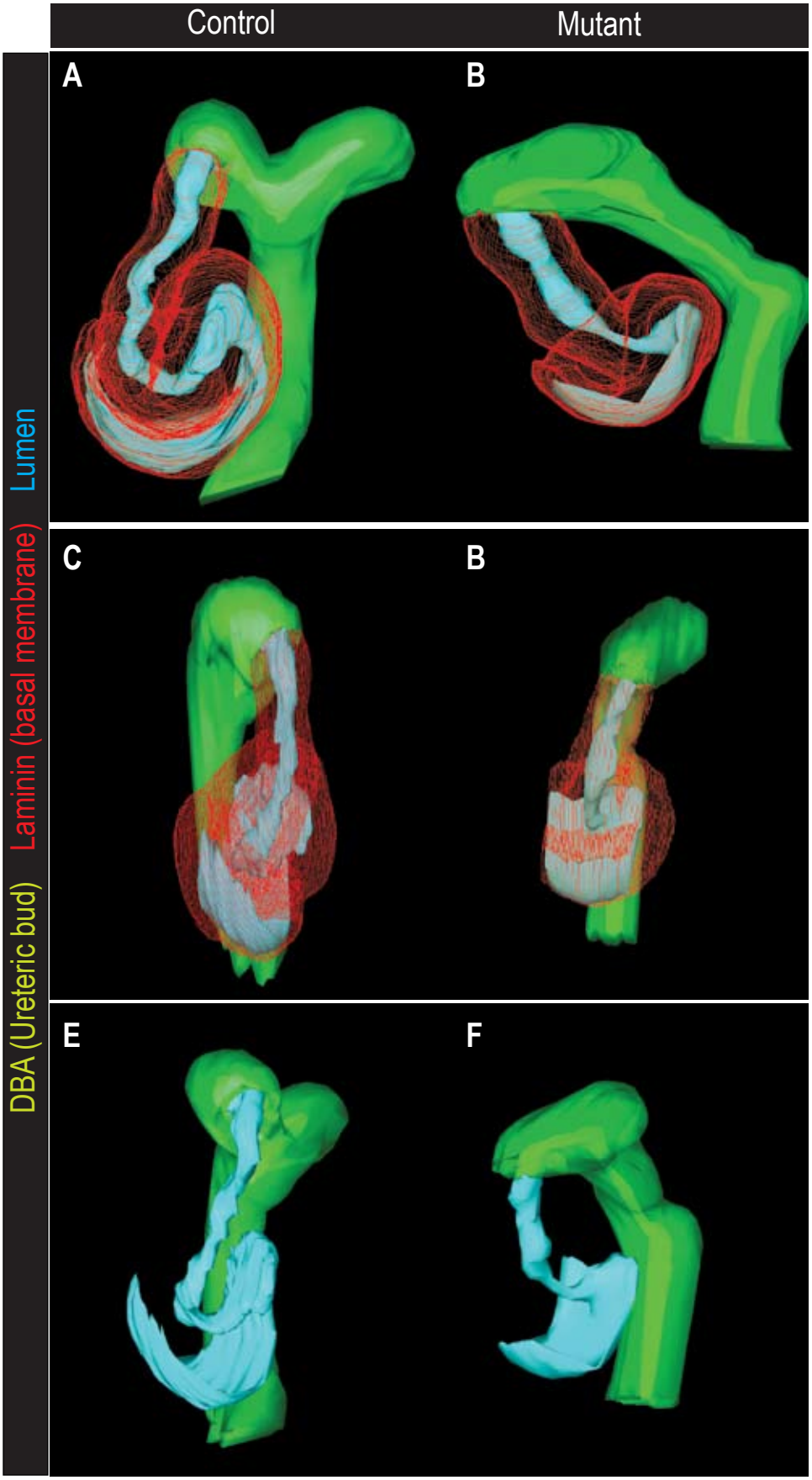

Supplementary results Figure 2

Bibliography

Bibliography

Abremski, K., and Hoess, R. (1984). Bacteriophage P1 site-specific recombination. Purification and properties of the Cre recombinase protein. J Biol Chem *259*, 1509-1514.

Ahlgren, U., Pfaff, S.L., Jessell, T.M., Edlund, T., and Edlund, H. (1997). Independent requirement for ISL1 in formation of pancreatic mesenchyme and islet cells. Nature *385*, 257-260.

Alarcon, P., Rodriguez-Seguel, E., Fernandez-Gonzalez, A., Rubio, R., and Gomez-Skarmeta, J.L. (2008). A dual requirement for Iroquois genes during Xenopus kidney development. Development *135*, 3197-3207.

Andersen, P., Uosaki, H., Shenje, L.T., and Kwon, C. (2012). Non-canonical Notch signaling: emerging role and mechanism. Trends Cell Biol *22*, 257-265.

Armstrong, J.F., Pritchard-Jones, K., Bickmore, W.A., Hastie, N.D., and Bard, J.B. (1993). The expression of the Wilms' tumour gene, WT1, in the developing mammalian embryo. Mech Dev *40*, 85-97.

Bach, I., Pontoglio, M., and Yaniv, M. (1992). Structure of the gene encoding hepatocyte nuclear factor 1 (HNF1). Nucleic Acids Res *20*, 4199-4204.

Badouel, C., Garg, A., and McNeill, H. (2009). Herding Hippos: regulating growth in flies and man. Curr Opin Cell Biol *21*, 837-843.

Barajas, L. (1970). The ultrastructure of the juxtaglomerular apparatus as disclosed by three-dimensional reconstructions from serial sections. The anatomical relationship between the tubular and vascular components. Journal of ultrastructure research *33*, 116-147.

Barajas, L. (1979). Anatomy of the juxtaglomerular apparatus. Am J Physiol *237*, F333-343.
Barak, H., Huh, S.H., Chen, S., Jeanpierre, C., Martinovic, J., Parisot, M., Bole-Feysot, C., Nitschke, P., Salomon, R., Antignac, C., *et al.* (2012). FGF9 and FGF20 maintain the stemness of nephron progenitors in mice and man. Dev Cell *22*, 1191-1207.

Barbacci, E., Reber, M., Ott, M.O., Breillat, C., Huetz, F., and Cereghini, S. (1999). Variant hepatocyte nuclear factor 1 is required for visceral endoderm specification. Development *126*, 4795-4805.

Barnes, J.D., Crosby, J.L., Jones, C.M., Wright, C.V., and Hogan, B.L. (1994). Embryonic expression of Lim-1, the mouse homolog of Xenopus Xlim-1, suggests a role in lateral mesoderm differentiation and neurogenesis. Dev Biol *161*, 168-178.

Basson, M.A., Akbulut, S., Watson-Johnson, J., Simon, R., Carroll, T.J., Shakya, R., Gross, I., Martin, G.R., Lufkin, T., McMahon, A.P., *et al.* (2005). Sprouty1 is a critical regulator of GDNF/RET-mediated kidney induction. Dev Cell *8*, 229-239.

Basson, M.A., Watson-Johnson, J., Shakya, R., Akbulut, S., Hyink, D., Costantini, F.D., Wilson, P.D., Mason, I.J., and Licht, J.D. (2006). Branching morphogenesis of the ureteric

epithelium during kidney development is coordinated by the opposing functions of GDNF and Sprouty1. Dev Biol *299*, 466-477.

Bellanne-Chantelot, C., Chauveau, D., Gautier, J.F., Dubois-Laforgue, D., Clauin, S., Beaufils, S., Wilhelm, J.M., Boitard, C., Noel, L.H., Velho, G., *et al.* (2004). Clinical spectrum associated with hepatocyte nuclear factor-1beta mutations. Ann Intern Med *140*, 510-517.

Bellanne-Chantelot, C., Clauin, S., Chauveau, D., Collin, P., Daumont, M., Douillard, C., Dubois-Laforgue, D., Dusselier, L., Gautier, J.F., Jadoul, M., *et al.* (2005). Large genomic rearrangements in the hepatocyte nuclear factor-1beta (TCF2) gene are the most frequent cause of maturity-onset diabetes of the young type 5. Diabetes *54*, 3126-3132.

Bingham, C., Bulman, M.P., Ellard, S., Allen, L.I., Lipkin, G.W., Hoff, W.G., Woolf, A.S., Rizzoni, G., Novelli, G., Nicholls, A.J., *et al.* (2001). Mutations in the hepatocyte nuclear factor-1beta gene are associated with familial hypoplastic glomerulocystic kidney disease. Am J Hum Genet *68*, 219-224.

Bjarnegard, M., Enge, M., Norlin, J., Gustafsdottir, S., Fredriksson, S., Abramsson, A., Takemoto, M., Gustafsson, E., Fassler, R., and Betsholtz, C. (2004). Endothelium-specific ablation of PDGFB leads to pericyte loss and glomerular, cardiac and placental abnormalities. Development *131*, 1847-1857.

Borke, J.L., Minami, J., Verma, A., Penniston, J.T., and Kumar, R. (1987). Monoclonal antibodies to human erythrocyte membrane Ca++-Mg++ adenosine triphosphatase pump recognize an epitope in the basolateral membrane of human kidney distal tubule cells. J Clin Invest *80*, 1225-1231.

Bouchard, M., Souabni, A., Mandler, M., Neubuser, A., and Busslinger, M. (2002). Nephric lineage specification by Pax2 and Pax8. Genes Dev *16*, 2958-2970.

Boyle, S., Misfeldt, A., Chandler, K.J., Deal, K.K., Southard-Smith, E.M., Mortlock, D.P., Baldwin, H.S., and de Caestecker, M. (2008). Fate mapping using Cited1-CreERT2 mice demonstrates that the cap mesenchyme contains self-renewing progenitor cells and gives rise exclusively to nephronic epithelia. Dev Biol *313*, 234-245.

Brenner-Anantharam, A., Cebrian, C., Guillaume, R., Hurtado, R., Sun, T.T., and Herzlinger, D. (2007). Tailbud-derived mesenchyme promotes urinary tract segmentation via BMP4 signaling. Development *134*, 1967-1975.

Brenner, M.B. (1996). The kidney. In, F.L. Rector, ed. (Saunders).

Brophy, P.D., Ostrom, L., Lang, K.M., and Dressler, G.R. (2001). Regulation of ureteric bud outgrowth by Pax2-dependent activation of the glial derived neurotrophic factor gene. Development *128*, 4747-4756.

Brou, C., Logeat, F., Gupta, N., Bessia, C., LeBail, O., Doedens, J.R., Cumano, A., Roux, P., Black, R.A., and Israel, A. (2000). A novel proteolytic cleavage involved in Notch signaling: the role of the disintegrin-metalloprotease TACE. Mol Cell *5*, 207-216.

Brunskill, E.W., Aronow, B.J., Georgas, K., Rumballe, B., Valerius, M.T., Aronow, J., Kaimal, V., Jegga, A.G., Yu, J., Grimmond, S., *et al.* (2008). cheng. Dev Cell *15*, 781-791.

Cacalano, G., Farinas, I., Wang, L.C., Hagler, K., Forgie, A., Moore, M., Armanini, M., Phillips, H., Ryan, A.M., Reichardt, L.F., *et al.* (1998). GFRalpha1 is an essential receptor component for GDNF in the developing nervous system and kidney. Neuron *21*, 53-62.

Cain, J.E., Di Giovanni, V., Smeeton, J., and Rosenblum, N.D. (2010). Genetics of renal hypoplasia: insights into the mechanisms controlling nephron endowment. Pediatric research *68*, 91-98.

Carette, C., Vaury, C., Barthelemy, A., Clauin, S., Grunfeld, J.P., Timsit, J., and Bellanne-Chantelot, C. (2007). Exonic duplication of the hepatocyte nuclear factor-1beta gene (transcription factor 2, hepatic) as a cause of maturity onset diabetes of the young type 5. The Journal of clinical endocrinology and metabolism *92*, 2844-2847.

Carroll, T.J., and Das, A. (2011). Planar cell polarity in kidney development and disease. Organogenesis *7*, 180-190.

Carroll, T.J., Park, J.S., Hayashi, S., Majumdar, A., and McMahon, A.P. (2005). Wnt9b plays a central role in the regulation of mesenchymal to epithelial transitions underlying organogenesis of the mammalian urogenital system. Dev Cell *9*, 283-292.

Chai, L., Yang, J., Di, C., Cui, W., Kawakami, K., Lai, R., and Ma, Y. (2006). Transcriptional activation of the SALL1 by the human SIX1 homeodomain during kidney development. J Biol Chem *281*, 18918-18926.

Chen, L., and Al-Awqati, Q. (2005). Segmental expression of Notch and Hairy genes in nephrogenesis. Am J Physiol Renal Physiol *288*, F939-952.

Chen, Y.Z., Gao, Q., Zhao, X.Z., Chen, Y.Z., Bennett, C.L., Xiong, X.S., Mei, C.L., Shi, Y.Q., and Chen, X.M. (2010). Systematic review of TCF2 anomalies in renal cysts and diabetes syndrome/maturity onset diabetes of the young type 5. Chinese medical journal *123*, 3326-3333.

Cheng, H.T., Kim, M., Valerius, M.T., Surendran, K., Schuster-Gossler, K., Gossler, A., McMahon, A.P., and Kopan, R. (2007). Notch2, but not Notch1, is required for proximal fate acquisition in the mammalian nephron. Development *134*, 801-811.

Cheret, C., Doyen, A., Yaniv, M., and Pontoglio, M. (2002). Hepatocyte Nuclear Factor 1 α Controls Renal Expression of the Npt1-Npt4 Anionic Transporter Locus. J Mol Biol *322*, 929-941.

Chi, L., Saarela, U., Railo, A., Prunskaite-Hyyrylainen, R., Skovorodkin, I., Anthony, S., Katsu, K., Liu, Y., Shan, J., Salgueiro, A.M., *et al.* (2011). A secreted BMP antagonist, Cer1, fine tunes the spatial organization of the ureteric bud tree during mouse kidney development. PloS one *6*, e27676.

Chi, X., Michos, O., Shakya, R., Riccio, P., Enomoto, H., Licht, J.D., Asai, N., Takahashi, M., Ohgami, N., Kato, M., *et al.* (2009). Ret-dependent cell rearrangements in the Wolffian duct epithelium initiate ureteric bud morphogenesis. Dev Cell *17*, 199-209.

Chouard, T., Jeannequin, O., Rey-Campos, J., Yaniv, M., and Traincard, F. (1997). A set of polyclonal and monoclonal antibodies reveals major differences in post-translational modification of the rat HNF1 and vHNF1 homeoproteins. Biochimie *79*, 707-715.

Clevers, H., and Nusse, R. (2012). Wnt/beta-catenin signaling and disease. Cell *149*, 1192-1205.

Coffinier, C., Barra, J., Babinet, C., and Yaniv, M. (1999a). Expression of the vHNF1/HNF1beta homeoprotein gene during mouse organogenesis. Mech Dev *89*, 211-213.

Coffinier, C., Gresh, L., Fiette, L., Tronche, F., Schutz, G., Babinet, C., Pontoglio, M., Yaniv, M., and Barra, J. (2002). Bile system morphogenesis defects and liver dysfunction upon targeted deletion of HNF1beta. Development *129*, 1829-1838.

Coffinier, C., Thepot, D., Babinet, C., Yaniv, M., and Barra, J. (1999b). Essential role for the homeoprotein vHNF1/HNF1beta in visceral endoderm differentiation. Development *126*, 4785-4794.

Costantini, F., and Shakya, R. (2006). GDNF/Ret signaling and the development of the kidney. Bioessays *28*, 117-127.

Courtois, G., Morgan, J.G., Campbell, L.A., Fourel, G., and Crabtree, G.R. (1987). Interaction of a liver-specific nuclear factor with the fibrinogen and alpha 1-antitrypsin promoters. Science *238*, 688-692.

Czerny, T., Schaffner, G., and Busslinger, M. (1993). DNA sequence recognition by Pax proteins: bipartite structure of the paired domain and its binding site. Genes Dev *7*, 2048-2061.

D'Angelo, A., Bluteau, O., Garcia-Gonzalez, M.A., Gresh, L., Doyen, A., Garbay, S., Robine, S., and Pontoglio, M. (2010). Hepatocyte nuclear factor 1alpha and beta control terminal differentiation and cell fate commitment in the gut epithelium. Development *137*, 1573-1582.

D'Souza, B., Meloty-Kapella, L., and Weinmaster, G. (2010). Canonical and non-canonical Notch ligands. Curr Top Dev Biol *92*, 73-129.

Dailey, L., Ambrosetti, D., Mansukhani, A., and Basilico, C. (2005). Mechanisms underlying differential responses to FGF signaling. Cytokine & growth factor reviews *16*, 233-247.

Davidson, A.J. (2008). Mouse kidney development. StemBook [Internet].

Davies, J.A., Ladomery, M., Hohenstein, P., Michael, L., Shafe, A., Spraggon, L., and Hastie, N. (2004). Development of an siRNA-based method for repressing specific genes in renal organ culture and its use to show that the Wt1 tumour suppressor is required for nephron differentiation. Hum Mol Genet *13*, 235-246.

De, A. (2011). Wnt/Ca2+ signaling pathway: a brief overview. Acta biochimica et biophysica Sinica *43*, 745-756.

De Robertis, E.M., and Kuroda, H. (2004). Dorsal-ventral patterning and neural induction in Xenopus embryos. Annu Rev Cell Dev Biol *20*, 285-308.

Di Giovanni, V., Alday, A., Chi, L., Mishina, Y., and Rosenblum, N.D. (2011). Alk3 controls nephron number and androgen production via lineage-specific effects in intermediate mesoderm. Development *138*, 2717-2727.

Donovan, M.J., Natoli, T.A., Sainio, K., Amstutz, A., Jaenisch, R., Sariola, H., and Kreidberg, J.A. (1999). Initial differentiation of the metanephric mesenchyme is independent of WT1 and the ureteric bud. Developmental genetics *24*, 252-262.

Dressler, G.R. (2006). The cellular basis of kidney development. Annu Rev Cell Dev Biol *22*, 509-529.

Dressler, G.R., Deutsch, U., Chowdhury, K., Nornes, H.O., and Gruss, P. (1990). Pax2, a new murine paired-box-containing gene and its expression in the developing excretory system. Development *109*, 787-795.

Drummond, I.A., and Davidson, A.J. (2010). Zebrafish kidney development. Methods in cell biology *100*, 233-260.

Dudley, A.T., Godin, R.E., and Robertson, E.J. (1999). Interaction between FGF and BMP signaling pathways regulates development of metanephric mesenchyme. Genes Dev *13*, 1601-1613.

Duncan, S.A., Navas, M.A., Dufort, D., Rossant, J., and Stoffel, M. (1998). Regulation of a transcription factor network required for differentiation and metabolism. Science *281*, 692-695.

Enomoto, H., Araki, T., Jackman, A., Heuckeroth, R.O., Snider, W.D., Johnson, E.M., Jr., and Milbrandt, J. (1998). GFR alpha1-deficient mice have deficits in the enteric nervous system and kidneys. Neuron *21*, 317-324.

Eremina, V., and Quaggin, S.E. (2004). The role of VEGF-A in glomerular development and function. Current opinion in nephrology and hypertension *13*, 9-15.

Eremina, V., Sood, M., Haigh, J., Nagy, A., Lajoie, G., Ferrara, N., Gerber, H.P., Kikkawa, Y., Miner, J.H., and Quaggin, S.E. (2003). Glomerular-specific alterations of VEGF-A expression lead to distinct congenital and acquired renal diseases. J Clin Invest *111*, 707-716.

Eswarakumar, V.P., Lax, I., and Schlessinger, J. (2005). Cellular signaling by fibroblast growth factor receptors. Cytokine & growth factor reviews *16*, 139-149.

Fajans, S.S., and Bell, G.I. (2011). MODY: history, genetics, pathophysiology, and clinical decision making. Diabetes care *34*, 1878-1884.

Fischer, E., Legue, E., Doyen, A., Nato, F., Nicolas, J.F., Torres, V., Yaniv, M., and Pontoglio, M. (2006). Defective planar cell polarity in polycystic kidney disease. Nat Genet *38*, 21-23.

Frain, M., Swart, G., Monaci, P., Nicosia, A., Stampfli, S., Frank, R., and Cortese, R. (1989). The liver-specific transcription factor LF-B1 contains a highly diverged homeobox DNA binding domain. Cell *59*, 145-157.

Georgas, K., Rumballe, B., Valerius, M.T., Chiu, H.S., Thiagarajan, R.D., Lesieur, E., Aronow, B.J., Brunskill, E.W., Combes, A.N., Tang, D., *et al.* (2009). Analysis of early nephron patterning reveals a role for distal RV proliferation in fusion to the ureteric tip via a cap mesenchyme-derived connecting segment. Dev Biol *332*, 273-286.

Gilland, E., Miller, A.L., Karplus, E., Baker, R., and Webb, S.E. (1999). Imaging of multicellular large-scale rhythmic calcium waves during zebrafish gastrulation. Proc Natl Acad Sci U S A *96*, 157-161.

Godart, F., Bellanne-Chantelot, C., Clauin, S., Gragnoli, C., Abderrahmani, A., Blanche, H., Boutin, P., Chevre, J.C., Froguel, P., and Bailleul, B. (2000). Identification of seven novel nucleotide variants in the hepatocyte nuclear factor-1alpha (TCF1) promoter region in MODY patients. Human mutation *15*, 173-180.

Gong, K.Q., Yallowitz, A.R., Sun, H., Dressler, G.R., and Wellik, D.M. (2007). A Hox-Eya-Pax complex regulates early kidney developmental gene expression. Mol Cell Biol *27*, 7661-7668.

Gordon, W.R., Vardar-Ulu, D., Histen, G., Sanchez-Irizarry, C., Aster, J.C., and Blacklow, S.C. (2007). Structural basis for autoinhibition of Notch. Nature structural & molecular biology *14*, 295-300.

Greger, R. (1985). Ion transport mechanisms in thick ascending limb of Henle's loop of mammalian nephron. Physiological reviews *65*, 760-797.

Greger, R., and Velazquez, H. (1987). The cortical thick ascending limb and early distal convoluted tubule in the urinary concentrating mechanism. Kidney Int *31*, 590-596.

Gresh, L., Fischer, E., Reimann, A., Tanguy, M., Garbay, S., Shao, X., Hiesberger, T., Fiette, L., Igarashi, P., Yaniv, M., *et al.* (2004). A transcriptional network in polycystic kidney disease. The EMBO journal *23*, 1657-1668.

Grieshammer, U., Cebrian, C., Ilagan, R., Meyers, E., Herzlinger, D., and Martin, G.R. (2005). FGF8 is required for cell survival at distinct stages of nephrogenesis and for regulation of gene expression in nascent nephrons. Development *132*, 3847-3857.

Grieshammer, U., Le, M., Plump, A.S., Wang, F., Tessier-Lavigne, M., and Martin, G.R. (2004). SLIT2-mediated ROBO2 signaling restricts kidney induction to a single site. Dev Cell *6*, 709-717.

Grote, D., Boualia, S.K., Souabni, A., Merkel, C., Chi, X., Costantini, F., Carroll, T., and Bouchard, M. (2008). Gata3 acts downstream of beta-catenin signaling to prevent ectopic metanephric kidney induction. PLoS Genet *4*, e1000316.

Grote, D., Souabni, A., Busslinger, M., and Bouchard, M. (2006). Pax 2/8-regulated Gata 3 expression is necessary for morphogenesis and guidance of the nephric duct in the developing kidney. Development *133*, 53-61.

Ha, N.C., Tonozuka, T., Stamos, J.L., Choi, H.J., and Weis, W.I. (2004). Mechanism of phosphorylation-dependent binding of APC to beta-catenin and its role in beta-catenin degradation. Mol Cell *15*, 511-521.

Hahn, S. (2004). Structure and mechanism of the RNA polymerase II transcription machinery. Nature structural & molecular biology *11*, 394-403.

Happe, H., van der Wal, A.M., Leonhard, W.N., Kunnen, S.J., Breuning, M.H., de Heer, E., and Peters, D.J. (2011). Altered Hippo signalling in polycystic kidney disease. The Journal of pathology *224*, 133-142.

Harada, Y., Yokota, C., Habas, R., Slusarski, D.C., and He, X. (2007). Retinoic acid-inducible G protein-coupled receptors bind to frizzled receptors and may activate non-canonical Wnt signaling. Biochem Biophys Res Commun *358*, 968-975.

Hartwig, S., Bridgewater, D., Di Giovanni, V., Cain, J., Mishina, Y., and Rosenblum, N.D. (2008). BMP receptor ALK3 controls collecting system development. J Am Soc Nephrol *19*, 117-124.

Haumaitre, C., Barbacci, E., Jenny, M., Ott, M.O., Gradwohl, G., and Cereghini, S. (2005). Lack of TCF2/vHNF1 in mice leads to pancreas agenesis. Proc Natl Acad Sci U S A *102*, 1490-1495.

Haumaitre, C., Fabre, M., Cormier, S., Baumann, C., Delezoide, A.L., and Cereghini, S. (2006). Severe pancreas hypoplasia and multicystic renal dysplasia in two human fetuses carrying novel HNF1beta/MODY5 mutations. Hum Mol Genet *15*, 2363-2375.

Hayashi, S., Lewis, P., Pevny, L., and McMahon, A.P. (2002). Efficient gene modulation in mouse epiblast using a Sox2Cre transgenic mouse strain. Mech Dev *119 Suppl 1*, S97-S101.

Heidet, L., Decramer, S., Pawtowski, A., Moriniere, V., Bandin, F., Knebelmann, B., Lebre, A.S., Faguer, S., Guigonis, V., Antignac, C., *et al.* (2010). Spectrum of HNF1B mutations in a large cohort of patients who harbor renal diseases. Clin J Am Soc Nephrol *5*, 1079-1090.

Hiesberger, T., Bai, Y., Shao, X., McNally, B.T., Sinclair, A.M., Tian, X., Somlo, S., and Igarashi, P. (2004). Mutation of hepatocyte nuclear factor-1beta inhibits Pkhd1 gene expression and produces renal cysts in mice. J Clin Invest *113*, 814-825.

Hildebrandt, F., and Zhou, W. (2007). Nephronophthisis-associated ciliopathies. J Am Soc Nephrol *18*, 1855-1871.

Horikawa, Y., Iwasaki, N., Hara, M., Furuta, H., Hinokio, Y., Cockburn, B.N., Lindner, T., Yamagata, K., Ogata, M., Tomonaga, O., *et al.* (1997). Mutation in hepatocyte nuclear factor-1 beta gene (TCF2) associated with MODY. Nat Genet *17*, 384-385.

Horiki, M., Imamura, T., Okamoto, M., Hayashi, M., Murai, J., Myoui, A., Ochi, T., Miyazono, K., Yoshikawa, H., and Tsumaki, N. (2004). Smad6/Smurf1 overexpression in cartilage delays chondrocyte hypertrophy and causes dwarfism with osteopenia. J Cell Biol *165*, 433-445.

Hossain, Z., Ali, S.M., Ko, H.L., Xu, J., Ng, C.P., Guo, K., Qi, Z., Ponniah, S., Hong, W., and Hunziker, W. (2007). Glomerulocystic kidney disease in mice with a targeted inactivation of Wwtr1. Proc Natl Acad Sci U S A *104*, 1631-1636.

Hsu, D.R., Economides, A.N., Wang, X., Eimon, P.M., and Harland, R.M. (1998). The Xenopus dorsalizing factor Gremlin identifies a novel family of secreted proteins that antagonize BMP activities. Mol Cell *1*, 673-683.

Hurd, T.W., and Hildebrandt, F. (2011). Mechanisms of nephronophthisis and related ciliopathies. Nephron *118*, e9-14.

Igarashi, P., and Somlo, S. (2002). Genetics and pathogenesis of polycystic kidney disease. J Am Soc Nephrol *13*, 2384-2398.

Imai, M., and Kokko, J.P. (1976). Mechanism of sodium and chloride transport in the thin ascending limb of Henle. J Clin Invest *58*, 1054-1060.

Iso, T., Kedes, L., and Hamamori, Y. (2003). HES and HERP families: multiple effectors of the Notch signaling pathway. Journal of cellular physiology *194*, 237-255.

James, R.G., Kamei, C.N., Wang, Q., Jiang, R., and Schultheiss, T.M. (2006). Odd-skipped related 1 is required for development of the metanephric kidney and regulates formation and differentiation of kidney precursor cells. Development *133*, 2995-3004.

Janda, C.Y., Waghray, D., Levin, A.M., Thomas, C., and Garcia, K.C. (2012). Structural basis of Wnt recognition by Frizzled. Science *337*, 59-64.

Jemc, J., and Rebay, I. (2007). The eyes absent family of phosphotyrosine phosphatases: properties and roles in developmental regulation of transcription. Annual review of biochemistry *76*, 513-538.

Jennings, B.H., and Ish-Horowicz, D. (2008). The Groucho/TLE/Grg family of transcriptional co-repressors. Genome biology *9*, 205.

Ji, J., Li, Q., Xie, Y., Zhang, X., Cui, S., Shi, S., and Chen, X. (2012). Overexpression of Robo2 causes defects in the recruitment of metanephric mesenchymal cells and ureteric bud branching morphogenesis. Biochem Biophys Res Commun *421*, 494-500.

Jokelainen, P. (1963). An electron microscopic study of the early development of the rat nephron., Vol Suppl. 47.

Jonassen, J.A., San Agustin, J., Follit, J.A., and Pazour, G.J. (2008). Deletion of IFT20 in the mouse kidney causes misorientation of the mitotic spindle and cystic kidney disease. J Cell Biol *183*, 377-384.

Jorgensen, M.C., Ahnfelt-Ronne, J., Hald, J., Madsen, O.D., Serup, P., and Hecksher-Sorensen, J. (2007). An illustrated review of early pancreas development in the mouse. Endocrine reviews *28*, 685-705.

Joseph, A., Yao, H., and Hinton, B.T. (2009). Development and morphogenesis of the Wolffian/epididymal duct, more twists and turns. Dev Biol *325*, 6-14.

Kaisaki, P.J., Menzel, S., Lindner, T., Oda, N., Rjasanowski, I., Sahm, J., Meincke, G., Schulze, J., Schmechel, H., Petzold, C., *et al.* (1997). Mutations in the hepatocyte nuclear factor-1alpha gene in MODY and early-onset NIDDM: evidence for a mutational hotspot in exon 4. Diabetes *46*, 528-535.

Kamiyama, M., Garner, M.K., Farragut, K.M., and Kobori, H. (2012). The establishment of a primary culture system of proximal tubule segments using specific markers from normal mouse kidneys. International journal of molecular sciences *13*, 5098-5111.

Kanai, Y., Lee, W.S., You, G., Brown, D., and Hediger, M.A. (1994). The human kidney low affinity Na+/glucose cotransporter SGLT2. Delineation of the major renal reabsorptive mechanism for D-glucose. J Clin Invest *93*, 397-404.

Kanwar, Y.S., Ota, K., Yang, Q., Wada, J., Kashihara, N., Tian, Y., and Wallner, E.I. (1999). Role of membrane-type matrix metalloproteinase 1 (MT-1-MMP), MMP-2, and its inhibitor in nephrogenesis. Am J Physiol *277*, F934-947.

Karavanov, A.A., Karavanova, I., Perantoni, A., and Dawid, I.B. (1998). Expression pattern of the rat Lim-1 homeobox gene suggests a dual role during kidney development. The International journal of developmental biology *42*, 61-66.

Karner, C.M., Das, A., Ma, Z., Self, M., Chen, C., Lum, L., Oliver, G., and Carroll, T.J. (2011). Canonical Wnt9b signaling balances progenitor cell expansion and differentiation during kidney development. Development *138*, 1247-1257.

Kellendonk, C., Opherk, C., Anlag, K., Schutz, G., and Tronche, F. (2000). Hepatocyte-specific expression of Cre recombinase. Genesis *26*, 151-153.

Kiefer, S.M., Robbins, L., Stumpff, K.M., Lin, C., Ma, L., and Rauchman, M. (2010). Sall1-dependent signals affect Wnt signaling and ureter tip fate to initiate kidney development. Development *137*, 3099-3106.

Kispert, A., Vainio, S., Shen, L., Rowitch, D.H., and McMahon, A.P. (1996). Proteoglycans are required for maintenance of Wnt-11 expression in the ureter tips. Development *122*, 3627-3637.

Kobayashi, A., Kwan, K.M., Carroll, T.J., McMahon, A.P., Mendelsohn, C.L., and Behringer, R.R. (2005). Distinct and sequential tissue-specific activities of the LIM-class homeobox gene Lim1 for tubular morphogenesis during kidney development. Development *132*, 2809-2823.

Kobayashi, A., Valerius, M.T., Mugford, J.W., Carroll, T.J., Self, M., Oliver, G., and McMahon, A.P. (2008). Six2 defines and regulates a multipotent self-renewing nephron progenitor population throughout mammalian kidney development. Cell stem cell *3*, 169-181.

Kobayashi, H., Kawakami, K., Asashima, M., and Nishinakamura, R. (2007). Six1 and Six4 are essential for Gdnf expression in the metanephric mesenchyme and ureteric bud formation, while Six1 deficiency alone causes mesonephric-tubule defects. Mech Dev *124*, 290-303.

Koinuma, D., Shinozaki, M., Komuro, A., Goto, K., Saitoh, M., Hanyu, A., Ebina, M., Nukiwa, T., Miyazawa, K., Imamura, T., *et al.* (2003). Arkadia amplifies TGF-beta superfamily signalling through degradation of Smad7. The EMBO journal *22*, 6458-6470.
Kokko, J.P. (1970). Sodium chloride and water transport in the descending limb of Henle. J Clin Invest *49*, 1838-1846.

Kovall, R.A. (2008). More complicated than it looks: assembly of Notch pathway transcription complexes. Oncogene *27*, 5099-5109.

Kreidberg, J.A., Sariola, H., Loring, J.M., Maeda, M., Pelletier, J., Housman, D., and Jaenisch, R. (1993). WT-1 is required for early kidney development. Cell *74*, 679-691.

Krivan, W., and Wasserman, W.W. (2001). A predictive model for regulatory sequences directing liver-specific transcription. Genome research *11*, 1559-1566.

Kuhn, R., Schwenk, F., Aguet, M., and Rajewsky, K. (1995). Inducible gene targeting in mice. Science *269*, 1427-1429.

Kume, T., Deng, K., and Hogan, B.L. (2000). Murine forkhead/winged helix genes Foxc1 (Mf1) and Foxc2 (Mfh1) are required for the early organogenesis of the kidney and urinary tract. Development *127*, 1387-1395.

Landschulz, W.H., Johnson, P.F., and McKnight, S.L. (1988). The leucine zipper: a hypothetical structure common to a new class of DNA binding proteins. Science *240*, 1759-1764.

Lehman, J.M., Michaud, E.J., Schoeb, T.R., Aydin-Son, Y., Miller, M., and Yoder, B.K. (2008). The Oak Ridge Polycystic Kidney mouse: modeling ciliopathies of mice and men. Dev Dyn *237*, 1960-1971.

Lemaigre, F., and Zaret, K.S. (2004). Liver development update: new embryo models, cell lineage control, and morphogenesis. Curr Opin Genet Dev *14*, 582-590.

Li, B., Carey, M., and Workman, J.L. (2007). The role of chromatin during transcription. Cell *128*, 707-719.

Li, B., and Greene, M.I. (2007). FOXP3 actively represses transcription by recruiting the HAT/HDAC complex. Cell Cycle *6*, 1432-1436.

Li, V.S., Ng, S.S., Boersema, P.J., Low, T.Y., Karthaus, W.R., Gerlach, J.P., Mohammed, S., Heck, A.J., Maurice, M.M., Mahmoudi, T., *et al.* (2012). Wnt signaling through inhibition of beta-catenin degradation in an intact Axin1 complex. Cell *149*, 1245-1256.

Lienkamp, S., Ganner, A., Boehlke, C., Schmidt, T., Arnold, S.J., Schafer, T., Romaker, D., Schuler, J., Hoff, S., Powelske, C., *et al.* (2010). Inversin relays Frizzled-8 signals to promote proximal pronephros development. Proc Natl Acad Sci U S A *107*, 20388-20393.

Lin, F., Hiesberger, T., Cordes, K., Sinclair, A.M., Goldstein, L.S., Somlo, S., and Igarashi, P. (2003). Kidney-specific inactivation of the KIF3A subunit of kinesin-II inhibits renal ciliogenesis and produces polycystic kidney disease. Proc Natl Acad Sci U S A *100*, 5286-5291.

Lindner, T.H., Njolstad, P.R., Horikawa, Y., Bostad, L., Bell, G.I., and Sovik, O. (1999). A novel syndrome of diabetes mellitus, renal dysfunction and genital malformation associated with a partial deletion of the pseudo-POU domain of hepatocyte nuclear factor-1beta. Hum Mol Genet *8*, 2001-2008.

Little, M., Georgas, K., Pennisi, D., and Wilkinson, L. (2010). Kidney development: two tales of tubulogenesis. Curr Top Dev Biol *90*, 193-229.

Logeat, F., Bessia, C., Brou, C., LeBail, O., Jarriault, S., Seidah, N.G., and Israel, A. (1998). The Notch1 receptor is cleaved constitutively by a furin-like convertase. Proc Natl Acad Sci U S A *95*, 8108-8112.

Lokmane, L., Haumaitre, C., Garcia-Villalba, P., Anselme, I., Schneider-Maunoury, S., and Cereghini, S. (2008). Crucial role of vHNF1 in vertebrate hepatic specification. Development *135*, 2777-2786.

Lokmane, L., Heliot, C., Garcia-Villalba, P., Fabre, M., and Cereghini, S. (2010). vHNF1 functions in distinct regulatory circuits to control ureteric bud branching and early nephrogenesis. Development *137*, 347-357.

Lu, B.C., Cebrian, C., Chi, X., Kuure, S., Kuo, R., Bates, C.M., Arber, S., Hassell, J., MacNeil, L., Hoshi, M., *et al.* (2009). Etv4 and Etv5 are required downstream of GDNF and Ret for kidney branching morphogenesis. Nat Genet *41*, 1295-1302.

Lu, W., Peissel, B., Babakhanlou, H., Pavlova, A., Geng, L., Fan, X., Larson, C., Brent, G., and Zhou, J. (1997). piont. Nat Genet *17*, 179-181.

Lyons, J.P., Mueller, U.W., Ji, H., Everett, C., Fang, X., Hsieh, J.C., Barth, A.M., and McCrea, P.D. (2004). Wnt-4 activates the canonical beta-catenin-mediated Wnt pathway and binds Frizzled-6 CRD: functional implications of Wnt/beta-catenin activity in kidney epithelial cells. Experimental cell research *298*, 369-387.

Malnic, G., Fernandez, R., and Lopes, M.J. (1994). The role of the distal nephron in the regulation of acid-base equilibrium by the kidney. Brazilian journal of medical and biological research = Revista brasileira de pesquisas medicas e biologicas / Sociedade Brasileira de Biofisica [et al *27*, 831-850.

Mansouri, A., Chowdhury, K., and Gruss, P. (1998). Follicular cells of the thyroid gland require Pax8 gene function. Nat Genet *19*, 87-90.

Mason, J.M., Morrison, D.J., Basson, M.A., and Licht, J.D. (2006). Sprouty proteins: multifaceted negative-feedback regulators of receptor tyrosine kinase signaling. Trends Cell Biol *16*, 45-54.

Maston, G.A., Evans, S.K., and Green, M.R. (2006). Transcriptional regulatory elements in the human genome. Annu Rev Genomics Hum Genet *7*, 29-59.

Matthews, J.M., and Sunde, M. (2002). Zinc fingers--folds for many occasions. IUBMB life *54*, 351-355.

McNeill, H. (2009). Planar cell polarity and the kidney. J Am Soc Nephrol *20*, 2104-2111.
Mendel, D.B., and Crabtree, G.R. (1991). HNF-1, a member of a novel class of dimerizing homeodomain proteins. J Biol Chem *266*, 677-680.

Menzel, R., Kaisaki, P.J., Rjasanowski, I., Heinke, P., Kerner, W., and Menzel, S. (1998). A low renal threshold for glucose in diabetic patients with a mutation in the hepatocyte nuclear factor-1alpha (HNF-1alpha) gene. Diabet Med *15*, 816-820.

Michael, L., and Davies, J.A. (2004). ji. Journal of anatomy *204*, 241-255.

Michos, O., Cebrian, C., Hyink, D., Grieshammer, U., Williams, L., D'Agati, V., Licht, J.D., Martin, G.R., and Costantini, F. (2010). Kidney development in the absence of Gdnf and Spry1 requires Fgf10. PLoS Genet *6*, e1000809.

Michos, O., Goncalves, A., Lopez-Rios, J., Tiecke, E., Naillat, F., Beier, K., Galli, A., Vainio, S., and Zeller, R. (2007). Reduction of BMP4 activity by gremlin 1 enables ureteric bud outgrowth and GDNF/WNT11 feedback signalling during kidney branching morphogenesis. Development *134*, 2397-2405.

Michos, O., Panman, L., Vintersten, K., Beier, K., Zeller, R., and Zuniga, A. (2004). Gremlin-mediated BMP antagonism induces the epithelial-mesenchymal feedback signaling controlling metanephric kidney and limb organogenesis. Development *131*, 3401-3410.

Mignatti, P., Morimoto, T., and Rifkin, D.B. (1992). Basic fibroblast growth factor, a protein devoid of secretory signal sequence, is released by cells via a pathway independent of the endoplasmic reticulum-Golgi complex. Journal of cellular physiology *151*, 81-93.

Miller, R.K., Canny, S.G., Jang, C.W., Cho, K., Ji, H., Wagner, D.S., Jones, E.A., Habas, R., and McCrea, P.D. (2011). Pronephric tubulogenesis requires Daam1-mediated planar cell polarity signaling. J Am Soc Nephrol *22*, 1654-1664.

Mishina, Y., Suzuki, A., Ueno, N., and Behringer, R.R. (1995). Bmpr encodes a type I bone morphogenetic protein receptor that is essential for gastrulation during mouse embryogenesis. Genes Dev *9*, 3027-3037.

Miyamoto, N., Yoshida, M., Kuratani, S., Matsuo, I., and Aizawa, S. (1997). Defects of urogenital development in mice lacking Emx2. Development *124*, 1653-1664.

Miyazaki, Y., Oshima, K., Fogo, A., Hogan, B.L., and Ichikawa, I. (2000). Bone morphogenetic protein 4 regulates the budding site and elongation of the mouse ureter. J Clin Invest *105*, 863-873.

Miyazono, K., Kamiya, Y., and Morikawa, M. (2010). Bone morphogenetic protein receptors and signal transduction. Journal of biochemistry *147*, 35-51.

Miyazono, K., Maeda, S., and Imamura, T. (2005). BMP receptor signaling: transcriptional targets, regulation of signals, and signaling cross-talk. Cytokine & growth factor reviews *16*, 251-263.

Mlodzik, M. (2002). Planar cell polarization: do the same mechanisms regulate Drosophila tissue polarity and vertebrate gastrulation? Trends Genet *18*, 564-571.

Mohammadi, M., Olsen, S.K., and Ibrahimi, O.A. (2005). Structural basis for fibroblast growth factor receptor activation. Cytokine & growth factor reviews *16*, 107-137.

Moore, A.W., McInnes, L., Kreidberg, J., Hastie, N.D., and Schedl, A. (1999). YAC complementation shows a requirement for Wt1 in the development of epicardium, adrenal gland and throughout nephrogenesis. Development *126*, 1845-1857.

Moore, M.W., Klein, R.D., Farinas, I., Sauer, H., Armanini, M., Phillips, H., Reichardt, L.F., Ryan, A.M., Carver-Moore, K., and Rosenthal, A. (1996). Renal and neuronal abnormalities in mice lacking GDNF. Nature *382*, 76-79.

Mugford, J.W., Sipila, P., Kobayashi, A., Behringer, R.R., and McMahon, A.P. (2008a). Hoxd11 specifies a program of metanephric kidney development within the intermediate mesoderm of the mouse embryo. Dev Biol *319*, 396-405.

Mugford, J.W., Sipila, P., McMahon, J.A., and McMahon, A.P. (2008b). Osr1 expression demarcates a multi-potent population of intermediate mesoderm that undergoes progressive restriction to an Osr1-dependent nephron progenitor compartment within the mammalian kidney. Dev Biol *324*, 88-98.

Mugford, J.W., Yu, J., Kobayashi, A., and McMahon, A.P. (2009). High-resolution gene expression analysis of the developing mouse kidney defines novel cellular compartments within the nephron progenitor population. Dev Biol *333*, 312-323.

Murdoch, C. (2000). CXCR4: chemokine receptor extraordinaire. Immunological reviews *177*, 175-184.

Nakai, S., Sugitani, Y., Sato, H., Ito, S., Miura, Y., Ogawa, M., Nishi, M., Jishage, K., Minowa, O., and Noda, T. (2003). Crucial roles of Brn1 in distal tubule formation and function in mouse kidney. Development *130*, 4751-4759.

Naray-Fejes-Toth, A., and Fejes-Toth, G. (1990). Glucocorticoid receptors mediate mineralocorticoid-like effects in cultured collecting duct cells. Am J Physiol *259*, F672-678.
Narlis, M., Grote, D., Gaitan, Y., Boualia, S.K., and Bouchard, M. (2007). Pax2 and Pax8 Regulate Branching Morphogenesis and Nephron Differentiation in the Developing Kidney. J Am Soc Nephrol *18*, 1121-1129.

Neild, G.H. (2011). Primary renal disease in young adults with renal failure. Nephrol Dial Transplant *25*, 1025-1032.

Nie, X., Xu, J., El-Hashash, A., and Xu, P.X. (2011). Six1 regulates Grem1 expression in the metanephric mesenchyme to initiate branching morphogenesis. Dev Biol *352*, 141-151.

Nishinakamura, R., Matsumoto, Y., Nakao, K., Nakamura, K., Sato, A., Copeland, N.G., Gilbert, D.J., Jenkins, N.A., Scully, S., Lacey, D.L., *et al.* (2001). Murine homolog of SALL1 is essential for ureteric bud invasion in kidney development. Development *128*, 3105-3115.

Nusslein-Volhard, C., Lohs-Schardin, M., Sander, K., and Cremer, C. (1980). A dorso-ventral shift of embryonic primordia in a new maternal-effect mutant of Drosophila. Nature *283*, 474-476.

Oberg, C., Li, J., Pauley, A., Wolf, E., Gurney, M., and Lendahl, U. (2001). The Notch intracellular domain is ubiquitinated and negatively regulated by the mammalian Sel-10 homolog. J Biol Chem *276*, 35847-35853.

Ohtani, K., and Dimmeler, S. (2011). Control of cardiovascular differentiation by microRNAs. Basic research in cardiology *106*, 5-11.

Ohto, H., Kamada, S., Tago, K., Tominaga, S.I., Ozaki, H., Sato, S., and Kawakami, K. (1999). Cooperation of six and eya in activation of their target genes through nuclear translocation of Eya. Mol Cell Biol *19*, 6815-6824.

Ohuchi, H., Hori, Y., Yamasaki, M., Harada, H., Sekine, K., Kato, S., and Itoh, N. (2000). FGF10 acts as a major ligand for FGF receptor 2 IIIb in mouse multi-organ development. Biochem Biophys Res Commun *277*, 643-649.

Ott, M.O., Rey-Campos, J., Cereghini, S., and Yaniv, M. (1991). vHNF1 is expressed in epithelial cells of distinct embryonic origin during development and precedes HNF1 expression. Mech Dev *36*, 47-58.

Panakova, D., Sprong, H., Marois, E., Thiele, C., and Eaton, S. (2005). Lipoprotein particles are required for Hedgehog and Wingless signalling. Nature *435*, 58-65.

Park, J.S., Valerius, M.T., and McMahon, A.P. (2007). Wnt/beta-catenin signaling regulates nephron induction during mouse kidney development. Development *134*, 2533-2539.

Patterson, L.T., Pembaur, M., and Potter, S.S. (2001). Hoxa11 and Hoxd11 regulate branching morphogenesis of the ureteric bud in the developing kidney. Development *128*, 2153-2161.

Pazour, G.J., San Agustin, J.T., Follit, J.A., Rosenbaum, J.L., and Witman, G.B. (2002). Polycystin-2 localizes to kidney cilia and the ciliary level is elevated in orpk mice with polycystic kidney disease. Curr Biol *12*, R378-380.

Pedersen, A., Skjong, C., and Shawlot, W. (2005). Lim 1 is required for nephric duct extension and ureteric bud morphogenesis. Dev Biol *288*, 571-581.

Pepicelli, C.V., Kispert, A., Rowitch, D.H., and McMahon, A.P. (1997). GDNF induces branching and increased cell proliferation in the ureter of the mouse. Dev Biol *192*, 193-198.

Petersen, C.P., and Reddien, P.W. (2009). Wnt signaling and the polarity of the primary body axis. Cell *139*, 1056-1068.

Phillips, K., and Luisi, B. (2000). The virtuoso of versatility: POU proteins that flex to fit. J Mol Biol *302*, 1023-1039.

Plotnikov, A.N., Hubbard, S.R., Schlessinger, J., and Mohammadi, M. (2000). Crystal structures of two FGF-FGFR complexes reveal the determinants of ligand-receptor specificity. Cell *101*, 413-424.

Pontoglio, M. (2000). Hepatocyte nuclear factor 1, a transcription factor at the crossroads of glucose homeostasis. J Am Soc Nephrol *11 Suppl 16*, S140-143.

Pontoglio, M., Barra, J., Hadchouel, M., Doyen, A., Kress, C., Bach, J.P., Babinet, C., and Yaniv, M. (1996). Hepatocyte nuclear factor 1 inactivation results in hepatic dysfunction, phenylketonuria, and renal Fanconi syndrome. Cell *84*, 575-585.

Pontoglio, M., Faust, D.M., Doyen, A., Yaniv, M., and Weiss, M.C. (1997). Hepatocyte nuclear factor 1alpha gene inactivation impairs chromatin remodeling and demethylation of the phenylalanine hydroxylase gene. Mol Cell Biol *17*, 4948-4956.

Pontoglio, M., Sreenan, S., Roe, M., Pugh, W., Ostrega, D., Doyen, A., Pick, A.J., Baldwin, A., Velho, G., Froguel, P., *et al.* (1998). Defective insulin secretion in hepatocyte nuclear factor 1alpha-deficient mice. J Clin Invest *101*, 2215-2222.

Porteous, S., Torban, E., Cho, N.P., Cunliffe, H., Chua, L., McNoe, L., Ward, T., Souza, C., Gus, P., Giugliani, R., *et al.* (2000). Primary renal hypoplasia in humans and mice with PAX2 mutations: evidence of increased apoptosis in fetal kidneys of Pax2(1Neu) +/- mutant mice. Hum Mol Genet *9*, 1-11.

Potter, E.L. (1965). Development of the Human Glomerulus. Archives of pathology *80*, 241-255.

Qiao, J., Uzzo, R., Obara-Ishihara, T., Degenstein, L., Fuchs, E., and Herzlinger, D. (1999). FGF-7 modulates ureteric bud growth and nephron number in the developing kidney. Development *126*, 547-554.

Qin, B.Y., Chacko, B.M., Lam, S.S., de Caestecker, M.P., Correia, J.J., and Lin, K. (2001). Structural basis of Smad1 activation by receptor kinase phosphorylation. Mol Cell *8*, 1303-1312.

Qin, B.Y., Lam, S.S., Correia, J.J., and Lin, K. (2002). Smad3 allostery links TGF-beta receptor kinase activation to transcriptional control. Genes Dev *16*, 1950-1963.

Quaggin, S.E., and Kreidberg, J.A. (2008). Development of the renal glomerulus: good neighbors and good fences. Development *135*, 609-620.

Quaggin, S.E., Schwartz, L., Cui, S., Igarashi, P., Deimling, J., Post, M., and Rossant, J. (1999). The basic-helix-loop-helix protein pod1 is critically important for kidney and lung organogenesis. Development *126*, 5771-5783.

Ramsay, R.G., and Gonda, T.J. (2008). MYB function in normal and cancer cells. Nat Rev Cancer *8*, 523-534.

Reginensi, A., Clarkson, M., Neirijnck, Y., Lu, B., Ohyama, T., Groves, A.K., Sock, E., Wegner, M., Costantini, F., Chaboissier, M.C., *et al.* (2011). SOX9 controls epithelial branching by activating RET effector genes during kidney development. Hum Mol Genet *20*, 1143-1153.

Reinke, H., and Horz, W. (2003). Histones are first hyperacetylated and then lose contact with the activated PHO5 promoter. Mol Cell *11*, 1599-1607.

Rey-Campos, J., Chouard, T., Yaniv, M., and Cereghini, S. (1991). vHNF1 is a homeoprotein that activates transcription and forms heterodimers with HNF1. The EMBO journal *10*, 1445-1457.

Rizzoni, G., Loirat, C., Levy, M., Milanesi, C., Zachello, G., and Mathieu, H. (1982). Familial hypoplastic glomerulocystic kidney. A new entity? Clin Nephrol *18*, 263-268.

Robert, B., St John, P.L., and Abrahamson, D.R. (1998). Direct visualization of renal vascular morphogenesis in Flk1 heterozygous mutant mice. Am J Physiol *275*, F164-172.

Roeder, R.G. (1996). Nuclear RNA polymerases: role of general initiation factors and cofactors in eukaryotic transcription. Methods in enzymology *273*, 165-171.

Rumballe, B., Georgas, K., Wilkinson, L., and Little, M. (2010). Molecular anatomy of the kidney: what have we learned from gene expression and functional genomics? Pediatric nephrology (Berlin, Germany) *25*, 1005-1016.

Saburi, S., Hester, I., Fischer, E., Pontoglio, M., Eremina, V., Gessler, M., Quaggin, S.E., Harrison, R., Mount, R., and McNeill, H. (2008). Loss of Fat4 disrupts PCP signaling and oriented cell division and leads to cystic kidney disease. Nat Genet *40*, 1010-1015.

Sainio, K., Hellstedt, P., Kreidberg, J.A., Saxen, L., and Sariola, H. (1997a). Differential regulation of two sets of mesonephric tubules by WT-1. Development *124*, 1293-1299.

Sainio, K., Suvanto, P., Davies, J., Wartiovaara, J., Wartiovaara, K., Saarma, M., Arumae, U., Meng, X., Lindahl, M., Pachnis, V., *et al.* (1997b). Glial-cell-line-derived neurotrophic factor is required for bud initiation from ureteric epithelium. Development *124*, 4077-4087.

Sajithlal, G., Zou, D., Silvius, D., and Xu, P.X. (2005). Eya 1 acts as a critical regulator for specifying the metanephric mesenchyme. Dev Biol *284*, 323-336.

Sanchez, M.P., Silos-Santiago, I., Frisen, J., He, B., Lira, S.A., and Barbacid, M. (1996). Renal agenesis and the absence of enteric neurons in mice lacking GDNF. Nature *382*, 70-73.

Satow, R., Chan, T.C., and Asashima, M. (2004). The role of Xenopus frizzled-8 in pronephric development. Biochem Biophys Res Commun *321*, 487-494.

Saxen, L., and Sariola, H. (1987). Early organogenesis of the kidney. Pediatric nephrology (Berlin, Germany) *1*, 385-392.

Schedl, A. (2007). Renal abnormalities and their developmental origin. Nat Rev Genet *8*, 791-802.

Schlessinger, J., Plotnikov, A.N., Ibrahimi, O.A., Eliseenkova, A.V., Yeh, B.K., Yayon, A., Linhardt, R.J., and Mohammadi, M. (2000). Crystal structure of a ternary FGF-FGFR-heparin complex reveals a dual role for heparin in FGFR binding and dimerization. Mol Cell *6*, 743-750.

Schuchardt, A., D'Agati, V., Larsson-Blomberg, L., Costantini, F., and Pachnis, V. (1994). Defects in the kidney and enteric nervous system of mice lacking the tyrosine kinase receptor Ret. Nature *367*, 380-383.

Self, M., Lagutin, O.V., Bowling, B., Hendrix, J., Cai, Y., Dressler, G.R., and Oliver, G. (2006). Six2 is required for suppression of nephrogenesis and progenitor renewal in the developing kidney. The EMBO journal *25*, 5214-5228.

Servitja, J.M., Pignatelli, M., Maestro, M.A., Cardalda, C., Boj, S.F., Lozano, J., Blanco, E., Lafuente, A., McCarthy, M.I., Sumoy, L., *et al.* (2009). Hnf1alpha (MODY3) controls tissue-specific transcriptional programs and exerts opposed effects on cell growth in pancreatic islets and liver. Mol Cell Biol *29*, 2945-2959.

Shah, M.M., Tee, J.B., Meyer, T., Meyer-Schwesinger, C., Choi, Y., Sweeney, D.E., Gallegos, T.F., Johkura, K., Rosines, E., Kouznetsova, V., *et al.* (2009). The instructive role of metanephric mesenchyme in ureteric bud patterning, sculpting, and maturation and its potential ability to buffer ureteric bud branching defects. Am J Physiol Renal Physiol *297*, F1330-1341.

Shakya, R., Watanabe, T., and Costantini, F. (2005). The role of GDNF/Ret signaling in ureteric bud cell fate and branching morphogenesis. Dev Cell *8*, 65-74.

Shawlot, W., and Behringer, R.R. (1995). Requirement for Lim1 in head-organizer function. Nature *374*, 425-430.

Shi, W., Chen, H., Sun, J., Chen, C., Zhao, J., Wang, Y.L., Anderson, K.D., and Warburton, D. (2004). Overexpression of Smurf1 negatively regulates mouse embryonic lung branching morphogenesis by specifically reducing Smad1 and Smad5 proteins. Am J Physiol Lung Cell Mol Physiol *286*, L293-300.

Shih, D.Q., Screenan, S., Munoz, K.N., Philipson, L., Pontoglio, M., Yaniv, M., Polonsky, K.S., and Stoffel, M. (2001). Loss of HNF-1alpha function in mice leads to abnormal expression of genes involved in pancreatic islet development and metabolism. Diabetes *50*, 2472-2480.

Simic, P., and Vukicevic, S. (2005). Bone morphogenetic proteins in development and homeostasis of kidney. Cytokine & growth factor reviews *16*, 299-308.

Simons, M., Gloy, J., Ganner, A., Bullerkotte, A., Bashkurov, M., Kronig, C., Schermer, B., Benzing, T., Cabello, O.A., Jenny, A., *et al.* (2005). Inversin, the gene product mutated in nephronophthisis type II, functions as a molecular switch between Wnt signaling pathways. Nat Genet *37*, 537-543.

Smith, C., and Mackay, S. (1991). Morphological development and fate of the mouse mesonephros. Journal of anatomy *174*, 171-184.

So, P.L., and Danielian, P.S. (1999). Cloning and expression analysis of a mouse gene related to Drosophila odd-skipped. Mech Dev *84*, 157-160.

Song, R., and Yosypiv, I.V. (2011). Genetics of congenital anomalies of the kidney and urinary tract. Pediatric nephrology (Berlin, Germany) *26*, 353-364.

Sourdive, D.J., Chouard, T., and Yaniv, M. (1993). The HNF1 C-terminal domain contributes to transcriptional activity and modulates nuclear localisation. Comptes rendus de l'Academie des sciences *316*, 385-394.

Stark, K., Vainio, S., Vassileva, G., and McMahon, A.P. (1994). Epithelial transformation of metanephric mesenchyme in the developing kidney regulated by Wnt-4. Nature *372*, 679-683.
Stoffel, M., and Duncan, S.A. (1997). The maturity-onset diabetes of the young (MODY1) transcription factor HNF4alpha regulates expression of genes required for glucose transport and metabolism. Proc Natl Acad Sci U S A *94*, 13209-13214.

Surendran, K., Boyle, S., Barak, H., Kim, M., Stomberski, C., McCright, B., and Kopan, R. (2010). The contribution of Notch1 to nephron segmentation in the developing kidney is revealed in a sensitized Notch2 background and can be augmented by reducing Mint dosage. Dev Biol *337*, 386-395.

Suzuki, M.M., and Bird, A. (2008). DNA methylation landscapes: provocative insights from epigenomics. Nat Rev Genet *9*, 465-476.

Taelman, V., Van Campenhout, C., Solter, M., Pieler, T., and Bellefroid, E.J. (2006). The Notch-effector HRT1 gene plays a role in glomerular development and patterning of the Xenopus pronephros anlagen. Development *133*, 2961-2971.

Tallquist, M.D., and Soriano, P. (2000). Epiblast-restricted Cre expression in MORE mice: a tool to distinguish embryonic vs. extra-embryonic gene function. Genesis *26*, 113-115.

Tamai, K., Zeng, X., Liu, C., Zhang, X., Harada, Y., Chang, Z., and He, X. (2004). A mechanism for Wnt coreceptor activation. Mol Cell *13*, 149-156.

Tena, J.J., Neto, A., de la Calle-Mustienes, E., Bras-Pereira, C., Casares, F., and Gomez-Skarmeta, J.L. (2007). Odd-skipped genes encode repressors that control kidney development. Dev Biol *301*, 518-531.

Tian, Y., Kolb, R., Hong, J.H., Carroll, J., Li, D., You, J., Bronson, R., Yaffe, M.B., Zhou, J., and Benjamin, T. (2007). TAZ promotes PC2 degradation through a SCFbeta-Trcp E3 ligase complex. Mol Cell Biol *27*, 6383-6395.

Tobin, J.L., and Beales, P.L. (2007). Bardet-Biedl syndrome: beyond the cilium. Pediatric nephrology (Berlin, Germany) *22*, 926-936.

Tomei, L., Cortese, R., and De Francesco, R. (1992). A POU-A related region dictates DNA binding specificity of LFB1/HNF1 by orienting the two XL-homeodomains in the dimer. The EMBO journal *11*, 4119-4129.

Torres, M., Gomez-Pardo, E., Dressler, G.R., and Gruss, P. (1995). Pax-2 controls multiple steps of urogenital development. Development *121*, 4057-4065.

Tsang, T.E., Shawlot, W., Kinder, S.J., Kobayashi, A., Kwan, K.M., Schughart, K., Kania, A., Jessell, T.M., Behringer, R.R., and Tam, P.P. (2000). Lim1 activity is required for intermediate mesoderm differentiation in the mouse embryo. Dev Biol *223*, 77-90.

Uematsu, F., Kan, M., Wang, F., Jang, J.H., Luo, Y., and McKeehan, W.L. (2000). Ligand binding properties of binary complexes of heparin and immunoglobulin-like modules of FGF receptor 2. Biochem Biophys Res Commun *272*, 830-836.

Ulinski, T., Lescure, S., Beaufils, S., Guigonis, V., Decramer, S., Morin, D., Clauin, S., Deschenes, G., Bouissou, F., Bensman, A., *et al.* (2006). Renal phenotypes related to hepatocyte nuclear factor-1beta (TCF2) mutations in a pediatric cohort. J Am Soc Nephrol *17*, 497-503.

Urist, M.R. (1965). Bone: formation by autoinduction. Science *150*, 893-899.

Vallania, F., Schiavone, D., Dewilde, S., Pupo, E., Garbay, S., Calogero, R., Pontoglio, M., Provero, P., and Poli, V. (2009). Genome-wide discovery of functional transcription factor binding sites by comparative genomics: the case of Stat3. Proc Natl Acad Sci U S A *106*, 5117-5122.

Veeman, M.T., Slusarski, D.C., Kaykas, A., Louie, S.H., and Moon, R.T. (2003). Zebrafish prickle, a modulator of noncanonical Wnt/Fz signaling, regulates gastrulation movements. Curr Biol *13*, 680-685.

Verdeguer, F., Le Corre, S., Fischer, E., Callens, C., Garbay, S., Doyen, A., Igarashi, P., Terzi, F., and Pontoglio, M. (2010). A mitotic transcriptional switch in polycystic kidney disease. Nat Med *16*, 106-110.

Verrey, F., Schaerer, E., Zoerkler, P., Paccolat, M.P., Geering, K., Kraehenbuhl, J.P., and Rossier, B.C. (1987). Regulation by aldosterone of Na+,K+-ATPase mRNAs, protein synthesis, and sodium transport in cultured kidney cells. J Cell Biol *104*, 1231-1237.

Wallingford, J.B., Ewald, A.J., Harland, R.M., and Fraser, S.E. (2001). Calcium signaling during convergent extension in Xenopus. Curr Biol *11*, 652-661.

Wallingford, J.B., and Habas, R. (2005). The developmental biology of Dishevelled: an enigmatic protein governing cell fate and cell polarity. Development *132*, 4421-4436.

Wang, J., Mark, S., Zhang, X., Qian, D., Yoo, S.J., Radde-Gallwitz, K., Zhang, Y., Lin, X., Collazo, A., Wynshaw-Boris, A., *et al.* (2005a). Regulation of polarized extension and planar cell polarity in the cochlea by the vertebrate PCP pathway. Nat Genet *37*, 980-985.

Wang, M.M. (2011). Notch signaling and Notch signaling modifiers. Int J Biochem Cell Biol *43*, 1550-1562.

Wang, Q., Lan, Y., Cho, E.S., Maltby, K.M., and Jiang, R. (2005b). Odd-skipped related 1 (Odd 1) is an essential regulator of heart and urogenital development. Dev Biol *288*, 582-594.

Wang, Y., Wysocka, J., Perlin, J.R., Leonelli, L., Allis, C.D., and Coonrod, S.A. (2004). Linking covalent histone modifications to epigenetics: the rigidity and plasticity of the marks. Cold Spring Harbor symposia on quantitative biology *69*, 161-169.

Watanabe, T., and Costantini, F. (2004). Real-time analysis of ureteric bud branching morphogenesis in vitro. Dev Biol *271*, 98-108.

Wellik, D.M., Hawkes, P.J., and Capecchi, M.R. (2002). Hox11 paralogous genes are essential for metanephric kidney induction. Genes Dev *16*, 1423-1432.

Wharton, K.A., Johansen, K.M., Xu, T., and Artavanis-Tsakonas, S. (1985). Nucleotide sequence from the neurogenic locus notch implies a gene product that shares homology with proteins containing EGF-like repeats. Cell *43*, 567-581.

Wu, G., Markowitz, G.S., Li, L., D'Agati, V.D., Factor, S.M., Geng, L., Tibara, S., Tuchman, J., Cai, Y., Park, J.H., *et al.* (2000). Cardiac defects and renal failure in mice with targeted mutations in Pkd2. Nat Genet *24*, 75-78.

Xu, P.X., Adams, J., Peters, H., Brown, M.C., Heaney, S., and Maas, R. (1999). Eya1-deficient mice lack ears and kidneys and show abnormal apoptosis of organ primordia. Nat Genet *23*, 113-117.

Xu, P.X., Zheng, W., Huang, L., Maire, P., Laclef, C., and Silvius, D. (2003). Six1 is required for the early organogenesis of mammalian kidney. Development *130*, 3085-3094.

Yamagata, K., Oda, N., Kaisaki, P.J., Menzel, S., Furuta, H., Vaxillaire, M., Southam, L., Cox, R.D., Lathrop, G.M., Boriraj, V.V., *et al.* (1996). Mutations in the hepatocyte nuclear factor-1alpha gene in maturity-onset diabetes of the young (MODY3). Nature *384*, 455-458.
Yoder, B.K. (2007). Role of primary cilia in the pathogenesis of polycystic kidney disease. J Am Soc Nephrol *18*, 1381-1388.

Yu, C.T., Tang, K., Suh, J.M., Jiang, R., Tsai, S.Y., and Tsai, M.J. (2012a). COUP-TFII is essential for metanephric mesenchyme formation and kidney precursor cell survival. Development *139*, 2330-2339.

Yu, J., Valerius, M.T., Duah, M., Staser, K., Hansard, J.K., Guo, J.J., McMahon, J., Vaughan, J., Faria, D., Georgas, K., *et al.* (2012b). Identification of molecular compartments and genetic circuitry in the developing mammalian kidney. Development *139*, 1863-1873.

Zhang, Y., Chang, C., Gehling, D.J., Hemmati-Brivanlou, A., and Derynck, R. (2001). Regulation of Smad degradation and activity by Smurf2, an E3 ubiquitin ligase. Proc Natl Acad Sci U S A *98*, 974-979.

Zhao, B., Lei, Q.Y., and Guan, K.L. (2009). Harness the power: new insights into the inhibition of YAP/Yorkie. Dev Cell *16*, 321-322.

Zhao, H., Kegg, H., Grady, S., Truong, H.T., Robinson, M.L., Baum, M., and Bates, C.M. (2004). Role of fibroblast growth factor receptors 1 and 2 in the ureteric bud. Dev Biol *276*, 403-415.

« O sancte deus, quanta mala patimur pro ecclesia dei…. Nunc bibendum est »

Papa Martino IV

Summary (English)

HNF1β is a transcription factor expressed during nephrogenesis in the ureteric bud and in the tubular epithelia derived from the metanephric mesenchyme. Mutations in HNF1B/MODY5 represent one of the most prevalent human genetic defects responsible for Congenital Abnormalities of Kidney and Urinary Tract (CAKUT). To investigate the role played by HNF1beta during kidney development, I made use of a CRE-LoxP strategy to inactivate *Hnf1b* in different compartments and at different time points during mouse kidney morphogenesis. My results showed that *Hnf1b* is required for the expression of several key genes including *Wnt9b*, *Emx2*, *Pax2* and *Lhx*. These genes are normally expressed in the ureteric bud and their absence leads to the formation of rudimentary kidneys, characterized by abnormal ureteric bud branching and lack of mesenchymal to epithelial transition. On the other hand, the specific inactivation of *Hnf1b* in the metanephric mesenchyme does not affect the early steps of epithelisation but leads to severe malformation of nephron precursors. In the absence of HNF1β, S-Shaped bodies lack the formation of a bulge of epithelial cells that normally give rise to Henle's loops and proximal tubules. At the molecular level, these defects are associated with a decreased expression of Dll1, a Notch ligand that is directly controlled by HNF1β. This downregulation leads to a defective activation of the Notch pathway in the prospective tubular compartment of comma and S-shaped bodies. Preliminary results using a highly chimeric inactivation of *Hnf1b* in the mesenchyme showed that the spotted absence of *Hnf1b* does not prevent nephrogenesis. However, tubules are shorter and partially cystic. My results showed that murine models for Hnf1b deficiency recapitulates many of the malformations described in MODY5 patients. All together, my results improved our understanding of the genetic program controlled by HNF1β during kidney development whose dysfunction may lead to CAKUT in patients.

Résumé (Français)

HNF1beta est un facteur de transcription exprimé pendant le développement rénal dans le bourgeon urétéral et les dérivés épithéliaux du blastème métanéphrique. Les mutations de HNF1B/MODY5 représentent l'une des anomalies génétiques les plus fréquentes à l'origine des CAKUT (Congenital Abnormalities of Kidney and Urinary Tract). Afin d'étudier le rôle de HNF1beta au cours du développement rénal, j'ai utilisé un système CRE-LoxP pour inactiver *Hnf1b* dans différents compartiments et à différents temps au cours de la morphogenèse rénale chez la souris. Mes résultats ont montré que *Hnf1b* est nécessaire pour l'expression de gènes clés exprimés dans le bourgeon urétéral, incluant *Wnt9b*, *Emx2*, *Pax2* et *Lhx1*.Leur absence est à l'origine de la formation de reins rudimentaires, caractérisés par un branchement anormal du bourgeon urétéral et une absence de transition mésenchyme-épithélium. D'autre part, l'inactivation spécifique de *Hnf1b* dans le blastème métanéphrique n'affecte pas les premiers dérivés épithéliaux mais conduit à la formation de précurseurs néphroniques anormaux. En l'absence de HNF1beta, les corps en S ne développent pas une protubérance de cellules épithéliales, à l'origine des tubules proximaux et des anses de Henlé. Au niveau moléculaire, ces anomalies sont associées à une diminution de l'expression de Dll1, un ligand de Notch, qui est directement contrôlé par HNF1beta. Cette diminution conduit à une activation défectueuse de la voie Notch dans le futur compartiment tubulaire du corps en virgule et du corps en S. Des résultats préliminaires concernant une inactivation très chimérique de *Hnf1b* dans le mésenchyme ont montré que dans ce modèle, les néphrons se forment normalement mais que les tubules sont plus courts et partiellement kystiques. Mes résultats ont montré que les modèles murins d'inactivation conditionnelle de *Hnf1b* récapitulent la plupart des anomalies observées chez les patients MODY5. L'ensemble de mes résultats améliore notre compréhension du programme génétique contrôlé par *Hnf1b* au cours du développement dont les anomalies peuvent conduire aux CAKUT chez les patients.